MULTIFUNCTIONAL ORGANIC-INORGANIC HYBRID NANOPHOTONIC DEVICES

Brett William Garner, B.S., M.S., M.I.P, J.D.

Dissertation Prepared for the Degree of

DOCTOR OF PHILOSOPHY

UNIVERSITY OF NORTH TEXAS

May 2008

APPROVED:

Arup Neogi, Major Professor
Tae-Youl Choi, Committee Member
Zhibing Hu, Committee Member
Arkadii Krokhin, Committee Member
William Deering, Graduate Advisor
Christopher L. Littler, Chair of the Department of Physics
Sandra L. Terrell, Dean of the Robert B. Toulouse School of Graduate Studies

Garner, Brett William, Multifunctional Organic-Inorganic Hybrid Nanophotonic Devices. Doctor of Philosophy (Physics), May 2008, 230 pp., 108 figures, references, 424 titles.

The emergence of optical applications, such as lasers, fiber optics, and semiconductor based sources and detectors, has created a drive for smaller and more specialized devices. Nanophotonics is an emerging field of study that encompasses the disciplines of physics, engineering, chemistry, biology, applied sciences and biomedical technology. In particular, nanophotonics explores optical processes on a nanoscale.

This dissertation presents nanophotonic applications that incorporate various forms of the organic polymer N-isopropylacrylamide (NIPA) with inorganic semiconductors. This includes the material characterization of NIPA, with such techniques as ellipsometry and dynamic light scattering. Two devices were constructed incorporating the NIPA hydrogel with semiconductors.

The first device comprises a PNIPAM—CdTe hybrid material. The PNIPAM is a means for the control of distances between CdTe quantum dots encapsulated within the hydrogel. Controlling the distance between the quantum dots allows for the control of resonant energy transfer between neighboring quantum dots. Whereby, providing a means for controlling the temperature dependent red-shifts in photoluminescent peaks and FWHM. Further, enhancement of photoluminescent due to increased scattering in the medium is shown as a function of temperature.

The second device incorporates NIPA into a 2D photonic crystal patterned on GaAs. The refractive index change of the NIPA hydrogel as it undergoes its phase change creates a controllable mechanism for adjusting the transmittance of light frequencies through a

linear defect in a photonic crystal. The NIPA infiltrated photonic crystal shows greater shifts in the bandwidth per °C than any liquid crystal methods.

This dissertation demonstrates the versatile uses of hydrogel, as a means of control in nanophotonic devices, and will likely lead to development of other hybrid applications. The development of smaller light based applications will facilitate the need to augment the devices with control mechanism and will play an increasing important role in the future.

ACKNOWLEDGEMENTS

I would like to acknowledge the hard work and guidance of my advisor Arup Neogi and my committee members Tae-Youl Choi, Arkadii Krokhin and Zhibing Hu. It is only with their mentoring and leadership that I was able to finish this dissertation. I also must thank Tong Cai for the help in preparing hydrogels and the instruction on their characterization.

Richard Reidy provided countless hours on his ellipsometer in determining the refractive index of the hydrogel. Also, Glenn Dillon and his staff at the UNT health sciences allowed access to his pipette puller.

A special thanks to Kiyoshi Asakawa at the University of Tsukuba and his photonic crystal group Nobuhiko Ozaki and Yoshinori Watanabe for the provided samples and instruction on modeling photonic crystals.

Finally, this work was supported by the National Science Foundation under the programs of International Research Experience for Students (IRES) and the Doctoral Dissertation Enhancement Program (DDEP) and a grant from the Department of Energy.

TABLE OF CONTENTS

LIST OF FIGURES

CHAPTER 1

INTRODUCTION

1.1 Light Interaction with Matter

The emergence of optical applications, such as lasers, fiber optics, and semiconductor based sources and detectors, has created a drive for smaller and specialized device applications. The theoretical and experimental fields of optical physics have flourished since the 1960's as optical applications have emerged in industrial and commercial sectors. The basis of the physics is the interactions between light and matter.

The development of the theoretical nature of light is one of the most interesting stories to be told in historical physics. The scientific awakening of the sixteenth and seventeen centuries brought forth two incompatible models of light, one based on a particle theory and the other a wave theory. It was not until the dawn of the twentieth century that a complete understanding of light's wave-particle duality came into being. Quantum electrodynamics successfully married the sub-disciplines of electricity, magnetism and atomic physics, to satisfactorily describe the nature of light and its interaction with matter.[1]

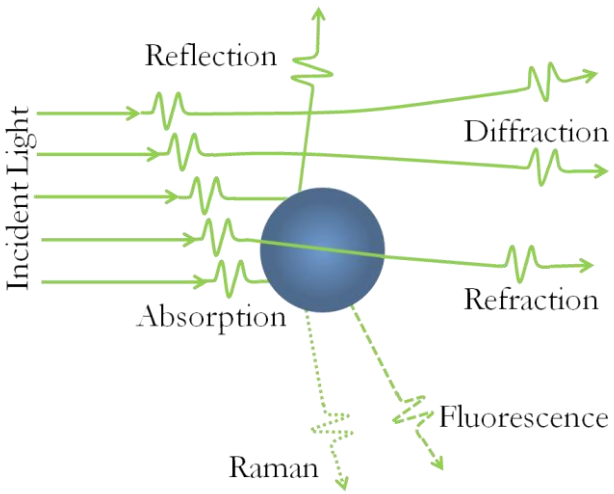

Figure 1.1 A depiction of the interactions of light with matter.

The basic interactions of light with matter include reflection, diffraction, refraction, and absorption,

depicted in figure 1.1. Each of these interactions, alter the energy, polarization and propagating direction of the EM wave. Absorption is unique among the basic interactions in that the EM radiation incident on the absorbing material is not the same EM radiation detected. The absorbed radiation is reradiated through fluorescent or Raman processes, which differ in wavelength from the incident radiation.

The first optical phenomenon, historically described was the refraction and reflection of light. Reflection is the simple concept of the direction of a wave being changed to the opposite direction of the incoming wave. However, refraction the bending of waves when they travel from one medium to another required a mathematical framework developed as Snell's law which describes the refraction of light in geometrical terms and the refractive indices of the materials. In figure 1.2, the change in angle is shown as a light wave from a low refractive index material enters a higher refractive index material and finally enters a material with a refractive index less than the second but greater than the first. The refraction process occurs because of the decrease in velocity with higher refractive index materials and is different for each unique material.

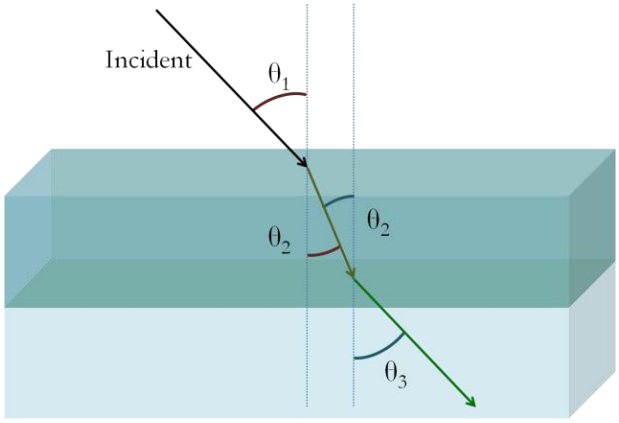

Figure 1.2 A diagram of the change in angle of a propagating wave as it moves through mediums with different refractive indices.

The process of diffraction is the bending of waves due to interactions with scattering objects. Waves interfere with one another and produce the familiar diffraction patterns according to the number of scatterers through which it interacts. These scatterers may be

objects or slits where even a single slit will produce a diffraction pattern as Young showed, to definitely prove the wave nature of light. The diffraction of light becomes most pronounced when the objects are on same order of size as the wavelength of the interacting wave. Figure 1.3 shows two intersecting wave fronts. The intensity of the wave fronts which intersect the wave peaks (blue intersections) will add together as constructive interference; while opposite wave fronts, peaks and valleys (a blue and a white) will cancel one another out.

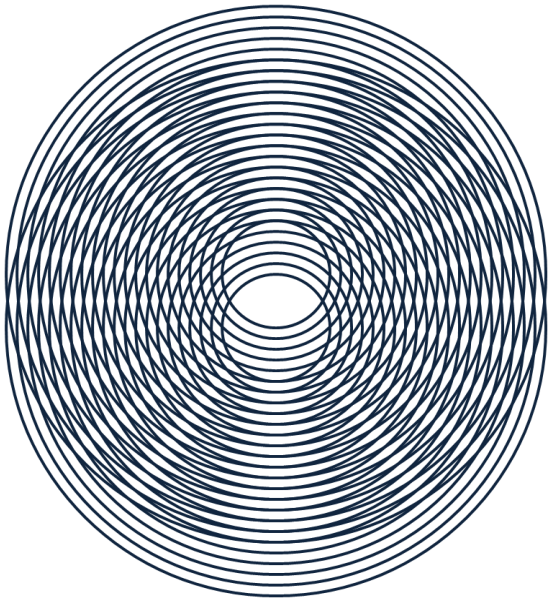

Figure 1.3 Diffraction patterns of two intersection circular wave patterns.

While most photons incident on a medium are elastically scattered, Raman scattered light occurs as a result of a change in vibrational, rotational or electronic energy. The total number of atoms or molecules scattering through Raman processes is small compared to the number scattering through Rayleigh or Mie process.

Fluorescence is a result of radiation absorbed at one wavelength followed by an emission of radiation at a different wavelength. The differences between the absorbed radiation and the emitted radiation are dissipated through vibrational or thermal processes. Materials that fluoresce include both organic and inorganic materials and are used extensively biomedical applications.

It is by the light—matter interaction that a material is characterization. These interactions yield information about the atomic and molecular structure, as well as the

electronic and optical properties of the material medium. An understanding of the fundamental properties of a material and its behavior in the presence of radiation allow for the material's use in a variety of applications. One such application is the fabrication and use in nanophotonic devices.

1.2 Nanophotonics

Nanophotonics is an emerging field of study that encompasses the disciplines of physics, engineering, chemistry, biology, applied sciences and biomedical technology. In particular, nanophotonics is the exploration of optical processes on a nanoscale. The investigations in this field can be placed into three categories: (1) nanoscale confinement of radiation; (2) nanoscale confinement of matter; and (3) nanoscale photophysical or photochemical transformation.[2] The first two categories define the field of nanomaterials, while the last is based on nanofabrication of photonic structures.[3] The field of nanophotonics is rather young in relation to other fields of study but will play an increasingly predominant role in future research and development.

1.3 Overview of Dissertation

This dissertation will present nanophotonic applications that incorporate various forms of N-isopropylacrylamide (NIPA). The information contained in the dissertation can be broken into four categories: (1) optical and physical properties NIPA; (2) low dimensional semiconductors; (3) tunable photonic crystals; and (4) historical development. The light interactions of matter discussed above are used in characterizing the devices incorporating the NIPA hydrogel.

Chapter 2 describes the physical properties of hydrogel and its response to various stimuli. This chapter is vital in understanding the following chapters as the optical

properties and applications are discussed. For example the process and mechanics of undergoing a volumetric phase change are foundational in understanding the material characteristics.

Chapter 3 is the first optical characterization section that deals exclusively with dynamic light scattering. Many researchers in the polymer world believe that the process of dynamic light scattering is due to Bragg diffraction. This is erroneous. It is based on scattering of light off individual particles and is shown in derivation format.

Chapter 4 is the second optical characterization section that introduces the concept of a change in refractive index of the material as the NIPA undergoes its phase change. Ellipsometric techniques are used to measure the refractive index at temperatures above and below the critical temperature.

Chapter 5 is the first chapter introducing a device application of the NIPA gel. Low dimensional semiconductors, CdTe quantum dots, are introduced into the pores of the hydrogel. As the NIPA undergoes its phase change, the relative distances between quantum dots change, thereby adjusting the resonant energy transfer between dots.

Chapter 6 is an introduction to photonic crystals including defects, bends and multiplexing. Methods of tuning the photonic bandgap are discussed as a backdrop for tuning via NIPA hydrogel.

Chapter 7 is a chapter based on computer simulations of a tunable photonic crystal incorporating NIPA hydrogel as a tunable refractive index material. The simulations compare the bandgaps for hydrogel in a swollen, low refractive index state to the gaps for the hydrogel in a collapsed high refractive index state.

Chapter 8 is the experimental verification of a photonic crystal incorporating NIPA hydrogel. Transmission experiments were performed to verify the tunability. Further, a discussion of the instrumentation developed for placing the gel inside the photonic crystal and used for characterization are included.

Chapter 9 is a brief summary of the results and their implications and future research directions for projects are discussed.

---

[1] J. Z. Buchwald, *The Rise of the Wave Theory of Light: Optical Theory and Experiment in the Early Nineteenth Century*, ed. (University of Chicago Press, Chicago 1989).

[2] Y. Shen, C. S. Friend, Y. Jiang, D. Jakubczyk, J. Swiatkiewics, P. N. Prasad, "Nanophotonics: Interactions, Materials, and Applications," J. Phys. Chem. **104**, 7577-7587 (2000).

[3] P. N. Prasad, *Nanophotonics*, ed. (Wiley-Interscience, New York 2004) p. 3-8.

CHAPTER 2

ON THE KINETICS OF

VOLUMETRIC HYDROGEL PHASE TRANSITIONS

2.1 Introduction to N-Isopropylacrylamide

The unique properties of NIPA gels, such as being water based and compatible with biological systems, have been of great interest in the biomedical industry for applications such as controlled drug delivery[1], artificial muscles, cell adhesion mediators[2], precipitation of proteins,[3] and chromatography.[4] These 'smart' polymers[1] respond to external physical environmental stimuli such as temperature[5], pH[6], electric field[7], magnetic field[8], light, salt and organic solvents.[9] Further these gel polymers may also respond to biomolecules such as glucose[10] and proteins.[11] Although biomedical applications are the most extensively studied, NIPA gels have other applications such as sensors, shape memory, tunable optics,[12] and molecular imaging[13].

The functionality and versatility of the hydrogel is derived from its ability to change shape and respond to many different stimuli. Hydrogels comprise randomly cross-linked

---

[1] The Maya are believe to be the first civilization to find an application for polymers. British explorers in the 1500's discovered that the Maya made rubber balls for their children from local rubber trees. [D. Hosler, S. Burkett, M. J. Tarkanian, "Prehistoric Polymers: Rubber Processing in Ancient Mesoamerica," *Science* **284**, 1988-1991 (1999)]. The first modern use was by Charles Goodyear when he combined natural rubber with sulfur at 270°C to create vulcanized rubber which is used extensively in today's automobile tires. [Charles Goodyear, Patent No. 240, "Improvement in the Process of Divesting Caoutchouc, Gum-Elastic, or India-Rubber of its Adhesive Properties, and Also of Bleach the Same, and Thereby adapting it to Various Useful Purposes, (June 17, 1873)]. The first artificial polymer was made by Leo H. Baekeland, in 1907. Bakelite was formed by mixing carbolic acid with formaldehyde and is used as an electrical insulator because of its hardness and high heat resistivity. [Leo Hendrick Baekeland, *Chemical Achievers: The Human Face of the Chemical Sciences*, Chemical Heritage Foundation, Accessed March 2008)]. In 1917, Michael Polanyi, employed x-ray diffraction to study polymers and in 1923 proposed a structure of long-chains with high molecular weight. [M. J. Nye, "Michael Polanyi (1891-1976)," *Inter. J. Phil. Chem.* **8**, 123-127 (2002)]. Finally in 1920, Staudinger proposed that polymers were made of long chains comprised of shirt repeating molecular units lined by covalent bonds. [H. Staudinger, "Über Polymerization," *Ber. Deut. Chem. Ges.* **53**, 1073 (1920)]. This idea ushered in molder polymer science.

polymer chains with water filling interstitial spaces of a formed network.[14] Using the molecular weight and the relation between the interpenetration function and expansion coefficients, it has been shown that the NIPA polymer molecules act as a flexible coil.[15]

These flexible coils can form two different varieties of the gel, a micro- or nano-spherical form (figure 2.1) and a bulk form (figure 2.2). The optical properties are such that while the bulk hydrogel is swollen with water in is typically clear but upon undergoing a volumetric phase transition the bulk gel becomes opaque. Figure 2.3 shows a photo of the bulk for below LCST and above LCST. The apparent change in opacity of the bulk gel is easily seen while that of the microgel, nano-particle form is less easy to observe due to size.

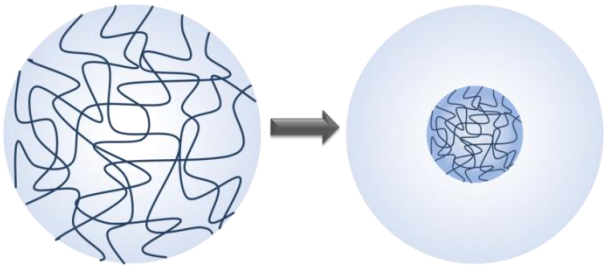

Figure 2.1 poly(N-isopropylacrylamide) microspheres in a hydrophilic state below LCST and in a hydrophobic state above LCST.

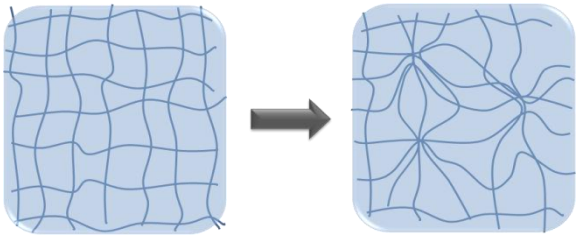

Figure 2.2 Bulk NIPA hydrogel in a network structure below LCST and the collapse gel above LCST.

Poly-N-isopropylacrylamide (PNIPA) gel systems exhibit strong temperature dependent characteristics; in particular, they exhibit a sharp volume phase transition at a critical temperature. Below the lower critical solution temperature (LCST), polymer chains are hydrophilic and swollen with water and remain swollen until heated beyond the critical temperature. Once the critical temperature has been attained the gel undergoes a discontinuous phase transition whereby the polymer chains become hydrophobic, decreasing in length causing the water to be expelled from the network. The process is

reversible, whereby lowering the temperature below the LCST reverses the transition causing the hydrogel to become swollen again with water.

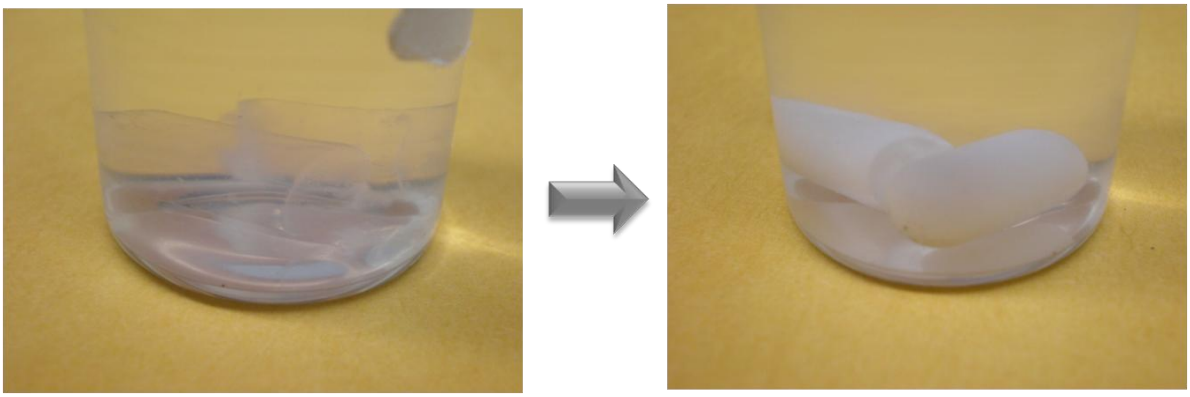

Figure 2.3 The photo to the right shows the bulk NIPA below 34°C, while the right photo shows the gel above 34°C.

2.2 Historical Development of Hydrogel

Materials having the ability to deform and then recover their original form have been studied extensively over the past century. This ability to deform and recover from 'extensive and prolonged deformation' is a significant feature of hydrogels.[16]

In 1942, Flory and Rehner began studying interactions between solvents and cross-linked network structures, and subsequently developed a statistical mechanical treatment.[17] The interaction of the solvent is expressed as function of two variables: (1) its concentration in the swollen network; and (2) the degree of cross-linking.[18] A gel in a solvent has a maximum swelling volume, related to the degree of cross-linking. Flory goes on to show that the interaction between the solvent and the network may be calculated from the temperature coefficient of maximum swelling. Flory's original statistical treatment used Gaussian distributions of polymer chains, which was later refined to account for large concentrations of cross-linking.[19] Huggins also devolved a similar

treatment concurrently with Flory.[20] Subsequently, the theory has come to be known as Flory-Huggins theory or Flory-Rehner Theory.

Dušek and Patterson, first predicted the collapse of polymer networks using the mean-field treatment of gel network systems in FH theory.[21] They predicted the phase would change between dense and dilute states via a volume transition.

Kuhn, first reported in 1950, experimentally measured volume changes in poly-acrylic acid and poly-methylacrylate acid gels.[22] Then in 1973, polyacrylamide-based hydrogels became of interest because of their 'half-liquidlike' and 'half-solidlike' material properties.[23] This particular gel maintained a crystal type rigid structure when stationary but when subjected to a shear force it deformed easily. The properties of the gel were explained as frictional forces between the liquid-solvent and the fibers comprising the polymer network. Using Flory's statistical treatment Tanaka explained the local motion of a polymer network with a diffusion equation where the diffusion coefficient was defined by the ratio of the elastic modulus of the network, to the frictional coefficient, between the network and the fluid.[24]

Tanaka's continued work, on polyacrylamide gels, produced studies on the temperature dependent network density fluctuations, using the intensity and correlation time of laser light experiments.[25] The gel consisted of a network of covalently cross-linked polyacrylamide polymers in an acetone-water mixture.[26] A theoretical treatment of density fluctuations of network density, using mode-coupling theory, was calculated using the elastic constant of the network and a frictional coefficient between the network and solvent.[27] The theoretical framework explained the experimental results of the light scattering measurement.

In 1979, Tanaka, demonstrated that the characteristic time of swelling is proportional to the square of the linear dimension of the gel and proportional to the diffusion coefficient of the gel network.[28] It was established that the swelling of the hydrogel is related to the diffusion of the polymer network in the solution instead of the solution into the polymer network. This recognized a difference of understanding from previous theories where the assumption was that the swelling time is determined by the diffusion coefficient of the fluid molecules. The diffusion coefficient is defined as

$$D = \frac{E}{f} \tag{2.1}$$

where E represents the longitudinal bulk modulus of the network and f represents the coefficient of friction between the network and solution.

Pelton and Chibante produced the first N-isopropylacrylamide microgels (spherical form), in 1986, with gel diameters of approximately 1μm.[29] The precipitation polymerization method used by Pelton was similar to the surfactant-free emulsion polymerization of styrene. The monomer and cross-linker were heated above LCST, to approximately 70°C, when an initiator was added causing the polymer chains to form. While this formation is occurring the polymer chains aggregate and are cross-linked into micro-particles that are stabilized by electrostatic and steric forces.[30] The micro-particles have a narrow size distribution, which have similar properties as the bulk gel such as the ability to undergo a sharp volumetric phase transition.

2.3 Volumetric Phase Transition Interactions

The phase transitions of macromolecules can be controlled by four main interactions: ionic, hydrophobic, van der Waals and hydrogen bonding.[31] These

interactions can be understood by observing the phase transitions in polymer gels. The volumetric transition is not unique to NIPA gel but general to all kinds of polymer networks.[32] The volumetric phase change of the NIPA gel are a consequence of the competition between repulsive intermolecular forces seeking to expand the network and an attractive force that acts to shrink the polymer.[33] Hydrogels comprise an elastic cross-linked polymer network and a fluidic solvent, filling interstitial space between the network fibers. The volumetric phase transition of hydrogel gel exhibits critical kinetic behavior near a critical point where the transition time goes to infinity. The volume transition is caused by interactions within the medium result in a coil—globule transition for a macromolecule polymer network in a dilute medium.[34] This coil—globule transition was first observed for a single temperature dependent polystyrene polymer chain which exhibited a low density state and a high density state.[35] The polymer interactions are a result of repulsive and attractive forces, which serve to expand or collapse the gel network.

2.3.1 Ionic Interactions

When a gel undergoes a volumetric phase transition it may do so by a continuous phase transition, or a first order discontinuous transition. The continuity of the transition is determined by the proportion of ionizable groups incorporated into the polymer network and the stiffness of the polymer chains comprising the network.[36] The higher the ionization of the groups, the greater the volume will change over a discontinuous transition.[37] There are several ways ionized polymer networks are created.

First, copolymerization of ionizable molecules placed into the network creates a discontinuous transition.[38] The discontinuous transition occurs when the counter-ions to the ionized groups and the stiffness of the polymer chains increase the osmotic pressure to

expand the polymer network. This process is similar to a gas-liquid transition dependent on an applied external pressure, which determines whether the transition is continuous or discontinuous. The conditions for creating a gel with a discontinuous phase change became more apparent when the swelling of hydrogel and a number of its ionized forms are measured as a function of temperature.[39] The nonionic NIPA hydrogels exhibited a sharp but continuous volumetric phase change. However, when a small concentration of ionizable groups is incorporated into the gel the phase change became discontinuous.

The second and third methods are similar in that ions are produced in the network group. First, hydrolysis may be used to produce charges in water or solvent electrostatically.[40] Secondly, ultraviolet light may be used to initiate an ionizing reaction in the gel, resulting in an internal osmotic pressure, thus inducing swelling.[41] When the UV light is removed the equilibrium moves toward the neutral polymer system causing the gel to collapse. Harrington et al. 1986, reported a reversible photoresponsive acrylamide gel in an electric field, where a rod shaped gel bent at a rate of 0.40 mm/s and 0.075 mm/s in the reverse bias.[42] The process is slow because it is dependent upon photochemical ionization and recombination of ions. Visible light is another option for light induced effects where hydrophobic interactions are predominant. The transition is induced by the heating of network polymers with visible light, and thus avoids the slow ionization processes.[43]

2.3.2 Hydrophobic Interactions

Interactions between non-polar molecules and polar molecules in a solvent, such as water, create a hydrophobic transition mechanism.[44] The interaction is a result in the difference in the Hammaker constants between the particle and solvent.[45] The water

molecules arrange themselves in an order considered to be 'tightly bound' water.[46] As the temperature of the system increases, the 'tightly bound' water molecules become less bound and around the hydrophobic groups. This decrease in molecular interactions increases the hydrophobic interaction as the temperature increases.

Adding molecules, which form hydrates, may weaken hydrophobic interactions in the gel network.[47] Molecules, which form hydrates in water, include alcohol[48], Me_2SO (dimethyl sulfoxide)[49], and DMF (dimethyl formamide). For example, a gel swollen in pure water will exhibit a reentrant behavior as an external stimulus is varied monotonically.[50] Consider a NIPA gel that gradually shrinks as Me_2SO is added to the gel, until the concentration reaches a critical value causing the gel to undergo a discontinuous volume change. However, if the concentration of Me_2SO continues to increase the gel undergoes a second first order discontinuous volumetric phase change, rewselling into its expanded state. Further, the hydrophobic interaction may be modified with the addition of surfactants.

2.3.3 van der Waals Interactions

A phase transition controlled by van der Waal forces is achieved by adding solvents, which reduce other interactions. Typically, van der Waal interactions are minimized when a gel is engineered to react to other stimuli such as temperature.[51] This interaction is dominant when the hydrophilic interactions of polymers and solvent are overcome by chain-chain attraction.[52]

2.3.4 Hydrogen Bonding Interactions

The last dominant attractive interaction in gel network systems is hydrogen bonding. Investigations of the balance between hydrophilic and hydrophobic states of

NIPA networks showed a dependence on size, configuration and mobility of alkyl side chains on substituted acrylamides.[53] Okano, who studied many different gels, found that only N-isopropylacrylamide showed a sharp phase transition of the gel network.

In 1991, Ilmain et al. developed a NIPA gel, which exhibited a phase transition as a result of hydrogen bonding, by slightly ionizing the gel of Okano.[54] Cooperativity between molecules provided the necessary interaction beyond the hydrogen bonds to yield a phase transition. This cooperativity or 'zipping' effect plays a crucial role in enhancing the attractive interaction. The unique feature of this particular gel was the volumetric phase change in swelling was induced by increasing rather than decreasing the temperature.

In regards to the microsphere poly(N-isopropylacrylamide) hydrogel, the hydrogen bonding interaction is paramount. Currently it is believed that the hydrogen bonding interactions form stable hydration shells around the hydrophobic groups of PNIPA. When the temperature is increased above LCST, the hydrophobic interactions between polymer chains increase, thus expelling the water.[55]

2.4 Flory-Huggins Theory

Although Tanaka used FH theory to model the behavior of the NIPA gel, on closer examination modifications have been required. The FH free energy of a gel is

$$\frac{\Delta}{\nu k_B T} = N\frac{1-\varphi}{\varphi}[\ln(1-\varphi)+\chi\varphi] + \frac{1}{2}\left[\alpha_x^2+\alpha_y^2+\alpha_z^2-\ln\left(\alpha_x\alpha_y\alpha_z\right)\right] + f\ln\varphi, \quad (2.2)$$

where k_B is the Boltzmann constant, T is the absolute temperature, φ is the volume fraction of polymer, the total number of chains is represented by ν, N is the total number of persistent units, χ is the reduced chain-solvent interaction energy, α_i is the linear swelling ration along the ith direction, and f is the number of ionized groups per chain.[56]

Typically experiments are carried out where the osmotic pressure, π, in the gel is held at a constant zero,

$$\pi = \varphi^2 \left(\frac{\partial \mu}{\partial \varphi}\right) = 0. \tag{2.3}$$

Defining the several variables, t, ρ, and S as

$$t \equiv \frac{(1-\chi)(2f+1)^{\frac{3}{2}}}{2\varphi_o} \tag{2.4}$$

$$\rho \equiv \left(\frac{\varphi}{\varphi_o}\right)(2f+1)^{3/2}, \tag{2.5}$$

and

$$S \equiv \left(\frac{vv}{N\varphi^3}\right)(2f+1)^4, \tag{2.6}$$

the expansion of the FH free energy[57] may be written as

$$t = S\left(\rho^{-5/3} - \frac{\rho^{-1}}{2}\right) - \frac{\rho}{3}. \tag{2.7}$$

This equation gives us the isobar in a single equation with only one adjustable parameter S, determining the continuity. If S has a value larger than a critical value S_0 the transition becomes discontinuous while a value of S is below the critical value the transition will be continuous. The critical point of the FH free energy equation is given by

$$\frac{\partial t}{\partial \rho} = \frac{\partial^2 t}{\partial \rho^2} = 0. \tag{2.8}$$

Unfortunately, when the critical value for NIPA gel is calculated, the theory predicts a continuous phase transition, counter to experimental evidence of a discontinuous transition. Oversimplification in the basic FH theory causes a failure predict a discontinuous transition for NIPA gel by neglecting such variables as defects within the gel

network, where large deformations are absorbed by a small number of chains. Li and Tanaka introduce the parameter σ to account for the fraction of chains that deform under the volume transition.[58] Later, an empirically modified FH theory was developed to account for the relations between the number of segments between junction points and the monomer concentration.[59] These empirical formulations extend FH theory to the transition of microgel nano-particles and have been shown to agree with experimental data.[60]

2.5 Kinetics of Volumetric Phase Transitions

The viscoelastic interactions of the gel polymer elasticity and friction between the network and the solvent determine the kinetic behavior of swelling and shrinking. The first theory of shrinking and swelling gel networks was derived from the theory of elasticity to describe experimental results gathered from light scattering experiments.[61] The equation of motion of the network according to Tanaka and Filmore is

$$f\frac{\partial \boldsymbol{u}(\boldsymbol{r},t)}{\partial t} = \nabla \cdot \overleftrightarrow{\sigma}, \tag{2.9}$$

where $\boldsymbol{u}(\boldsymbol{r},t)$ is the displacement vector of the network and f is the frictional coefficient between the network and solvent, the stress tensor $\overleftrightarrow{\sigma}$, is given by

$$\sigma_{ik} = K\nabla \cdot \boldsymbol{u}(\boldsymbol{r},t)\delta_{ik} + 2\mu\left(u_{ik} - \frac{1}{3}\nabla \cdot \boldsymbol{u}(\boldsymbol{r},t)\delta_{ik}\right), \tag{2.10}$$

and the strain tensor is defined as

$$u_{ik} = \frac{1}{2}\left(\frac{\partial u_i}{\partial x_k} + \frac{\partial u_k}{\partial x_i}\right). \tag{2.11}$$

Later, with the assumptions that the shear modulus of the gel is negligible compared with the osmotic bulk module, this theory was applied to spherical gels.[62] With these assumptions, Tanaka reported that the relaxation time of the gel network was proportional

to the square of the linear size and inversely proportional to the collective diffusion constant of the network. However, most gels have a shear modulus of the same order of magnitude as the bulk modulus.[63] The theory was then generalized to include solutions for infinitely long cylinders, and disks having infinite diameters.[64] The motion of a network chain during the process of swelling or deswelling, as described by Tanaka and Filmore can be written as

$$\frac{\partial \boldsymbol{u}(\boldsymbol{r},t)}{\partial t} = D_0 \nabla^2 \boldsymbol{u}(\boldsymbol{r},t) + \frac{1}{f}\left(K + \frac{\mu}{3}\right) \boldsymbol{\nabla} \times (\boldsymbol{\nabla} \times \boldsymbol{u}), \tag{2.12}$$

where $\boldsymbol{u}(\boldsymbol{r},t)$ is the displacement vector measured from the final equilibrium state.[65] The collative diffusion coefficient is given by

$$D_0 = \frac{1}{f}\left(K + \frac{4}{3}\mu\right). \tag{2.13}$$

The cross term in the equation of motion is zero for symmetrical geometries such as spheres, long cylinders, and large disks.[66]

These early theories ignored the polymer interaction with the solvent medium. The motion of the gel is controlled by the solvent, which seeks to minimize the total energy of the system, and over-damps the network motion, resulting in a diffusion-like relaxation.[67]

What has become known as LT theory (Li and Tanaka) solves this by defining a dimensional quantity d_i that accounts for each orthogonal direction in which the gel may swell (i.e. a disk is defined by $d_i = 1$, a cylinder by $d_i = 2$ and a sphere $d_i = 3$).[68] The swelling of the gel will be fastest along the orthogonal directions, assuming the swelling process is solely a diffusion process, and given that the relaxation time of a diffusion process is proportional to the square of the length scale. The gel swelling will cause anisotropic deformation at the cost of shear energy. This requires an additional term to

minimize the overall shear energy during the kinetic process. The change in volume caused by the diffusion occurring only in the d_i directions is redistributed to the remaining dimensions $d - d_i$ through shear processes. The redistribution, thus, reduces the rate of diffusion in the allowed d_i direction.

A more complete description of the displacement vector can be made by considering first a purely network diffusion process using a collective diffusion process with zero solvent velocity and second considering the movement of the solvent together with the network. To accomplish this LT theory writes the displacement vector using two operators, one to describe the shear energy relaxation, $\boldsymbol{S}(\boldsymbol{r}, i)$, and the other the diffusion process, $D(\boldsymbol{r}, 0)$.

$$\boldsymbol{u}(\boldsymbol{r}, t) = \left[\prod_i \boldsymbol{S}(\boldsymbol{r}, i) \cdot D(\boldsymbol{r}, 0)\right] \boldsymbol{u}(\boldsymbol{r}, 0) \tag{2.14}$$

where the index $i = 1, 2, 3 \ldots \infty$ characterizes steps of time (i.e. $t = i\Delta t$). LT theory describes the diffusion constant with three terms: (1) the time; (2) the position within the gel; (3) the shape of the gel. Making use of the dimensional quantity the diffusion constant becomes

$$D_e = D_d \frac{d_d}{d}$$

where d is the total number of dimension ($d = 3$ a spherical gel particle). The fractional reductions of the different diffusion constants are thus, $1/3$ for a disk, $2/3$ for a cylinder and $3/3$ for a sphere.

LT theory seeks to describe the swelling of a gel at the boundary by separating the motion of the network and solvent from the diffusion process. Others have sought to directly solve the coupled equations of motion for a network and solvent for specific cases

such as a long cylinder or large disk.[69] These later papers further refine the basic fractional reductions with additional terms to account for specific geometries and more closely relate to experimental data.

A gel undergoing a discontinuous volume transition will approach a critical point where the bulk elastic modulus K becomes zero and the relaxation time approaches infinity.[70] This phenomena was first observed in 1977 by Tanaka et al.[71] The bulk elastic modulus, K, shear modulus, μ, and coefficient of friction, f, are no longer constants but functions of time that change as the discontinuity is approached.[72]

2.6 Preparation of N-isopropylacrylamide Gels

Hydrogels may be prepared in three different forms, bulk, nano-particle or micro-particle. The bulk form is easily made and easy to handle but reacts slowly to external stimulation. The micro-particle and nano-particle react very quickly to external stimuli because of their size but are more difficult to prepare and handle. The three forms may be prepared through three different methods. The first method requires the co-polymerization of two different monomers.[73, 74] The second method requires the forming of inter-penetrating polymer networks.[75] Lastly, hydrogels may be prepared by creating networks with micro-porous structures.[76]

2.6.1. Bulk Form

The NIPA gel was prepared using free radical polymerization.[77] A mixture of mixture of 7.8 g of N-isopropylacrylamide (Kodak, Co.), 133 mg of methylene-bis-acrylamide as cross-linker, tetra-methyl-ethylene-diamine (240 μl) as accelerator, and sodium acrylate (SA), ionic group, were dissolved in 100 ml of deionized and distilled

water. Nitrogen gas was bubbled through the solution to remove dissolved oxygen. Then ammonium persulfate (40 mg) as an initiator was added to the solution.[78]

2.6.2 Micro-particle Form

The preparation of the micro-particle form, poly(N-isopropylacrylamide) or PNIPAM, includes the insertion of quantum dots for photonic applications of the hydrogel. This is a multi step process consisting of (1) PNIPAM particle synthesis; (2) CdTe nanocrystal preparation; and (3) encapsulation of nanocrystals in PNIPAM micro-spheres.[79]

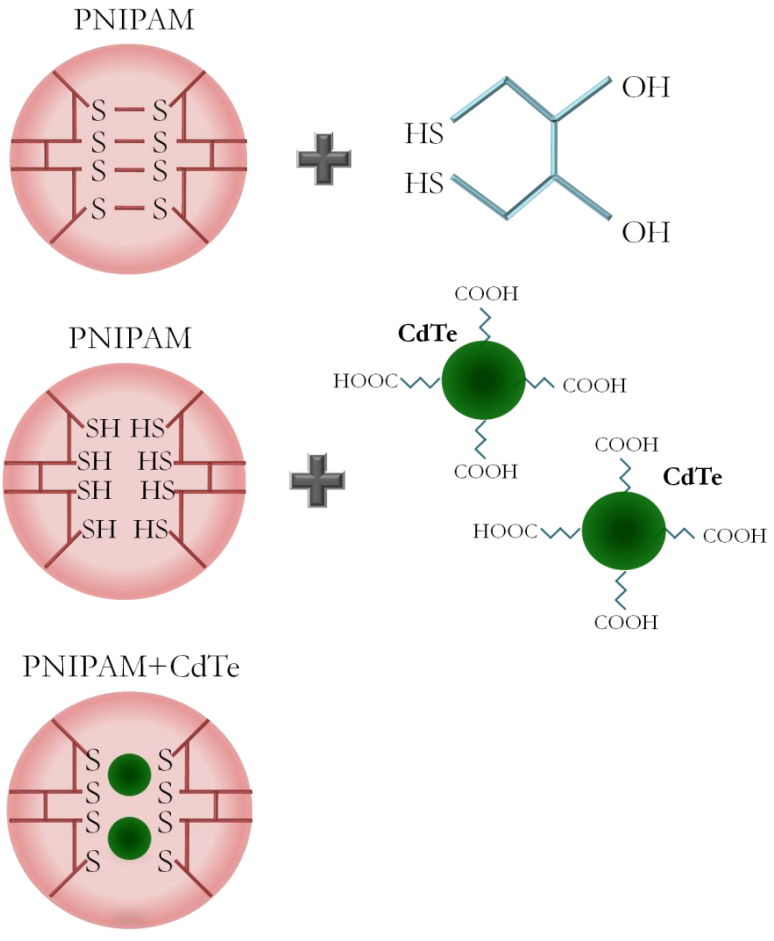

Figure 2.3 A depiction of the steps to encapsulate CdTe quantum dots within PNIPAM.

Poly-N-isopropylacrylamide (PNIPAM) particles were synthesized by mixing NIPA monomer, N(3-aminopropyl) methylacrylamide chloride monomer, methylene bisacrylamide and N,N-Cysteine-bisacrylamide in deionized water.

A hybrid material comprised of PNIPAM and CdTe was made. Cadmium Teluride (CdTe) nanocrystals were synthesized from sodium hydrogen telluride (NaHTe).

Cd(ClO4)2..6H2O with proper pH adjustment. Quantum dot sizes of 2 nm (green) and 4 nm (red) were of particular interest, as the emission wavelength of the resultant fluorescence is dependent on the physical dimensions of the quantum dot. The CdTe nanocrystals were then encapsulated inside the PNIPAM spheres. A basic schematic is shown in figure 2.3.

---

[1] A. Kikuchi, T. Okano, "Pulsatile drug release control using hydrogels," Adv. Drug Deliv. Rev. **54**, 53 (2002).

[2] M. Yamato, C. Konno, M. Utsumi, A. Kikuchi, T. Oano, "Thermally responsive polymer-grafted surfaces facilitate patterned cell seeding and co-culture," Biomaterials. **23**, 561 (2002).

[3] S.R. Carter and S. Rimmer "Aqueous compatible polymers in bionanotechnology," IEE Proc.-Nanobiotechnol. **152**, 169 (2005).

[4] J. Gao, B. J. Frisken, "Cross-Linker-Free N-Isopropylacrylamide Gel Nanospheres," Languir **19**, 5212-5216 (2003).

[5] Yamashita, K., O. Hashimoto, T. Nishimura, M. Nango, "Preparation of stimuli-responsive water absorbent," React. Funct. Poly. **51**, 61 (2002).

[6] Caykara T., C. Ozyurek, O. Kantoglu, O.J. Guven, "Equilibrium swelling behavior of pH- and temperature-sensitive poly(N-vinyl 2-pyrrolidone-g-citric acid) polyelectrolyte hydrogels," Polym. Sci. B **38**, 2063-2071 (2000).

[7] T. Tanaka, I. Nishio, S. Sun, S. Nisho, "Collapse of Gels in an Electric Field," Science **218**, 467-469 (1982).

[8] M. Zrìnyi, "Intelligent polymer gels controlled by magnetic fields," Colloid Poly. Sci. **278**, 98-103 (2000).

[9] Y. Qui, K. Park, "Environment-sensitive hydrogels for drug delivery," Adv. Drug Delivery Rev. **54**, 321-339 (2002).

[10] K. Kubota, S. Fujishige, I. Ando, "Solution properties of poly(N-isopropyl-acrylamide) in water," Polym. J. **22**, 15-20 (1990).

[11] T. Miyata, T. Uragami, K. Nakamae, "Biomolecule-sensitive hydrogels," Adv. Drug Delivery Rev. **54**, 79-98 (2002).

[12] J. Kim, M.J. Serpe, A.L. Lyon, "Hydrogel Microparticles as Dynamically Tunable Microlenses," J. Am. Chem. Soc. **126**, 9512-13 (2004).

[13] R. Apkarian, E. R. Wright, V. A. Seredyuk, S. Eustis, L. A. Lyon, V. P. Conticelo, F. M. Menger, "In-Lens Cry-High Resolution Scanning Electron Microscopy: Methodologies for Molecular Imaging of Self-Assembled Organic Hydrogels," Microsc. Microanal. **9**, 286-295 (2003).

[14] Z. Hu, X. Lu, J. Gao, "Hydrogel Opals," Adv. Maters. **13**, 1708-1712 (2001).

[15] K. Kubota, S. Fujishige, I. Ando, "Solution properties of poly(N-isopropyl-acrylamide) in water," Polym. J. **22**, 15-20 (1990).

[16] A. T. Walter, "Elastic Properties of Polvinyl Chloride gels," J. Poly. Sci. **8**, 207-228 (1954).

[17] P. J. Flory, "Thermodynamics of High Polymer Solutions," J. Chem. Phys. **10**, 51-61 (1942).

[18] P. J. Flory, J. Rehner Jr., "Statistical Mechanics of Cross-Linked Polymer Networks II. Swelling," J. Chem. Phys. **11**, 521-526 (1943).

[19] P. J. Flory, "Statistical Mechanics of Swelling of Network Structures," J. Chem. Phys. **18**, 108-111 (1950).

[20] M. L. Huggins, "Solutions of Long Chain Compounds," J. Chem. Phys. **9**, 440 (1941).

[21] K. Dušek, D. Patterson, "Transition in Swollen Polymer Networks Induced by Intramolecular Condensation," J. Polym. Sci. **6**, 1209-1216 (1968).

[22] W. Kuhn, B. Hargitay, A. Katchalsky, H. Eisenberg, "Reversible Dilation and Contraction by Changing the State of Ionization of High-Polymer Acid Networks," Nature **165**, 514-516 (1950).

[23] T. Tanaka, L. O. Hocker, G. B. Benedek, "Spectrum of light scattered from a viscoelastic gel," J. Chem. Phys. **59**, 5151-5159 (1973).

[24] T. Tanaka, L. O. Hocker, G. B. Benedek, "Spectrum of light scattered from a viscoelastic gel," J. Chem. Phys. **59**, 5151-5159 (1973).

[25] T. Tanaka, S. Ishiwata, C. Ishimoto, "Critical Behavior of Density Fluctuations in Gels," Phys. Rev. Lett. **38**, 771-774 (1977).

[26] T. Tanaka, "Collapse of Gels and the Critical Endpoint," Phys. Rev. Lett. **40**, 820-823 (1978).

[27] T. Tanaka, "Dynamics of critical concentration fluctuations in gels," Phys. Rev. A **17**, 763-766 (1978).

[28] T. Tanaka, D. J. Fillmore, "Kinetics of swelling of gels," J. Chem. Phys. **70**, 1214-1218 (1979).

[29] R. H. Pelton, P. Chibante, "Preparation of aqueous lattices with N-isopropylacrylamide," Colloids and Surf. **20**, 247-256 (1986).

[30] J. Gao, B. J. Frisken, "Cross-Linker-Free N-Isopropylacrylamide Gel Nanospheres," Langmuir **19**, 5212-5216 (2003).

[31] F. Ilmain, T. Tanaka, E. Kokufuta, "Volume transition in a gel driven by hydrogen bonding," Nature **349**, 400 (1991).

[32] T. Amiya, T. Tanaka, "Phase Transitions in Cross-Linked Gels of Natural Polymers," Macromolecules **20**, 1162-1164 (1987).

[33] T. Tanaka, E. Sato, Y. Hirokawa, S. Hirotsu, J. Peetermans, "Critical Kinetics of Volume Phase Transition of Gels," Phys. Rev. Lett. **55**, 2455 (1985).

[34] I. Nisho, G. Swislow, S. –T. Sun, T. Tanaka, "Critical density fluctuations within a single polymer chain," Nature **300**, 243-244 (1982).

[35] G. Swislow, S. –T. Sun, I. Nisho, T. Tanaka, "Coil-Globule Phase Transition in a Single Polystyrene Chain in Cyclohexane," Phys. Rev. Lett. **44**, 796-798 (1980).

[36] Y. Hirokawa and T. Tanaka, "Volume phase transition in a nonionic gel," J. Chem. Phys. **81**, 6379-6380 (1984).

[37] Y. Li, T. Tanaka, "Phase Transitions of Gels," Annu. Rev. Mater. Sci. **22**, 243-277 (1992).

[38] S. Hirotsu, Y. Hirokawa, T. Tanaka, "Volume-phase transitions of ionized N-isopropylacrylamide gels," J. Chem Phys. **87**, 1392-1395 (1987).

[39] S. Hirotsu, Y. Hirokawa, T. Tanaka, "Volume-Phase transitions of ionized N-isopropylacrylamide gels," J. Chem. Phys. **87**, 1392-1395 (1987).

[40] M. Ilavsky, "Phase transition is Swollen Gels. 2. Effect of Charge Concentration on the Collapse and Mechanical Behavior of Polyacrylamide Networks," Macromolecules **15**, 782-788 (1982).

[41] A. Mamada. T. Tanaka, D. Kungwatchakun, M. Irie, "Photoinduced Phase Transistion of Gels," Macromolecules **23**, 1517-1519 (1990).

[42] M. Irie, "Photoresponsive Polymers. Reversible Bending of Rod-Shaped Acrylamide Gels in an Electric Field," Macromolecules **19**, 2890-2892 (1986).

[43] A. Suzuki, T. Tanaka, "Phase transition in polymer gels induced by visible light," Nature **346**, 345-347 (1990).

[44] H. B. Lee, M. S. Jhon, J. D. Andrade, "Nature of water in synthetic hydrogels. I Dilatometry, specific conductivity, and differential scanning calorimetry of polyhydroxyethyl methacrylate," J. Colloid Interface Sci. **51**, 225-231 (1975).

[45] J. Wu, B. Zhou, Z. Hu, "Phase Behavior of Thermally Responsive Microgel Colloids," Phys. Rev. Lett. **90**, 48304 (2003).

[46] A. Takizawa, T. Kinoshita, O. Nomura, Y. Tsujita, "Characteristics of Water in Copoly(methyl methacrylate—N—vinylpyrrolidone) Membranes," Polym. J. **17**, 747-752 (1985).

[47] T. Amiya, Y. Hirokawa, Y. Hirose, Y. Li, T. Tanaka, "Reentrant phase transition of N-isopropylacrylamide gels in mixed solvents," J. Chem Phys. **86**, 2375-2379 (1987).

[48] S. Hirotsu, "Phase Transition of a Polymer Gel in Pure and Mixed Solvent Media," J. Phys. Soc. Jpn. **56**, 233-242 (1987).

[49] K. Otake, H. Inomata, M. Konno, S. Saito, "Thermal Analysis of the Volume Phase Transition with N-Isopropylacrylamide Gels," Macromolecules **23**, 283-289 (1990).

[50] S. Katayama, Y. Hirokawa, T. Tanaka "Reentrant Phase Transition in Acrylamide-Derivative Copolymer Gels," Macromolecules **17**, 2641-2643 (1984).

[51] C. L. A. Berli, D. Quemada, "Prediction of the Interaction Potential of Microgel Particles from Rheometric Data. Comparison with Different Models," Langmuir **16**, 10509-10514 (2000).

[52] Y. Li, T. Tanaka, "Phase Transitions of Gels," Annu. Rev. Mater. Sci. **22**, 243-277 (1992).

[53] T. Okano, Y. H. Bae, H. Jacobs, S. W. Kim, "Thermally on-off switching polymers for drug permeation and release," J. Conrl. Rel. **11**, 255-265 (1990).

[54] F. Ilmain, T. Tanaka, E. Kokufuta, "Volume transition in a gel driven by hydrogen bonding," Nature **349**, 400 (1991).

[55] V. V. Fernandez, N. Tepale, J. F. A. Soltero, "Thermoresponsive nanostructured poly(N-isopropylacrylamide) hydrogels made via inverse microemulsion polymerization," Colloid. Polym. Sci. **284**, 387-395 (2006).

[56] Y. Li, T. Tanaka, "Phase Transitions of Gels," Annu. Rev. Mater. Sci. **22**, 243-277 (1992).

[57] T. Tanaka, D. Fillmore, S. –T. Sun, I. Nishio, G. Swislow, A. Shah, "Phase Transitions in Ionic Gels," Phys. Rev. Lett. **45**, 1636-1639 (1980).

[58] Y. Li, T. Tanaka, "Phase Transitions of Gels," Annu. Rev. Mater. Sci. **22**, 243-277 (1992).

[59] T. Hino, J. M. Prausnitz, "Swelling equlibria for heterogeneous polyacrylamide gels," J. App. Polym. Sci. **62**, 1635-1640 (1996).

[60] L. Arleth, X. Xia, R. P. Hjelm, J. Wu, Z. Hu, "Volume transition and internal structures of small poly(N-isopropylacrylamide) microgels," J. Polym. Sci. Part B **43**, 849-860 (2004).

[61] T. Tanaka, L. Hocker, G. Benedek, "Spectrum of light scattered from a viscoelastic gel," J. Chem. Phys. **59**, 5151-5159 (1973).

[62] T. Tanaka, D. J. Fillmore, "Kinetics of swelling of gels," J. Chem. Phys. **70**, 1214-1218 (1979).

[63] A. Peters, S. J. Candau, "Kinetics of Swelling Polyacrylamide Gels," Macromolecules **19**, 1952-1955 (1986).

[64] A. Peters, S. J. Candau, "Kinetics of Swelling of Spherical and Cylindrical Gels," Macromolecules **21**, 2278-2282 (1988).

[65] T. Tanaka, D. J. Fillmore, "Kinetics of swelling of gels," J. Chem. Phys. **70**, 1214-1218 (1979).

[66] Y. Li, T. Tanaka, "Kinetics of swelling and shrinking of gels," J. Chem. Phys. **92**, 1365-1371 (1990).

[67] Y. Li, T. Tanaka, "Phase Transitions of Gels," Annu. Rev. Mater. Sci. **22**, 243-277 (1992).

[68] Y. Li, T. Tanaka, "Phase Transitions of Gels," Annu. Rev. Mater. Sci. **22**, 243-277 (1992).

[69] C. Wang, Y. Li, Z. Hu, "Swelling Kinetics of Polymer Gels," Macromolecules **30**, 4727-4732 (1997).

[70] A. Onuki, "Paradox in phase transitions with volume change," Phys. Rev. A **38**, 2192-2195 (1988).

[71] T. Tanaka, S. Ishiwata, C. Ishimoto, "Critical Behavior of Density Fluctuations in Gels," Phys. Rev. Lett. **38**, 771-774 (1977).

[72] T. Tanaka, E. Sato, Y. Hirokawa, S. Hirotsu, J. Peetermans, "Critical Kinetics of Volume Phase Transition of Gels," Phys. Rev. Lett. **55**, 2455-2458 (1985).

[73] Y. H. Bae, T. Okano, S. W. Kim, "'On—Off" Thermocontrol of Solute Transport. I. Temperature Dependence of Swelling of N-Isopropylacrylamide Networks Modified with Hydrophobic Components in Water," Pharm. Res. **8**, 531-537 (1991).

[74] Y. H. Bae, T. Okano, S. W. Kim, "'On—Off" Thermocontrol of Solute Transport. II. Temperature Dependence of Swelling of N-Isopropylacrylamide Networks Modified with Hydrophobic Components in Water," Pharm. Res. **8**, 624-628 (1991).

[75] Y. Qui, K. Park, "Environment-sensitive hydrogels for drug delivery," Adv. Drug Del. Rev. **53**, 321-339 (2001).

[76] B. G. Kabra, S. H. Gehrke, R. J. Spontak, "Microporous, Responsive Hydroxypropyl Cellulose Gels. 1. Synthesis and Microstructure," Macromolecules **31**, 2166-2173 (1998).

[77] T. Tanaka, "Collapse of Gels and the Critical Endpoint," Phys. Rev. Lett. **40**, 820-823 (1978).

[78] G. Huang, J. Gao, Z. Hu, J. V. St. John, B. C. Ponder, D. Moro, "Controlled drug release from hydrogel nanoparticle networks," J. Cont. Rel. **94**, 303-311 (2004).

[79] A. Neogi, S. Ghosh, J. Li, T. Cai, Z. Hu, "Enhanced Luminesence Efficiency from Hydrogel Microbead Encapsulated Quantum Dots," Mater. Res. Soc. Symp. Proc. **959**, 0959-M02-09 (2007).

CHAPTER 3

DYNAMIC LIGHT SCATTERING

3.1 Introduction to Light Scattering

When an electromagnetic wave interacts with a medium, a portion of energy is removed from the incident wave and scattered in all directions. A scattering medium is comprised of scattering units or molecules having a light electronic charge bound to a massive nucleus. The electric field of the incoming EM wave induces an oscillating polarization of the bound charges in the molecules. The molecules with oscillating bound charges radiate the EM field, resulting in scattered light.[1] The size, shape and molecule-molecule interactions may then be determined through study of the polarization, frequency shift, angular distribution, and intensity of the scattered light.

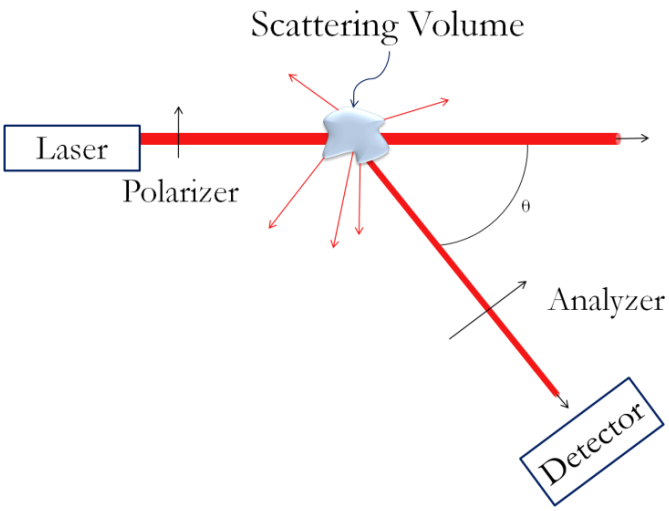

Figure 3.1 A schematic view of a basic scattering experiment.

In determining these quantities the light scattering experiments requires an incident, monochromatic and coherent light source. The scattered incident light can be broadly categorized as an either inelastic or elastic interaction. The inelastic interaction is an absorption process such as Raman, fluorescence and phosphorescence, while in the elastic interaction there is no absorption.[2] In the polymer and colloidal arts, elastic interactions

are referred to as a static measurement and quasi-elastic interactions are dynamic measurements.

In practice, as shown in figure 3.1, a laser is used as the incident light source and scatters in a dilute solution of suspended colloidal particles or macromolecules. The incident light will scatter off the macromolecules given that the refractive index of the solvent and the macromolecules differ.[3] The destructive and constructive interference from each scattering macromolecule are recorded by a detector and are recorded as a net scattered intensity or a photon count. The net scattered intensity will fluctuate with time because of the Brownian motion of the macromolecules in the solvent. The rate of change in the intensity can be related to translational, rotational and internal motions of the macromolecules.

The non-invasive nature of dynamic light scattering has made it a standard measurement in the polymer arts. Commercialized instrumentation have simplified and decreased the time required for the measurement.[4] Employing theoretical electrodynamics and statistical mechanics, the structure and molecular dynamics can be measured in a scattering medium.

3.2 Historical Development of Dynamic Light Scattering

The first experiments conducted on light scattering were performed by Tyndall in 1869 on the light scattering from aerosols.[5, 6, 7] The first theoretical work was done by Lord Rayleigh in describing atmospheric phenomena.[8] The theoretical works involve describing the refractive index of small scattering particles[9] and electromagnetic theory.[10] After these initial papers, Rayleigh explained the blue color of the sky by extended the theory to include assemblies of non-interacting particles with a diameter comparable to the

wavelength of incident light.[11] Rayleigh's final contributions to scattering theory came when he derived a scattering formula for spheres of an arbitrary size and showed a fixed phase relation of scattered waves from different points on the same particle with each element of the particle as an independent dipole oscillator.[12, 13, 14] Scattering theory was further extended by Debye when he performed the calculation for non-spherical particles.[15]

The description of large particles proved to be rather difficult because of fixed spatial relations between scatters and the dependence upon the amplitude of the electric field on the particles position. In 1908, Mie[16] and Debye[17]solved the problem independently for the case for spherical scatterers. This large spherical particle scattering theory now bares Mie's name, as Mie Scattering. Gans extended the theory by considering aspect ratios of the particles rather than well defined dimensions.[18] These studies by Gans involved a suspension of gold particles and silver particles[19] in solution. Later he described the scattering by a large particle in a medium where the ratio of the refractive indices is approximate one.[20]

Out of Rayleigh's scattering theory, fluctuation theory was born. Rayleigh's theory had failed to accurately predict the intensity of scattered radiation by condensed phases. The destructive interferences between the wavelets, scattered from molecule to molecule, accounted for the difference in the experimental and theoretical prediction. The development of fluctuation theory brought a theoretical model to account for the condensed phase scattering. Smoluchowski[21] and Einstein[22] developed fluctuation theory and solved the problem by considering a liquid to be a continuous medium. Smoluchowski described the optical effects that occur near the gas-liquid critical point of a binary mixture of liquids. Einstein was able to show that critical opalescence could be explained by density

fluctuations. Within the continuous medium thermal fluctuations can give rise to local inhomogeneities and thus density and concentration fluctuations.[23] Thus the intensity of light can be found without a detailed description of the scattering medium.

The fluctuation approach calculates the mean square fluctuations of density and concentration from fluctuations in the scattered light. These mean square fluctuations then are used to calculate the isothermal compressibility and the concentration dependence of the osmotic pressure.[24] The phenomenological approach to light scattering was objected to by some on the grounds that light scattering arises from density fluctuations in a region with dimensions small compared to the wavelength of incident light.[25, 26] However, Fixman in 1955 was able to show that the Einstein-Smoluchowski phenomenological scattering theory agrees with the molecular scattering theory.[27]

Ornstein and Zernike's work in correlation functions provided the step in describing the scattering process in liquids. Their studies centered on the scattering of light in a fluid critical opalescence.[28, 29, 30] They showed that the pair correlation function becomes infinity long, when the turbidity of a fluid in a region is in close proximity to the gas-liquid critical point. In 1927, Zernike and Prins showed that the pair correlation function could be used to correlate the positions of particles in a liquid with scattered x-rays.[31]

Debye, in 1947, was able to show a method for measuring the molecular weight of large particles in solution by expanding the concentration as a power series and considering a distribution of masses and diameters.[32, 33] Concurrently, Zimm developed a method of deriving molecular mass by performing scattering experiments at several angles and at least four different concentrations.[34] The plot of the data is known as the Zimm

plot.[35] Debye's method differed from Zimm's method in that Debye only required scattered data from only one angle.

Another light scattering method was developed by the Brillouin, which measured the frequency distribution of scattered light from acoustic vibrations a medium.[36, 37] Brillouin scattering is similar to Raman scattering[38] in that Brillouin scattering results from acoustic phonons, while Raman scattering is derived form optic phonons and molecule vibrations. The Brillouin scattering measurement determines a frequency shift with an interferometer and is limited to the detection of quasi-particles. Brillouin predicted a doublet frequency distribution, now baring his name, which was observed by Gross in liquids.[39, 40] Along with the Brillouin doublet, Gross also observed a central line with an unshifted maximum, which represented the fine structure of Rayleigh scattering due to acoustic waves in condensed matter. The unshifted frequency was explained as the entropy fluctuation component of density fluctuations.[41] The ratio of the integrated intensity of the central line to that of the doublet could be written as

$$\frac{I_c}{I_d} = \frac{c_p - c_v}{c_v}.$$

This relation is known as the Landau-Placzek ratio. In their 1934 paper they also noted that the spectral width of the light scattered by the non-propagating density fluctuations would be proportional to the thermal diffusivity of the fluid.

The invention of the laser, by Gould in the late 1950's, brought new and increasingly accurate scattering experiments. Using the frequency distribution of scattered light from suspended macromolecules the diffusion coefficient could be found.[42] Finally, in 1964 Cummins et al. introduced optical mixing as a method for resolving scattered light from a

suspension of dilute polystyrene spheres.[43] With this technique of optical mixing spectroscopy, the modern era of laser light scattering emerged to be widely used in physics, material science, biology and chemistry.

3.3 Theory of Light Scattering

Light scattering as formulated from classical electromagnetic theory occurs when incident light falls upon a medium containing charges. The electromagnetic field exerts a force on the charges which in turn re-radiate the electromagnetic field. If the medium is comprised of many scatterers, then the scatterers are assumed to receive the same incident field. The resulting scattered electric filed from the particles will then be a superposition of scattered fields.

The direction of the scattered field depends on the characteristics of the scattering medium. If the medium is composed of particles with identical dielectric constants, the only scattered light will be in the forward direction. Scattered wavelets from each volume element will differ only by a phase factor which is determined by relative positions in the volume. For a large volume, each scattered wavelet from a volume element can always be matched with a corresponding wavelet with equal amplitude but opposite phase from another volume element. Conversely, if the medium is comprised of particles with differing dielectric constants, then the amplitudes from the various volume elements will no longer have equal amplitudes. Thus, the wavelets will not be canceled and scattered light will propagate from the medium. Fluctuation theory as introduced by Einstein brings a semi-classical view of scattering based on molecular translation and rotation in the medium.[44]

Particles in a solution, such as the PNIPA are not stationary but undergoing constant Brownian motion. These motions within the solution result in fluctuations in the intensity of scattered radiation from the medium. The fluctuation rate of the scattered light gives information related to relaxation processes such as translation and rotational diffusions and molecular internal motions.

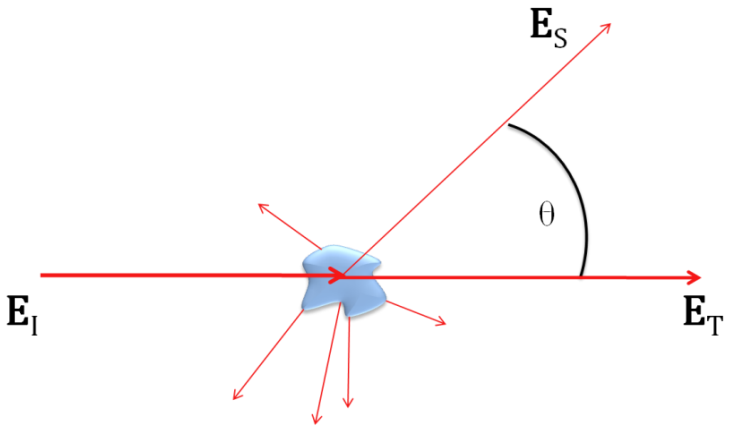

Figure 3.2 The interaction of electromagnetic radiation with a medium depicted as the incident, scattered and transmitted electric fields.

Consider a light scattering experiment where a laser is focused onto a fluid containing macromolecules in a suspension. The incident electric field, $\boldsymbol{E}_I$, of the plane wave impinging upon the suspended macromolecules is then scattered, $\boldsymbol{E}_S$, in all directions and a component of the electric field is transmitted through the scattering medium, $\boldsymbol{E}_T$, as shown in figure 3.2. Polarizers can be inserted, as in figure 3.3, to control the polarization of the incident light, allowing for study of the polarization by detectors in the

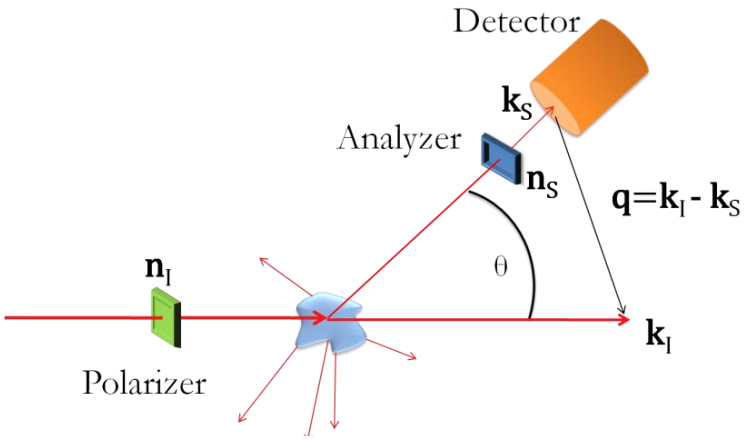

Figure 3.3 A basic schematic of the scattering experiment showing the relative positions of the polarizer, analyzer and detector. The wavevectors k_I and k_S and the scattering vector are also defined.

setup. Information about the macromolecules in solution can be determined from both the scattered electric field and the transmitted electric field.

The study of the resulting electric fields can be studied through optical mixing techniques. The beating of electromagnetic waves was first studied in the radio frequency[45] regime but is also applicable to other EM frequencies. The study of the scattered light is called the homodyne method where only scattered light is collected by the detector. The second method is called heterodyne where non-scattered light is mixed with the scattered light at the photomultiplier tube. The signal from the PM is then analyzed with an autocorrelator.

3.3.1 Scattering of Electromagnetic Waves

In understanding the operation of the light scattering experiment it is first required to appreciate the interaction of the electromagnetic radiation with the medium. A detailed derivation of the scattered field is given in section 8.1 at then end of this chapter. In this section an expression for the amplitude of the scattered wavevector will be shown.

Consider the electric field of an incident plane wave

$$\boldsymbol{E}(\boldsymbol{r},t) = E_0 e^{i(\boldsymbol{k}_I \cdot \boldsymbol{r} - \omega_I t)} \hat{n}_I \tag{3.1}$$

where E_0 is the amplitude of the electric field, $\boldsymbol{k}_I$ is the wavevector, ω_I is the angular frequency and $\hat{n}_I$ is the unit vector in the direction of the incident electric field. Further, the local dielectric constant is given in terms of a fluctuation tensor **I**, the position **r** and time t

$$\boldsymbol{\varepsilon}(\boldsymbol{r},t) = \varepsilon_0 \boldsymbol{I} + \delta\boldsymbol{\varepsilon}(\boldsymbol{r},t) \tag{3.2}$$

A scattering vector q may be defined in terms of the incident, $\boldsymbol{k}_I$, and scattered wave $\boldsymbol{k}_S$ vectors.

$$\boldsymbol{q} = \boldsymbol{k}_I - \boldsymbol{k}_S. \tag{3.3}$$

The wavevectors have magnitudes of

$$k_I = \frac{2\pi n}{\lambda_I} \tag{3.4}$$

and

$$k_S = \frac{2\pi n}{\lambda_S} \tag{3.5}$$

where n is the refractive index of the scattering media. The wavelength of light will not change during the non-absorption scattering process allowing

$$|\boldsymbol{k}_I| \cong |\boldsymbol{k}_S| \tag{3.6}$$

Using the law of cosines the scattering vector can be found

$$q^2 = |\boldsymbol{k}_S - \boldsymbol{k}_I|^2 = k_S^2 + k_I^2 - 2\boldsymbol{k}_I \cdot \boldsymbol{k}_S \tag{3.7}$$

$$= 2k_I^2 - 2k_I^2 cos\theta = 4k_I^2 \sin^2\frac{\theta}{2} \tag{3.8}$$

Finally, taking the square root the magnitude of the scattering vector becomes

$$q = 2k_I \sin\frac{\theta}{2}. \tag{3.9}$$

Many authors erroneously refer to equation (3.9) as the Bragg Condition. The Bragg condition comes from the father-son physicist team of William Henry Bragg and William Lawrence Bragg and was derived in 1914 to describe the x-ray scattering off a crystal lattice.[46] The Bragg condition is noted as

$$m\lambda = 2d \sin\theta. \tag{3.10}$$

In figure 3.4, it is apparent that the angle Θ_D is equivalent to 2θ in equation (3.9). However, there is a subtle difference between equations (3.9) and (3.10). The two equations are only equivalent for a single crystalline plane, which without multiple planes, Bragg Diffraction

does not occur. Thus, by some authors calling equation (3.9) the Bragg condition they are implicitly stating that more than one crystalline plane exists. This is never assumed in the derivation nor is it a physical representation of reality. The signal of scattered light received by the detector is due to fluctuations of the macromolecule, not a lattice type ordering of macromolecules. Further, disorder in a medium of suspended scatterers would preclude any assumption of Bragg diffraction.

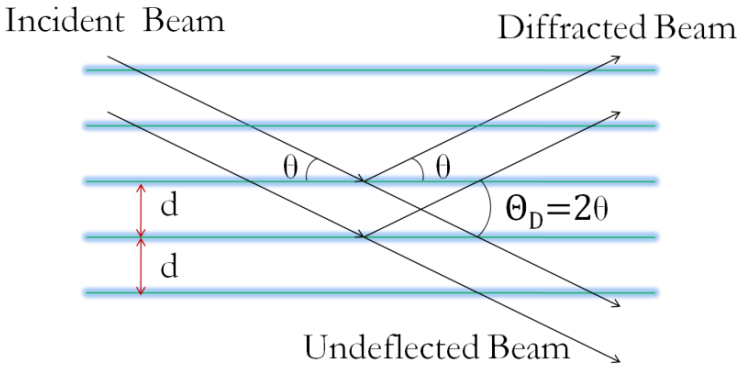

Figure 3.4 A depiction of Bragg Diffraction and the angles associated with the crystal phenomena.

3.3.2 The Correlation Function

A correlation function associates random variables at two different points in space or time. In other words, these functions provide a technique for measuring the extent to which two random variables are related over a period of time. The autocorrelation function is the correlation of random variables at the same point but different times and is a measure of random variables in a system as they change with respect to time. Further, sometimes the autocorrelation may refer to the correlation of random variables in a system with multiple random variables.

Advancement in time-dependent correlations became realized with the theory of noise and stochastic processes.[47] The correlation between random variables has become an extensively employed technique in light scattering spectroscopic experiments and in describing the scatterers which are governed by statistical mechanics.

In the dynamic light scattering experiment, changes in the properties of the electromagnetic radiation is measured, such as frequency shifts, intensity fluctuation and polarization changes from interactions with the macromolecules. The incident EM wave is assumed to be weak and the macromolecules are assumed to interact linearly with the wave. The theory of linear response was developed to measure reaction the light to macromolecules, when they are weakly coupled.[48] The theory states that if the response of each system in the absence of coupling is known then the response of one system to the other is also known.[49] Simply, the time-correlation function is determined by taking one dependent quantity $X(t)$, multiplied by another time dependent quantity $X'(t+\tau)$ and averaged over an equilibrium ensample.[50] The time-correlation functions of the random variables then describes the response of one system to the other. Time-correlations occur widely in classical and quantum statistical mechanics.

An example of time correlation functions in statistical mechanics is demonstrated with a cylinder of gas which is in thermal equilibrium.[51] The random, Brownian motion of the particles of the gas will change the particles positions and momenta as functions of time. The pressure on a cylinder wall is proportional to the total force per unit area, which is also proportional on the distance of various particles from the wall. Consider pressure as the property X which depends on both the positions and momenta. If the pressure on the cylinder wall is measured instantaneously, the measurement will reflect the random molecular motion of the particles as fluctuations. A plot of the property X as a function of time will be similar to a noise pattern. If the measurement of X, is made over a long time compared to the fluctuation period, instead of instantaneously, the measurement will approach an average value.

The autocorrelation of the property X will measure the similarity between two noise signals at different times and is derived in section 8.2. The property X will be measured at an initial moment $X(t)$ and after a time $X(t+\tau)$. If the autocorrelation function decays as a single exponential function then, the fluctuation of the property from its average value is given by

$$\langle \delta X(0)\delta X(\tau)\rangle = \langle \delta X^2\rangle e^{\frac{-\tau}{\tau_r}} \tag{3.11}$$

In general the fluctuation does not decay exponentially, thus a time scale for the decay of the correlation can be defined as

$$\tau_r \equiv \int_0^\infty d\tau \frac{\langle \delta X(0)\delta X(\tau)\rangle}{\langle \delta X^2\rangle}. \tag{3.12}$$

3.3.3 Spectral Density

Often the measurement made in light scattering experiments is the spectral density of the electric field of the incident light on a medium. In the typical scattering experiment light scatters off a particle, then the scattered light passes through a filter with a given band-width and then is collected by a detector. The spectral intensity of a property X is given by

$$\lim_{T\to\infty} \langle |X_{T0}|^2\rangle_T = I_X(\omega_0)\Delta\omega \tag{3.13}$$

where T is the interval of time tending toward infinity, $\Delta\omega$ is the range of frequencies allowed through the filter, and I_X is the spectral density of the property X autocorrelation function. The spectrum of X can then be found by tuning the filter to allow different values of ω_0.

In practice the property $X(t)$ is the scattered electric field $E_T(t)$, passes through a filter such as an interferometer, or grating, and collected by a photomultiplier tube (PM). Equation (3.13) becomes

$$\lim_{T\to\infty}\langle|E_{T0}|^2\rangle_T = I_E(\omega_0)\Delta\omega. \tag{3.14}$$

The spectral density or power spectrum is found by Fourier inversion and using the time-correlation,

$$I_E(\omega) = \frac{1}{2\pi}\int_{-\infty}^{+\infty} d\tau\,\langle E^*(t)E(t+\tau)\rangle e^{i\omega t}. \tag{3.15}$$

Thus, the in practice the spectral density $I_E(\omega)$ is measured with a filter or by heterodyne methods using a spectrum analyzer.

3.4 Static Light Scattering

The static light scattering experiment measures, the time averaged photon count, using a photomultiplier tube. Fluctuation theory governs changes in the poarizability of the scattering. The scattered intensity depends upon three variables: (1) the molecular weight, M_w; (2) the average root mean square of the radius of gyration; and (3) the second-order virial coefficient A_2. Fluctuations in simple media are typically due to variations in temperature and pressure, while in polymer solutions the fluctuation is due to concentration fluctuations.

3.4.1 Excess Rayleigh Ratio

The Rayleigh Ratio is a measure of the intensity of electromagnetic radiation per unit scattering volume. The first excess Rayleigh ratio measurements were performed in the early 60's, but deviated greatly from theoretical predictions.[52] Later, measurements became reasonably closer to predicted values.[53, 54, 55]

The scattered intensity for a single particle is given by

$$I_s = \frac{k_s^4 \sin^2\theta}{r^2}\alpha^2 I_0 \tag{3.16}$$

where I_s is the scattered intensity, I_0 is the incident radiation, θ is the angle of the scattered light, r is the distance from the scattering particle to the detector, α is the polarizability, and $k_s = {}^{2\pi n}/_{\lambda_o}$. Now consider a volume V, containing N scattering particles. Equation (3.16) may be altered to account for the multiple particles

$$I_s = \frac{k_s^4 \sin^2\theta}{r^2}\alpha^2 \frac{N}{V} I_0. \tag{3.17}$$

Gathering the intensities

$$\frac{I_s r^2}{I_0} = k_s^4 \sin^2\theta\ \alpha^2 \frac{N}{V} \tag{3.18}$$

allows the definition of the Rayleigh ratio as

$$R = \frac{I_s r^2}{I_0}. \tag{3.19}$$

The excess Rayleigh ratio is found by using the Clausius-Mosotti equation[56]

$$\frac{(n^2-1)}{(n^2+2)} = 4\pi\alpha \frac{N}{V}. \tag{3.20}$$

However, in free space $n \sim 1$, then

$$n^2 - 1 = 4\pi\alpha \frac{N}{V}. \tag{3.21}$$

For a solvent medium with a refractive index of n_0 then

$$n^2 - n_0^2 = 4\pi\alpha_{ex} \frac{N}{V}. \tag{3.22}$$

where α_{ex} is the excess polarizability. Solving for α_{ex} and writing N in terms of the concentration

$$C = \frac{M}{N_a}\frac{N}{V}$$

$$\alpha_{ex} = \frac{2}{4\pi C}\frac{(n-n_0)}{n}\frac{CV}{N}, \tag{3.23}$$

or in differential form

$$\alpha_{ex} = \frac{1}{2\pi n_0}\frac{M}{N_A}\left(\frac{\partial n}{\partial C}\right)^2\left(\frac{\partial \mu}{\partial C}\right)_{T,P}^{-1}, \tag{3.24}$$

where $\partial\mu/\partial C$ is the fluctuation of chemical potential due to the fluctuation in concentration, N_A is Avogadro's number and M is the molecular weight . Writing equation (3.19) as the excess Rayleigh ratio

$$R_{ex} = \frac{I_{ex}r^2}{I_0}, \tag{3.25}$$

where $I_{ex} = I_{Solution} - I_{Solvent}$. Substituting equation (3.24) and (3.25) into equation (3.18) yields

$$R_{ex} = \frac{4\pi^2 n_o^2}{\lambda_o^4}\frac{CM}{N_a} sin^2\theta \left(\frac{\partial n}{\partial C}\right)^2\left(\frac{\partial \mu}{\partial C}\right)_{T,P}^{-1}. \tag{3.26}$$

where λ_0 is the wavelength of the incident light. For dilute polymer solutions it is often more convenient to write equation (3.26) in terms of the osmotic pressure π_0,

$$R_{ex} = \frac{4{\pi_0}^2 n_0^2}{\lambda_0^4}\sin^2\theta \left(\frac{dn}{dC}\right)^2\frac{k_B TC}{\partial\pi_0/\partial C}, \tag{3.27}$$

where k_B is the Boltzmann constant and T is the absolute temperature. The virial expansion of the ratio of the osmotic pressure

$$\frac{\pi_0}{C} = N_a k_B T\left(\frac{1}{M} + 2A_2C + 3A_3C \ldots\right)^{-1} \tag{3.28}$$

or in differential form

$$\frac{\partial \pi_0}{\partial C} = N_a k_B T \left(\frac{1}{M} + 2A_2 + \cdots\right)^{-1} \tag{3.29}$$

or

$$\frac{\partial \pi_0}{\partial C} = N_a k_B T \frac{1}{M}(1 + 2A_2 M + \cdots)^{-1} \tag{3.30}$$

where A_2 is the second virial coefficient and A_3 is the third virial coefficient which is ignored. Substituting (3.30) into equation (3.27) and allowing $\theta = \pi/2$ for the incident angle, gives

$$R_{ex} = \frac{4{\pi_0}^2 n_0^2}{\lambda_0^4}\left(\frac{dn}{dC}\right)^2 \frac{CM}{1 + 2A_2 CM + \cdots}. \tag{3.31}$$

An optical constant may be defined to simplify equation (3.31)

$$\frac{KC}{R_{ex}} = \frac{1}{M} + 2A_2 C + \cdots \tag{3.32}$$

where

$$K = \frac{4\pi^2 n^2}{\lambda_0^4 N_0}\left(\frac{dn}{dC}\right)^2. \tag{3.33}$$

In general the Rayleigh ratio is dependent upon the scattering vector q

$$q = \frac{4\pi n}{\lambda} sin\frac{\theta}{2}, \tag{3.34}$$

where λ is the wavelength of light in the medium and θ is the scattering angle. Given that there are many scatterers, interference will arise that can be described in terms of a structure factor

$$P(\theta) = \frac{1}{N^2}\sum_i^N \sum_j^N \langle e^{i\boldsymbol{q}\boldsymbol{r}_{ij}} \rangle, \tag{3.35}$$

where N is the number of scatterers per molecule. Expanding for small values of $\boldsymbol{q}$

$$P_z(\theta) = 1 - \frac{1}{3} q^2 \langle R_g^2 \rangle_z + \cdots, \tag{3.36}$$

where the mean-square radius of gyration is

$$\langle R_g^2 \rangle_z = \frac{1}{N} \sum |R_i|^2 \ldots \tag{3.37}$$

and the z-average of the mean-square is

$$\langle R_g^2 \rangle_z = \frac{\sum m_i M_i \langle R_g^2 \rangle_i}{\sum m_i M_i}. \tag{3.38}$$

Defining the z-average of $P(\theta)$

$$P_z(\theta) = \frac{\sum m_i M_i P_i(\theta)}{\sum m_i M_i} \tag{3.39}$$

where $P_i(\theta)$ is the structure factor of the ith particle and m_i is the mass fraction of particle ith with molecular weight M_i. Thus writing equation (3.32) in terms of (3.36) yields[57, 58, 59]

$$\frac{KC}{R(\theta)} = \frac{1}{M_w P_z(\theta)} + 2A_2 C + \cdots. \tag{3.40}$$

Combining equation (3.40) and (3.36) yields the Zimm equation

$$\frac{KC}{R(\theta)} = KCMP(\theta) = KCM \left[1 - \frac{1}{3} q^2 \langle R_g^2 \rangle_z + \cdots \right]. \tag{3.41}$$

Equation (3.41) may be simplified if $q^2 \langle R_g^2 \rangle \ll 1$ and ignoring higher order terms[60]

$$\frac{KC}{R(\theta)} = \frac{1}{M_w} \left[1 + \frac{1}{3} q^2 \langle R_g^2 \rangle_z \right] + 2A_2 C \tag{3.42}$$

where

$$M_w = \frac{\sum_i C_i M_i}{\sum_i C_i}. \tag{3.43}$$

3.5 Dynamic Light Scattering

Dynamic light scattering, also referred to as Quasi Elastic Light Scattering (QELS) is determined from an autocorrelation of the intensity fluctuations due to the Brownian motion of the suspended scatterers. The quantities typically measured in the dynamic

scattering experiment are the translational diffusion coefficient D, the half width at full maximum Γ and the hydrodynamic radius R_h. The measurement is made essentially using the Doppler Effect, where incident light on scatterers undergoing Brownian motion is shifted due to their motion. The quantities measuring the fluctuation are either scattered intensity or frequency broadening. These methods of measurement refer to the techniques of heterodyne and homodyne optical mixing. Heterodyne mixing is the optical mixture of the scattered light with an unshifted unscattered reference beam. The homodyne or self beating method does not require mixing of a reference beam but measures the beating directly.[61] While the frequency broadening will be extremely small compared to the incident light in the frequency domain, the broadening can be measured in the time domain through a time-correlation function.

The Seigert relation, as derived in section 8.4, makes use of the time-time correlation function in determining Γ and D. The Siegert relation relates the second order autocorrelation curve with the first autocorrelation function

$$g^{(2)}(\tau) = A\left[1 + \beta\left|g^{(1)}(\tau)\right|^2\right] \tag{3.44}$$

$$A = \langle I(t)I(t)\rangle \tag{3.45}$$

and

$$g^{(2)}(\tau) = \langle I(t)I(t+\tau)\rangle, \tag{3.46}$$

where $g^{(1)}$ is the first autocorrelation function, $g^{(2)}$is the second autocorrelation function, β is a correlation factor which is dependent upon the scattering geometry of the experiment and τ is the decay time.

The intensities in the Seigert relation may be written in terms of the components of the scattering medium, particularly the solvent and solute (macromolecules). Equation (3.46) becomes

$$g^{(2)}(\tau) = \langle [I_{solvent}\,(t) + I_{solute}\,(t)][I_{solvent}\,(t+\tau) + I_{solute}\,(t+\tau)] \rangle \qquad (3.47)$$

and equation (3.45) becomes

$$g^{(2)}(\tau) = A\left[1 + \beta\left(\frac{I_{solvent}}{I_{solution}}\right)\left|g^{(1)}(\tau)\right| + \frac{I_{solute}}{I_{solution}}\left|g^{(1)}_{solute}\,(\tau)\right|\right]^2. \qquad (3.48)$$

It should be noted that the cross terms have been eliminated because the light scattered by the solvent is not correlated with light scattered by the solute. Since the small molecules of the solvent diffuse faster than the solute, the decay of the first correlation function, $\left|g^{(1)}_{solvent}\,(\tau)\right|$ is faster than the second correlation function $\left|g^{(2)}_{solute}\,(\tau)\right|$. Thus the approximation can be made

$$g^{(2)}(\tau) = A\left[1 + \beta\left(\frac{I_{solute}}{I_{solution}}\right)^2\left|g^{(1)}_{solute}\,(\tau)\right|^2\right]. \qquad (3.49)$$

Writing equation (3.49) in the same form as equation (3.44)

$$g^{(2)}(\tau) = A\left[1 + \beta_A\left|g^{(1)}_{solute}\right|^2\right], \qquad (3.50)$$

where β_A is dependent upon the ratio of the intensity of the solute to the solution and β and is called the apparent coherence

$$\beta_A = \beta\left(\frac{I_{solute}}{I_{solution}}\right)^2. \qquad (3.51)$$

The determination of the intensity—intensity correlation function $g^{(2)}(\tau)$ requires a definition of the first correlation function $\left|g^{(1)}(\tau)\right|$. Assuming the medium is comprised of

monodisperse, spherical scatterers the first correlation function can be represented as an exponential decay function

$$\left|g^{(1)}(\tau)\right| = G(\Gamma)\mathrm{e}^{-\Gamma t}, \tag{3.52}$$

where $G(\Gamma)$ is the line width coefficient distribution having a full width at half maximum Γ. The FWHM is defined as $\Gamma^{-1} = \tau_c$ the characteristic decay time of the rate of dynamic relaxation in self beating.

Equation (3.52) can be generalized as a Laplace integral, for a polydisperse polymer

$$\left|g^{(1)}(\tau)\right| = \int_0^\infty G(\Gamma)e^{-\Gamma t}d\Gamma, \tag{3.53}$$

where the polymer has a continuous molar mass M and the quantity $G(\Gamma)d\Gamma$ can be considered the statistical weight of the particles with a FWHM of Γ.

Another method of dealing with equation (3.52) is to apply a cumulant fit to the logarithmic correlation function

$$\ln\left(g^{(1)}(\tau)\right) = -\Gamma t + \frac{\mu_2}{2}\Gamma^2 t^2 - \frac{\mu_3}{6}\Gamma^3 t^3 + \cdots. \tag{3.54}$$

where the cumulants μ_2 and μ_3 are measures of the degree of polydispersion. In practice, the cumulant analysis of narrowly dispersed polymer chains in a dilute is sufficient to determine an accurate line width Γ.[62] Defining an apparent diffusion constant in terms of the scattering vector q and inverse characteristic decay time Γ

$$D_A(q) = \frac{\Gamma}{q^2}. \tag{3.55}$$

In the limit of a small scattering vector $\boldsymbol{q}$, D_0 can be expanded and written in terms of the radius of gyration

$$D_A(q) = D_z\left(1 + f\langle R_g^2\rangle_z q^2 + \cdots\right) \tag{3.56}$$

and the diffusion coefficient D_z can be written as

$$D_z = D_o(1 + k_d C + \cdots. \tag{3.57}$$

Thus, combining equation (3.56) and (3.57), equation (3.55) can be written as[63, 64, 65]

$$\frac{\Gamma}{q^2} = D(1 + k_d C)\left(1 + f q^2 \langle R_g^2 \rangle_z\right), \tag{3.58}$$

where D is the translational diffusion coefficient of the solute molecule at $C \to 0$, k_d is the second diffusion virial coefficient and f is a dimensionless parameter characterizing the polymer chain structure and solvent.

The translational diffusion coefficient distribution $G(D)$ can be defined as

$$G(D) = q^2 G(\Gamma) \tag{3.59}$$

In the limit as $\tau \to 0$, the first correlation function can be written as

$$\left|g^{(1)}(\tau \to 0)\right| = \frac{\langle E(t)E^*(\tau \to 0)\rangle}{\langle E(t)E^*(t)\rangle} \tag{3.60}$$

or

$$\left|g^{(1)}(\tau \to 0)\right| = \int_0^\infty G(\Gamma)dT = \int_0^\infty G(D)dD = 1. \tag{3.61}$$

Thus, the average diffusion coefficient $\langle D \rangle$ is defined as

$$\langle D \rangle = \int_0^\infty G(D)D\ dD. \tag{3.62}$$

The Stoke-Einstein relation associates translational diffusion coefficient D and f the molecular friction factor.

$$D = \frac{k_B T}{f} \tag{3.63}$$

where k_B is the Bolzmann constant and T is the absolute temperature. For a spherical particle

$$f = 6\pi\eta \tag{3.64}$$

where η is the viscosity of the solvent. Defining a hydrodynamic radius R_h, in terms of the diffusion coefficient and friction factor[66]

$$R_h = \frac{k_B T}{6\pi\eta} \tag{3.65}$$

Assuming spherical colloidal particles, rotational and internal motion can be ignored, allowing $G(\Gamma)$ to be converted into a hydrodynamic size distribution of the colloidal particles. In this way dynamic light scattering determines the radii of disperse, dilute, colloidal particles.

3.6 Experimental Dynamic Laser Light Scattering

Studying the angular cross section of photon correlation measurements on a few particles can yield information about particles and particle interactions.[67] The technique of photon correlation measurement was introduced in the early 1970's.[68, 69] These first calculations assumed the scattered light amplitude to be governed by Gaussian statistics and the autocorrelation was measured at a single sample time.[70] Unfortunately, these first calculations contained a number of inaccuracies and errors.[71] Improvements came when an accurate knowledge of the statistical precision of the measurement was understood.[72]

Photon correlation techniques allow the measurement of Doppler shifts in the scattered laser light which characterizes colloidal suspensions.[73] The development of correlation techniques have led to production of commercially available light scattering instruments with the capability of making static and dynamic measurements. Currently, with the mathematics of the photon correlation largely developed for scattering, improvements are made in regard to sensitivity of detecting intensity fluctuations.[74]

Further, with increased computing power, data acquisition is an ongoing improvement in light scattering studies.[75]

3.6.1 DLS Instrumentation

These experiments were performed using a commercially available laser light scattering spectrometer (ALV/DLS/SLS-5000) equipped with an ALV 500 digital time correlator. The scattering laser source was a Helium-Neon laser manufactured by Uniphase, model 1145 P, with a power output of 22 mW operating at a wavelength of 632.8 nm. The incident laser light is vertically polarized with respect to the scattering plane and regulated with a Newport M-925B beam attenuator. Light scattered from the medium is gathered and guided, with a ~40μm diameter fiber, to the detector, an active quenched avalanche photodiode. The avalanche photodiode provides a higher sensitivity, 2 orders of magnitude, over photomultiplier tubes. The higher sensitivity is such that a 22 mW laser will have an equivalent count rate as a 400 mW laser used in conjunction with a photomultiplier tube.

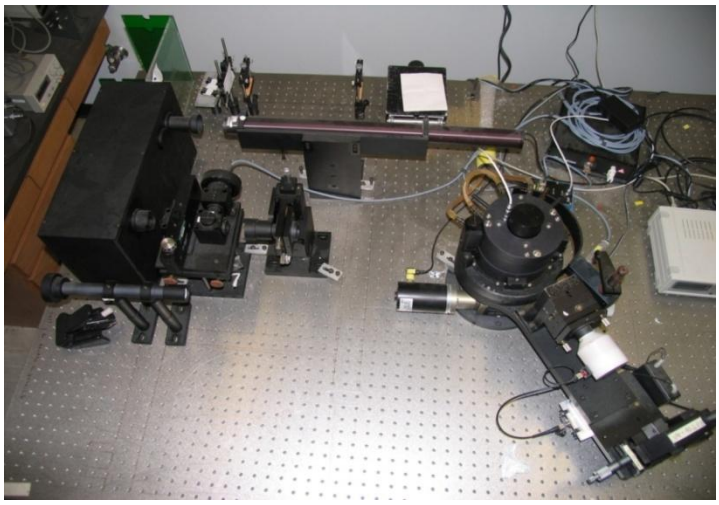

Figure 3.5 The Dynamic Light Experiment (DLS) showing the laser as the incident source , and the ALV 5000 digital autocorrelator.

3.6.2 Correlation Algorithm

The ALV-5000 digital correlator is capable of real-time computation of photon correlation functions with fixed simultaneous lag time ranging from 0.2 μs to several hours.

Two independent correlation functions of two different input signals can be sampled simultaneously.

The basic commercial light scattering apparatus contains digital correlator software to perform the following: (1) counting photoelectron pulses over a sampling time interval t_s; (2) delaying samples for a lag time, that is a integer multiple of t_s, $t = \kappa t_s$; (3) multiplying delayed and direct data samples; and (4) summing these products.[76] Steps (3) and (4) are typically done for many different delays in parallel. A corresponding number of channels are used to keep the results of these computations.

3.7 DLS Experimental Results

Scattering techniques of particles incident on gels has become the major technique for measuring gel properties. In particular, dynamic light scattering provides a non-invasive, small interaction probing tool for understanding gel polymer chain interactions and motions. Tanaka, used intensity and time-correlation of laser light in the initial studies of acrylamide gels and their responses.[77] The phase transitions of NIPA hydrogel is dependent upon the ionic concentrations of the network, temperature, pH and solvent composition.[78] The hydrogel has been found to undergo a discontinuous transition when a charged co-monomer, typically acrylic acid is added to the gel network, where the free energy of counter-ions lead to swelling and the elastic energy of the network maintains the shape of the gel.[79]

3.7.1 Temperature Response

Temperature responsive colloidal gels have been extensively studied since 1986, when Pelton and Chibante first synthesized NIPA base microgels. Poly(N-isopropylacrylamide) has a temperature sensitive phase behavior with a lower critical

temperature (LCST) where the microgel is in a hydrophilic state below LCST and in a hydrophobic state above LCST.[80] The LCST can be changed by incorporating comonomers into the gel network where hydrophobic comonomers lower the LCST and hydrophilic comonomers raise the LCST. The relevant forces which drive the volume transition in temperature dependent hydrogel is the balance of hydrophilic and hydrophobic interactions between inter-polymer and intra-polymer chains.

The temperature of the NIPA hydrogel is maintained with a ISO Thermo water bath manufactured by Fisher Scientific. The temperature of the dilute microgel sample was allowed to come to a constant temperature for one-hour, to ensure temperature stability within the sample. Each data measurement was made after one-hour of constant temperature. The data depicted in figure 3.6 shows the volumetric phase change with 34°C being the LCST. The hydrodynamic radius of the gel sphere below LCST is approximately 460 nm and shrinks to 300 nm above LCST.

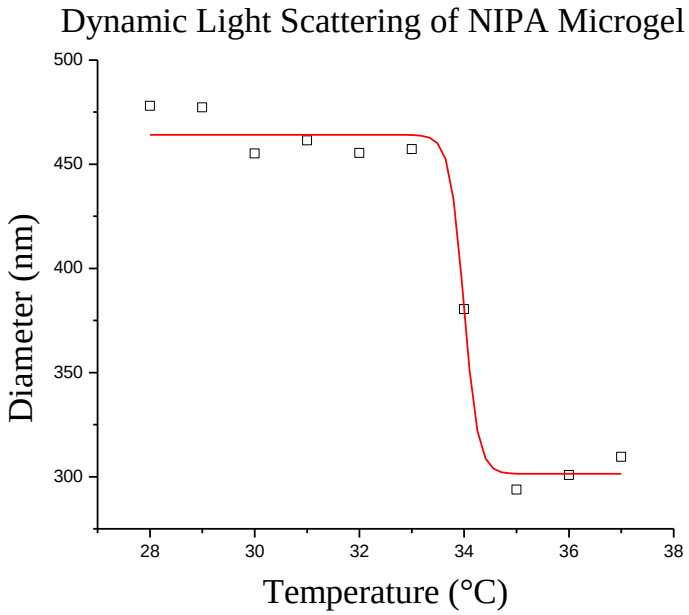

Figure 3.6 The results from NIPA microgel under a temperature stimulus.

3.7.2 Electric Field Response

One of the more convientient environmental stimuli, which NIPA gel is responsive to is the electric field. Since PNIPA hydrogel contains ions, when an electric field, of sufficient

strength to over come hydrohylic forces, is applied, the gel will undergo its discontinuous volumetric phase change. The first electric field, sensitive gel was reported by Hamlen in 1965, where a PVA gel fiber sharnk under an applied voltage of 5 V.[81] Gel shrinking and swelling behavior is responsive to both ac and dc excitations.[82, 83] Tanaka, was able to explain the collapse of bulk polyacrylamide gel with FH theory, described in the previous chapter.[84] The degree of collapse is dependent upon the field intensity, the concentration of polyions in the gel and the size of the gel particles.[85] The collaspe is based upon the change in osmotic pressure due to ion concentration differences between the inside and outside of the gel. Although most electrolyte gels are rather slow to respond to an applied field, some have been shown to respond within miliseconds.[86]

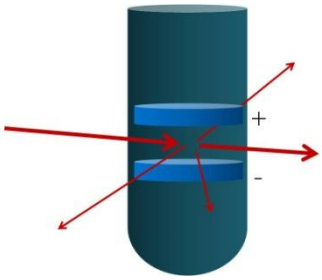

Figure 3.7 A schematic of laser light incident on scatterers between the parallel plates.

The electric field stimulus applied to the microgel particles is provided by two parallel electrodes sized to fit inside a test tube. The incident laser light is adjusted to scatter off the medium disposed between the two electrodes depicted in figure 3.7. The actual electrodes used in the experiment are shown in figure 3.8. The electrodes were constructed of copper with stiff wire leads soldered onto the outward side of the electrode.


Figure 3.8 The electrodes used in the DLS-Electric Field experiment.

Data in the experiment was taken every 5 minutes over a sampling interval of 1 minute. The data was gathered much more quickly than the thermal experiment because of electrolysis of the solvent (water) causes anomalous readings due to gas bubbles. In figure 3.9, the resulting graph of the hydrogel undergoing a volumetric phase change is shown. The gel undergoes the discontinuous phase change at a field strength of approximately 2.1 V cm^{-1}, where the initial diameter of the microgel particles being 312 nm which collapsed to a size of 180 nm.

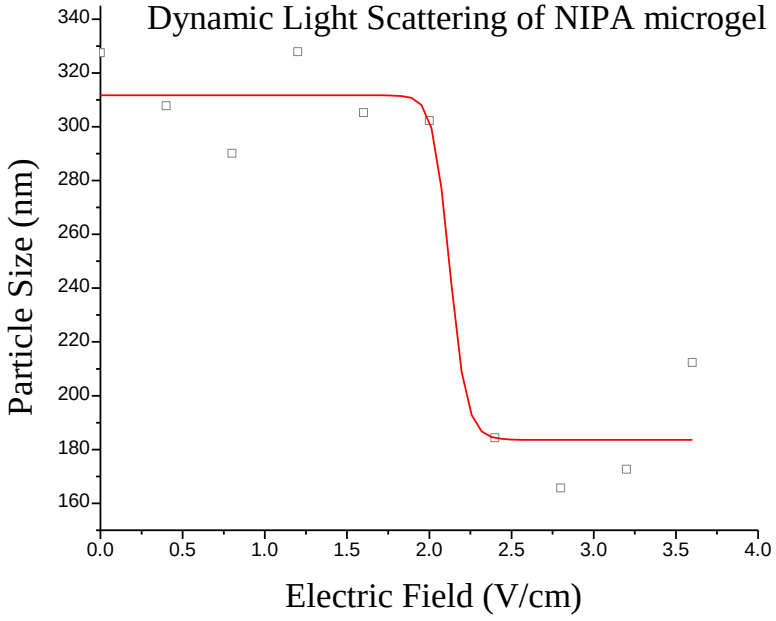

Figure 3.9 A depiction of the collapse of NIPA microspheres exposed to an electric field, measured my DLS.

3.8 Derivations

The following sections show some of the assumed derivations in detail. The detail is shown to give the reader a better understanding of the underlying physical processes.

3.8.1 Derivation of Scattered Field[87]

The equations governing the electromagnetic interaction are the Maxwell equations. The Maxwell equations for a non-conducting, non-magnetic medium in the absence of source are

$$\boldsymbol{\nabla} \cdot \boldsymbol{H} = 0, \tag{3.66}$$

$$\boldsymbol{\nabla} \cdot \boldsymbol{D} = 0, \tag{3.67}$$

$$\boldsymbol{\nabla} \times \boldsymbol{E} = -\frac{1}{c}\frac{\partial \boldsymbol{H}}{\partial t}, \tag{3.68}$$

$$\boldsymbol{\nabla} \times \boldsymbol{H} = \frac{1}{c}\frac{\partial \boldsymbol{D}}{\partial t}. \tag{3.69}$$

The vector $\boldsymbol{E}$ represents the electric field, $\boldsymbol{D}$ the electric displacement is written in terms of $\boldsymbol{E}$ and $\boldsymbol{P}$ the dipole moment per unit volume.

$$\boldsymbol{D} \equiv \varepsilon_0 \boldsymbol{E} + \boldsymbol{P},$$

and $\boldsymbol{H}$ is the auxiliary field given by

$$\boldsymbol{H} \equiv \frac{1}{\mu_o}\boldsymbol{B} - \boldsymbol{M}$$

where $\boldsymbol{B}$ is the magnetic field and $\boldsymbol{M}$ is the magnetization, but $\boldsymbol{M} = 0$ for a nonmagnetic medium. The local dielectric constant will be considered the tensor

$$\boldsymbol{\varepsilon}(\boldsymbol{r}, t) = \varepsilon_0 \boldsymbol{I} + \delta\boldsymbol{\varepsilon}(\boldsymbol{r}, t) \tag{3.70}$$

where $\boldsymbol{I}$ is a second rank unit tensor, and the term $\delta\boldsymbol{\varepsilon}(\boldsymbol{r}, t)$is the dielectric constant fluctuation tensor.

The total fields at a point in the scattering medium are given as the sum of the incident and scattered fields. Thus

$$\boldsymbol{E} = \boldsymbol{E}_I + \boldsymbol{E}_S \tag{3.71}$$

$$\boldsymbol{D} = \boldsymbol{D}_I + \boldsymbol{D}_S \tag{3.72}$$

$$\boldsymbol{H} = \boldsymbol{H}_I + \boldsymbol{H}_S. \tag{3.73}$$

Since the total fields obey Maxwell's equations, the individual fields must also obey Maxwell's equations, in particular the scattered field.

The total displacement vector, (3.72), can be written in terms of the dielectric tensor, equation (3.70)

$$\boldsymbol{D} = (\varepsilon_o \boldsymbol{I} + \delta\boldsymbol{\varepsilon}) \cdot (\boldsymbol{E}_I + \boldsymbol{E}_S) = \varepsilon_o \boldsymbol{E}_I + (\delta\boldsymbol{\varepsilon}) \cdot \boldsymbol{E}_I + \epsilon_o \boldsymbol{E}_S + (\delta\boldsymbol{\varepsilon}) \cdot \boldsymbol{E}_I. \tag{3.74}$$

Further, using the fact that the polarization for the incident wave is zero the incident displacement vector may be written as

$$\boldsymbol{D}_I = \varepsilon_0 \boldsymbol{E}_I. \tag{3.75}$$

This allows the scattered displacement vector to be written as

$$\boldsymbol{D}_I = \varepsilon_o \boldsymbol{E}_S + (\delta\boldsymbol{\varepsilon}) \cdot \boldsymbol{E}_S, \tag{3.76}$$

where the second order term $(\delta\boldsymbol{\varepsilon}) \cdot \boldsymbol{E}_s$ is ignored.

The scattered auxiliary field, $\boldsymbol{H}_s$, may be eliminated from Maxwell's equations by taking the curl of equation (3.68)

$$\boldsymbol{\nabla} \times \boldsymbol{\nabla} \times \boldsymbol{E} = -\frac{1}{c}\frac{\partial}{\partial t}\boldsymbol{\nabla} \times \boldsymbol{H}.$$

Substituting into equation (3.69) gives

$$\boldsymbol{\nabla} \times \boldsymbol{\nabla} \times \boldsymbol{E}_S = -\frac{1}{c^2}\frac{\partial^2 \boldsymbol{D}_S}{\partial t^2}. \tag{3.77}$$

The inhomogeneous wave equation can then be arrived at by solving equation (3.76) for $\boldsymbol{E}_s$ and substituting into equation (3.77).

$$\nabla^2 \boldsymbol{D}_S - \left(\frac{\varepsilon_o}{c}\right)\frac{\partial^2 \boldsymbol{D}_S}{\partial t^2} = -\boldsymbol{\nabla} \times \boldsymbol{\nabla} \times (\partial\boldsymbol{\varepsilon} \cdot \boldsymbol{E}_I) \tag{3.78}$$

Equation (3.78) may be simplified further by introducing a polarization potential or Hertz vector.[88, 89, 90]

$$\boldsymbol{D}_S = \nabla \times \nabla \times \boldsymbol{\pi} \tag{3.79}$$

The Hertz vector can be shown to satisfy the inhomogeneous wave equation with the source term $-(\delta\boldsymbol{\varepsilon})\cdot\boldsymbol{E}_i$, by substituting equation (3.79) into equation (3.78)

$$\nabla^2\boldsymbol{\pi}-\frac{\varepsilon_o}{c^2}\frac{\partial^2\boldsymbol{\pi}}{\partial t^2}=-(\delta\boldsymbol{\varepsilon})\cdot(\boldsymbol{E}_I). \tag{3.80}$$

The integral form of equation (3.80) can be written as

$$\boldsymbol{\pi}(\boldsymbol{R},t)=\frac{1}{4\pi}\int d^3r\,\frac{\delta\boldsymbol{\varepsilon}(\boldsymbol{r},t')}{|\boldsymbol{R}-\boldsymbol{r}|}\cdot\boldsymbol{E}_I(\boldsymbol{r},t') \tag{3.81}$$

where $\boldsymbol{R}$ and $\boldsymbol{r}$ are depicted in figure 3.9 and t' is the retarded time

$$t'=t-\frac{\sqrt{\varepsilon_o}}{c}|\boldsymbol{R}-\boldsymbol{r}|$$

The incident electric field, $\boldsymbol{E}_I$ can be written as

$$\boldsymbol{E}_I(r,t)=E_o e^{i(\boldsymbol{k}_I\cdot\boldsymbol{r}-\omega_I t)}\hat{n}_I, \tag{3.82}$$

where $\hat{n}_I$ is the unit vector in the direction of the incoming electric field. If we assume that the detector is immersed into the scattering medium or is refractive index matched to the medium (i.e. $\boldsymbol{D}_s=\varepsilon_0\boldsymbol{E}_s$) and substitute equation (3.82) into equation (3.78) then

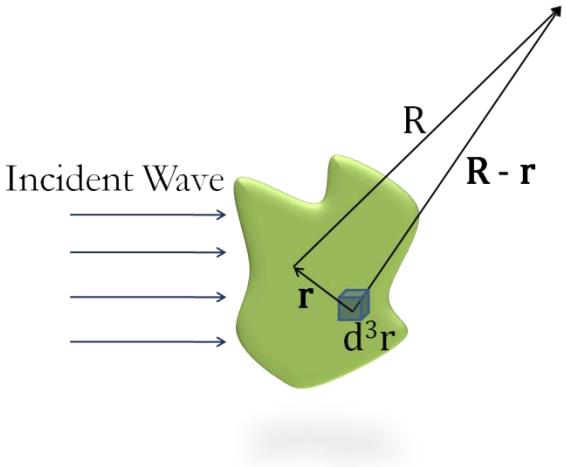

Figure 3.10 The scattered field from an incident wave on a volume element of a scattering medium.

$$\boldsymbol{E}_s(\boldsymbol{R},t)=\boldsymbol{\nabla}\times\boldsymbol{\nabla}\times\left[\frac{E_o}{4\pi\varepsilon_o}\int d^3r\,\frac{1}{|\boldsymbol{R}-\boldsymbol{r}|}[\delta\boldsymbol{\varepsilon}(\boldsymbol{r},t')\cdot\hat{n}_I]e^{\,i(\boldsymbol{k}_I\cdot\boldsymbol{r}-\omega_I t')}\right] \tag{3.83}$$

If the detector is also, assumed to be a large distance form the scattering volume the denominator of the integrand, $|\boldsymbol{R}-\boldsymbol{r}|$, may be expanded in power series as

$$|\boldsymbol{R}-\boldsymbol{r}|\cong R-\boldsymbol{r}\cdot\hat{k}_f+\cdots$$

where $\hat{\mathrm{k}}_f$ is the unit vector in the direction of $\boldsymbol{R}$. Thus, the retarded time can be written as

$$t' \cong t - \frac{\sqrt{\varepsilon_o}}{c}\left(R - \boldsymbol{r} \cdot \hat{k}_f\right) \tag{3.84}$$

It is now necessary to perform a Fourier transform of $\delta\boldsymbol{\varepsilon}(\boldsymbol{r}, t')$ over an interval T, yielding

$$\delta\boldsymbol{\varepsilon}(\boldsymbol{r}, t') = \sum_p \delta\boldsymbol{\varepsilon}_p(\boldsymbol{r}) e^{i\Omega_o t'} \tag{3.85}$$

where

$$\Omega_o = \left(\frac{2\pi}{T}\right) p.$$

The scattered frequency can be defined as

$$\omega_f \equiv \omega_I - \Omega_o. \tag{3.86}$$

Consider the relative frequencies for translational and rotational motions of a macromolecule in solution. The translational and rotational motions will be much less than the frequency of incident light.

$$\Omega_o \ll \omega_I$$

The wave vector can be defined as

$$\boldsymbol{k}_o \equiv \frac{\sqrt{\varepsilon_o}}{c}\omega_f \hat{k}_f \tag{3.87}$$

and the scattering vector or the wavevector component of the dielectric constant fluctuation that will give rise to the scattering

$$\boldsymbol{q}_0 \equiv \boldsymbol{k}_i - \boldsymbol{k}_o. \tag{3.88}$$

Substituting equations (3.84), (3.85) and (3.86) into equation (3.82), using the approximation and ignoring terms over order greater than $1/R$

$$\boldsymbol{E}_s(\boldsymbol{R},t) = \frac{E_o}{4\pi\varepsilon_o R}\sum_o e^{i(k_o R-\omega_I t)}\boldsymbol{k}_o$$

$$\times\left[\boldsymbol{k}_o \times \int_V d^3r\; e^{i(\boldsymbol{k}_I-\boldsymbol{k}_o\hat{k}_f)}\cdot r\;\delta(\boldsymbol{r})(e^{i\Omega_o t})\cdot\hat{n}_I\right]. \tag{3.89}$$

The following approximation can now be made

$$k_o \approx \frac{\sqrt{\varepsilon_o}}{c}\omega_I = k_I \cong k_f$$

$$k_o\hat{k}_f \approx k_I\hat{k}_f$$

and definitions

$$\boldsymbol{k}_f = k_I\hat{k}_f$$

$$\boldsymbol{q} = \boldsymbol{k}_I - \boldsymbol{k}_f$$

Using these approximations, definitions and equation (3.85), (3.89) becomes

$$\boldsymbol{E}_s(\boldsymbol{R},t) = \frac{E_o}{4\pi\varepsilon_o R}e^{i(\boldsymbol{k}_f\cdot\boldsymbol{R}-\omega_I t)}\boldsymbol{k}_f \times\left[\boldsymbol{k}_f \times \int_V d^3r\; e^{i\boldsymbol{q}\cdot\boldsymbol{r}}(\delta\boldsymbol{\varepsilon}(\boldsymbol{r},t)\cdot\hat{n}_I)\right]. \tag{3.90}$$

3.8.2 Derivation of Correlation Time[91]

Consider a property X having a time dependence, which exhibits a noise pattern as shown in figure 3.10, the motions of a macromolecule in solution. If the property X is measured over a time interval, the equilibrium of the system is also the time average

$$\bar{X}(\boldsymbol{r},t) = \frac{1}{T}\int_{t_0}^{t_0+T} dt\; X(\boldsymbol{r},t). \tag{3.91}$$

where T is the time which the measurement is performed, and t_0 is the time when the measurement is initiated. However, the average is only meaningful if the measurement is performed over a time interval much longer that an individual fluctuation. The idealized

measurement will be conducted over an infinite time with X averaged over the infinite time:

$$\bar{X}(t_o) = \lim_{T\to\infty} \frac{1}{T} \int_{t_0}^{t_0+T} dt\, X(t). \tag{3.92}$$

In general for dilute scattering experiments the infinite time average is independent of t_0. This is called a stationary property since the average depends only on the measurement duration rather than a starting point. The property X fluctuates, as depicted in figure 3.10, about its time average $\langle A \rangle$, independent of t_0.

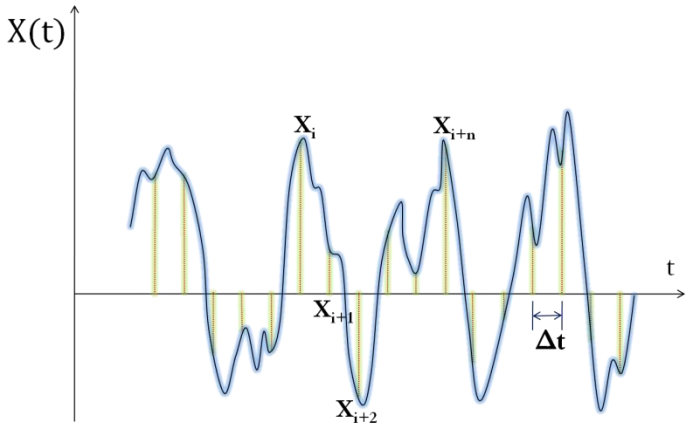

Figure 3.11 A property X with a time dependence fluctuates similar to the movement of molecules in a fluid.

$$\langle A \rangle = \lim_{T\to\infty} \frac{1}{T} \int_{0}^{T} dt\, A(t) \tag{3.93}$$

In other words, the joint probability distribution depends on x_i, x_{i+1} and not on values of t_i, t_{i+1}.

The general noise function depicted in figure 3.10, shows that the property X at time t and $t + \tau$ where τ is the delay time, will have different values. Thus

$$X(t + \tau) \neq X(t)$$

However, if τ is sufficiently short to be comparable to fluctuations in X then $X(t + \tau)$ will nearly approximate $X(t)$ and $X(t + \tau)$ will be correlated with $X(t)$. However, an increasing τ that causes a deviation of $X(t + \tau)$ tending toward a non-zero value, results in a loss of

correlation. The measure of correlation between the two functions is the autocorrelation of the property X.

$$\langle X(0)X(\tau)\rangle = \lim_{T\to\infty}\frac{1}{T}\int_0^T dt\, X(t)X(t+\tau). \tag{3.94}$$

Consider a non-conserved, non-periodic process with the correlation function

$$\langle X(t+\tau)X(t)\rangle = \langle X(\tau)X(0)\rangle \tag{3.95}$$

which is independent of t. To create a graphical representation of the correlation function first let $\tau \to 0$, then

$$\langle X(t+\tau)X(t)\rangle \to \langle |X(t)|^2\rangle \tag{3.96}$$

But if $\tau \to \infty$, then

$$\langle X(t+\tau)X(t)\rangle \to \langle X(\tau)\rangle\langle X(0)\rangle \to \langle X\rangle^2$$

In practice, the scattering experiment has a correlator which computes time-correlation functions of the scattered field. This requires the time axis in figure 3.10, to be divided into discrete intervals of time Δt, allowing the following variables to be rewritten assuming the property X does not vary greatly over the time interval.

$$t = i\Delta t$$

$$\tau = n\Delta t$$

$$T = N\Delta t$$

$$t + \tau = (i+n)\Delta t$$

Thus equations (3.93) and (3.94) can be written as a summation rather than integral form as

$$\langle X\rangle \cong \lim_{N\to\infty}\frac{1}{N}\sum_{i=1}^{N} X_i \tag{3.95}$$

$$\langle X(0)X(\tau)\rangle \cong \lim_{N\to\infty}\frac{1}{N}\sum_{i=1}^{N} X_i X_{i+n} \tag{3.96}$$

The decay of the time correlation function is more easily proved for the discrete case. Using Schwartz's inequality which states

$$\left|\sum_j A_j B_j\right|^2 \leq \left|\sum_j A_j^2\right|\left|\sum_j B_j^2\right| \tag{3.97}$$

In using the inequality the quantity $B_j = X_{i+n}$ and $A_j = X_i$. Thus

$$\lim_{N\to\infty}\frac{1}{N}\sum_{i=1}^{N} X_i^2 = \langle X^2\rangle \tag{3.98}$$

$$\lim_{N\to\infty}\frac{1}{N}\sum_{i=1}^{N} X_{i+n}^2 = \langle X^2\rangle \tag{3.99}$$

and

$$\lim_{N\to\infty}\frac{1}{N}\sum_{i=1}^{N} X_i X_{i+n} = \langle X(0)X(\tau)\rangle. \tag{3.100}$$

The inequality becomes

$$|\langle X(0)X(\tau)\rangle|^2 \leq \langle X^2\rangle^2. \tag{3.101}$$

Since $\langle X(0)X(\tau)\rangle$ is real

$$\langle X(0)X(\tau)\rangle \leq \langle X^2\rangle. \tag{3.102}$$

Therefore, the autocorrelation function either remains equal to its initial value for all τ, or decays from its initial value as depicted in figure 3.11. When τ becomes large compared to the fluctuation time of X, $X(t)$ and $X(t+\tau)$ become uncorrelated

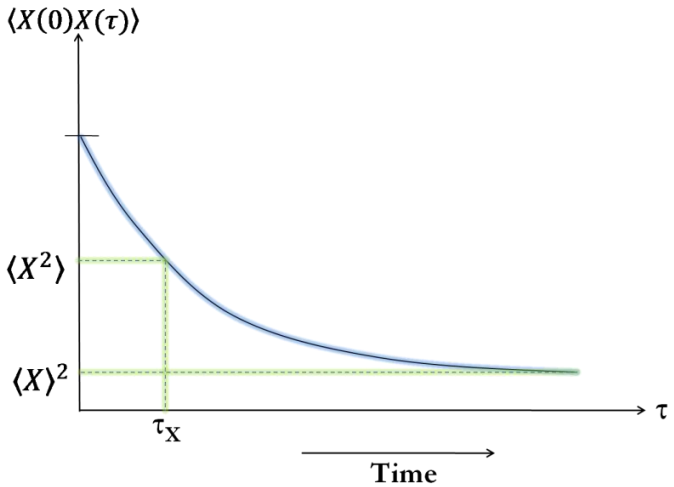

Figure 3.12 The time correlation of a non-conserved, non-periodic property X.

$$\lim_{\tau\to\infty}\langle X(0)X(\tau)\rangle = \langle X(0)\rangle\langle X(\tau)\rangle = \langle X\rangle^2. \tag{3.103}$$

Therefore, for a non-periodic, non-conservative property, the time correlation function will decay from $\langle X^2\rangle$ to $\langle X\rangle^2$.

When performing the scattering experiment, using an exponentially decaying autocorrelation function is typical.[92]

$$\langle X(0)X(\tau)\rangle = \langle X\rangle^2 + [\langle X^2\rangle - \langle X\rangle^2]\mathrm{e}^{-\frac{\tau}{\tau_r}} \tag{3.104}$$

where τ_r is defined as the correlation or relaxation time. The basic shape of the exponential autocorrelation function can be seen in figure 3.11.

The determination of the correlation time requires the a definition of a deviation from the average value of $X(t)$.

$$\delta X(t) \equiv X(t) - \langle X\rangle \tag{3.105}$$

The term $\delta X(t)$ is referred to as the fluctuation. Substituting equation (3.105) into equation (3.94)

$$\langle X(0)X(\tau)\rangle = \lim_{T\to\infty}\frac{1}{T}\int_0^T dt\,[\langle X\rangle^2 + \langle X\rangle[\delta X(t) + \delta X(t+\tau)] + \delta X(t)\delta X(t+\tau)]. \tag{3.106}$$

Since $\langle X\rangle$ is a constant and

$$\langle \delta X(t)\rangle = 0 = \langle \delta X(t+\tau)\rangle.$$

Equation (3.106) becomes

$$\langle X(0)X(\tau)\rangle = \langle X\rangle^2 + \langle \delta X(0)\delta X(\tau)\rangle.$$

Solving for $\langle \delta X(0)\delta X(\tau)\rangle$yields

$$\langle \delta X(0)\delta X(\tau)\rangle = \langle X(0)X(\tau)\rangle - \langle X\rangle^2 \tag{3.107}$$

and

$$\langle \delta X^2 \rangle = \langle \delta X(0) \delta X(0) \rangle = [\langle X^2 \rangle - \langle X \rangle^2]. \tag{3.108}$$

Substituting equation (3.107) and (3.108) into equation (3.104) gives

$$\langle \delta X(0) \delta X(\tau) \rangle = \langle \delta X^2 \rangle \mathrm{e}^{-\frac{\tau}{\tau_r}}. \tag{3.109}$$

More generally the time correlation may be written as

$$\tau_r \equiv \int_0^\infty d\tau \frac{\langle \delta X(0) \delta X(\tau) \rangle}{\langle \delta X^2 \rangle}, \tag{3.110}$$

since not all fluctuations decay exponentially.

3.8.3 Derivation of the Power Spectral Density[93]

The power spectral density of a time-correlation function is defined as

$$S_x(\omega) \equiv \frac{1}{2\pi} \int dt\, e^{-i\omega t} \langle X^*(0) X(t) \rangle \tag{3.111}$$

where X^* is the complex conjugate of X. The Fourier inversion of equation (3.111) yields a time correlation function in terms of the spectral density.

$$\langle X^*(0) X(t) \rangle = \int_{-\infty}^{+\infty} d\omega\, e^{i\omega t}\ S_x(\omega) \tag{3.112}$$

Since $S_x(\omega)$ and $\langle X^*(0) X(t) \rangle$ are Fourier transforms of one another, if one is found experimentally, then the other is also known. Typically in the scattering experiment the spectral density is measured rather than the time-correlation function.

In practice, a signal, X_T, is measured, over a period T, by a detector whose output is proportional to $|X_{To}(t)|^2$. The output of the detector is recorded as an average over the time interval, T, as the mean-square value, $|X|^2$, which is found by setting $t = 0$ in equation (3.112),

$$\langle |X|^2 \rangle = \langle |X(0)| \rangle^2 = \int_{-\infty}^{+\infty} d\omega\, S_x(\omega). \tag{3.113}$$

The property $X(t)$ may be expressed in terms of its Fourier Components over a time interval $(-T/2, T/2)$

$$X_T = \frac{1}{\sqrt{T}} \sum_n X_n \mathrm{e}^{i\omega_n t} \tag{3.114}$$

where the Fourier coefficients are represented by X_n.

The frequency components of X_n are given by $\omega_n = \frac{2\pi}{T} n$ and can be filtered out by employing a filter in the scattering experiment. The filter can be described by defining a set of numbers represented by F_n such that

$$F_n = \begin{cases} 1 & \omega_o \leq \omega \leq \omega_o + \Delta\omega \\ 0 & \text{otherwise} \end{cases}$$

Equation (4.114) becomes

$$X_{To}(t) = \frac{1}{\sqrt{T}} \sum_n F_n X_n \mathrm{e}^{i\omega_n t}. \tag{3.115}$$

The square of (3.115) measured by the detector is

$$|X_{To}(t)|^2 = \frac{1}{T} \sum_{n,n'} F_{n'} F_n X_{n'} \mathrm{e}^{i(\omega_n - \omega_{n'})t} \tag{3.116}$$

The time average value of $X_{To}(t)$ is given by

$$\langle |X_{To}|^2 \rangle = \frac{1}{T} \int_{-T/2}^{T/2} dt \, |X_{To}(t)|^2 \tag{3.117}$$

Substituting equation (3.116) into (3.117)

$$\langle |X_{To}|^2 \rangle = \frac{1}{T} \int_{-T/2}^{T/2} \frac{dt}{T} \sum_{n,n'} F_{n'} F_n X_{n'} e^{i(\omega_n - \omega_{n'})t}. \tag{3.118}$$

Integrating over time

$$\langle |X_{To}|^2 \rangle = \frac{1}{T} \sum_n F_n^2 |X_n|^2. \tag{3.119}$$

Writing this in terms of a time correlation function

$$\langle X^*(t)X(t+\tau)\rangle_T = \frac{1}{T}\int_{-T/2}^{T/2} dt\, X_T^*(t)X_T(t+\tau) \tag{3.120}$$

where $X^*(t)$ is the complex conjugate of $X(t)$ and τ is the relaxation time. Substituting equation (3.114) into (3.120) yields

$$\langle X^*(t)X(t+\tau)\rangle_T = \sum_{n,n'} \frac{1}{T} X_{n'}^* X_n \int_{-T/2}^{T/2} \frac{dt}{T} \mathrm{e}^{i(\omega_n - \omega_{n'})t}\, \mathrm{e}^{i\omega_n \tau}. \tag{3.121}$$

Performing the integration

$$\int_{-T/2}^{T/2} dt\, \mathrm{e}^{i(\omega_n - \omega_{n'})t} = T\delta_{n,n'}.$$

Equation (3.121) becomes

$$\langle X^*(t)X(t+\tau)\rangle_T = \sum_n \frac{|X_n^2|}{T} e^{i\omega_n \tau} \tag{3.122}$$

Multiplying by $\mathrm{e}^{-i\omega_m \tau}$ and integrating over τ yields

$$|X_m|^2 = \int_{-T/2}^{T/2} d\tau\, \langle X^*(t)X(t+\tau)\rangle_T \mathrm{e}^{-i\omega_n \tau}$$

or

$$|X_m|^2 = 2\pi I_X^T(\omega_m) \tag{3.123}$$

where $I_X^T(\omega_m)$ is defined as the spectral density of the time correlation function.

Substituting equation (3.123) into (3.119)

$$\langle |X_{To}|^2\rangle_T = \frac{2\pi}{T}\sum_n I_X^T(\omega_n) F_n^2. \tag{3.124}$$

Equation (3.124) may be written in terms of a range of frequencies

$$\Delta\omega_n = \omega_{n+1} - \omega_n = \frac{2\pi}{T}$$

Transforming equation (3.124) into

$$\langle |X_{To}|^2 \rangle_T = \sum_n \Delta\omega_n I_X^T(\omega_n) F_n^2 \tag{3.125}$$

Writing the sum of equation (3.125) in integral form by $T \to \infty, \Delta\omega_n \to 0$

$$\lim_{T\to\infty} \langle |X_{To}|^2 \rangle_T = \int_{-\infty}^{+\infty} d\omega\, I_X(\omega) |F(\omega)|^2, \tag{3.126}$$

gives the spectral density. Given that the filter has a band-width then

$$|F(\omega)|^2 = \begin{cases} 1 & \omega_o \le \omega \le \omega_o + \Delta\omega \\ 0 & \text{otherwise} \end{cases}$$

If the wavelength lies within the band then equation (3.126) becomes

$$\lim_{T\to\infty} \langle |X_{To}|^2 \rangle_T = I_X(\omega_o)\Delta\omega \tag{3.127}$$

In practice, the spectral density $I_A(\omega_o)$ is found from the time average of $|X_{To}|^2$. Thus by scanning the values of ω_o, the spectrum of the fluctuation of X is determined.

3.8.4 Derivation of the Siegert Relation[94]

The characterization of an electromagnetic field governed by Gaussian statistics consists of two correlation function, a first order and a second order.[95] The Seigert equation relates the two correlation functions $g^{(2)}(\tau)$and $g^{(1)}(\tau)$ in the equation[96]

$$g^{(2)}(\tau) = 1 + \left| g^{(1)}(\tau) \right|^2 \tag{3.128}$$

In deriving the Seigert equation first the total scattered electric field off a suspension of particles

$$E(t) = \sum_k^N E_k e^{i\varphi_k(t)}, \tag{3.129}$$

where N is the number of particles, E_k is the amplitude from individual particles and φ_k is the phase of each individual particle.

The intensity of the scattered field is into a solid angle $d\Omega = \sin\theta\ d\theta\ d\varphi$ is given by

$$I_S = \frac{1}{2}\left(\frac{\varepsilon}{\mu}\right)^{1/2} \langle E_S \cdot E_S^* \rangle$$

where ε is the electric permittivity and μ is the permeability. Thus the intensity as a function of time may be written as

$$I(t) \propto E^*(t)E(t)$$

or

$$I(t) \propto \sum_{k,l} E_k E_l e^{i\varphi_l(t) - i\varphi_k(t)}. \tag{3.130}$$

The amplitude of the autocorrelation function is thus given by

$$G^{(1)}(\tau) = \langle E^* E(t+\tau) \rangle. \tag{3.131}$$

And substituting equation (3.129) into (3.131)

$$= \sum_{k,l}^{N} \langle E_k E_l e^{i\varphi_l(t+\tau) - i\varphi_k(t)} \rangle \tag{3.132}$$

Similarly the second order correlation function for the intensity—intensity correlation is given by

$$G^{(2)}(\tau) = \langle I(t) I(t+\tau) \rangle \tag{3.133}$$

and substituting in for the intensity yields

$$G^{(2)}(\tau) = \langle \sum_{k,l,m,n}^{N} E_k E_l E_m E_n e^{i(\varphi_l - \varphi_k + \varphi_n(t+\tau) - \varphi_m(t+\tau)} \rangle. \tag{3.134}$$

It should be noted that the second order correlation function will vanish unless the indices of the sum are pairwise equal. There are of three different cases for the summation.

Case I: If $k = l$ and $m = n$, but $k \neq m$, the summation is equal to

$$N(N-1)\langle E_k^2 \rangle \langle E_m^2 \rangle = \left(1 - \frac{1}{N}\right) \left| \sum_k^N E_k^2 \right|^2 = \left(1 - \frac{1}{N}\right) \left[G^{(1)}(0) \right]^2. \tag{3.135}$$

Case II: If $k = n$ and $l = m$ but $k \neq l$, the summation is equal to

$$N(N-1)\langle E_k^2\rangle\langle e^{i\varphi_k(t+\tau)-i\varphi_k(t)}\rangle\langle E_l^2\rangle\langle e^{i\varphi_l(t)-i\varphi_l(t+\tau)}\rangle \tag{3.136}$$

$$= \left(1-\frac{1}{N}\right)\left|\sum_k^N E_k^2\langle e^{i\varphi_k(t+\tau)-i\varphi_k(t)}\rangle\right|^2$$

$$\left(1-\frac{1}{N}\right)\left|G^{(1)}(\tau)\right|^2. \tag{3.137}$$

Case III: If $k = l = m = n$, the summation is equal to

$$N\langle E_k^4\rangle = N\langle E_k^2\rangle^2 = \frac{1}{N}\left[G^{(1)}(0)\right]^2. \tag{3.138}$$

Letting $N \to \infty$ in each case and summing the elements of the summation

$$\frac{G^{(2)}}{G^{(2)}(0)} = 1 + \left|\frac{G^{(1)}}{G^{(1)}(0)}\right|.$$

Defining the variables

$$g^{(2)}(\tau) = \frac{G^{(2)}}{G^{(2)}(0)} \tag{3.139}$$

and

$$g^{(1)}(\tau) = \frac{G^{(1)}}{G^{(1)}(0)} \tag{3.140}$$

yields

$$g^{(2)}(\tau) = 1 + \left|g^{(1)}(\tau)\right|^2. \tag{3.141}$$

Equation (3.140) and (3.139) may be written in terms of the normalized field—field and normalized intensity—intensity correlation functions.

$$g^{(1)}(\tau) = \frac{\langle E^*(t)E(t+\tau)\rangle}{\langle E^*(t)E(t)\rangle} \tag{3.142}$$

$$g^{(2)}(\tau) = \frac{\langle I(t)I(t+\tau)\rangle}{\langle I(t)\rangle^2} \tag{3.143}$$

Allowing equation (3.141) to be written as

$$\langle I(t)I(t+\tau)\rangle = \langle E^*(t)E(t)\rangle^2 + \langle E^*(t)E(t+\tau)\rangle^2 \tag{3.144}$$

Although a laser is typically used as the incident light the scattered light will not be purely coherent requiring an instrument parameter β

$$g^{(2)}(\tau) = A\left[1 + \beta\left|g^{(1)}(\tau)\right|^2\right] \tag{3.145}$$

where τ is the delay time and β is a measure of the coherence of the detected field. A is defined as

$$A = \langle I(t)I(t+\tau)\rangle. \tag{3.146}$$

Equation (3.145) relates the intensity—intensity correlation function with the time correlation function for the self beating technique in optical mixing.

---

[1] J. D. Jackson, *Classical Electrodynamics*, 3rd ed., (John Wiley & Sons, New York 1998), p. 456.

[2] F. L. Pedrotti, L. S. Pedrotti, *Introduction to Optics*, 2nd ed. (Prentics Hall, New Jersey, 1993), p. 305.

[3] C. Wu, B. Chu, in *Experimental Methods in Polymer Science: Modern Methods in Polymer Research and Technology*, edited by T. Tanaka, (Academic Press, San Diego, CA 2000), pp. 1.

[4] W. Brown, *Dynamic Light Scattering*, edited by W. Brown, (Clarendon Press, Oxford 1993), Preface.

[5] J. Tyndall, "On the blue colour of the sky, the polarisation of skylight, and the polarisation of light by cloudy matter generally," Phil. Mag. **37**, 384-394 (1869).

[6] J. Tyndall, "On the chemical rays, and the light from the sky," Proc. Roy. Inst. **5**, 429-450 (1869).

[7] J. Tyndall, "On the action of rays of high refrangibility upon gaseous matter, Phil Trans. Roy. Soc. **160**, 333-365 (1870).

[8] Lord Rayleigh, "On the light from the sky, its polarization and coulour," Phil. Mag. **41**, 107-120 (1871).

[9] Lord Rayleigh, "On the scattering of light by small particles," Phil. Mag. **41**, 274-279, 447, (1871).

[10] Lord Rayleigh, "On the electromagnetic theory of light," Phil. Mag. **12**, 81-102 (1881).

[11] Lord Rayleigh, "On the transmission of light through an atmosphere containing small particles in suspension, and on the origin of the blue sky," Phil. Mag. **47**, 375-394 (1899).

[12] Lord Rayleigh, "The Incidence of Light upon a Transparent Sphere of Dimensions Comparable with the Wave-Length," Proc. Roy. Soc. A, **84**, 25-46 (1910).

[13] Lord Rayleigh, "On the Diffraction of Light by Spheres of Small Relative Index," Proc. Roy. Soc. A **90**, 219-225 (1914).

[14] Lord Rayleigh, "On the Scattering of Light by Spherical Shells, and by Complete Spheres of Periodic Structure, when the Refractivity is Small," Proc. Roy. Soc. A **94**, 296-300 (1918).

[15] P. Debye, "Zerstreuung von Röntgenstrahlen," Annalen der Physik (Leipzig) **351**, 809-823 (1915).

[16] G. Mie, "Beiträge zur Optik tuber Medien, speziell kolloidaler Metallösungen," Annalen der Physik (Leipzig) **330**, 377-445(1908).

[17] P. Debye, "Das Verhalten von Lichtwellen in der Nähe eines Brennpunktes oder einer Brennlinie, Annalen der Physik (Leipzig) **335**, 755-776 (1909).

[18] R. Gans, "Uber die from ultramikroskopischer Goldteilchen," Annalen der Physik (Leipzig) **342**, 881 (1912).

[19] R. Gans, "Über die Form ultramikroskopischer Silberteilchen," Annalen der Physik (Leipzig) **352**, 270-284 (1915).

[20] R. Gans, "Strahlunsdiagramme ultramikroskopischer Teilchen," Annalen der Physik (Leipzig) **381**, 29-38 (1925).

[21] M. Smoluchowski, " Molekular-kinetische Theorie der Opaleszenz von Gasen im kritischen Zustande, sowie einiger verwandter Erscheinungen," Annalen der Physik (Leipzig) **25**, 205-226 (1908).

[22] A. Einstein, "Theorie der Opaleszenz von homogenen Flüssigkeitsgemischen in der Nähe des kritischen Zustandes," Annalen der Physik (Leipzig) **14,** 368-391 (1910).

[23] B. J. Berne, R. Pecora, *Dynamic Light Scattering*, ed. (John Wiley & Sons, New York 1976) p.4.

[24] B. J. Berne, R. Pecora, *Dynamic Light Scattering*, ed. (John Wiley & Sons, New York 1976) p.4.

[25] K. R. Ramanathan, Indian J. Phys. **1**, 413 (1927).

[26] Y. Rocard, Annales de Physique (Paris) **10**, 116 (1928).

[27] M. Fixman, "Molecular Theory of Light Scattering," J. Chem. Phys. **23**, 2074-2079 (1955).

[28] L. S. Ornstein, F. Zernike, "Accidental deviation of density and opalescence at the critical point of a substance," Proc. Acad. Sci. Amst. **17**, 793 (1914).

[29] L. S. Ornstein, F. Zernike, Proc. Acad. Sci. Amst. **19**, 1312 (1916).

[30] L. S. Ornstein, F. Zernike, Z. Phys. **27**, 761 (1926).

[31] F. Zernike, T. H. Prins, Z. Physik. **41**, 184 (1927).

[32] P. Debye, " Molecular-weight determination by light scattering," J. Phys. Coll. Chem. **51**, 18-32 (1947).

[33] P. Debye, "Light Scattering in Solutions," J. Appl. Phys. **15**, 338-342 (1944).

[34] B. H. Zimm, "The Scattering of Light and the Radial Distribution Function of High Polymer Solutions," J. Chem. Phys. **16**, 1093-1099 (1948).

[35] B. H. Zimm, "Molecular Theory of Scattering of Light in Fluids," J. Chem Phys. **13**, 141-145 (1945).

[36] L. Brillouin," Über die Fortpflanzung des Lichtes in dispergierenden Medien," Annalen der Physik (Leipzig) **349**, 203-240 (1914).

[37] L. Brillouin, "Diffusion de la lumiere et des rayonnes X par un corps transparent homogene; influence del'agitation thermique," Annales de Physique (Paris) **17**, 88-122 (1922).

[38] V. V. Raman, K. S. Krishnan, "A new type of secondary radiation," Nature **121**, 501-502 (1928).

[39] E. Gross, "Change of wave-length of light due to elastic heat waves at scattering in liquids," Nature **126**, 201 (1930).

[40] E. Gross, "Modification of light quanta by elastic heat oscillations in scattering media," Nature **129**, 722 (1932).

[41] L. Landau, G. Placzek, "Struktur der unverschobenen Streulinie," Phys. Zeitt. Sow. **5**, 172-173 (1934).

[42] R. Pecora, "Doppler Shifts in Light Scattering from Pure Liquids and Polymer Solutions," J. Chem. Phys. **40**, 1604-1614 (1964).

[43] H. Z. Cummins, N. Knable, L. Yeh, "Observation of Diffusion Broadening of Rayleigh Scattered Light," Phys. Rev. Lett. **12**, 150 (1964).

[44] A. Einstein, "Theorie der Opaleszenz von homogenen Flüssigkeitsgemischen in der Nähe des kritischen Zustandes," Annalen der Physik (Leipzig) **14,** 368-391 (1910).

[45] A. T. Forrester, R. A. Gudmandesen, P. O. Johnson, "Photoelectric Mixing of Incoherent Light," Phys. Rev. **99**, 1691 (1955).

[46] W.L. Bragg, "The Diffraction of Short Electromagnetic Waves by a Crystal", Proc. of the Cambridge Phil. Soc. **17**, 43–57 (1914).

[47] N. Wax, *Selected Papers on Noise and Stochastic Processes*, edited by N. Wax (Dover, New York 1954).

[48] R. Zwanzig, "Time-Correlation Functions and Transport Coefficients in Statistical Mechanics," Ann. Rev. Phys. Chem. **16**, 67-102 (1965).

[49] B. J. Berne, R. Pecora, *Dynamic Light Scattering*, ed. (John Wiley & Sons, New York 1976) p11.

[50] R. Zwanzig, "Time-Correlation Functions and Transport Coefficients in Statistical Mechanics," Ann. Rev. Phys. Chem. **16**, 67-102 (1965).

[51] B. J. Berne, R. Pecora, *Dynamic Light Scattering*, ed. (John Wiley & Sons, New York 1976) p. 11.

[52] J. P. Kratohvil, Gj. Deželić, M. Kerker, E. Matijević, "Calibratin of Light Scattering Instruments: A Critical Survey," J. Poly. Sci. **57**, 59-78 (1962).

[53] T. M. Bender, R. J. Lewis, R. Pecora, "Absolute Rayleigh ratios of four solvents at 488 nm," Macromolecules **19**, 244-245 (1986).

[54] J. A. Finnigan, D. J. Jacobs, "Light scattering from benzene, toluene, carbon disulphide and carbon tetrachloride," Chem. Phys. Lett. **6**, 141-143 (1970).

[55] O. J. Ehl, C. Loucheux, C. Reiss, H. Benoit, "Mesure de l' incrément d' indice de refraction de différentes solutions de hauts polymers, et du rapport de Rayleigh de quelques liquids, en function de la temperature," Makromol. Chem. **75**, 35-51 (1964).

[56] R. L. Schmidt, H. L. Clever, "Thermodynamics of Binary Liquid Mixtures by Rayleigh Light Scattering," J. Chem. Phys. **72**, 1529-1536 (1968).

[57] X. Lu, Z. Hu, J. Gao, "Synthesis and Light Scattering Study of Hydroxypropyl Celloulose Microgels," Macromolecules **33**, 8698-8702 (2000).

[58] C. Wu, K. K. Chan, K. Q. Xia, "Experimental Study of the Spectral Distribution of the Light Scattered from Flexible Macromolecules in Very Dilute Solution," Macromolecules **28**, 1032-1037 (1995).

[59] G. Zhang, C. Wu, "The Water/Methanol Complexation Induced Reentrant Coil-to-Globule Transition of Individual Homopolymer Chains in Extremely Dilute Solution," J. Am Chem. Soc. **123**, 1376-1380 (2001).

[60] B. Chu, Q. Ying, C. Wu, J. R. Ford, H. S. Dhadal "Characterization of poly(1,4-phenyleneterephthalamide) in concentrated sulphuric acid. 2: Determination of molecular weight distributions," Polymer **26**, 1408 (1985).

[61] K. Jubota, S. Fujishige, I. Ando, "Single-Chain Transition of Poly(N-isopropylacrylamide) in Water," J. Phys. Chem. **94**, 5154-5158 (1990).

[62] X. Wang, C. Wu, "Light-Scattering Study of Coil-to-Globule Transition of a Poly(N-isopropyacrylamide) Chain in Deuterated Water," Macromolecules **32**, 4299-4301 (1999).

[63] W. Bruchard, M. Schmidt, W. H. Stockmayer, "Information on Polydispersity and Branching from Combined Quasi-Elastic and Integrated Scattering," Macromolecules **13**, 1265-1272 (1980).

[64] C. Wu, S. Zhou, "Laser Light Scattering Study of the Phase Transition of Poly(N-isopropylacrylamide in Water. 1. Single Chain," Macromolecules **28**, 8381-8387 (1995).

[65] M. Meewes, J. Rička, M. De Silva. R. Nyffenegger, Th. Binkert, "Coil-Globule Transition of Poly(N-isopropylacrylamide). A study of Surfactant Effects by Light Scattering," Macromolecules **24**, 5811-5816 (1991).

[66] X. Qui, C. M. S. Kwan, C. Wu, "Laser Light Scattering Study of the Formation and Structure of Poly(N-isopropylacrylamide-co-acrylic acid) Nanoparticles," Macromolecules **30**, 6090-6094 (1997).

[67] K. Schätzel, M. Drewel, "Laser light scattering and correlation techniques for characterization of colloidal suspensions," Z. Physik B **68**, 229-232 (1987).

[68] E. Jakeman, E. R. Pike, S. Sqain, "Statistical accuracy in the digital autocorrelation of photon counting fluctuations," J. Phys. A. : Gen. Phys. **4**, 517-534 (1971).

[69] V. Degiorgoi, J. B. Lastovka, "Intensity—correlation spectroscopy," Phys. Rev. A **4**, 2033-2050 (1971).

[70] B. E. A. Saleh, M. F. Cordoso, "The effect of channel correlation on the accuracy of photon counting digital autocorrelators," J. Phys. A.: Math. Nuc. Gen. **6**, 1897-1909 (1973).

[71] Z. Kojro, "Influence of statistical errors on size distributions obtained from dynamic light scattering data. Experimental limitations in size distribution determination," J. Phys. A: Math. Gen. **23**, 1363-1383 (1990).

[72] K. Schätzel, "Noise on photon correlation data: I. Autocorrelation functions," Quantum Opt. **2**, 287-305 (1990).

[73] K. Schätzel, M. Drewel, "Laser light scattering and correlation techniques for characterization of colloidal suspensions," Z. Physik B **68**, 229-232 (1987).

[74] R. G. W. Brown, "Homodyne Optical Fiber Dynamic Light Scattering," App. Opt. **40**, 4004-4010 (2001).

[75] K. Schätzel, "Correlation techniques in dynamic light scattering," App. Phys. B **42**, 193-213 (2004).

[76] ALV Laser Vertiebsgesellschaft, *ALV/DLS/SLS 5000 Digital Correlator Reference Manual*, June 1993.

[77] T. Tanaka, S. Ishiwata, C. Ishimoto, "Critical Behavior of Density Fluctuations in Gels," Phys. Rev. Lett. **38**, 771-774 (1977).

[78] S. Hirotsu, T. Hirokawa, T. Tanaka, "Volume-phase transitions of ionized N-isopropylacrylamide gels," J. Chem. Phys. **87**, 1392-1395 (1987).

[79] M. Shibayama, T. Fujikawa, S. Nomura, "Dynamic Light Scattering Study of Poly(N-isopropylacrylamide-co-acrylic acid) Gels," Macromolecules **29**, 6535-6540 (1996).

[80] Z. B. Hu, X. Lu, J. Gao, "Hydrogel Opals," Adv. Mater. **13**, 1708 (2001).

[81] R. Hamlen, C. Kent, S. Shafer, "Electrochemically activated contractile polymer," Nature **206**, 1149-1150 (1965).

[82] S. Hirotsu, "Electric-Field Induced Phase Transition in Polymer Gels," Jpn. J. Appl. Phys. Suppl. **24**, 396-388 (1985).

[83] T. Shiga, T. Kurauchi, "Deformation of Polyelectrolyte Gels under the Influence of Electric Field," J. App. Poly. Sci. **39**, 2305-2320 (1990).

[84] T. Tanaka, I. Nishio, S. Sun, S. Nisho, "Collapse of Gels in an Electric Field," Science **218**, 467-469 (1982).

[85] T. Schica, Y. Hirose, A. Okada, T. Kurauchi, "Bending of Poly (Vinal Alcohol) –Poly (Sodium Acrylate) Composite Hdrogels in Electric Fields," J. App. Polymer. Sci. **44**, 249-253 (1992).

[86] C. Nanavati, J. M. Fernandez, "The secretory granule matrix: a fast-acting smart polymer," Science **259**, 963-965 (1993).

[87] L. D. Landau, E. M. Lifshitz, *Electrodynamics of Continuous Media*, 2nd ed. Translated by J. B. Sykes, J. S. Bell, M. J. Kearsley (Pergamon Press, New York 1984) p. 422-462.

[88] H. Hertz, "The Forces of Electrical Oscillations Treated According to Maxwell's Theory, Weidemann's Ann. **36**, 1 (1889); reprinted in Chap. 9 of H. Hertz, *Electric Waves*, Dover, New York 1962).

[89] A. Righi, "Sui campi elettromagnetici e particolarmente su quelli create da cariche elettriche o da poli magnetic in movimento," Nuovo Cimento **2**, 104-121 (1901).

[90] A. Righi, "Sulla questione del campo magneico generato dalla convenzione elettrica, e su alter questioni, Nuovo Cimento **2**, 233-256 (1901).

[91] B. Chu, *Laser Light Scattering,* 2nd ed. (Academic Press, San Diego, CA, 1991) p. 35.

[92] B. J. Berne, R. Pecora, *Dynamic Light Scattering*, ed. (John Wiley & Sons, New York 1976).

[93] B. J. Berne, R. Pecora, *Dynamic Light Scattering*, ed. (John Wiley & Sons, New York 1976) p. 18.

[94] E. O. Schulz-Du Bois, In *Photon Correlation Techniques in Fluid Mechanics* ed., edited by E. O. Schulz-Du Bois, (Springer-Verlag, Berlin 1983) p. 15.

[95] L. Mandel, Prog. Opt. **2**, 181 (1963).

[96] A. J. F. Seigert, "MIT Radiation Lab. Report" *No. 465*, (1943).

CHAPTER 4

ON THE REFRACTIVE INDEX OF HYDROGEL

4.1 Historical Introduction

Greek philosophical thought on the nature of light shaped ideas governing optical natural philosophy in the centuries to follow. Euclid, in 300 BC, made the first mathematical study of light where he described light traveling in straight lines and described the laws of reflection.[1] The Greeks had postulated that eyesight was a result of an interaction from a beam from the observer's eye and a light source transmitted through the element of fire.[2] From this postulate, Euclid went on to reason that light would travel infinitely fast. In the fifth century BC, Empedocles proposed the natural theory of four elements, earth, water, air and fire, composed and governed all interactions in the universe. Lucretius, whose theory was the most accurate among the Greeks but given little attention, proposed that light was composed of minuscule atoms which shoot across the sky when imparted by a shove.[3] The observation of refraction and its importance was not described until around 140 AD by Ptolemy, when measuring the

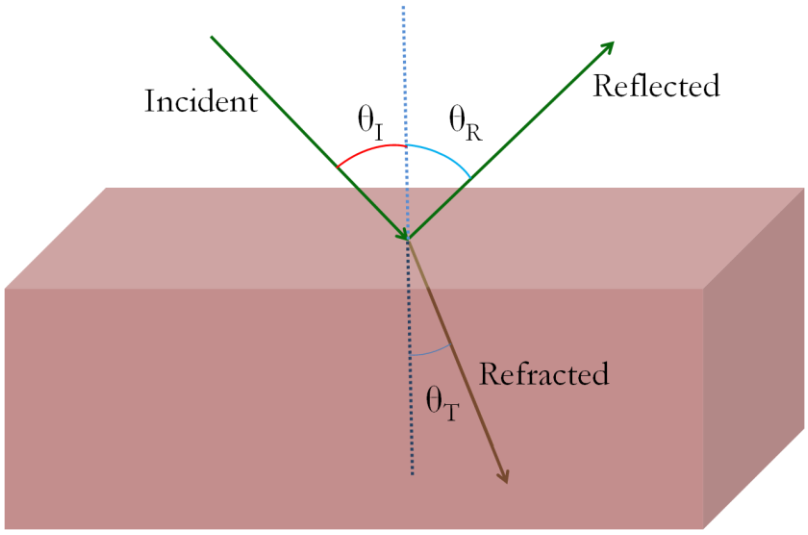

Figure 4.1 A beam of light incident upon a surface will partially reflect and partially be transmitted into the medium at an angle θ_T.

positions of the stars, he realized that light from the stars was being refracted by the atmosphere.[4]

The first ray theory, or geometrical explanation of the refraction of light was proposed by a Dutch astronomer in 1621, and a schematic diagram of the phenomena is shown in Figure 4.1. This became known as Snell's law[5]

$$n_1 \sin\theta_1 = n_2 \sin\theta_2.$$

However, Snell's law was not published by Snell but first by Descartes[6] in 1637 and then by Christian Huygens[7]. Although Descartes does not mention Snell by name it is largely believed he had seen a manuscript of Snell's law. Fermat also derived a refraction law based upon the principle that light will travel the path with requires the least time. Later he was able to show that, although he and Snell had begun with different assumptions, both formulations were in agreement.[8]

The father of modern light theory, Sir Isaac Newton defined refraction in his 1704 treatise on optics as

> "Refrangibility of the Rays of Light, is the Disposition to be refracted or turned out of their Way in passing out of one transparent Body or Medium into another. And a greater or less Refrangibility of Rays, is their Disposition to be turned more or less out of their Way in like Incidences on the Same Medium."[9]

At the time of Newton, two theories of light existed, a corpuscular or particle based theory and a wave theory. Euler in 1746, argued for a wave theory of light because of the difficulties in describing diffraction with a corpuscular theory.[10]

1804 marked the first major evidence of the wave theory of light when Thomas Young published his experimental results on interference patterns.[11] Conducting his experiments at Cambridge, Young showed that when light is passed through two pin holes, the result on the screen is an interference pattern.[12] Young explained the interference phenomena using Newton's wave theory of light.

The polarization of light reflecting of a surface, a phenomenon used in many modern instruments, was discovered by Malus.[13, 14] Malus also introduce the idea of geometric ray optics as straight lines which are relected or refracted at surface interfaces. A more complete understanding of the polarization phenomena reported by Malus, was given by Brewster in 1811, in what became known as Brewster's Law.[15]

$$\theta_p = \tan^{-1}\left(\frac{n_2}{n_1}\right)$$

Brewster stated, "If light is incident under this angle, the electric field vector of the reflected light has no component in the plane of incidence."[16] In other words the maximum polarization of an incident beam occurs when the angle of incidence is such that the refracted ray makes an angle of 90° normal to the surface.

Fresnel, unaware of the work of Huygens, Euler or Young, developed his own wave theory of light based on his observations of diffraction patterns formed by the shadow of a small obstruction.[17, 18] The first accurate measurement of the speed of light came in 1849, when Fizeau used a series of pulses created by a rotating cog wheel to find a value of 300,000 ±1000 km/s.[19] Foucault then used a similar method with a rotating mirror to measure the speed of light in air and water, discovering that the speed was slower in water.[20]

In 1845, Faraday studied light passing through a polarizing medium where the plane of polarization is rotated by a magnetic field parallel to the beam.[21] Faraday also proposed lines of electric and magnetic force to connect particles of mass.[22] With the ideas of Faraday, Maxwell was able to develop the formalism of modern electromagnetic wave theory.

First in 1862, Maxwell discovered that electromagnetic phenomena traveled at the same speed as light. He wrote

> We can scarcely avoid the inference that light consists in the traverse undulations of the same medium which is the cause of electric and magnetic phenomena.[23]

Then two years later in regards to the velocity calculated from his electromagnetic theory

> This velocity is so nearly that of light that it seems we have strong reason to conclude that light itself (including radiant heat and other radiations) is an electromagnetic disturbance in the form of waves propagated through the electromagnetic field according to electromagnetic laws. [24]

The equations derived by Maxwell were published in 1873, and fully describe what is now called classical electromagnetic theory.[25] The theory developed by Maxwell then provided the formalism upon which electromagnetic interactions with matter could be described.

4.2 Theory of Mie Scattering

A light beam interacting with a particle will result in oscillatory motion of electric charges in the particle. The electric charge will then reradiate the energy as scattered light thus becoming a transport mechanism for electromagnetic radiation.

Many theoretical studies have been made regarding the scattering of light by small particles. Lord Rayleigh made the first study of scattering by particles of 'extremely small' size.[26] Interested in the colloidal suspension of metals, Mie calculated the scattering of particles of various sizes.[27] Ryde and Cooper, used Rayleigh's and Mie's formulation, to make an experimental studies of the optical properties of opal glasses.[28,29]

Light scattering can broadly be categorized in three classes: (1) Elastic scattering where the wavelength of the scattering light is unchanged form the incident beam; (2) Quasi-elastic scattering where there are small frequency shifts due to Doppler effects and diffusion broadening; and (3) Inelastic scattering where the scattered light has a wavelength different from the incident beam.

The theory governing elastic scattering depends upon the wavelength of incident radiation, the particle size and the particles optical properties relative to the surrounding medium. Typically, the particle size is expressed as a size parameter

$$\alpha = \frac{\pi D_p}{\lambda}. \tag{4.1}$$

There are many theories which govern scattering processes and only three will be mentioned here. The theory governing the scattering of light incident on a particle with a size parameter, α, falls into three regimes:

(1) $\alpha \ll 1$ Rayleigh Regime;

(2) $\alpha \cong 1$ Mie Regime; and

(3) $\alpha \gg 1$ Geometric Regime.

The poly-(N-isopropylacrylamide) hydrogel discussed in the preceding chapter had diameters on the order of hundreds of nanometers. The wavelengths of operation for an

ellipsometric experiment are also based upon wavelengths of hundreds of nanometers. Thus, Mie scattering will be the Regime that will be discussed. Further, the microgel particles comprised of hydrogel will also be considered spherical.

In understanding Mie scattering, consider that the energy scattered by a particle is proportional to the intensity of the incident beam

$$I_s = C_s I_o \tag{4.2}$$

where C_s is the individual particle scattering cross-section area. Likewise, the absorption energy will be

$$I_a = C_a I_o \tag{4.3}$$

where C_a is the individual particle absorption cross-sectional area.

The law of conservation of energy mandates that any light removed from the incident beam is either scattered or absorbed by the particle. Extinction accounts for both the scattering and absorption that may occur in such an interaction. The extinction sometimes is referred to as a "shadow" of influence that may be greater or less than a particles geometrical cross-section. The extinction is defined as

$$C_E = C_s + C_{a.} \tag{4.4}$$

A scattering efficiency can be defined based upon the particles geometrical cross-section as

$$Q_s = \frac{C_s}{A}. \tag{4.5}$$

The absorbing efficiency is likewise defined allow an extinction efficiency to be defined as

$$Q_E = Q_s + Q_{a.} \tag{4.6}$$

The optical properties of the particle are defined in terms of the complex index of refraction

$$N = n + i\kappa \tag{4.7}$$

where the real part represents the non-absorbing interaction and the imaginary part represents the absorbing interaction. The wavelength is accounted for by allowing both the real and imaginary parts to be functions of the incident wavelength. The refractive index of the surrounding medium is accounted for by defining a normalized refractive index

$$m = \frac{N}{N_0} \tag{4.8}$$

where N_0 is the refractive index of the surrounding medium (i.e. air for atmospheric scattering, or solvent for colloidal suspensions).

An exact solution for the scattering and extinction efficiencies can be derived for a spherical particle.[30]

$$Q_s(m,\alpha) = \frac{2}{\alpha^2}\sum_{j=1}^{\infty}(2j+1)\left[\left|a_j\right|^2 + \left|b_j\right|^2\right] \tag{4.9}$$

$$Q_E(m,\alpha) = \frac{2}{\alpha^2}\sum_{j=1}^{\infty}(2j+1)Re\left[a_j + b_j\right] \tag{4.10}$$

where

$$a_j = \frac{\alpha\psi_j^{'}(x)\psi_j(\alpha) - x\,\psi_j^{'}(\alpha)\psi_j(x)}{\alpha\psi_j^{'}(x)\zeta_j(\alpha) - x\zeta_j^{'}(\alpha)\psi_j(x)} \tag{4.11}$$

$$b_j = \frac{x\,\psi_j^{'}(x)\psi_j(\alpha) - \alpha\,\psi_j^{'}(\alpha)\psi_j(x)}{x\,\psi_j^{'}(x)\zeta_j(\alpha) - \alpha\zeta_j^{'}(\alpha)\psi_j(x)} \tag{4.12}$$

and $x = \alpha m$. The functions $\psi_j(z)$ and $\zeta_j(z)$ are the Riccati—Bessel functions[31]

$$\psi_j(z) = \left(\frac{\pi z}{2}\right)^{\frac{1}{2}} J_{j+\frac{1}{2}}(z) \tag{4.13}$$

$$\zeta_j(z) = \left(\frac{\pi z}{2}\right)^{1/2}\left[J_{j+\frac{1}{2}}(z) + i(-1)^j\, J_{-j-\frac{1}{2}}(z)\right] \tag{4.14}$$

At this point the problem of calculating the coefficients becomes a computational problem that can be solved through various techniques.[32]

4.2.1 Mie Scattering for an Ensample of Particles

The problem of Mie scattering by an ensample of particles is a complex problem that may be simplified with the following assumptions: (1) the average distance between particles is large compared to the particle size; (2) the total scattered intensity is the sum of individual intensities from each particle and (3) the single particle formulation may be used and summed. These assumptions largely depend on the concentration of the sample.

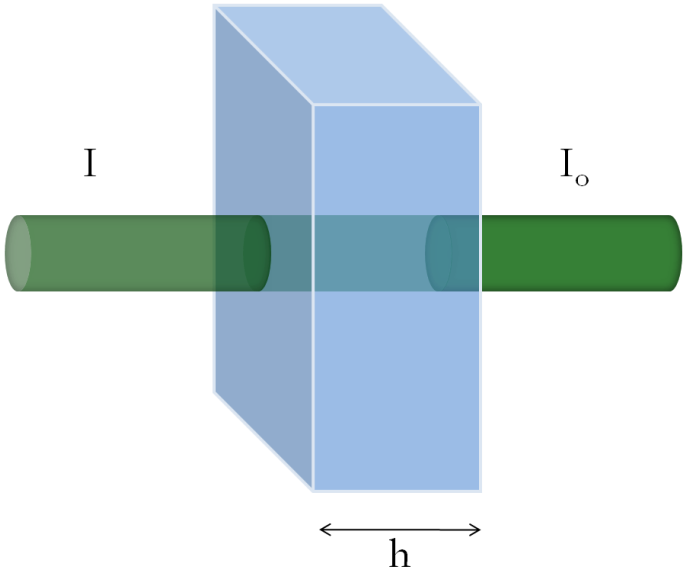

Figure 4.2 A beam of light incident on a medium with thickness h, containing scattering particles.

Light extinction, in a medium being traversed by a beam, occurs through scattering and absorption by particles within the medium, as shown in Figure 4.2. The reduction in intensity can be written

$$dI = -b_E I \, dh, \tag{4.15}$$

where dh is the an incremental length and b_E is the extinction coefficient written for a monodisperse collection of particles in terms of N the total particle number concentration.

$$b_E = C_E N \tag{4.16}$$

A population of monodisperse particles with a number concentration N, allows the extinction coefficient to be related to the dimensionless extinction efficiency

$$b_{ext} = \frac{\pi D_p^2}{4} N Q_{ext}. \tag{4.17}$$

Thus the extinction coefficient can be expressed as the sum of the scattering coefficient b_{scat} and an absorption coefficient b_{abs}

$$b_{ext} = b_{scat} + b_{abs}. \tag{4.18}$$

If the incident intensity at the surface layer, $h = 0$ then the intensity, in equation (4.15), at any point in the layer is given by

$$\frac{I}{I_o} = \mathrm{e}^{-b_E h}. \tag{4.19}$$

This is known as the Beer-Lambert law.[33]

4.2.2 The Extinction Coefficient from Mie Scattering

The poly(N-isopropylacrylamide) microgel undergoes a volumetric change, meaning equation (4.17) is no longer a constant. Further, the degree of shrinking will not be uniform throughout the medium, requiring equation (4.17) to be written in terms of a population distribution $n(D_p)$,

$$b_E(\lambda) = \int_0^{D_p^{max}} \frac{\pi D_p^2}{4} Q_E(m, \alpha) n\big(D_p\big) dD_p \tag{4.20}$$

where D_p^{max} is an upper limit diameter for the particle population. Similarly the coefficient of scattering and absorption may be written as

$$b_s(\lambda) = \int_0^{D_p^{max}} \frac{\pi D_p^2}{4} Q_s(m, \alpha) n\big(D_p\big) dD_p \tag{4.21}$$

and

$$b_a(\lambda) = \int_0^{D_p^{max}} \frac{\pi D_p^2}{4} Q_a(m, \alpha) n\big(D_p\big) dD_p. \tag{4.22}$$

Typically these coefficients are written in terms of a mass distribution function

$$n_M = \rho_p \frac{\pi D_p^3}{6} n(D_p) \tag{4.23}$$

where ρ_p is the scattering particle density. Thus equation (4.20) becomes

$$b_E(\lambda) = \int_0^{D_p^{max}} \frac{3}{2\,\rho_p D_p} Q_E(m,\alpha) n_M(D_p) dD_p. \tag{4.24}$$

If the a mass extinction efficiency is defined as

$$E_E(D_p, \lambda, m) = \frac{3}{2\rho_p D_p} Q_E(m,\alpha) \tag{4.25}$$

then equation (4.25) becomes

$$b_{ext}(\lambda) = \int_0^{D_p^{max}} E_{ext}(D_p, \lambda, m) n_M(D_p) dD_p. \tag{4.26}$$

Likewise, the mass scattering efficiency and mass absorption efficiency are written in a similar fashion

$$E_s(D_p, \lambda, m) = \frac{3}{2\rho_p D_p} Q_s(m,\alpha) \tag{4.27}$$

$$E_a(D_p, \lambda, m) = \frac{3}{2\rho_p D_p} Q_a(m,\alpha). \tag{4.28}$$

4.2.3 Scattering at the Extrema

Consider the light interactions at the two extremes governed by Rayleigh theory, $D_p \ll \lambda$ and geometrical optics, $D_p \gg \lambda$. First, in the Rayleigh regime the scattering efficiency is given by

$$Q_S^R(m,\alpha) = \frac{8}{3}\alpha^4 \left|\frac{m^2-1}{m^2+2}\right|^2. \tag{4.29}$$

Thus, in terms of the particle diameter

$$Q_S^R \approx D_p^4. \tag{4.30}$$

Conversely, in the geometrical regime the scattering efficiency becomes independent of particle size. Therefore, for the Rayleigh regime

$$E_S(D_p, \lambda, m) \approx D_p^3 \qquad D_p \ll \lambda \tag{4.31}$$

and for the geometrical optic regime

$$E_S(D_p, \lambda, m) \approx D_p^{-1} \qquad D_p \gg \lambda. \tag{4.32}$$

The mass scattering efficiency, therefore, increases as D_p^3 for small particles and falls off as D_p^{-1} for the largest particles.

4.2.4 Scattering in the Mie Regime

The scattering dependence on particle size in the Mie regime is not as simple as the extrema examples, and thus requires complex calculations. Many authors have solved this problem with varying assumption and methods.[34, 35 36, 37, 38, 39, 40, 41]

Consider the hydrogel made of identical microspheres that act as scatterers in a medium of water. Generally, for a suspension of identical scatterers in a medium the effective refractive index is

$$n_{eff} = n_m \left[1 + i\left(\frac{3}{2}\frac{f}{\alpha^3}\right) S(0)\right] \tag{4.33}$$

where n_m is the refractive index of the medium and $S(0)$ is the forward scattering amplitude of a particle embedded in the medium calculated from Mie. Mie scattering assumes spherical particles therefore, for non-spherical particles most authors average the particle over all possible orientations to find an effective diameter. The volume fraction f is defined by the scattering spheres and recall α the size parameter from equation (4.1) is

$$\alpha = \frac{\pi D_p}{\lambda}.$$

Although the effective refractive index will be a complicated function depending upon the forward scattering amplitude, it is also inversely dependent upon the volume of the scattering particle. As the size of the particles decrease the scattering will increase and thus the index of refraction will increase as well. Therefore, when the poly(N-isopropylacrylamide) undergoes its volumetric phase change and shrinks, the effective refractive index should increase.

4.3 Ellipsometric Measurement of Refractive Index

Ellipsometry is a method that measures the change in the polarization of light reflecting of thin films, surfaces and interfaces. The basic concept is a collimated beam of mono-chromatic light with a given polarization, impinges upon an unknown sample, the reflected light, having a new polarization is collected and analyzed. Using the incident and reflected polarizations, ratios of two incident polarizations are determined. The ratios then are modeled using properties of the sample interfaces and the optical constants are determined by solving the inverse problem.

4.3.1 Types of Ellipsometry

The methods of performing ellipsometry fall into three categories depending upon the quantities measured: (1) multiple angle of incidence ellipsometry (MAIE) where the ellipsometric measurement ρ as a function of φ [42, 43,44,45,46]; (2) spectroscopic ellipsometry (SE) makes use of the wavelength λ [47, 48, 49, 50]; and (3) variable angle spectroscopic ellipsometry (VASE) measures ρ in with two real variable φ and λ[51, 52].

4.3.2 Introduction to Ellipsometric Theory

An ellipsometer consists of three basic elements, a light source, an unknown medium such as a thin film and a detector. The polarization state is determined by the superposition of orthogonal components of the electric field vector of two co-propagating orthogonally polarized waves. The measurement is made with the relative phase and amplitude of the two propagating beams. Linearly polarized light becomes elliptically polarized as it reflects off the surface and the ellipse of polarization is measured.[53, 54] Light impinging the sample at an oblique angle, is linearly polarized, with the electric-field vibration parallel *p* or perpendicular *s* to the plane of incidence. The reflected light will also be *p*-polarized or *s*-polarized, making *p* and *s* eigen-polarizations of reflection.[55]

The complex reflection coefficients R_P and R_S form the associated eigenvalues for arbitrary electric field components E_{IP} and E_{IS}. They are related through

$$E_{RP} = R_P E_{IP} \tag{4.34}$$

and

$$E_{RS} = R_S E_{IS}. \tag{4.35}$$

Taking the ratio of equation (4.34) and (4.35) to describe the ratio of the complex coefficients for the *p* and *s* polarizations

$$\frac{E_{RS}}{E_{RP}} = \frac{R_P}{R_S}\frac{E_{IP}}{E_{IS}} \tag{4.2.3}$$

and defining

$$\rho = \frac{R_p}{R_s}$$

$$\chi_i = \frac{E_{is}}{E_{ip}}$$

and

$$\chi_r = \frac{E_{rs}}{E_{rp}}$$

ρ may be written as

$$\rho = \frac{\chi_i}{\chi_r} \tag{4.36}$$

where χ_i describes the incident polarization and χ_r describes the reflected polarization.[56]

Consider a function written in polar coordinates

$$\rho = \tan\psi \, e^{i\Delta} \tag{4.37}$$

where ρ is a measure of two ellipsometric angles ψ and Δ such that

$$0 \leq \psi \leq 90°$$

$$0 \leq \Delta \leq 360°$$

The reflection coefficients enter the equation as the relative amplitude attenuation

$$\tan\psi = \frac{|R_p|}{|R_s|} \tag{4.38}$$

and the relative phase shift of p and s upon reflection from the sample is given by

$$\Delta = \arg(R_p) - \arg(R_s) \tag{4.39}$$

Thus the measurement can be made using only the relative amplitude and phase shift and not absolutes.

4.4 Experimental Ellipsometry

Refractive index measurements were made using a commercial spectroscopic ellipsometer shown in figure 4.3 (manufactured by J.A. Woollam Co., model VUV-VASE). The sample was mounted in a vertical position via a vacuum pump on the instrument. The

ellipsometer measures both ψ and Δ and are plotted versus wavelength. Figures 4.4 and 4.5 depict ψ data for a sample of silicon on insulator with different thin films of Si and SiO_2.

Vertical mounting of the ellipsometer posed some difficulties when making an the measurement because the microgel is liquid and the bulk gel is a non-rigid material. Since liquid is free flowing it is necessary to hold it to a surface for a sufficient time period to make a measurement.

Figure 4.3 The commercially available ellipsometer used in measuring the refractive index of the hydrogel.

Previous methods reported in journals have incorporated a rough surface to eliminate back surface scattering and provide a rigid surface to which liquid can be applied.[57] The rigid surface slows the flow of the liquid down the slide long enough for an optical measurement to be made.[58] Although the surface may not be completely smooth, an ellipsometric measurement is ratiometric where the ratio of *p* and *s* reflections are measured,

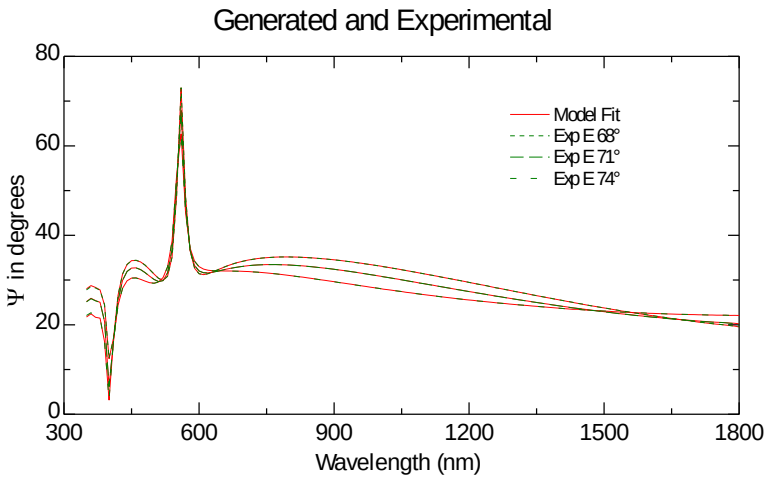

Figure 4.4 Ellipsometric data and model for a sample of SOI with a SiO_2 layer 408.43±0.108nm under a Si layer 1308.00±0.368nm.

not the absolute intensity. This technique allows for rewetting the sample are to account for evaporative losses.

Although this may be an appropriate technique for some liquid samples, it is not for PNIPA gel. Since, PNIPA microspheres are held in a suspension of water, any evaporation and subsequent rewetting would increase the concentration of microspheres yielding a false result.

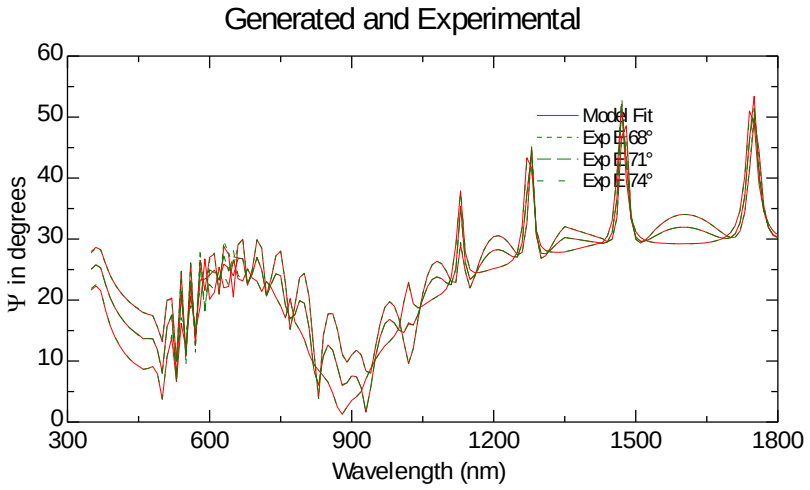

Figure 4.5 Ellipsometric data and model for a sample of SOI with a SiO_2 layer 152±0.0527nm under a Si layer 68.558±0.00321nm.

The technique used in this experiment incorporated the rough surface method where a frosted glass slide was used to eliminate back surface scattering of the underlying substrate and a Corning glass cover slip covering the suspension of microspheres. The purpose of the cover slip is twofold: first it reduces the exposed surface area, reducing evaporation and second it maintains an even layer of liquid in a vertical position. The

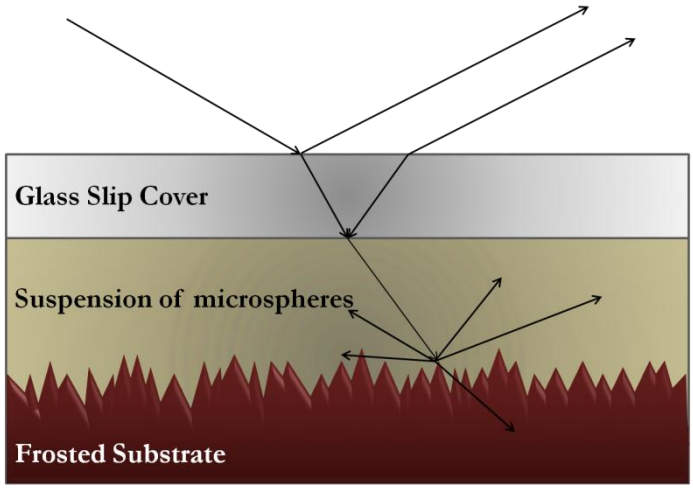

Figure 4.6 A schematic of the sample holder showing the rough surface, the suspended microgel layer and the glass cover slip.

configuration depicted in figure 4.6 shows the frosted substrate, the Aqueous PNIPA and the confining glass cover slip.

4.5 Ellipsometric Results

The data acquired from the ellipsometer and the model fit data are depicted in figure 4.7. In figure 4.7 the model data appears to coincide well with the model fit data. Further, as a general indication of the closeness of the fit, figure 4.8 shows the difference between the measured data and the model fit data. The VASE software provided by the manufacturer of the ellipsometer was used to build a model. The gel layer was fit using the Cauchy dispersion relation,

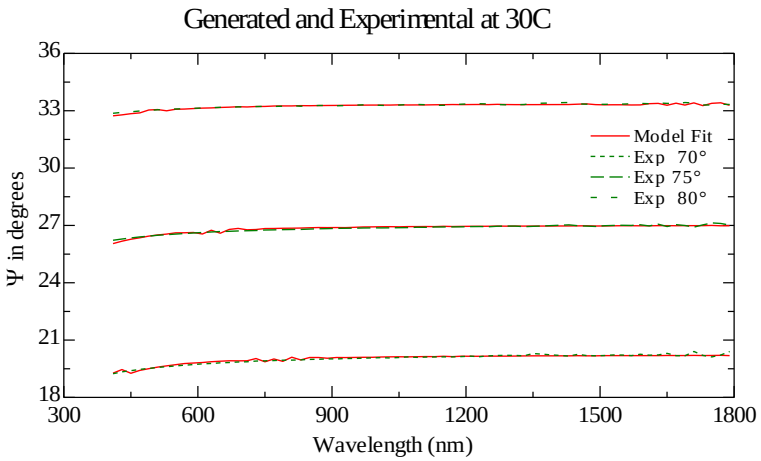

Figure 4.7 Data taken for a suspension of poly(N-isopropylacrylamide) microspheres, at three different angles.

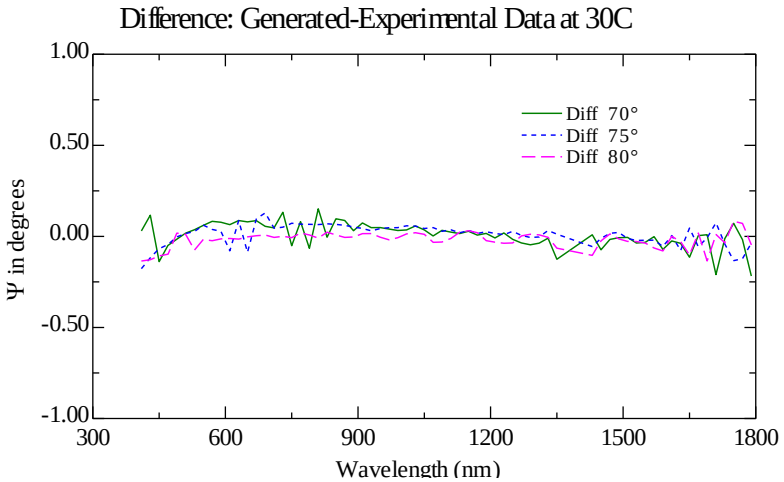

Figure 4.8 The differences between the model and the data. If the model were a perfect fit the lines would be absolutely flat.

$$n(\lambda) = A_n + \frac{B_n}{\lambda^2} + \frac{C_n}{\lambda^4} \tag{4.40}$$

Where λ is the wavelength of incident light, A_n, B_n, and C_n are fit parameters. The Cauchy relation is particularly adept at describing the dispersion of the index of refraction in materials in which the spectral ranges in which the given material is transparent.

Data was collected at three angles 70°, 75° and 80° over a range from 300nm to 1800 nm, as shown in figure 4.9. However, the model was constructed to fit only data ranging from 400 nm to 1800 nm to avoid lower wavelength regions which are strongly absorbed by the glass cover slip. Further, the AutoRetarder was used on the VUV vase

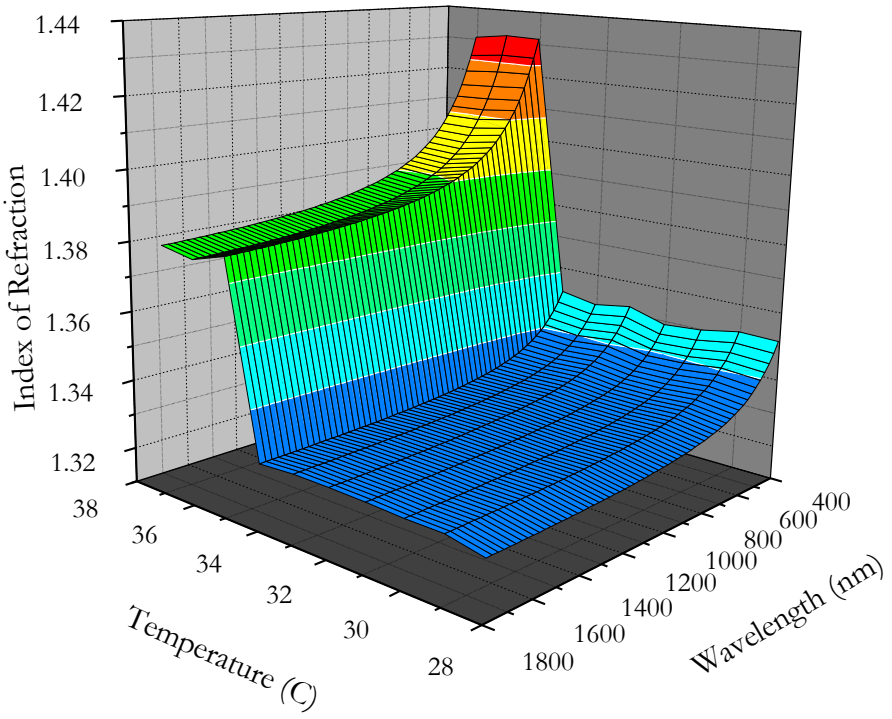

Figure 4.9 Refractive index data showing the change in refractive index in relation to wavelength and temperature.

ellipsometer. The AutoRetarder distinguishes non-polarized light from circularly polarized light by use of a compensator in the optical path.[59] Depolarization of the light beam can be caused from a non-uniform film, backside reflection from a transparent substrate, spatial

incoherence of a patterned film or from the spectral resolution.[60] In figure 4.8, the difference between the measured data and the constructed model show a close fit. If the model were perfectly matched the difference would be a straight line at ψ = 0.

Figure 4.9 shows the results for the survey of refractive index over the spectral range 400 nm to 1800 nm at temperatures ranging from 28°C to 37°C. A rapid increase in the index of refraction can be seen around the temperature of 34°C, which corresponds to the critical temperature where the gel sphere collapses. This increase in index of refraction is what is expected when scattering spheres shrink and increase the scattering of light. In figure 4.10, we look at a cross section of figure 4.9 at the wavelength of 1500

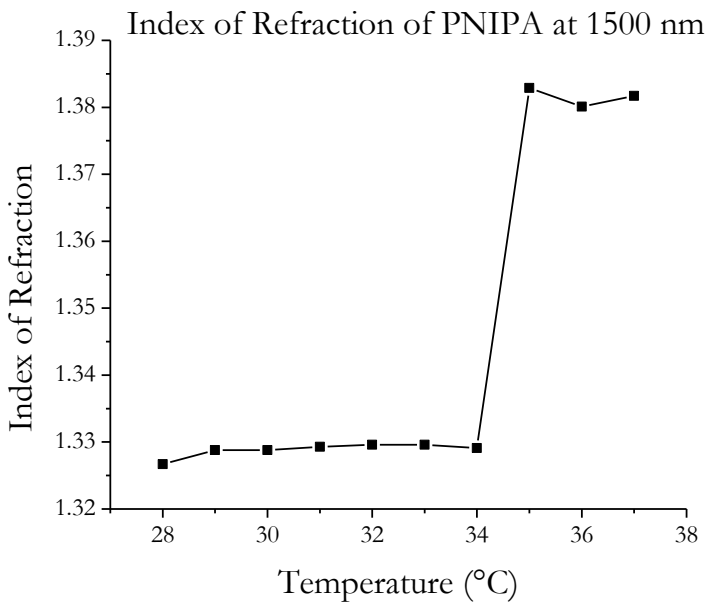

Figure 4.10 The refractive index measured at 1500nm.

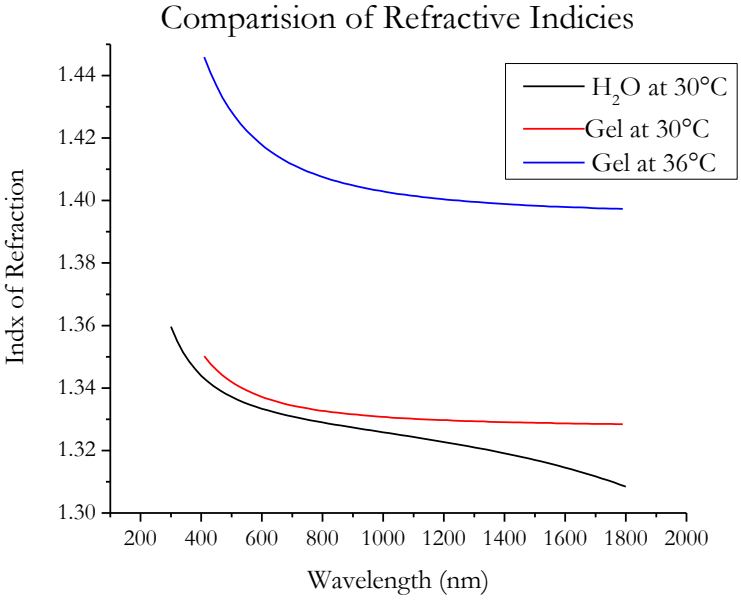

Figure 4.11 A plot showing the refractive index change of water, hydrogel microspheres below LCST and hydrogel microspheres above LCST.

nm, and see the jump in refractive index more clearly.

We expect that the refractive index of PNIPA at a temperature below the critical temperature would be comparable to water[61] since the gel particles are engorged with water and not strongly scattering light. Figure 4.11 shows that indeed the index of refraction is close to water at the shorter wavelengths. The two curves do diverge at the longer wavelengths, however this is due to the different methods used to calculate the indices. The significant finding is the change in index of refraction when the temperature is varied from below the critical temperature to above the critical temperature.

---

[1] Euclid, *Optica*, (300 BC); translated by Heiberg; in M. R. Cohen, I. E. Drabkin, *A source book in Greek science*, (Cambridge, Harvard University Press, 1958) p. 257-168.

[2] Aristotle, *On the Soul II* (335 BC) ; translated by R. D. Hicks (Cambridge 1907); in M. R. Cohen, I. E. Drabkin, *A source book in Greek science*, (Cabbridge, Harvard University Press, 1958) p. 285-286.

[3] Lucretius, *On the Nature of Things II*, (55 BC); translated by Cyril Bailey (Oxford, 1921); in M. R. Cohen, I. E. Drabkin, *A source book in Greek science*, (Cabbridge, Harvard University Press, 1958) p. 212-217.

[4] Ptolemy, *Almagest*, (140 AD); in M. R. Cohen, I. E. Drabkin, *A source book in Greek science*, (Cambridge, Harvard University Press, 1958) p. 212-217.

[5] J. A. Vollgraff, "Snellius' Notes on the Reflection and Refraction of Rays," Osiris, **1**, 718-725 (1936).

[6] R. Descartes, *La Dioptrique*, (Leiden, 1639); Discourse on Method, Optics, Geometry and Meteorology (Indianapolis: Bobbs-Merrill 1965).

[7] C. Huygens, *Traité de la lumière*, (Leyden 1960).

[8] P. de Fermat, "Principle of Least Time," Oeuvres de Fermat vol 2, (Paris, 1891) p. 354.

[9] Isaac Newton, *Opticks: or, A Treatise on the Reflexions, Refractions, Inflexions and Colours of Light*, (Printers of the Royal Society, London, 1705).

[10] L. Euler, "Nova theoria lucis et colorum," Opuscala varii argumenti **1**, 169 (Berlin 1746).

[11] T. Young, "The Bakerian Lecture: On the Theory of Light and Colours," Phil. Trans. Roy. Soc. London, **92**, 12-48 (1802); T. Young, "An Account of Some Cases of the Production of Colours, not Hitherto Describes," Phil. Trans. Roy. Soc. **92**, 387-397 (1802).

[12] T. Young, "The Bakerian Lecture: Experiments and Calculations Relative to Physical Optics," Phil. Trans. Roy. Soc (London) **94**, 1-16 (1804).

[13] É. L Malus, "Mémoire sur la mesure du pouvoir réfringent des corps opaques," Nouveau Bull. D. Sci. par. la Soc. Philimatique 1, 77-81 (1807); Also in"Ueber die Messung des Brechungsvermögens der undurchsichtigen Körper," Annalen der Physik. **31**, 225-234 (1809).

[14] É. L. Malus "Sur une propriété de la lumière réfléchie," Nouveau Bull. D. Sci. par. la Soc. Philimatique **1**, 266-269 (1808), translation in Ann. Phys. 31, 286-297, 1809.

[15] D. Brewster, "On the Laws Which Regulate the Polarisation of Light by Reflexion from Transparent Bodies," Phil. Trans. Roy. Soc. **105**, 125-159 (1815).

[16] D. Brewster, "Experiments on the Depolarisation of Light as Exhibited by Various Mineral, Animal and Vegetable Bodies, with a Reference of the Phenomena to the General Principles of Polarisation, Phil. Trans. Roy. Soc. **105**, 29-53 (1815).

[17] A. Fresnel, " Mémoire sur la diffraction de la lumière," Ann. Chim, et Phys. **1**, 239-281 (1816).

[18] A. Fresnel, *Oeuvres Complètes d'Augustin Fresnel*, Edited by H. de Senarmont, É. Verdet, L. Fresnel, (IImprimiere Imperiale, Paris 1866-1870)

[19] A. H. L. Fizeau, Compt. Rend. Acad. Sci. Paris **30**, 562, 771 (1850).

[20] L. Foucault, Compt. Ren. Acad. Sci. Paris **30,** 551 (1850).

[21] M. Faraday, *Extraits des recherché expérimentales en électricité,* edited by Germaine Hirtz (Paris, Gauthier-Villars, 1967).

[22] J. Tyndall, *Faraday as a discoverer*, electronic ed. (Champaign, Ill, Project Gutenberg; Boulder, Co, Netlibrary 1999).

[23] J. C. Maxwell, On the physical lines of force IV. The teory of molecular vortices applied to the action of magnetism on polarized light," Proc. Roy. Soc. **13**, 531-536 (1862).

[24] J. C. Maxwell, "A dynamical theory of the electromagnetic field," Phil. Trans. Roy. Soc. **155**, 459-512 (1865).

[25] J. C. Maxwell, "On double diffraction of a viscous fluid in motion," Proc. Roy. Soc. **22**, 46-47 (1873).

[26] Lord Rayleigh, "On the Light from the Sky, Its Polarization and Color," Phil. Mag. **41**, 107-120 (1871).

[27] G. Mie, "Beiträge zur Optik trüber Medien, speziell kolloidaler Metallösungen," Annalen der Physik **330**, 377-445 (1908).

[28] J.W. Ryde, B. S. Cooper, "Scattering of Light by Turbid Media—Part I," Proc. Roy. Soc. Series A **131**, 451 (1931).

[29] J.W. Ryde, B. S. Cooper, "Scattering of Light by Turbid Media—Part II," Proc. Roy. Soc. Series A **131**, 464 (1931).

[30] C. F. Bohren, D. R. Huffman, *Absorption and Scattering of Light by Small Particles*, (Wiley, New York 1983).

[31] M. Abramowitz, I. A. Stegun, "Riccati-Bessel Functions." §10.3 in Handbook of Mathematical Functions with Formulas, Graphs, and Mathematical Tables, (Dover, New York 1972) p. 445.

[32] N. C. Wickramasinghe, *Light Scattering Functions for Small Particles with Applications in Astronomy*, (Wiley, New York 1973).

[33] A. Beer, "Versuch die Absorptions-Verhältnisse des Cordierites für rothes Licht zu bestimmen," Ann. der Physik **84**, 37-44 (1951); A Beer, "Bestimmung der Absorption des rothen Lichts in farbigen Flüssigkeiten," Ann. der Physik **86**, 78-88 (1852).

[34] R. G. Berra, A. García-Valenzuela, "Coherent reflectance in a system of random Mie scatterers and its relation to the effective-medium approach," J. Opt. Soc. Am. A **20**, 296-311 (2003).

[35] A. Reyes-Coronado, A. García, C. Sánchez-Pérez, R. G. Barrera, "Measurement of the effective refractive index of a turbid colloidal suspension using light refraction," New J. Phys. **7**, 89 (2005)

[36] A. García-Valenzuela, R. G. Barrera, "Electromagnetic response of a random half-space of Mie scatterers within the effective medium approximation and the determination of the effective optical coefficients," J. Quant. Spectrosc. Radiat. Transfer **79-80**, 627-647(2003).

[37] L. Tsang, J. A. Kong, *Scattering of Electromagnetic Waves: Advanced Topics*, (Wiley, New York 2001).

[38] L. Tsang, J. A. Kong, "Effective propagation constants for coherent electromagnetic waves propagating in media embedded with dielectric scatterers," J. Appl. Phys. **53**, 7162-7173 (1982).

[39] M. Lax, "Multiple scattering of waves II. The effective field in dense systems," Phys. Rev. **85**, 621-629 (1952).

[40] C. F. Bohren, D. R. Huffman, *Absorption and Scattering of Light by Small Particles*, (Wiley, New York 1983).

[41] H. C. van de Hulst, *Light Scattering by Small Particles*, (Wiley, New York 1957).

[42] M. M. Ibrahim, N. M. Bashara, "Parameter-Correlation and Computational Considerations in Multiple-Angle Ellipsometry," J. Opt. Soc. Am. **61**, 1622-1629 (1971).

[43] O. Hunderi, "On the problems of multiple overlayers in ellipsometry and a new look at multiple angle of incidence ellipsometry," Surf. Sci. **61**, 515-520 (1976).

[44] J. Humlicek, "Sensitivity extrema in multiple-angle ellipsometry," J. Opt. Soc. Am. A **2**, 713-722 (1985).

[45] W. H. Weedon, S. W. McKnight, A. J. Devaney, "Selection of optimal angles for inversion of multiple-angle ellipsometer and reflectometry equations," J. Opt. Soc. Am. A **8**, 1881-1891 (1991).

[46] R. Roseler, *Infrared Spectroscopic Ellipsometry*, Akademie-Verlag, Berlin (1990).

[47] D. E. Aspnes, "Characterization of Materials and Interfaces by Visible-Near UV Spectrophotometry and Ellipsometry," J. Mat. Educ. **7**, 849-901 (1985).

[48] P. J. McMarr, K. Vedam, J. Narayan, "Spectroscopic Ellipsometry: A New Tool for Nondesctructive Depth Profiling and Characterization of Interfaces," J. Appl. Phys. **59**, 664-701 (1986).

[49] R. Drevillon, "Spectroscopic Ellipsometry of Ultrathin Films: From UV to IR," Thin Solid Films **163** 157-166 (1988).

[50] R. W. Collins and Y. –T. Kim, "Ellipsometry for Thin-Film and Surface Analysis," Anal. Chem. **62**, 887A-900a (1990).

[51] P. G. Snyder, M. C. Rost, G. H. Bu-Abbud, J. A. Woollam, J. Appl. Phys. **60**, 3293-3302 (1986).

[52] J. Hilfiker, J. Woollam, G. Mowry, P. Chow, J. Elman, "Automated Spectroscopic Ellipsometry," Industrial Physicist **2**, 30-34 (1996).

[53] A. Rothen, "The Ellipsometer, an Apparatus to Measure Thickness of Thin Surface Films," Rev. Sci. Instrum. **16**, 26-30 (1945).

[54] A. C. Hall, "A century of ellipsometry," Surf. Sci. **16**, 1-13 (1969).

[55] R. M. A. Azzam and N. M. Bashara, *Ellipsometry and Polarized Light*, (North-Holland, New York 1977) p. 97.

[56] R. M. A. Azzam, N. M. Bashara, *Ellipsometry and Polarized Light*, (North-Holland, New York 1977) p. 28.

[57] R. A. Synowicki, T. E. Tiwald, U.S. Patent No. 6,738,139 (18 May 2004).

[58] R. A. Synowicki, et al. "Fluid refractive index measurements using rough surface and prism minimum deviation techniques," J. Vac. Sci Technol. B **22**, 3450 (2004).

[59] S. E. Green, C. M. Herzinger, B. D. Johs, J. A. Woollam, U.S patent 5,757,494 (26 May 1998).

[60] J. N. Hilfiker, B. Singh, R.A. Synowicki, C. L. Bungay, "Optical characterization in the vacuum ultraviolet with Variable Angle Spectroscopic Ellipsometry: 157nm and below," SPIE Microlithography Conf. (2000).

[61] P. Schiebener, J. Straub, J. M. H. Levelt Sengers, and J. S. Gallagher, "Refractive index of water and steam as function of wavelength, temperature and density," J. Phys. Chem. Ref. Data **19**, 677-717 (1990).

CHAPTER 5

PHOTOLUMINESCENCE OF ENCAPSULATED QUANTUM DOT—HYDROGEL HYBRID MATERIALS

5.1 A History of Luminescence

One of the first documented references to luminescence is found in Shih Ching or Book of Odes (1500-1000 B.C.), which states in verse "i-yao hsiaohsing" or "Glowing intermittently are the fireflies."[1] Perhaps the first industrial uses of luminescent material is reported by the Chinese in regards to a Japanese boat which was covered by paint derived from seashells that luminesced.[2] The Greeks with their curiosity of natural philosophy wrote about luminescent bodies. Aristotle, for example, in De Anima states

> "Some things, indeed, are not seen in daylight, though they produce sensation in the dark: as for example the things of fiery and glittering appearance for which there is no distinguishing name, like fungus (mukes) horn (keras) and the head scales and eyes of fishes. But in no one of these cases is the proper color seen. Why these objects are seen must be discussed elsewhere."[3]

Many species of fungi are luminescent and the bacteria on dead fish are also luminescent. One branch of the study of luminescence is the study of phosphors, which is derived from Greek meaning "light bearer." However, the term was not used in reference to an actual material until an alchemist named Vincentinus Casiarolo of Bologna, Italy discovered a glass stone at the foot of a volcano. Intending to create a noble metal he fired the stone.

Ultimately he failed in changing it to a metal but did create a substance, which emitted red light in the dark after being exposed to sunlight. In figure 5.1, we see a representation of the stone printed after its discovery.[4] Modern chemistry has shown that the rock was in fact was barite and once sintered became BaS, a well known phospor material.[5]

Figure 5.1 An Allegorical representation of the magical phenomenon of light emission by the Stone of Bologna (M. Cellio).

Unfortunately with the onset of the Middle Ages, reports of luminescent phenomena ceased. It wasn't until the late 15th century and early 16th century that reports began to be written. One of the most prevalent, is the ring of Catharine of Aragon, Queen of England (1485-1536), which is reported to have luminesced at night.[6] Most likely, the jewel was a diamond since some are known to be phosphorescent. The first serious scientific study of luminescent behavior and its causes were performed by Francis Bacon in the early 17th century.[7]

As scientific thought began to flourish, rudimentary experimental based theories concerning luminescence began to emerge, although they still lacked the quantum mechanical understanding. Stokes showed that the incident light differed in color or refrangibility from the emitted light.[8] In particular, he stated *Stokes' Law*, that the light emitted at longer wavelengths was less frangible than the incident light. Becquerel in 1867 measured the decay in the luminescence in uranyl salts and showed that the decay was either exponential or hyperbolic which he credited to monomolecular decay and bimolecular decay.[9] However, in 1928 Leonard suggested that the decay of the alkaline

earth sulfides were monomolecular and the hyperbolic decay was the superposition of centers with different decay constants.[10] These experimental findings had to wait for the development of quantum mechanics for a complete explanation.

5.2 Theoretical Development

In this chapter luminescence is discussed as a general process where a material absorbs a photon, elevating the material to an excited electronic state, which in turn decays emitting an electromagnetic wave. Luminescence emissions are different from other emissions such as Raman effect, Rayleigh scattering, Compton scattering and Cherenkov radiation in that there is a short delay between excitation and emission. These delay times are long when compared to period of radiation λ/c .[11]

The terms used for light emission are dependent upon whether the material is an organic or inorganic material.[12, 13] For an inorganic molecule, fluorescence is the light emission caused by the absorption a photon followed by the virtually instantaneous emission at a different wavelength that stops when the incident light stops.

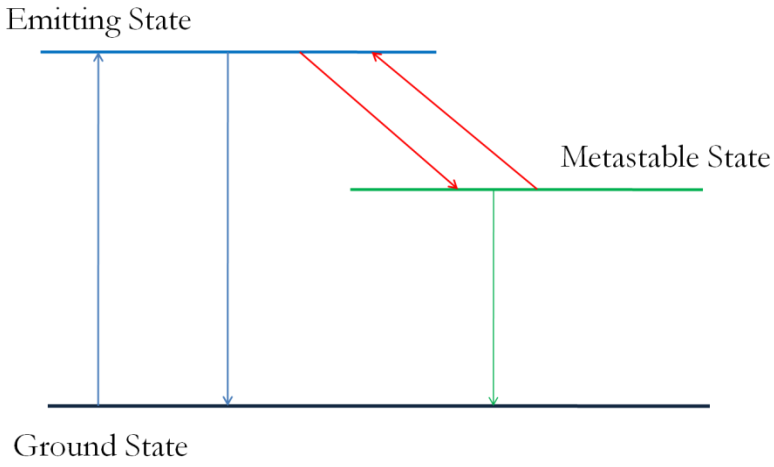

Figure 5.2 A basic schematic of a two level system with a metastable state.

Phosphorescence in an inorganic molecule is defined as the after-glow of the material once the exciting radiation ceases. Conversely, in an organic molecule fluorescence is emission

from a singlet excited state and phosphorescence is emissions from a triplet excited state.[14, 15]

5.2.1 Basic Model Development

Beginning in 1933 Jablonski, proposed an energy level model for the emitting center of organic molecules.[16] His visualization of luminescence included a thermally activated metastable state shown in figure 5.2. In this system an incident photon excites the system, which in turn decays to a metastable state and finally decays back to the ground state emitting a photon. The theory became further developed with the introduction of ion impurities in the atomic lattice. Seitz in his study on thamllium ions found that homopolar forces between the excited ion and its neighbor depressed singlet excited levels more so than triplet.[17] Figure 5.3, a modification of figure 5.2 came to emerge as a more accurate picture.[18]

Luminescence as described by quantum mechanics built a theory of band structures based on electrons in periodic potentials. Seitz and Mott theory included spectral differences based on the nuclear coordinates of the atoms comprising the material.[19] Further complexities in the theory of luminescent behavior were added to account for charge transfer between

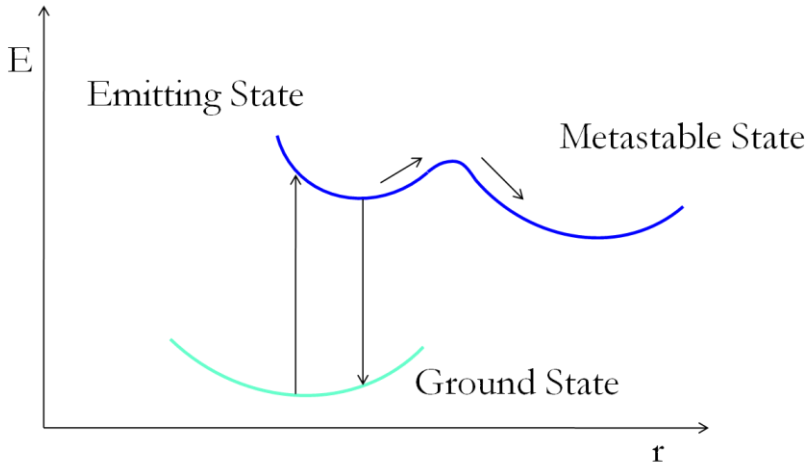

Figure 5.3 The configuration model of luminescence developed by Seitz (1938) and Mott (1939).

impurities and defect crystals which involved both bands and localized electronic states.[20, 21]

Quantum confinement in quantum dots began to be studied in the early 1980s as a result of the work of Efros and Ekimov[22, 23] at the Ioffe in St. Petersburg and Brus[24, 25] at Bell Labs. These seminal studies involved correlating the size of the semiconductor to its emitting color. Other studies soon followed that described oscillator strengths[26] in different semiconductor materials[27] and radiative lifetimes[28] of low dimensional structures. The key to understanding the radiative transitions in quantum dots begins with an understanding of the density of states in a low dimensional system.

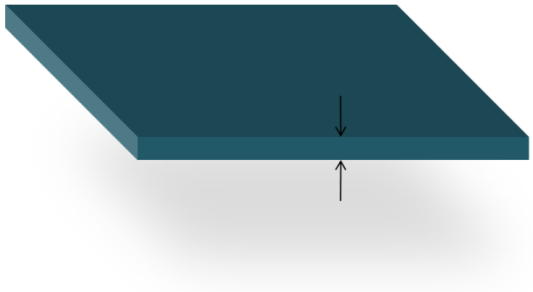

Figure 5.4 2D structure with quantum confinement in the z-direction.

5.3 Low Dimensional Density of States

The density of states for a 3D bulk material system is given by

$$\rho_{3D}(E) = \frac{1}{2\pi^2}\left(\frac{2\mu}{\hbar^2}\right)^{3/2}\left(E - E_g\right)^{1/2}.$$

In this section the density of states for low dimensional systems, 2D, 1D and 0D will be discussed.

Consider the 2D laminar sheet, in figure 5.4, where electrons are free to move in the x and y-directions but are confined in the z-direction. The density of states for a 2D structure is the number of states per unit area and unit energy. The wavefunction from elementary quantum mechanics for an infinitely deep potential well is

$$\psi_n(z) = \left(\frac{2}{L_z}\right)^{1/2}\cos\frac{n\pi z}{L_z}, \qquad (5.1)$$

and the energies arising from such a system are given by

$$E_n = \frac{\hbar^2}{2m}\left(\frac{\pi n}{L_z}\right)^2, \qquad n = 1, 2, 3, \ldots \tag{5.2}$$

However, in the x and y-directions the Schrödinger equation is separable, thus the energy in the xy-plane is

$$E_{xy} = \frac{\hbar^2}{2m}\left(k_x^2 + k_y^2\right) \tag{5.3}$$

Thus the total energy for the electron and holes respectively will be the sum of E_n, E_{xy}, and E_g the gap energy. The energy levels for electrons and holes are given by

$$E_e = E_g + \frac{\hbar^2}{2m_e^*}\left[\left(\frac{\pi n_h}{L_z}\right)^2 + \left(k_x^2 + k_y^2\right)\right] \tag{5.4}$$

$$E_e = E_h + \frac{\hbar^2}{2m_h^*}\left[\left(\frac{\pi n_e}{L_z}\right)^2 + \left(k_x^2 + k_y^2\right)\right] \tag{5.5}$$

where m_e^* is the effective mass of the electron and m_h^* is the effective mass of the hole. The space reduced from the 3D to the 2D leaves only coordinates in the xy-plane. In figure 5.5 the surface energy is a constant circle in the k-space with the coordinates k_x and k_y.

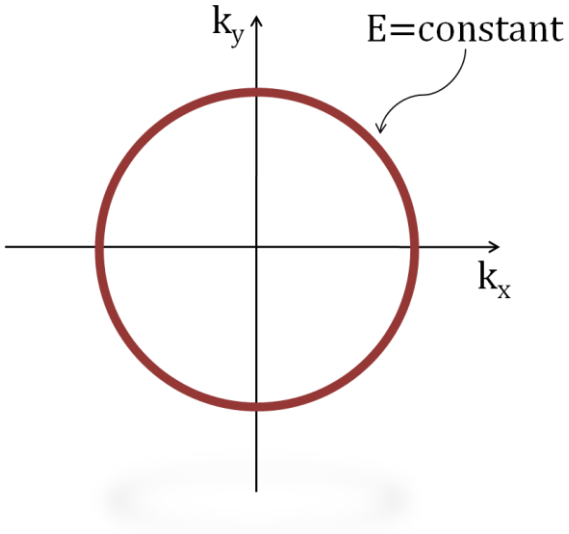

Figure 5.5 The surface energy for a 2D system in k-space.

The total energy of the electronic system, for an optical transition, is the sum of the energy for the electron and the hole

$$E = E_e + E_h \tag{5.6}$$

or

$$E = E_g + \frac{\hbar^2}{2\mu}\left[\left(\frac{\pi n}{L_z}\right)^2 + \left(k_x^2 + k_y^2\right)\right] \tag{5.7}$$

where μ is the reduced mass, defined as

$$\frac{1}{\mu} = \frac{1}{m_e^*} + \frac{1}{m_h^*}$$

The volume of k-space is found by

$$V_{2D}(E) = dE \int_S \frac{1}{\nabla_k E(k)} dS = \frac{2\pi\mu}{\hbar^2} \tag{5.8}$$

Since two electrons with opposite spin can fill the same phase space the density of states is

$$\rho_{2D}(E) = \frac{\mu}{\pi\hbar^2} \ (E \geq E_0). \tag{5.9}$$

Assuming the semiconductor has more than one quantum state, the total density of states can be written as

$$\rho_{2D}(E) = \frac{\mu}{\pi\hbar^2} \sum_n \theta\big(E - E_n - E_g\big) \tag{5.10}$$

where θ is a step function, E_n are quantized energy states and E_g is the gap energy.

Similarly, for a 1D system

$$V_{1D}(E) = \int_S \frac{\delta(k_x - k_{x0})}{\nabla_k E(k_x)} dS = \sqrt{\frac{\mu}{2\hbar^2} \frac{1}{(E - E_0)}} \quad (E \geq E_0). \tag{5.11}$$

More generally

$$V_{1D}(E) = \sqrt{\frac{\mu}{2\hbar^2} \frac{1}{(E - E_m - E_n - E_g)}}\,. \tag{5.12}$$

Recall that in phase space two electrons with opposite spin give a volume of 2π, thus

$$\rho_{1D}(E) = \frac{(2\mu)^{1/2}}{\pi\hbar} \sum_{m,n} \frac{1}{\big(E - E_m - E_n - E_g\big)^{1/2}}. \tag{5.13}$$

Finally, for a 0D system, the electron is confined in all three spatial dimensions leaving no k-space for the electrons to fill. Thus, each quantum state of a 0D system is occupied by only two electrons.

The density of states in such a case is given by

$$\rho_{0D} = 2\sum_{l,m,n} \delta\left(E - E_l - E_m - E_n - E_g\right) \tag{5.14}$$

where δ is a delta function and the indices l, m, and n refer to quantum numbers associated with each spatial direction.

5.4 Basic Theory of Quantum Dots

The density of states of a material describes the allowed energy of the particular material. A bulk 3D material has a continuum of states,

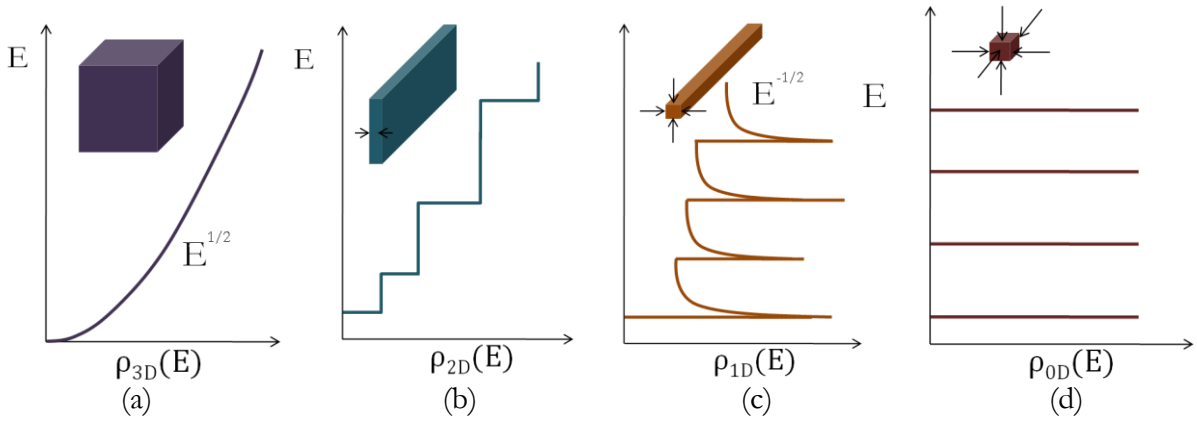

Figure 5.6 The density of states for (a) 3D bulk materials, (b) 2D layer structures; (c) 1D quantum wires; (d) 0D quantum dots.

shown in figure 5.6(a). The optical properties of a 3D system differ fundamentally from low-dimensional systems. In low-dimensional systems spatial confinement of holes and electrons radically alter the states. Layered 2D structures, figure 5.6(b) exhibit a step function density of states. Often 2D structures are used as quantum wells commonly used in electronic applications. In 1D structures, figure 5.6(c) there is only one-degree of freedom, creating a quantum wires. 0D structures, figure 5.6(d) are structures that exhibit discrete energy states and called quantum dots.

Quantum dots are nanostructures composed of semiconductor materials having periodic groups of class II-VI, III-V or IV-VI materials. Quantum dot semiconductors are a distinctive from bulk semiconductors in that their diameters are on the order of 2-10 nanometers. However, to understand the radiative processes in the quantum dot, the processes in the bulk structure will first be discussed.

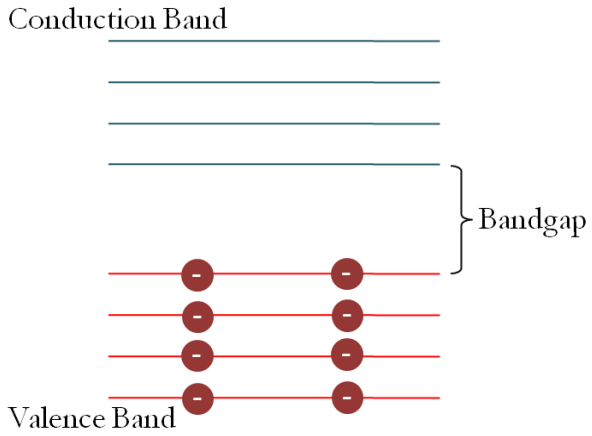

Figure 5.7 A schematic of the electronic structure of a bulk semiconductor with the electrons in the valence band.

The electrons in bulk 3D semiconductors have a continuum of energies as shown in figure 5.6(a). In fact there are energy levels in bulk semiconductors but adjacent energy levels are so close together they are described as forming a continuous spectrum of energies. Within each of these energy levels two electrons are allowed to reside. Further, there are some energy levels that are forbidden called a bandgap. Electrons below the bandgap are in the valence band while those occupying levels above the bandgap are in the conduction band.

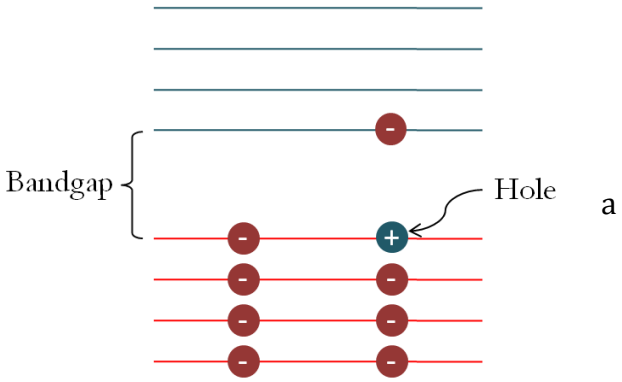

Figure 5.8 A schematic of an electron that has jumped into the conduction band leaving a positive hole in the valence band.

In the typical bulk semiconductor there are very few electrons occupying the conduction band, leaving the majority of electrons to nearly fill the valence band. An electron can move from the valence band to the conduction band by absorbing enough energy to jump the bandgap. When an electron is able to jump into the conduction band the vacancy in the valence band is called a "hole", as shown in figure 5.8.

The same concepts of bulk semiconductors also apply to quantum dot semiconductors such as energy levels, a conduction band and a valence band and a bandgap. The difference between the bulk material and the quantum dot is the size, which plays a vital role in exciton separation. In the bulk semiconductor material the exciton Bohr radius is allowed to extend to its expected limit as shown in figure 5.9. However, in a quantum dot with a physical size less than the exciton Bohr radius, the electron levels become discrete, quantum mechanically confining the electron. The size of the bandgap in a quantum dot is

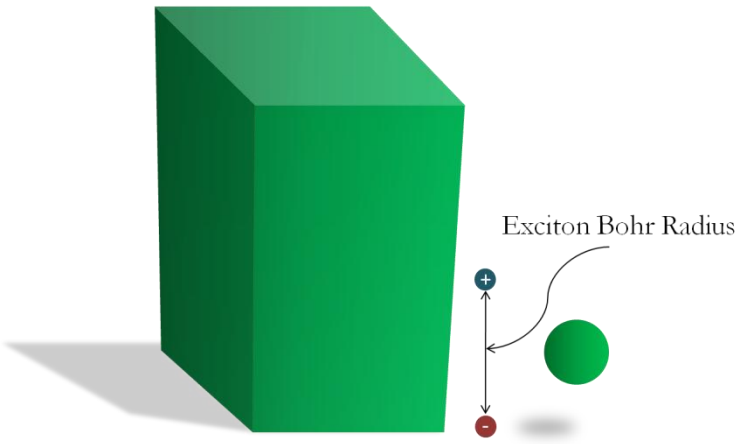

Figure 5.9 A schematic depicting the a bulk material and a quantum dot in relation to the exciton Bohr radius.

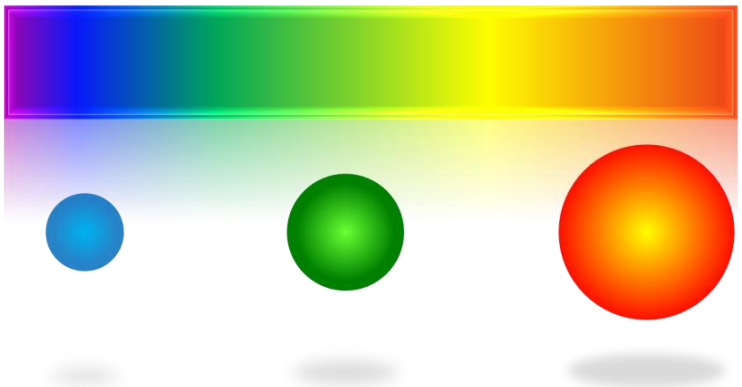
Figure 5.10 A representation of the size of quantum dots and their radiating wavelengths.

determined by its diameter,[29] with larger quantum dots emitting in the red and smaller in the blue, as depicted in figure 5.10. Thus, a quantum dot can be tailored to emit at a desired wavelength.

5.4.1 Quantum Confinement

The exciton exists as a bound state of an electron and a hole, through Coulomb attraction. In a 3D bulk material the lowest energy bound state is described by the effective Rydberg energy

$$Ry^* = \frac{\mu}{\varepsilon^2 m_e} Ry \tag{5.15}$$

and the effective Bohr radius

$$a_B^* = \frac{\varepsilon m_e}{\mu} a_B \tag{5.16}$$

where m_e is the electron mass, and ε is the dielectric constant. Further, the Rydberg energy, $Ry = 13.6\ eV$ and the Bohr radius of the hydrogen atom $a_B = 52.9$ pm. Thus, the energy levels of the exciton can similarly be written as[30]

$$E_n = E_g - \frac{Ry^*}{n^2} \qquad (n = 1, 2, 3, \dots) \tag{5.17}$$

Similar terminology is used to describe microcrystallines or quantum dots. The quantum confinement is classified into three different confinement regimes: (1) strong; (2) intermediate; and (3) weak.[31, 32] These different categories are dependent upon the relative size of the quantum dot in relation to the exciton Bohr radius.[33] Assuming the quantum dots are spherical the Bohr radii for the hole, a_h^*, and electron, a_e^* are

$$a_e^* = \frac{\hbar^2 \varepsilon}{m_e^* e^2}, \tag{5.18}$$

$$a_h^* = \frac{\hbar^2 \varepsilon}{m_h^* e^2}. \tag{5.19}$$

where e is the fundamental charge of an electron. Combining equations (5.18) and (5.19) yield the exciton Bohr radius

$$a_B^* = \frac{\hbar^2 \varepsilon}{\mu e^2} \tag{5.20}$$

where $a_e^* < a_B^*, a_h^* < a_B^*,\ \mu$ is the reduced mass and ε is the dielectric constant.

5.4.1.1 Strong Confinement

Strong confinement occurs when the Coulomb interaction energy is much smaller than the quantized energy. Further, the motion of electrons and holes must be quantized. Under these conditions $R \ll a_e^*$ and $a_h^* < a_B^*$. The ground state energy is given a sum of the kinetic energy of electrons and hole, the gap energy and Coulomb energy[34, 35, 36]

$$E(R) = E_g + \frac{\hbar^2 \pi^2}{2\mu R^2} - \frac{1.786 e^2}{\varepsilon R} - 0.248 Ry^* \tag{5.21}$$

where the term $0.248 Ry^*$ is the correlation energy. Typical semiconductors which exhibit strong confinement are GaAs, CdS, CdSe, and CdTe quantum dots.

5.4.1.2 Intermediate Confinement

Intermediate confinement occurs under the conditions that the electron motion is quantized and the hole is electron and hole are bound by Coulomb interactions. Mathematically stated $a_h^* < R < a_e^*$. Type II-VI quantum dots such as CuBr, belong to this regime.

5.4.1.3 Weak Confinement

Weak confinement exists when only the motion of the excitons center of mass is quantized. Under these conditions $R \gg a_B^* > a_e^*$ and $R \gg a_B^* > a_h^*$. The ground state energy in the weak regime is[37]

$$E = E_g - Ry^* + \frac{\hbar^2 \pi^2}{2MR^2}. \tag{5.22}$$

where the total mass $M = m_e^* + m_h^*$. The most common semiconductor belonging to this class is CuCl.[38]

5.4.2 Other Considerations

Although the diameter of a quantum dot and the ability to confine the exciton as discussed above is an integral, in practice there are other considerations when characterizing quantum dots. The largest consideration is the shape of the quantum dot. In the above discussion the quantum dot was always assumed to be a sphere. In the preparation of quantum dots the diameters are never identical but are represented by a distribution of diameters. The more uniform the diameter of the quantum dots the more narrow the luminescent spectral peak. Other considerations include the ambient surroundings of the quantum dots and the impurities in the dots themselves.

5.5 Förster Resonant Energy Transfer

Theodor Förster, a German scientist was the first to propose fluorescence resonance energy transfer (FRET).[39, 40, 41, 42] In simple terms the process occurs when an excited donor chromophore transfers energy by dipole-dipole coupling to an acceptor chromophore. The energy is not transferred through by fluorescent processes. When both the donor and acceptor are fluorescent, some apply the term "fluorescence energy transfer" is to the

process, but the process is still non-radiative. Thus, the preferred term is "Förster resonance energy transfer."

FRET processes remained relatively unexplored from when it was initially articulated to the mid 1960s. In the mid 70s the biochemical community came to realize the potential worth of a FRET system for tracking global structural changes in macromolecules.[43] The processes offered an experimental technique for estimating molecular distances as reactions occur. Depending on the materials FRET has been found to occur between 10-80 Å.

The Förster formalism is based upon the transfer of energy between two neighboring chromophores. A chromophore is a term used to describe the part of a molecule responsible for its color. The chromophore is a chemical group, in the molecule where the energy difference between two orbitals, fall within a specific range of the EM spectrum. Thus, when the chromophore is illuminated at a specific wavelength corresponding to the orbitals an electron is excited from the ground state to an excited one. There are two conditions which are required for resonant energy transfer. First, a large overlap in the first absorption band of the acceptor and the emission band of the donor, creates the necessary transfer region. Second, the donor must have a high fluorescence yield.[44]

5.5.1 Förster Formalism

The transfer of energy from an donor to an acceptor molecule will involve the electronic states of the donor and acceptor and may be accomplished through different mechanisms. However, regardless of the mechanism, conservation of total energy is required for a resonant process to occur. The conservation of energy requires that the

donor molecule be greater than or equal to the acceptor molecule. The transfer of energy between the donor and acceptor competes with other deexcitation processes such as vibration. For example, once the transfer has been accomplished any surplus energy remaining with the donor is dissipated as vibration energy.

The formalism of FRET requires several assumptions.[45] The first being, the donor and acceptor chromophores are stationary, in relation to a time scale, on the same order as the lifetime of the excited state. Second, the interaction energy is weak such that the rate of transfer is proportional to the square of vibrational interaction energy.[46] Third, the donor and acceptor interaction is only a dipole-dipole interaction so the overlap between the electronic wavefunctions of the donor and acceptor is not a means of deexcitation.[47]

The Förster formulation for the rate of energy transfer, k_T, is given by

$$k_T = \frac{9(\ln 10)\kappa^2 Q_d J}{128\pi^5 n^4 N_A \tau_d R^6} \tag{5.23}$$

where κ is the orientation factor for a dipole-dipole interaction; Q_d is the fluorescence quantum yield of the donor in the absence of the acceptor, J is the normalized spectral overlap integral, n is the refractive index of the medium surrounding the donor and acceptor, N_A is Avogadro's number, τ_d is the fluorescence lifetime of the donor in the absence of the acceptor, and R is the distance between the centers of the donor and acceptor. Notice that equation (5.23) does not require that the donor and acceptor be identical molecules.

The orientation factor κ is a measured with respect to the angle between the donor and acceptor molecules θ_T giving

$$\kappa^2 = [\cos\theta_T - 3\cos\theta_d \cos\theta_a]^2 \tag{5.24}$$

where θ_d and θ_a are angles defined by the vector joining the donor and acceptor with the emission and absorption dipoles. The orientation factor κ^2can vary from 0 to 4.0.[48] The normalized spectral overlap is given by

$$J = \frac{\int \varepsilon_a(\lambda)\lambda^4 d\lambda}{\int F_d(\lambda)\, d\lambda} \tag{5.25}$$

where $F_d(\lambda)$ is the fluorescence intensity of the donor in the absence of the acceptor at wavelength λ, and $\varepsilon_a(\lambda)$ is the molar absorption coefficient of the acceptor at λ. Equation (5.25) corresponds to the amount of overlap of the donor and acceptor emission spectra.

An alternative form of the Förster transfer rate can be stated in terms of a critical distance at which 50% of the excitation energy is transferred to the acceptor.

$$k_T = \frac{1}{\tau_d}\left(\frac{R_0}{R}\right)^6 \tag{5.26}$$

where R_0 is a spatial relation between the donor and acceptor where the probability of donor deexcitation by energy transfer equals the probability of deexcitation by other processes. Substituting equation (5.26) into equation (5.23) and solving for into equation (5.23) and solving for R_0

$$R_0^6 = \frac{9(\ln 10)\kappa^2 Q_d\, J}{128\pi^5 n^4 N_A}. \tag{5.27}$$

If the units of the variables are in terms of cm^{-1} and M^{-1} then R_0 can be written as[49]

$$R_0^6 = 9.78 \times 10^3 \frac{Q_d \kappa^2 J}{n^4} \text{Å}^6. \tag{5.28}$$

The transfer efficiency(E), of energy from the donor to the acceptor, is written as

$$E = \frac{R_0^6}{(R_0^6 + R^6)} \tag{5.29}$$

where R_0 and E are found experimentally allowing the donor-acceptor distance R to be determined.

5.5.2 Experimental Verification of FRET

Equation (5.29) shows the energy to be inversely proportional to the sixth power of the donor-acceptor separation, R. Three experimental papers represent this verification. In 1965, Latt et al. showed that the transfer efficiency between donor and acceptor chromophores attached to fused steroids showed a nearly R^{-6} dependence.[50] Then Stryer and Haugland in a more controlled experiment showed transfer efficiencies between a series of poly-t-proline oligomers had a $R^{5.9\pm.3}$ dependence.[51] Finally, Buecher et al. used sheets of fatty acids to measure the separation between multilayers, to confirm the R^{-6} dependence.[52] The validation of J was made by Haugland et al, in 1969 when they varied the magnitude of J and showed that the transfer rate was proportional to J the spectral overlap.[53]

5.5.3 Modern Advances in FRET

Modern biochemistry makes extensive use of the FRET phenomena to measure conformational changes, such as molecular rotations and distance on a nanometer scale.[54] Using near-field scanning optical microscopy emission spectra from donor and acceptor fluorophores in a short DNA molecule can be imaged.[55, 56] Techniques and new fluorescent materials have improved spatial resolution, distance range and sensitivity.[57]

One material that is now being commonly used as a FRET marker is the quantum dot. For example quantum dots allow specific labeling of cellular constitutions.[58] Further, quantum dots have been used as donors for FRET in imaging the binding and uptake of biotinylated transferin on living cells.[59]

The types of quantum dot used as FRET markers are colloidal dots which have a narrow emission bandwidth ad broad absorption spectra. Unlike organic dyes, which require complex arrangement of excitation sources and filters, a population of quantum dots can be excited with a single source.[60] Further advantages of quantum dots include their brightness and photostability.[61]

5.6 Quantum Dots-Encapsulated in Hydrogel

Encapsulating quantum dots in materials to create optical gains was seen early in their development. For example, the II-VI semiconductor CdS were embedded in a sodium borosilcate glass matrix to create a gain material.[62] Thermoresponsive hydrogel has been realized as a controlled medium to adjust the distances between quantum dots, due to the relationship in the quantum dot size and hydrogel pore size.[63] One well known thermoresponsive hydrogel is PNIPAM hydrogel, discussed in previous chapters, that undergoes a volumetric phase change at a lower critical solution temperature. CdTe quantum dots were first embedded in the bulk form of the PNIPAM hydrogel to yield an enhancement in photoluminescence.[64] Later the quantum dots were embedded in poly(N-isopropylacrylamide-acrylic acid) a microsphere form of the NIPA gel which is tunable in

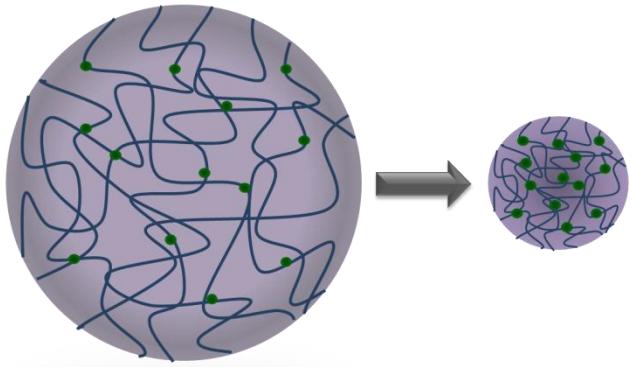

Figure 5.11 A microsphere with embedded CdTe quantum dots undergoing a volumetric phase change, bringing the QD into close proximity to one another.

response to pH stimuli.[65] The CdTe offered a way to control the self assembly of the gel network. In another study, researchers loaded two different sized CdTe nanocrystals into PNIPAM in an effort to realize multiple optical encoding.[66] However, they found that the "average distance between CdTe nanocrystals was still greater than that required for Förster energy transfer."[67]

In the following sections in this chapter CdTe quantum dots encapsulated in PNIPAM hydrogel will be discussed. There are two separate stimuli applied in the experiments namely temperature and electric field. When the stimuli is applied to the swollen PNIPAM microsphere, it undergoes a phase change bringing the quantum dots into close proximity (see figure 5.11), resulting in Förster resonant energy transfer.

Figure 5.12 A quart glass cuvette containing green QD illuminated under a black light.

The experimental setup of each, the results and the interpretations thereof will also be discussed. Finally, a transmission experiment was performed to indicate the level of scattering in the medium.

5.6.1 Temperature Dependent Photoluminescence

In the previous sections the foundation for a PNIPAM hydrogel—Quantum Dot hybrid material was laid. In this section the experimental setup and results will be discussed.

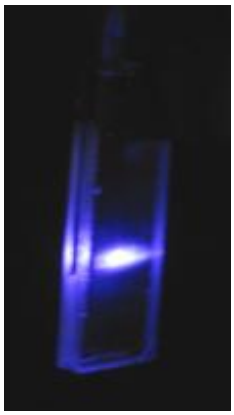

Figure 5.13The sample illuminated by the 404nm laser source.

Samples of the hydrogel-QD material were placed in quartz glass cuvettes and placed in a heater. Figure 5.12 shows a glass cuvette containing the hydrogel-QD material illuminated under a

black light. In the experimental setup, the sample was excited by a 404nm diode laser source, shown in figure 5.13, manufactured by Power Technology Incorporated .

The illuminating laser was placed at 45° angle to the spectrometer, as shown in figure 5.14. Once the laser (purple) illuminated the source, luminescent emission from the sample (green) was focused into the spectrometer via optical lens. The spectrometer used to gather and record data is the TRIAX 320 spectrometer manufactured by Jobin Yvon. The sample holder was built as a small enclosure containing a heater and a forward window to allow for sample excitation. Thermoelectric heaters manufactured by Melcor Incorporated were used to drive the temperature. The temperature of

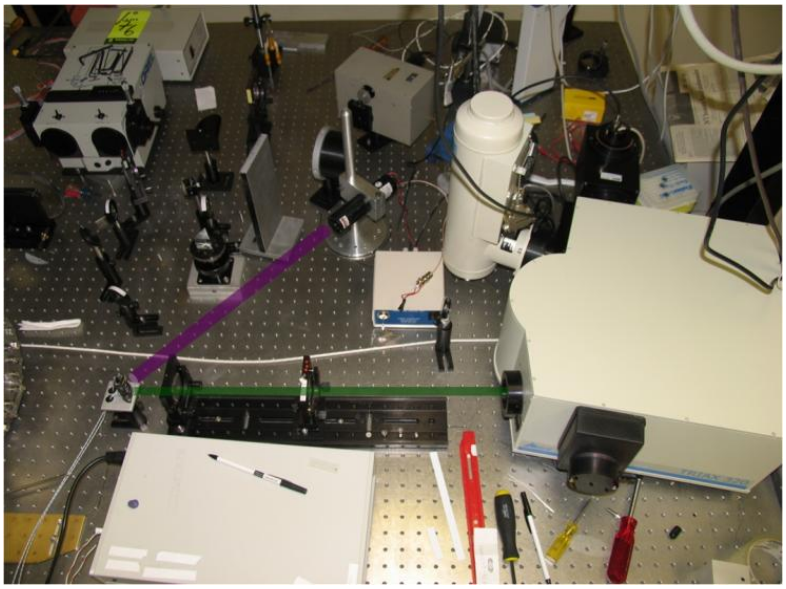

Figure 5.14 The geometrical setup of the PL experiment.

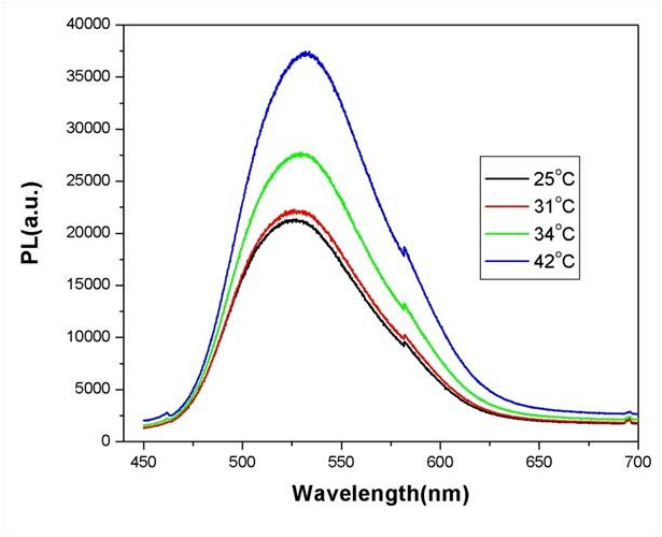

Figure 5.15 The PL of the hydrogel-QD hybrid material showing luminescent enhancement as a function of temperature.

the sample was varied from 25°C to 41°C, to ensure measurement below the hydrogel LCST and above LCST. A Lakeshore 332 Temperature Controller was used to set and monitor the temperature of the sample.

The spectral data, shown in figure 5.15 indicates that as the temperature increases the photoluminescence also increases. Further, the wavelength of the peak shifts toward the red as the temperature increases. The shape of the curve also changes with temperature, where the spectral width increases with temperature.

5.6.2 Temperature Dependent Peak Red-Shift Analysis

The quantum dots encapsulated in the hydrogel are not represented by a single diameter. Rather, there is a distribution of sizes, shown in figure 5.16, some of which are more excitable at a wavelength of 404nm. Consider the blue dots as a representation of the smallest dots within the distribution. These dots because of there size will more efficiently absorb the UV laser source. The other quantum dots may or may not be excited by the laser depending upon their size. . Although the size of the quantum dots is represented by a distribution, there sizes do not significantly depart from one another and there bandgaps should have some overlap. Therefore, when the gel undergoes its phase change the quantum dots are brought into close proximity of one another the smallest quantum dots can transfer energy to the larger

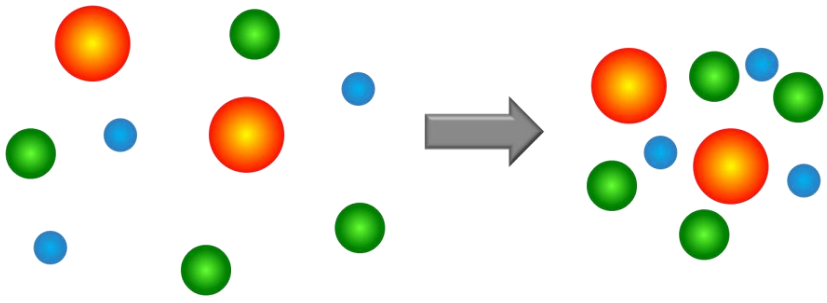

Figure 5.16 A hypothetical distribution of quantum dots encapsulated in a gel microsphere. When the hydrogel undergoes its volumetric phase change the quantum dots are brought within close proximity to one another.

quantum dots. Returning to figure 5.16, the blue dots now are able to transfer energy to the green dots and the green dots to the red dots (the larges size in the distribution). The evidence of this process is seen in figure 5.16. The red-shift in the spectral peak indicates that a larger number of dots with slightly redder bandgaps are being excited. Further, the increase in spectral width and in particular the tail in the red indicates that larger dots are also being excited. In summary, as the hydrogel undergoes its phase change: (1) dots of all sizes are brought closer together; (2) smaller dots are able to more efficiently transfer energy through the FRET process to the larger quantum dots; and (3) the larger quantum dots with redder spectrums become more and more dominant in the emitted spectrum.

5.6.3 Luminescent Enhancement

Perhaps the most notable feature in figure 5.15 is the increased in photoluminescence, one the temperature rises above 34°C. Recall in the previous chapters that the refractive index of the hydrogel—water material was dependent upon the scattering in the medium. Thus, below LCST there a given amount of scattering that occurs that subsequently excites a fixed number of quantum dots. As the PNIPAM gel spheres undergo their volumetric phase change the scattering in the medium also increases. Since the scattering has now increased more quantum dots will be excited, resulting in an increase in photoluminescence yield from the medium.

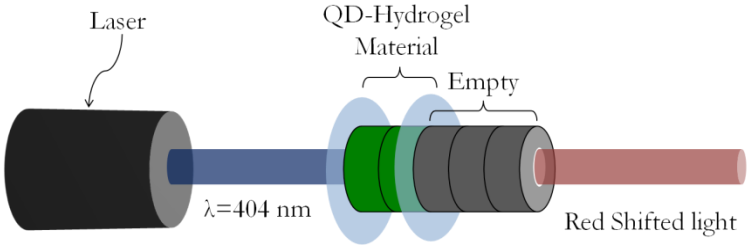

Figure 5.17 In line photoluminescent of transmitted light.

5.6.4 Transmission through Hydrogel-QD Material

Another experiment that indicated the above process, is the transmission experiment where laser light is passed through a volume of the hydrogel-QD material. The experimental setup requires a linear setup where, the laser light passes through the volume and from the volume into the spectrometer. A basic depiction is shown in figure 5.17. In the experiment the path length of the volume transacted by the laser beam was increased from 1 cylinder or by 3mm. In figure 5.17, two cylinders are filled with the hydrogel-QD material and were held in place by two windows.

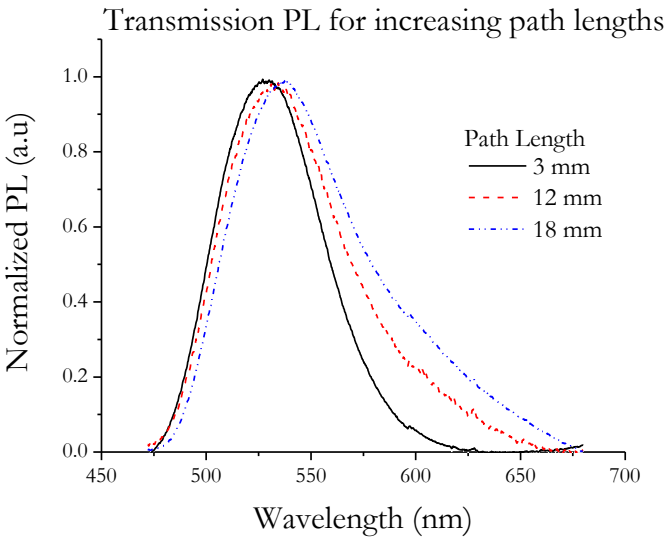

Figure 5.18The transmission PL spectra of the hydrogel-QD at various path lengths.

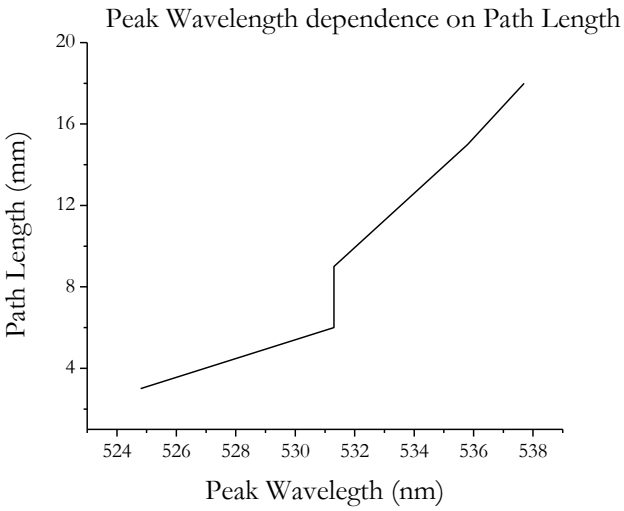

Figure 5.19A plot of the peak wavelength of the spectra in figure 5.16 plotted against the path length.

The first sample analyzed was a well prepared sample with the quantum dot distribution showing a narrow spectral distribution. In figure 5.18, the peak shifts toward the red and a tail develops in the red, as the path length is increased. The peak wavelength is plotted against path length in figure 5.19.

The discontinuity in figure 5.19 may be due to a change in intensity of the laser light passing through the material. Both figures 5.18 and 5.19 support the FRET process discussed above. The larger quantum dots play a larger role in the emitted light as the path length increases. This is to be expected since as the path length increases energy is able to be passed to increasingly larger dots.

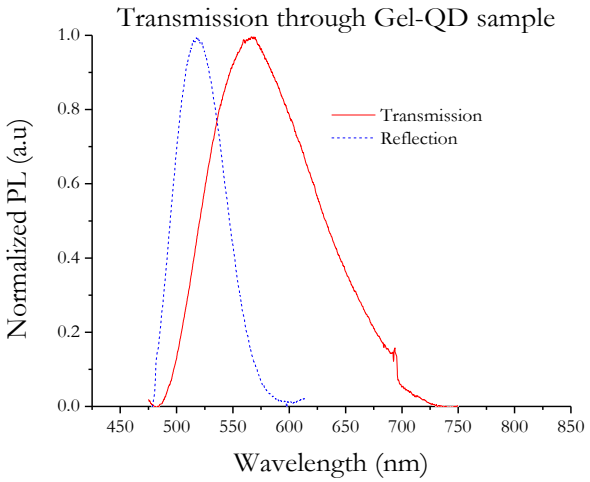

Figure 5.20 The PL for a transmission through 1.5 cm path and PL for reflection geometry.

The second experiment illustrates this point of larger quantum dots being excited as the path length increases. In this experiment a wide distribution of dots was prepared and transmission data was obtained for a 1.5 cm path length. Also data was collected for the reflection geometry used in the temperature measurement. Figure 5.20 indicates that indeed a longer path length is allowing larger dots to be excited. The shift in the spectral peak amounts to approximately 60nm. This again bolsters the claim that the FRET process is occurring where energy is transferred from smaller dots to larger ones which then emit the energy according to the larger dot's bandgap.

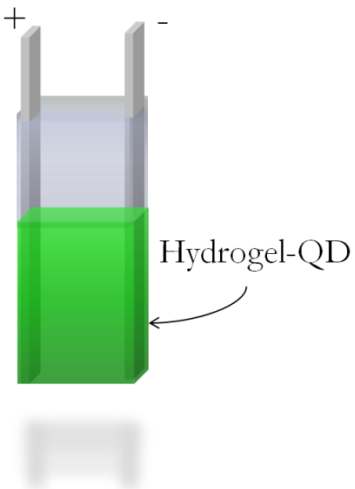

Figure 5.21 A schematic of the electro-chemical cell created to generate an electric field across the hydrogel-QD material.

5.6.5 Electric Field Enhancements

The experimental setup to test for electric field enhancements is similar to that of the temperature dependent methods. The geometry of the exciting laser and spectrometer remain the same. The sample holder, however, is altered to accommodate electrodes disposed on opposite sides of the holder and lay within in the material. Several different materials for the electrodes were tried in this experiment. The best material for the electrodes was found to be Al. Other metals such as Pt and Cu reacted with the with the quantum dots causing them to precipitate out of solution and loose their luminescent features.

An enhancement was also found four the hydrogel-QD material when an electric field was applied to the sample. However, the enhancement was found when the temperature was above LCST. Figure 5.22 shows the increase in luminescence as a function of electric field. The data was taken at 36°C, every 3 minutes in intervals of 0.2 V/cm. The dramatic jump occurs at 5.4 V/cm. The curious feature of figure 5.22 is the fact that the enhancement is occurring above the critical temperature. Most likely this is again due to an increase in scattering in the medium. However, the scattering in this instance is due to a deformation

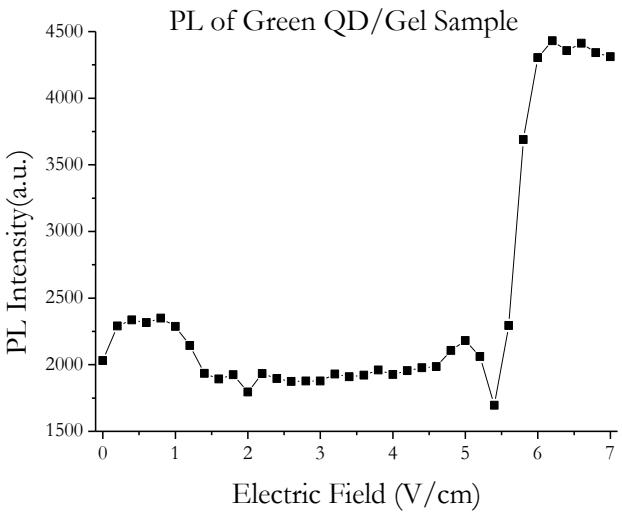

Figure 5.22 The enhancement of hydrogel-QD using an electric field, at 36°C, above LCST.

of the collapsed gel sphere. A net charge exists on the gel particles. When the particle is placed within an electric field a natural charge separation occurs, which naturally deforms the particle. Since the particle is no longer a sphere, the scattering will increase, explaining the enhancement.

---

[1] J. Legge, *The Chinese classics*, vol. 4, (1893) pp. 237.

[2] S. Shionoya, "Introduction to the Handbook," in *Phosphor Handbook*, edited by S. Shionoya, W. M. Yen, (CRC Press, New York 1999).

[3] Aristotle, *De Anima*, Book II, Ch. 7, Sec. 4; translated by R. D. Hicks, *Aristotle De Anima*, (Cambridge Press, 1907) p. 80-81.

[4] M. Cellio, *Il Fosforo o vero la Pietra Bolognese*, (1680); original volume at University Library of Bologna, Italy.

[5] A. Roda, *Bioluminescence & Chemiluminescence: Perspectives for the 21st Century*, A Roda, M Pazzagli, L.J Kricka & PE Stanley (Eds) (Wiley, New York, 1999).

[6] C. Gesner, *De raris et admirandis herbis quae sive nactu luceant, sive alias ob causas, Lunariae nominantur et obiter de alia etiam rebus, quae in tenebris lucent, Commentariolus*, (Tiguri 1555) p. 82; in E. N. Harvey, *A History of Luminescence: From the Earliest Times Until 1900*, (J. H. Furst, Baltimore, MD 1957).

[7] F. Bacon, *Topics of inquiry concerning light and the nature of light*, (1612); in Basil Montagu, Esq., *The works of Francis Bacon*, **15**, 82-87 (London, 1834).

[8] G. Q. Stokes, "On the change of refrangibility of light," Phil. Trans. Roy. Soc. London **142**, 463-562 (1852).

[9] E. Becquerel, *La Lumière, ses causes et ses effets*, (Grautheir-Villars, Paris 1867).

[10] P. Leonard, *Handbuch der Experimental Physik* **23**, Pt. 1 and 2 "Phosphoreszenz und Fluoreszenz," (Akad. Verlagsges. Leipzig, 1928)

[11] E. I. Adirowitsch, *Einige Fragen Zur Theorie der Lumineszens der Kristalle*, (Akademie-Verlag, Berlin 1953).

[12] S. Shionoya, "Introduction to the Handbook," in *Phosphor Handbook*, edited by S. Shionoya, W. M. Yen, (CRC Press, New York 1999).

[13] P. Pringsheim, *Fluorescence and Phosphorescence*, (Interscience Publishers, New York 1949).

[14] F. A. Kröger, W. Hoogenstraaten, "Decay and quenching of fluorescence in willemite," *Physica*, **14**, 425-441 (1948).

[15] D. Curie, *Luminescence in Crystals,* (Wiley, New York 1963)

[16] A. Jabloński, "Efficiency of anti-Stokes fluorescence in dyes," Nature **131**, 839 (1933).

[17] F. Seitz, "Interpretation of the properties of Alkali Halide-Thallium phosphors," J. Chem. Phys. **6**, 150-162 (1938).

[18] N. F. Mott, "The theory of crystal rectifiers," Proc. Roy. Soc. A (London), **171**, 27-38 (1939).

[19] F. Williams, *Luminescence of Inorganic Solids*, edited by P. Goldberg, (Academic Press, New York 1966) p. 5.

[20] N. Riehl, M. Schön, "Der Leuchtmechanismus von Kristallphosphoren," Z. Physik **114**, 682 (1939).

[21] R. P. Johnson, "Luminescence of sulfide and silicate phosphors," J. Opt. Soc. Am. **29**, 387-391 (1939).

[22] A. I. Ekimov, A. A. Onuschenko, "Quantum size effect in the spectra of semiconductor microcrysals," Sov. Phys. Semicond. **16**, 775-778 (1982).

[23] A. I. Ekimov, A. L. Efros, A. A. Onushcenko, "Quantum Size Effect in Semiconductor Microcrystals," Solid St. Comm., **56**, 921-924 (1985).

[24] L. E. Brus, "A simple model for the ionization potential, electron affinity and aqueous redox potential of small semiconductor crystallites," J. Chem. Phys. **79**, 5566-5571 (1983).

[25] L. E. Brus, "Electron-electron and electron-hole interactions in small semiconductor crystallites: The size dependence of the lowest excited electronic state," J. Chem. Phys., **80**, 4403-4409 (1984).

[26] M. Matsuura, T. Kamizoto, "Oscillator strength of excitons in quantum wells," Surf. Sci. **174**, 183-187 (1986).

[27] T. Itoh, T. Kirihara, "Excitons in CuCl Microcrystals Embedded in NaCl," J. Lumin. **31**, 120-22 (1984).

[28] J. Feldmann, G. Peter, E. O. Göbel, P. Dawson, K. Moore, C. Foxon, R. J. Elliott, "Linewidth dependence of radiative excitons lifetimes in quantum wells," Phys Rev. Lett. **59**, 2337-2340 (1987).

[29] R. N. Bhargave, D. Gallagher, X. Hong, A. Nurmikko, "Optical properties of manganese-doped nanocrystals of ZnS," Phys. Rev. Lett., **72**, 416-419 (1994)

[30] C. Weisbuch, B. Vinter, *Quantum Semicondutor Structures*, (Academic Press, Boston 1991).

[31] A. D. Yoffe, "Low-dimensional systems; quantum size effects and electronic properties of semiconductor microcrytallites (zero-dimensional systems) and some quasi-two-dimensional systems," Adv. Phys. **42**, 173-262 (1993).

[32] A. I. Ekimov, "Optical Properties of Semiconductor Quantum Dots in Glass Matrix'" Phys. Scr. **T39**, 217-222 (1991).

[33] Y. Matsumoto, T. Kawamura, T. Ohzeki, S. Urabe, "Lifetime of indirect excitons in AgBr quantum dots," Phys. Rev. B **46**, 1827-1830 (1992)

[34] M. Chamarro, C. Gourdon, P. Lavallard, O. Lublinskaya, A. I. Ekimov, "Enhancement of electron-hole exchange interaction in CdSe nanocrystals: A quantum confinement effect," Phys. Rev. B **53**, 1336-1342 (1996).

[35] A. I. Ekimov, F. Hache, M. C. Schanne-Klein, D. Ricard, C. Flytzanis, I. A. Judryavtsec, T. V. Yazeva, A. V. Rodina, A. L. Efros, "Absorption and intensity-dependent photoluminescence measurements on CdSe quantum dots: assignment of the first electronic transitions," J. Opt. Soc. Am. B **10**, 100 (1993).

[36] M. G. Bawendi, W. L. Wilson, L. Rothberg, P.J. Carroll, T.M. Jedju, M. L. Steigerwald, L. E. Brus, "Electronic structure and photo excited-carrier dynamics in nanometer-size CdSe clusters," Phys. Rev. Lett. **65**, 1623-1626 (1990).

[37] T. Itoh, T. Iwabuchi, M. Kataoka, "Study on the Size and Shape of CuCl Microcrystals Embeddedin Alkali-Chloride Matrices and Their Correlation with Exciton Confinement," Phys. Stat. Solidi (b) **145**, 567-577 (1988).

[38] Y. Masumoto, T. Kawamura, K. Era, "Biexciton lasing in CuCl quantum dots," Appl. Phys. Lett., **62**, 225-227 (1993).

[39] T. Förster, "Zwischenmolekulare Energiewanderung und Fluoreszenz," Annalen der Physik (Leipzig) **437**, 55-75 (1948); Translation by R.S. Knox, "Intermolecular energy migration and fluorescence."

[40] T. Förster, "Transfer Mechanisms of Electronic Excitation," Discuss. Faraday Soc. **27**, 7-17 (1959).

[41] T. Förster, "Part III Action of Light and Organic Crystals," In *Modern Quantum Chemistry*, ed. O Sinanoglu, (Academic Press, New York 1965).

[42] T. Förster, Mechanism of energy transfer, in: *Comprehensive Biochemistry* (M. Florkin and E. H. Statz, eds), Vol. 22, pp. 61-77, (Elsevier, New York 1967).

[43] G. Karreman, R. H. Steele, A. Szent-Györgyi, "On Resonance Transfer of Excitation Energy Between Aromatic Amino acids in Proteins," Proc. Nat. Acd. Sci. U.S.A. **44**, 140-143 (1958).

[44] C. A. Parker, *Photoluminescence of Solutions: With Applications to Photochemistry and Analytical Chemistry*, (Elsevier Pub. Co., New York 1968).

[45] H. C. Cheung, "Resonance Energy Transfer," in *Topics in Fluorescence Spectroscopy, Volume 2: Principles*, ed. by J. R. Lakowicz, (Plenum Press, New York 1991) p. 128.

[46] H. C. Cheung, "Resonance Energy Transfer," in *Topics in Fluorescence Spectroscopy, Volume 2: Principles*, ed. by J. R. Lakowicz, (Plenum Press, New York 1991) p. 128.

[47] H. C. Cheung, "Resonance Energy Transfer," in *Topics in Fluorescence Spectroscopy, Volume 2: Principles*, ed. by J. R. Lakowicz, (Plenum Press, New York 1991) p. 128.

[48] H. C. Cheung, "Resonance Energy Transfer," in *Topics in Fluorescence Spectroscopy, Volume 2: Principles*, ed. by J. R. Lakowicz, (Plenum Press, New York 1991) p. 131.

[49] L. Stryer, "Fluorescence Energy Transfer as a Specroscopic Ruler," Ann. Rev. Biochem., **47**, 819-846 (1978).

[50] S. Latt, H. T. Cheung, E. R. Blout, "Energy Transfer: A system with relatively fixed donor-acceptor separation," J. Am. Chem. Soc. **87**, 995-1003 (1965).

[51] L. Stryer R. P. Haugland, "Energy transfer: A spectroscopic ruler," Proc. Natl. Acad. Sci. U.S.A. **58**, 718-726 (1967).

[52] H. Buecher, K. H. Drexhage, M. Fleck, H. Kuhn, D. Mobius, F. Schafer, J. Sondermann, W. Sperling, P. Tillman, J. Weigand, Controlled transfer of excitation energy through thin layers, Mod. Cryst. **2**, 199-230 (1967).

[53] R. P. Haugland, G. J. Yguerabide, L. Stryer, Dependence of the kinetics of singlet-singlet energy transfer on the spectral overlap integral, Proc. Natl. Acad. Sci. U.S.A. **63**, 23-30 (1969).

[54] S. Weiss, Fluorescence Spectroscopy of Single Biomolecules," Science **283**, 1676-1683 (1999).

[55] T. Ha, T. Enderle, D. F. Ogletree, D. S. Chemla, P. R. Selvins, S. Weiss, "Probing the interaction between two single molecules: Fluorescence resonance energy transfer between a single donor and a single acceptor," Proc. Natl. Acad. Sci. U.S.A. **93**, 6264-6268 (1996).

[56] S. Weiss, "Measuring conformational dynamics of biomolecules by single molecule fluorescence spectroscopy," Nat. Struct. Bio. **7**, 724-729 (2000).

[57] P. R. Selvin, "The renaissance of fluorescence resonance energy transfer," Nat. Struct. Bio., **7**, 730-734 (2000).

[58] T. M. Jovin, "Quantum dots finally come of age," Nature Biotechnol., **21**, 32-33 (2003).

[59] H. E. Grecco, K. A. Lidke, R. Heintzmann, D. S. Lidke, C. Spagnuolo, O. E. Martinez, E. A. Jares-Erijman, T. M. Jovin, "Ensamble and Single Particle Photophysical Properties (Two-Photon Excitation, Anisotropy, FRET, Lifetime Spectral Conversion) of Commercial Quantum Dots in Solution and in Live Cells," Micro. Res. Tech., **65**, 169-179 (2004).

[60] R. Clapp, I. L. Medintz, H. T. Uyeda, E. R. Goldman, H. Mattoussi, "Quantum dot-based multiplxed fluorescence resonance energy transfer," in *Genetically Engineered and Optical Probes for Biomedical Applications III*, edited by D. J. Bornhop, S. I Achilefu, R. Raghavachari, A. P. Savitsky (2005).

[61] S. Hohng, T. Ha, "Single-Molecule Quantum Dot Fluorescence Resonance Energy Transfer," Chem. Phys. Chem. **6**, 956-960 (2005).

[62] J. Butty, N. Peyghambarian, "Room temperature optical gain in sol-gel derived CdS quantum dots," Appl. Phys. Lett. **69**, 3224-3226 (1996).

[63] M. Kuang, D. Wang, H. Möhwald, "Fabrication of Thermoresponsive Plasmonic Microspheres with Long-Term Stability from Hydrogel Spheres," Adv. Mater., **15**, 1611-1616 (2005).

[64] J. Li, X. Hong, Y. Liu, D. Li, Y. Wang, J. Li, Y. Bai, T. Li, "Highly Photoluminescent CdTe/Poly(N-isopropylacrylamide Temperature-Sensitive Gels," Adv. Mater., **17**, 163-166 (2005).

[65] J. Li, B. Lin, J. Li, "Controllable Self-Assembly of CdTe/Poly(N-isopropylacrylamide-acrylic acid) Microgels in Response to pH Stimuli," Langmuir, **22**, 528-531 (2006).

[66] Y. Yang, Z. Wen, Y. Dong, M. Gao, "Incorporating CdTe Nanocrystals into Polystyrene Microspheres: Towards Robust Fluorescent Beads," Small, **2**, 898-901 (2006).

[67] Y. Gong, M. Gao, D. Wang, H. Möhwald, "Incorporating Fluorescent CdTe Nanocrystals into a Hydrogel via Hydrogen Bonding: Toward Fluorescent Microspheres with Temerature-Responsive Properties," Chem. Mater., **17**, 2648-2653 (2005).

CHAPTER 6

ON TUNABLE PHOTONIC CRYSTALS

6.1 Introduction to Photonic Crystals

The language used in describing photonic crystals strongly overlaps the field of solid state physics, borrowing many terms of art which describe similar phenomena, but on different length scales. Solid state describes the motion of electrons with respect to a lattice structure, whereas in a photonic crystal the propagation of an electromagnetic wave is described with respect to period scatterers. Similarly the density of states, described for an electron in solid state, carries over to describe the density of states for confined EM radiation.

Figure 6.1 A one-dimensional photonic crystal comprised of the dielectric materials A and B, with a periodicity of a.

A photonic crystal requires two elements. First, the crystal aspect requires two periodically ordered materials with differing dielectric materials. Second, the photonic portion requires electromagnetic radiation to interact with the two materials. Photonic crystals are grouped into three main categories depending upon the dimensionality of the periodicity of the dielectric materials, namely, one-dimensional (1D), two-dimensional (2D) and three dimensional (3D).[1]

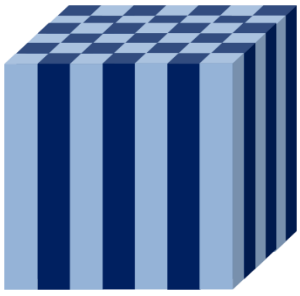
Figure 6.2 Alternating dielectric materials in two dimensions.

The simplest photonic crystal, shown in figure 6.1, is

formed by alternating dielectric materials A and B with a periodicity of a. This is termed a one-dimensional crystal because the dielectric materials alternate in only one direction. Similarly, in a two-dimensional photonic crystal the dielectric materials alternate in two dimensions as in figure 6.2. The 2D crystal is the easiest to fabricate with current technologies and will be discussed in further detail later in the chapter. Although the 3D photonic crystal, shown in figure 6.3 is the most difficult to fabricate, it offers complete control of EM radiation in all directions.

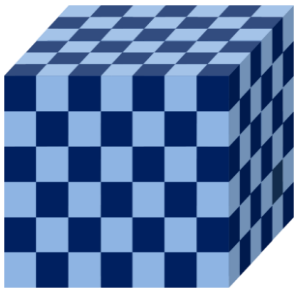

Figure 6.3 A schematic of a 3D photonic crystal with differing dielectric materials in 3 dimensions.

Recall that the frequency of an EM field in free space is given by

$$c = \lambda_0 \nu, \tag{6.1}$$

where λ_0 is the wavelength of the EM wave, c represents the speed of light, and ν is the frequency. Further, a wavenumber can be defined as

$$k = \frac{2\pi}{\lambda_0}. \tag{6.2}$$

Combining equations (6.1) and (6.2) yields the dispersion relation for an EM field.

$$\omega = ck. \tag{6.3}$$

Although these three equations are valid only for free space they are easily modified for materials with a uniform refractive index n. This is accomplished by letting

$$c \rightarrow \quad v = \frac{c}{n} \tag{6.4}$$

and

$$\lambda_o \rightarrow \quad \lambda = \frac{\lambda_o}{n}. \tag{6.5}$$

The density of states for EM radiation from an oscillating dipole in free space, is found by considering the number of eigenmodes in a volume V with eigenfrequencies less than ω_o. There are two polarizations for each wavevector

$$N(\omega_o) = 2\frac{V}{(2\pi)^3}\int_{k<\omega_o/c} d\boldsymbol{k}$$

$$= \frac{\omega_o^3 V}{3\pi^2 c^3}. \tag{6.6}$$

Thus, the density of states is given by

$$D(\omega) = \frac{\partial N(\omega)}{\partial \omega} = \frac{\omega^2 V}{\pi^2 c^3}. \tag{6.7}$$

Further, the density of states for a material with a uniform refractive index is found by allowing $c \to v$, just as before. Therefore, from equation (6.7), the optical properties of a material is strongly dependent upon $D(\omega)$, and can significantly be altered by modifying $D(\omega)$.[2] A more in depth discussion of the density of states and its relation to the radiated energy of an oscillating dipole is given in appendix 6.A.

A photonic crystal with specific values will exhibit a range of frequencies where no electromagnetic eigenmodes exist. The range of forbidden frequencies is called the photonic bandgap, similar in concept to the electron bandgaps in atomic crystal structures. The photonic crystal is tailored to have a specific bandgap, which is used to control the flow of an electromagnetic wave through the crystal.

Few 3D photonic crystals have been fabricated using fabrication techniques common in the semiconductor industry. One early method was infiltrating synthetic opal spheres with conducting polymer.[3, 4] However, there have been some who have successfully created photonic crystals based upon silicon processing techniques.[5]

2D photonic crystal structures are the most common and easily fabricated with attempts to create photonic crystals out of two-dimensionally ordered spheres.[6, 7, 8] Although these alternative methods office promise, they are often painstaking precision. For example, a two dimensional photonic crystal was created using dielectric sphere created by mechanically arranging ninety-one spheres in a scanning electron microscope.[9]

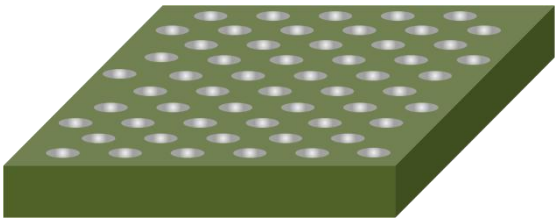

Figure 6.4 A photonic crystal slab comprised of a triangle lattice of holes.

The most commonly fabricated photonic crystals are the 2D variety, in the form of photonic crystal slabs, which draw on the fabrication technologies of the semiconductor industry. 2D photonic crystals can exist as a lattice of holes, as in figure 6.4, or as a lattice of columns, as in figure 6.5. These slabs consist of a semiconductor material on top of an insulating material. Slab structures offer easy fabrication as well as high coupling efficiencies for transmitting light into and out of, high refractive index semiconductors.[10] This discussions contained within this chapter will center on slab structures and their use in tunable photonic crystals. Other applications of the 2D slab photonic crystal include the incorporation of other nano-photonic structures such as quantum dots. The photoluminescence of InAs quantum dots as an internal photonic source was recognized early in the development of photonic crystals.[11] Others have created lasers using 2D photonic crystals slabs which form an optical microcavity for the capture of photons.[12]

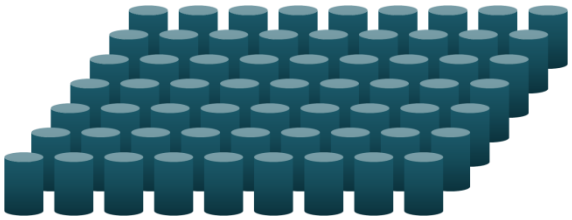

Figure 6.5 A 2D photonic crystal comprised of a square lattice of columns.

6.2 Historical Development

Our understanding of light and its interaction with matter was born with James Clerk Maxwell in 1864. He developed the first theory to describe lights interaction with matter and just as his equations were valid then they are today.[13] Later, Oliver Heaviside used differential operators to simply these fundamental equations into Maxwell's equations into their modern form.

The first photonic crystals were never man made but appear naturally in minerals butterfly wings and abalone shells.[14] Although he did not call them photonic crystals, John Strutt (Lord Rayleigh) in 1887, was the first to describe their properties with respect to a natural crystalline mineral.[15] These 1D crystals are created by alternating dielectric layers which have a narrow bandgap, reflecting a particular color. As the angle of the light changes so does the periodicity of the layers, thus altering the color reflected. With the one-dimensional periodicity Lord Rayleigh was able to show a band gap of forbidden wavelength, which would be later known as a Bragg mirror.[16]

The next development came with the Bloch-Floquet Theorem, which describes how a wave can travel through a period medium without scattering.[17] Lord Rayleigh actually formulated a solution for 1D periodic material that showed a bandgap, however he abandoned the solution for a more simplistic one.

One-dimensional structures have become widely used in the areas of thin films, optical coatings, and diode lasers, while two and three dimensional structures were ignored up until the 1970's and early 1980's when a small amount of research was done for periodic lattices in higher dimensions without bandgaps.

The theoretical benchmark in the development of photonic crystals came in 1979, when Ohtaka used the vector-spherical wave expansion to model the dispersion relation and transmittance of an array of identical dielectric spheres.[18, 19] Ohtaka's inspiration for the work was the number of materials created in the mid 70's exhibiting lattice constants comparable to that of light, such as polymers[20, 21, 22, 23] , lattice voids in ion-bombarded[24] or neutron-bombarded[25] metals and ordered biological systems[26]. This method he employed is also known as the vector KKR (Korigna-Kohn-Rostker) method a direct extension of the LEED (Low Energy Electron Diffraction)[27, 28, 29]. The work of Korigna calculated the energy $E(\boldsymbol{k})$ of a Bloch wave with a reduced wave vector $\boldsymbol{k}$ using the dynamical theory of lattice interferences to electron waves[30] and the work of Kohn and Kostker calculated the conduction band structure of metallic lithium by solving the Schrödinger equation in a periodic lattice using a variation-iteration method.[31] Previous to this treatment a two different formulations were used in LEED calculations for band structure including Boudreaux-Heine[32, 33], and Hartree-Fock[34, 35 ,36].

In 1987, Yablanovitch announced the existence of photonic band gaps in 3D periodic structures and their applications in optoelectronic devices.[37] The inspiration for the revolutionary idea was born out of photonic semiconductor applications and their bandgap properties.[38, 39, 40, 41] Although other researchers that same year were working towards a theory describing the localization of electromagnetic waves[42, 43, 44] it was John who described the localization of electromagnetic waves in disordered crystals and predicted quantum optical phenomena such as non-exponential decay of spontaneous emission and a bound state of photons.[45] While Yablanovitch's work was driven by

bandgap theory, John's work derives from the interactions of an electromagnetic wave with matter and the effects of ordering.[46, 47, 48, 49]

With this newfound application of Maxwell's equations researchers began exploring the nature of light propagation through two and three-dimensional periodic structures.[50] In 1997, researchers at MIT announced the theoretical prediction that light confined to a periodic lattice could be made to bend around tight corners with minimal losses.[51] One year later the same group was able to show experimentally the confinement of light around a sharp bend.[52] Others soon followed with confinement with different geometries.[53]

These first experimental studies were done with two-dimensional periodic geometries because of the ease of fabrication.[54,55] The fabrication of a true three-dimensional period structure with a band gap is very complicated and labor intensive. The solution is a slab structure which confines the light in the x-y plane by the periodicity of the lattice and index waveguiding in the z-direction.[56] Thus a period structure can be made on a two dimensional surface that will reflect electromagnetic radiation within the band gap.[57] The radiation will be confined in a third direction by lower refractive indexes above and below the two-dimensional plane.

These initial discoveries, of a photonic bandgap and the localization of light within a lattice, have been followed by research which has sought to release the full potential of photonic crystals. With increased research, a theoretical understanding and modeling techniques have been further developed. For example, the group theory for a vector field with two degrees of freedom describing symmetry properties in a photonic crystal.[58, 59, 60] Two standards for computational purposes have emerged, the plane-wave expansion

method and the FDTD method. With these methods the expected optical properties of a particular photonic can be calculated.

6.3 Basic Photonic Band-Gap Theory

The elements required for a photonic crystal are (1) a periodic dielectric structure that (2) exhibits a forbidden range of frequencies. In this section basic bandgap theory is discussed in terms of a 1D crystal, for simplicity and conceptual purposes. However, 2D structures, which are the most commonly made, will be discussed in regards to their geometries, materials and fabricated structures.

6.3.1 The Photonic Band-Gap

The calculation of the bandgap structure for a 1D photonic crystal is the simplest to perform and easiest to see conceptually. Assuming that the magnetic permeability of the material is equivalent to that of free space, Maxwell's equations written for an EM wave in a varying dielectric in the x direction is

$$\frac{c^2}{\varepsilon(x)}\frac{\partial^2 E(x,t)}{\partial x^2} = \frac{\partial^2 E(x,t)}{\partial t^2} \tag{6.8}$$

where $E(x,t)$ is the electric field as a function of position x and time t, c is the speed of light and $\varepsilon(x)$ is the position dependent dielectric constant. Further, since $\varepsilon(x)$ is a periodic function a constant may be added without changing the function

$$\varepsilon(x) = \varepsilon(x+\alpha). \tag{6.9}$$

Since dielectric constant, $\varepsilon(x)$ is a periodic function, $\varepsilon^{-1}(x)$in equation (6.8) is also a periodic function that is can be expanded by a Fourier series

$$\varepsilon^{-1}(x) = \sum_{n=-\infty}^{\infty} A_n e^{\left(i\frac{2\pi n x}{\alpha}\right)}, \tag{6.10}$$

where n denotes an integer. A_n are the Fourier coefficients, which are real, since $\varepsilon(x)$ is real. Thus

$$A_{-n} = A_n^* \tag{6.11}$$

Bloch's theorem is used to describe the electronic eigenstates in crystals having a spatial periodicity. The electron's motion through the crystal is dependent upon the potential energy of the regular periodicity of atomic nuclei. Bloch's theorem is also valid for EM waves encountering a periodic dielectric structure, and is derived in appendix 6.B. Solutions to equation (6.8) can be written in the form of

$$E(x,t) \equiv E_k(x,t) = u_k(x)e^{i(kx-\omega t)}, \tag{6.12}$$

where $u_k(x)$ is also a periodic function so that

$$u_k(x) = u_k(x+\alpha) \tag{6.13}$$

and ω_k is s the angular frequency. Equation (6.12) can be expanded a Fourier series

$$E_k(x,t) = \sum_{m=-\infty}^{\infty} E_m e^{i\left[\left(k+\frac{2\pi m}{\alpha}\right)x-\omega_k t\right]} \tag{6.14}$$

where E_m are the Fourier coefficients. The only terms of equation (6.10) that are dominant are $n = 0, \pm 1$, thus

$$\varepsilon^{-1}(x) \approx A_0 + A_1 e^{i\frac{2\pi x}{\alpha}} + A_{-1}e^{-i\frac{2\pi x}{\alpha}} \tag{6.15}$$

Substituting equations (6.14) and (6.15) into the wave equation (6.8) and cancelling exponential terms yields

$$A_1\left[k+\frac{2\pi(m-1)}{\alpha}\right]^2 E_{m-1} + A_{-1}\left[k+\frac{2\pi(m+1)}{\alpha}\right]^2 E_{m+1} \approx \left[\frac{\omega_k^2}{c^2} - A_0\left(k+\frac{2\pi m}{\alpha}\right)^2\right]E_m \tag{6.16}$$

The next step in determining the bandgap for the 1D crystal is to find an equation for E when $m = -1$ and $m = 0$. Thus

$$E_{-1} = \frac{1}{\frac{\omega_k^2}{c^2} - A_0\left(k - \frac{2\pi}{a}\right)^2}\left[A_1\left(k - \frac{4\pi}{\alpha}\right)^2 E_{-2} + A_{-1}k^2 E_0\right] \tag{6.17}$$

and

$$E_0 = \frac{1}{\frac{\omega_k^2}{c^2} - A_0 k^2}\left[A_1\left(k - \frac{2\pi}{\alpha}\right)^2 E_{-1} + A_{-1}\left(k + \frac{2\pi}{\alpha}\right)^2 E_1\right] \tag{6.18}$$

A further simplification is made to equations (6.17) and (6.18) when E_{-1} and E_0 are the dominant coefficients in equation (6.14). These coefficients are dominant when $\omega_k^2/c^2 \approx A_0 k^2$ and $k \approx \left|k - \frac{2\pi}{\alpha}\right|$ in equations (6.17) and (6.18). Thus, the coupled equations become

$$-A_{-1}c^2k^2E_0 + \left[\omega_k^2 - A_0c^2\left(k - \frac{2\pi}{\alpha}\right)^2\right]E_{-1} = 0 \tag{6.19}$$

$$(\omega_k^2 - A_0c^2k^2)E_0 - A_1c^2\left(k - \frac{2\pi}{\alpha}\right)^2 E_{-1} = 0 \tag{6.20}$$

These two equations are linearly independent and have a nontrivial solution when the determinant of the coefficients is set to zero.

$$\begin{vmatrix} \omega_k^2 - A_0c^2k^2 & -A_1c^2\left(k - \frac{2\pi}{\alpha}\right)^2 \\ -A_{-1}c^2k^2 & \omega_k^2 - A_0c^2\left(k - \frac{2\pi}{\alpha}\right)^2 \end{vmatrix} = 0 \tag{6.21}$$

Solving the determinant for the eigenfrequency

$$\omega_\pm = \frac{\pi c}{\alpha}\sqrt{A_0 \pm |A_1|} \pm \frac{\alpha c}{\pi|A_1|\sqrt{A_0}}\left[A_0^2 - \frac{|A_1|^2}{4}\right]\left(k - \frac{\pi}{\alpha}\right)^2 \tag{6.22}$$

If $k - \frac{\pi}{\alpha} \ll 1$, then there are no eigenmodes over the interval

$$\frac{\pi c}{\alpha}\sqrt{A_0 - |A_1|} < \omega < \frac{\pi c}{\alpha}\sqrt{A_0 + |A_1|}\,, \tag{6.23}$$

and thus a photonic bandgap of forbidden frequencies is created, as schematically shown in figure 6.6. From equation (6.23), the bandgap collapses when $A_1 = 0$.

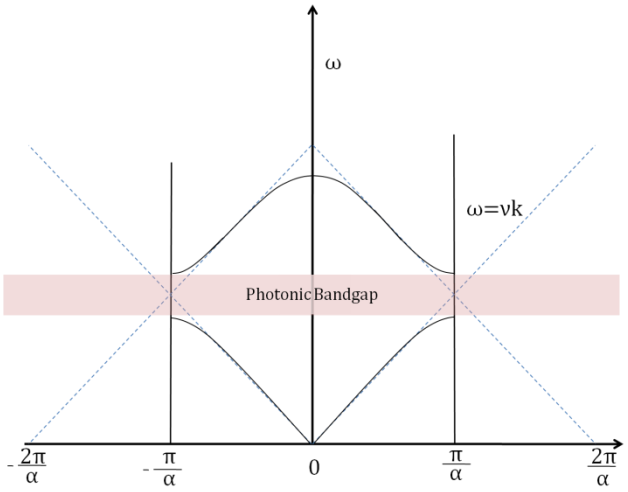

Figure 6.6 A schematic of the dispersion relation for a 1D photonic crystal.

6.3.2 Two-Dimensional Geometries

The requirement of a periodic varying dielectric, in the x and y directions, are met by creating a background material with holes of a different dielectric constant. Thus there are two possibilities (1) a photonic crystal can be formed by a series of high refractive index columns in a background of low refractive index material or (2) a series of low refractive index columns in a high refractive index material. The lattice structure of the colomns are most often triangular or sqauare lattices but other lattices geometries are possible.[61] The key is that periodicity of the scatterers in the photonic crystal gives rise to a range of forbidden frequencies or bandgap.[62] Although the periodicity of the colomns varies in only two-dimensions, they exist in a 3D world.[63]

2D strucutres are created on slab materials where EM wave interacts with the periodic structure is in the xy plane but is confined in the z direction (figure 6.7), within the slab, through total internal reflection.[64, 65] The materials typically used are

semiconductors and are fabricated using techniques borrowed from the semiconductor industry.[66, 67]

These 2D structures can be used to create microcavities for use in low threshold laser, and waveguides with low-loss bends.[68] Most photonic crystals fabricated are confined to operate in the near infrared or infrared range of the spectrum because of fabrication limitations.[69, 70] The methods of fabrication include e-beam or x-ray beam lithography[71], deep UV lithography[72], wet etching techniques[73] and focused ion beam milling.

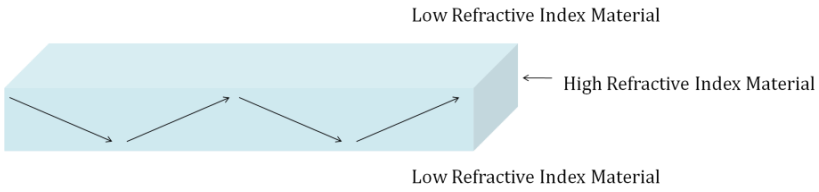

Figure 6.7 A slab of high refractive index surrounded by a low refractive index confines an EM wave inside the slab.

6.3.2.1 Air-bridges/Membranes

The slab structures which maximize the concept of indexing in the z direction are air-bridges or membranes.[74] In this structure the high index material is surrounded by air above and below the high index material.[75, 76, 77, 78] In other words a high index material, typically semiconductor material such as GaAs, AlGaAs or Si, are suspended in the air and in the suspended structure the photonic crystal features created.[79] These materials are selected because they are transparent at IR communication wavelengths of 1.55μm and 1.3μm.[80] Although membranes are the optimal structures for maintaining an EM wave in the material, they are not durable and suffer from structural failure. However, being the optimal structures it is easy to observe true modes created by the photonic crystal structure and leaky slab modes.[81, 82]

6.3.2.2 SOI (Silicon-on-Insulator)

The semiconductor industry offers another material that is well adapted for use in fabricating 2D photonic crystals in SOI.[83] A SOI wafer is composed of a top surface of silicon atop an insulator which is typically SiO_2. The SiO_2 having a refractive index of approximately 1.45 is still much less than the refractive index of Si with a value of 3.5. Thus the air above and the SiO_2 below the silicon provide the necessary indexing to maintain the EM wave in the Si layer.[84] SOI offers several advantages over bridge-type structures (1) the wafer cost; (2) fabrication cost; and (3) durability of the structure. However, SOI material can also be used to make membrane type photonic crystal as discussed above.[85]

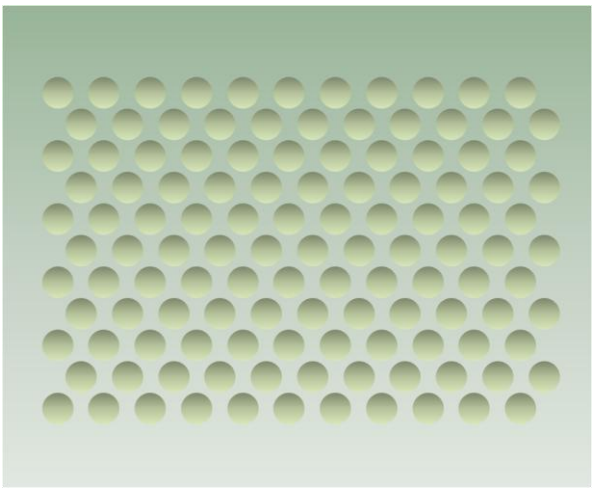

Figure 6.8 An array of scatterers form a photonic crystal, which acts as a Bragg mirror to an EM wave traveleing left to right.

6.3.3 Defects

A photonic crystal acts as a perfect Bragg mirror, reflecting EM waves with frequencies that fall within the bandgap. Figure 6.8 shows such a structure. If a row of the Bragg mirror is removed, as in figure 6.9, light falling within the bandgap will be allowed to propagate down the defect,

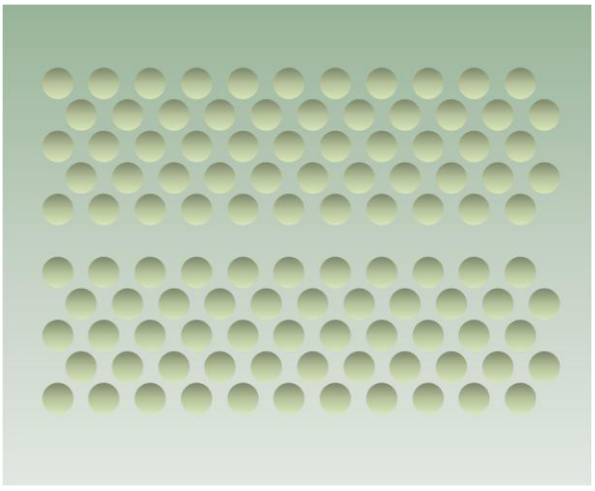

Figure 6.9 A row has been removed from the photonic crystal of figure 6.8 allowing an EM wave with a frequency in the bandgap to propagate from left to right.

while being confined by the photonic crystal on either side.[86] Thus, the photonic crystal with a defect can act as a near lossless waveguide.[87] Analysis of the light propagating through the waveguide will yield the bandgap structure of the photonic crystal.[88, 89]

6.3.4 Bends

The waveguiding ability of photonic crystals with line defects introduced an apparatus for transporting EM radiation from one point to another. In 1996, the first theoretical predications for using a photonic crystal to waveguide light around corners began to appear. The numerical simulations indicated a transmission of 98% around 90° bends with a radius of curvature of zero.[90] This provided a leap forward over conventional dielectric waveguides which exhibit a maximum of 30% transmission. A couple years later this as shown experimentally, thus providing a new mechanism which could be used in large-scale all optical circuits.[91] In

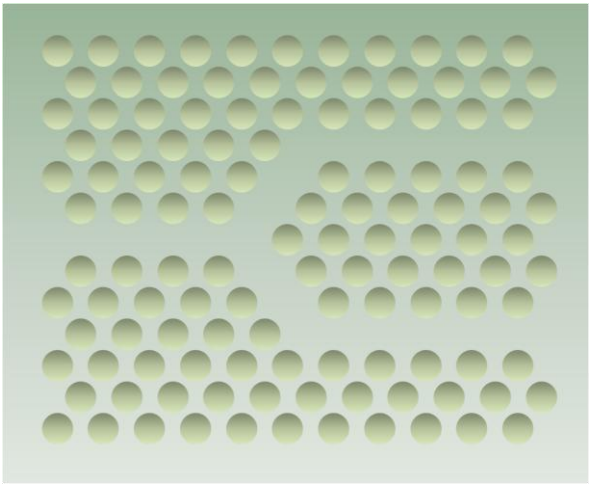

Figure 6.10 A photonic crystal with a Y-Bend structure used in multiplexing.

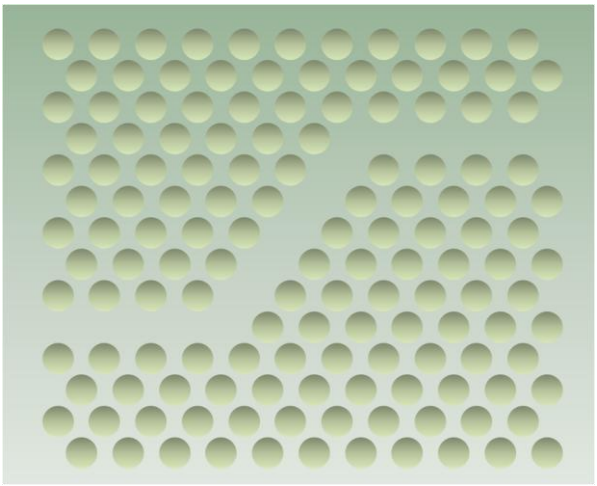

Figure 6.11 A photonic crystal with a 120° bend.

More complex structures for multiplexing and demultiplexing that are required for optical circuits were introduced. Using scattering matrix computational methods the losses

for Y structures (shown in figure 6.10), abrupt bends and a directional coupler were calculated.[92] Experimentally structures with 120° bends began being fabricated in 2000 (shown in figure 6.11) on SOI, operating at a wavelength of 1550 where the radius of curvature is on the same order as the wavelength of light.[93, 94] As a theoretical understanding has developed, the sophistication of creating bending waveguides has also become more sophisticated in created low loss structures.[95, 96]

6.4 Tunable Photonic Crystals

When a photonic crystal is designed the considerations include, the operating wavelength, fabrication materials, and proposed use of the crystal. For example photonic crystals have been used to experimentally demonstrate an ultracompact biochemical sensor operating at a wavelength near 1550 nm that senses the evaporation of waver from glycerol.[97]

The first photonic crystal designed for specific systems were designed by adjusting the lattice spacing, scatterer diameters and defect widths.[98] This is called structural tuning. With the first structurally tuned photonic crystals, once the crystal was fabricated the properties of the structure could not be changed.

Thus, the need arose for the ability to change the photonic band gap, without the need to fabricate a new photonic crystal. The photonic crystal may be tuned by changing (1) the lattice constant; (2) the scatterer diameter; (3) the optical properties of the background material; (4) the refractive index of the scatterers. One early proposal was to change the optical properties of the semiconductor material by introducing temperature dependent impurities.[99] Another common method of tuning the bandgap is by inserting a material into a defect, such as using quartz and high permittivity ceramics to create a

tunable defect.[100] Finally, the other solution has been to insert a material into the lattice holes that is responsive to external stimuli, such as a magnetic field.[101] For example a thermooptic effect was shown on SOI where hearing the holes changed the RI and thus the bandgap.[102] Using this thermooptic effect Mach-Zehnder interferometers have been fabricated with a switching time of approximately 20 μs.[103, 104]

6.4.1 Lattice Constant Tuning

Changing the lattice constant by some external means is the most simplistic method of changing the photonic bandgap. One brute force method is to construct a photonic crystal that is sensitive to mechanical stresses, so when as a force is applied the lattice responds by changing the lattice spacing and scatterer diameter.[105] Another example is the use of thermal expansion of the lattice to achieve bandgap tuning. If Si is heated to 425°C the thermal expansion of the lattice is significant enough to shift the bandgap.[106]

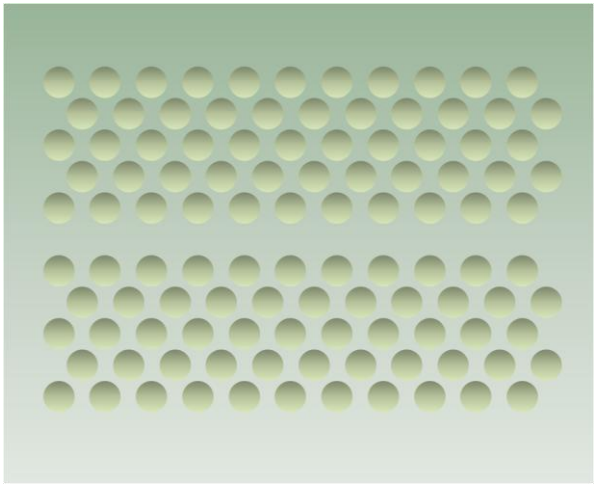

Figure 6.12 A 2D photonic crystal with air holes that act as scatterers.

Although thermal expansion and mechanical tuning of the bandgap achieve their respective goals the processes cause severe fatigue of the photonic crystal. Further, such extreme heating will cause problems with components, in close proximity to the heat source, making this solution unattractive for integrated optical circuitry.

6.4.2 Scatterer Refractive Index Tuning

Currently the most practical solution to bandgap tuning is to introduce a material to the lattice structure which has the ability to change its refractive index. There are many practical applications of tunable photonic crystals that encompass the fields of microwave engineering, quantum optics, semiconductor technology, lasers, and biosciences.[107] For example, nonlinear optical polymers have been introduced to the scatterers that can be modulated by a high electric field.[108] In the bio-sciences, sensors have been created where the level of protein concentrations in the scatterers effect the refractive index, thus, changing the transmission properties of the photonic crystal.[109]

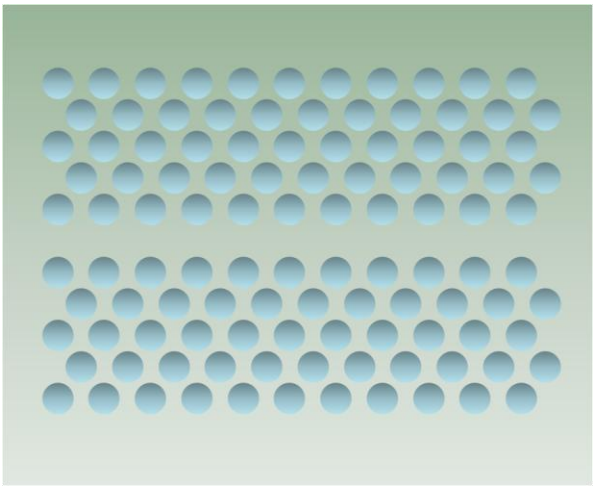

Figure 6.13 A 2D photonic crystal with the scatterers filled with a tunable material. Thus, making the bandgap tunable.

The basic idea is to take a photonic crystal with air voids as the scatterers, as shown in figure 6.12, and fill the scatterers with a tunable material, as shown in figure 6.13. The light transmitted through the defect waveguide then is dependent on the tunable material in the scatterers. More complex structure incorporating tunable materials can be

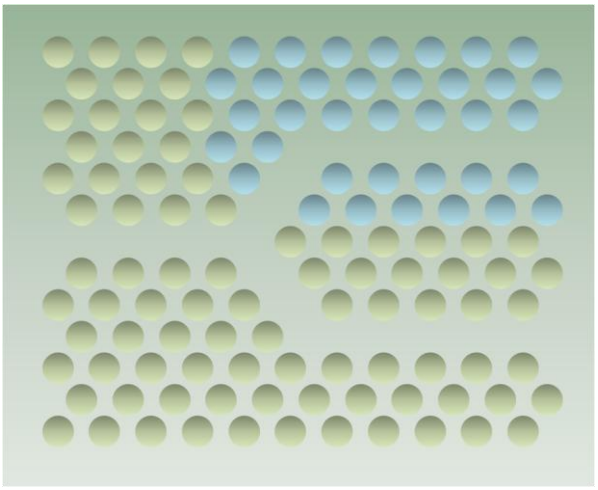

Figure 6.14 A 2D photonic crystal with a tunable multiplexing structure.

used for multiplexing. For example, in figure 6.14, the path of the transmitted EM radiation through the crystal is dependent upon the tunable scatterers.

6.4.2.1 Liquid Crystals

Early in the development of photonic crystals, liquid crystals[i] were seen as a likely candidate as a tunable material. The first work in liquid crystal-photonic crystal hybrids, by Busch and John, showed that the bandgap could be controlled by the orientation of the liquid crystal.[110] The attractiveness of the liquid crystal is its ability to be externally tuned thermally or by applying an electric field.[111, 112, 113, 114] Over the past years many theoretical[115] and experimental[116] investigations have been made to increase there tunability[117, 118], applications[119] and fabrication techniques[120]. Liquid crystals, however, suffer from the problem of offering only a small wavelength shift in the bandgap per degree of temperature or volt of electric field. Many studies show only a 0.18 nm/°C change[121] and a total theoretic shift of 14 nm.[122] Recently, larger 3D photonic crystal operating in the 3 and 4 μm range, have been able to achieve tunability of 70 nm.[123] However, to achieve such a wide tunability voltages in excess of 600V where applied and an average of only 0.117 nm/V was achieved. Although the tunability in the mid IR and microwave range makes liquid crystals attractive they are do not offer they same tunability in the communications

[i] Liquid crystals were discovered in 1888 by Austrian, Friedrich Reinitzer at the German University of Prague. While extracting cholesterol from carrots he observed that cholesteryl benzoate did not melt like in the usual ways. The compound had two melting points at 145.5°C when it became a cloudy liquid and at 178.5°C became a clear liquid. He presented his results on May 3, 1888 and shared the credit with collegues Otto Lehmann and von Zepharovich. The term liquid crystal was not termed until 1922 by Georges Friedel. However, liquid crystals were not qidely studied until after 1969 when Hans Kelker synthesized a nematic phase at room temperature. Finally in 1991, Pierre-Gilles de Gennes receive the Nobel Prize in Physics "for discovering that methods developed for studying order phenomena in simple systems can be generalized to more complex forms of matter, in particular to liquid crystals and polymers."

wavelengths or even the visible wavelengths. The large problem with liquid crystals is their high viscosity, making it difficult to infiltrate a photonic crystal lattice.

6.4.2.2 Hydro-Gel Based Methods

Another method for tuning photonic crystal is to make use of hydrogel polymer materials that offer a wide range of tunability.[124] The methods of using hydrogel vary widely. One method is to use hydrogel as a nanofluidic channel selector.[125] The hydrogel is used to select a row on the photonic crystal, and then fluid is allowed to flow over the selected row creating a defect waveguide for EM radiation transmission. Other methods include inserting nano-silicon columns in the hydrogel and using the hydrogel to manipulate the position of the columns for the creating of a photonic crystal.[126] One dimensional photonic crystals have been created employing layers of hydrogel. As the hydrogel undergoes its phase change the thickness of the layers change, tuning the 1D bandgap.[127] This method showed a 575% change in the bandgap.

Hydrogel offers an unrealized method of tuning photonic crystals. In the previous chapters it has been shown that as the hydrogel undergoes its volumetric phase change the refractive index changes. This change in refractive index provides a tuning mechanism. In figure 6.15 a schematic of a photonic crystal with hydrogel infiltrating the lattice structure is shown. The remainder of this thesis will describe the process of building and the characteristics of a tunable hydrogel hybrid photonic crystal.

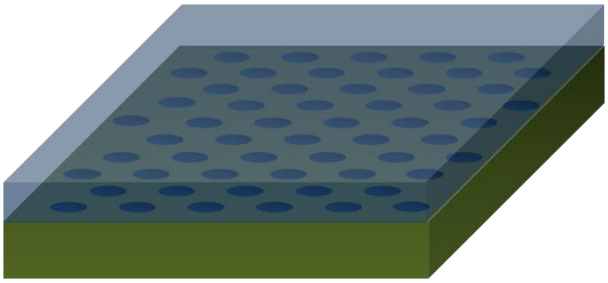

Figure 6.15 A photonic crystal where hydrogel has infiltrated the scatterers and a small layer overlying the photonic crystal.

6.5 Derivations

The following derivations in this section are given for a more thorough understanding of the subjects discussed above.

6.5.1 Energy of an Oscillating Dipole[128]

The density of states is a quantity that describes the allowed energies in a particular system. In solid state physics it is used to describe the packing of the electronic energy levels in a quantum mechanical system. The density of states in regards to EM waves describes the optical properties of the material and can describe the rate of spontaneous emission.

The derivation for the density of states begins with an understanding of dipole radiation. Consider a single dipole oscillating with a frequency ω at a position $\boldsymbol{r}_0$. Using a delta function, the polarization can be written in terms of a dipole moment, $\boldsymbol{p}$, and a positive infinitesimal, $\eta \to 0^+$.

$$P_p(\boldsymbol{r}, t) = \boldsymbol{p}\delta(\boldsymbol{r} - \boldsymbol{r}_o)e^{-i\omega t}\, e^{\eta t}. \tag{6.24}$$

The infinitesimal is included so the electric field is switched on adiabatically at $t = -\infty$.

Maxwell's equations in matter are written as

$$\boldsymbol{\nabla} \cdot \boldsymbol{D}(\boldsymbol{r}, t) = \rho_f \tag{6.25}$$

$$\boldsymbol{\nabla} \cdot \boldsymbol{B}(\boldsymbol{r}, t) = 0 \tag{6.26}$$

$$\boldsymbol{\nabla} \times \boldsymbol{E}(\boldsymbol{r}, t) = -\frac{\partial \boldsymbol{B}}{\partial t} \tag{6.27}$$

$$\boldsymbol{\nabla} \times \boldsymbol{H}(\boldsymbol{r}, t) = \boldsymbol{J}_f + \frac{\partial \boldsymbol{D}}{\partial t} \tag{6.28}$$

In the case of this derivation free currents and free charge density will be ignored, thus

$$\boldsymbol{J}_f = 0 \tag{6.29}$$

and

$$\rho_f = 0 \tag{6.30}$$

Further, the magnetic field B can be written in terms of the auxiliary field, which will simply be called the magnetic field,

$$\boldsymbol{H} \equiv \frac{1}{\mu_0}\boldsymbol{B} - \boldsymbol{M} \tag{6.31}$$

where the magnetization $\boldsymbol{M} = 0$ for nonmagnetic materials. The electric displacement $\boldsymbol{D}(\boldsymbol{r}, t)$ can be written in terms of the electric field and the polarization

$$\boldsymbol{D}(\boldsymbol{r}, t) \equiv \varepsilon_0 \varepsilon(\boldsymbol{r})\boldsymbol{E}(\boldsymbol{r}, t) + \boldsymbol{P}_{ext}(\boldsymbol{r}, t). \tag{6.32}$$

Substituting equations (6.29), (6.30), (6.31) and (6.32) into Maxwell's equations yields[129]

$$\boldsymbol{\nabla} \cdot [\varepsilon_0 \varepsilon(\boldsymbol{r})\boldsymbol{E}(\boldsymbol{r}, t) + \boldsymbol{P}_{ext}(\boldsymbol{r}, t)] = 0. \tag{6.33}$$

$$\boldsymbol{\nabla} \cdot \boldsymbol{H}(\boldsymbol{r}, t) = 0 \tag{6.34}$$

$$\boldsymbol{\nabla} \times \boldsymbol{E}(\boldsymbol{r}, t) = -\frac{1}{\mu_0}\frac{\partial}{\partial t}\boldsymbol{H}(\boldsymbol{r}, t) \tag{6.35}$$

$$\boldsymbol{\nabla} \times \boldsymbol{H}(\boldsymbol{r}, t) = \frac{\partial}{\partial t}[\varepsilon_0 \varepsilon(\boldsymbol{r})\boldsymbol{E}(\boldsymbol{r}, t) + \boldsymbol{P}_{ext}(\boldsymbol{r}, t)] \tag{6.36}$$

The inhomogeneous wave equation is obtained by eliminating the magnetic field in equations (6.34) and (.6.35).

$$-\left[\frac{1}{c^2}\frac{\partial^2}{\partial t^2} + \mathcal{H}\right]\boldsymbol{E}(\boldsymbol{r}, t) = \frac{1}{c^2 \varepsilon_0 \varepsilon(\boldsymbol{r})}\frac{\partial^2}{\partial t^2}\boldsymbol{P}_{ext}(\boldsymbol{r}, t) \tag{6.37}$$

where the differential operator $\mathcal{H}$ is defined as

$$\mathcal{H}[\boldsymbol{A}(\boldsymbol{r}, t)] \equiv \nabla \times [\nabla \times \boldsymbol{A}(\boldsymbol{r}, t)]. \tag{6.38}$$

Further, defining the vector function $\boldsymbol{Q}(\boldsymbol{r}, t)$,

$$\boldsymbol{Q}(\boldsymbol{r}, t) \equiv \sqrt{\varepsilon(\boldsymbol{r})}\boldsymbol{E}(\boldsymbol{r}, t), \tag{6.39}$$

equation (6.37) may be written

$$-\left[\frac{1}{c^2}\frac{\partial^2}{\partial t^2}+\mathcal{H}\right]\boldsymbol{Q}(\boldsymbol{r},t)=\frac{1}{c^2\varepsilon_0\sqrt{\varepsilon(\boldsymbol{r})}}\frac{\partial^2}{\partial t^2}\boldsymbol{P}_{ext}(\boldsymbol{r},t). \tag{6.40}$$

The solution to (6.40) is found in terms of a Green's tensor function[130]

$$\boldsymbol{Q}(\boldsymbol{r},t)=\int_V d\boldsymbol{r}'\int_{-\infty}^{\infty}dt'\overleftrightarrow{\boldsymbol{G}}(\boldsymbol{r},r',t-t')\frac{1}{c^2\varepsilon_0\sqrt{\varepsilon(r')}}\frac{\partial^2}{\partial t^2}P_{ext}(r',t') \tag{6.41}$$

where V is the volume of the photonic crystal and the Green's function is

$$\begin{aligned}\overleftrightarrow{\boldsymbol{G}}(\boldsymbol{r},\boldsymbol{r}',t)=&\frac{c^2}{2\pi V}\sum_{\boldsymbol{k}}\frac{\boldsymbol{Q}_{\boldsymbol{k}}^{(T)}(\boldsymbol{r})\otimes\boldsymbol{Q}_{\boldsymbol{k}}^{(T)}(\boldsymbol{r}')}{2\omega_{\boldsymbol{k}}^{(T)}}\\&\times\int_C\left[\frac{1}{\omega-\omega_{\boldsymbol{k}}^{(T)}+i\eta}-\frac{1}{\omega+\omega_{\boldsymbol{k}}^{(T)}+i\eta}\right]e^{-i\omega t}\,d\omega\\&+\frac{c^2}{2\pi V}\sum_k\boldsymbol{Q}_{\boldsymbol{k}}^{(L)}(\boldsymbol{r})\otimes\boldsymbol{Q}_{\boldsymbol{k}}^{(L)}(\boldsymbol{r}')\int_C\frac{e^{-i\omega t}}{(\omega+i\eta)^2}d\omega.\end{aligned}$$

where (T) represents the transverse component and (L) represents the longitudinal components. The Green's function can be simplified to

$$\overleftrightarrow{\boldsymbol{G}}(\boldsymbol{r},\boldsymbol{r}',t)=-\frac{c^2}{V}\sum_k\left[\frac{sin\left(\omega_{\boldsymbol{k}}^{(T)}t\right)}{\omega_{\boldsymbol{k}}^{(T)}}\boldsymbol{Q}_{\boldsymbol{k}}^{(T)}(\boldsymbol{r})\otimes\boldsymbol{Q}_{\boldsymbol{k}}^{(T)}(\boldsymbol{r}')+t\boldsymbol{Q}_{\boldsymbol{k}}^{(L)}(\boldsymbol{r})\otimes Q_{\boldsymbol{k}}^{(L)\dagger}(\boldsymbol{r}')\right] \tag{6.42}$$

Substituting (6.39) into (6.38)

$$\begin{aligned}\boldsymbol{Q}(\boldsymbol{r},t)=-\frac{1}{\varepsilon_0 V}\sum_k\int_V d\boldsymbol{r}'\int_{-\infty}^{t}dt'\left[\frac{\sin\omega_{\boldsymbol{k}}^{(T)}(t-t')}{\omega_{\boldsymbol{k}}^{(T)}}\boldsymbol{Q}_{\boldsymbol{k}}^{(T)}(\boldsymbol{r})\otimes Q_{\boldsymbol{k}}^{(T)\dagger}(\boldsymbol{r}')+(t-t')\boldsymbol{Q}_{\boldsymbol{k}}^{(L)}(\boldsymbol{r})\right.\\\left.\otimes\boldsymbol{Q}_{\boldsymbol{k}}^{(L)}(\boldsymbol{r}')\right]\frac{1}{\sqrt{\varepsilon(\boldsymbol{r}')}}\frac{\partial^2}{\partial t^2}P_{ext}(\boldsymbol{r}',t')\end{aligned} \tag{6.42}$$

This integral is solved by first integrating by parts

$$\boldsymbol{Q}(\boldsymbol{r},t) = -\frac{1}{\varepsilon_0 V}\sum_{\boldsymbol{k}}\int_V d\boldsymbol{r}' \int_{-\infty}^{t} dt'\Big[\cos\omega_{\boldsymbol{k}}^{(T)}(t-t')\boldsymbol{Q}_{\boldsymbol{k}}^{(T)}(\boldsymbol{r}) \otimes \boldsymbol{Q}_{\boldsymbol{k}}^{(T)\dagger}(\boldsymbol{r}') + \boldsymbol{Q}_{\boldsymbol{k}}^{(L)}(\boldsymbol{r})$$

$$\otimes \boldsymbol{Q}_{\boldsymbol{k}}^{(L)\dagger}(\boldsymbol{r}')\Big]\frac{1}{\varepsilon(\boldsymbol{r}')}\frac{\partial}{\partial t'}\boldsymbol{P}_{ext}(\boldsymbol{r}',t'). \tag{6.43}$$

Using partial integration again

$$\boldsymbol{Q}(\boldsymbol{r},t) = -\frac{1}{\varepsilon_0 V}\sum_{\boldsymbol{k}}\int_V dr'\Big[\boldsymbol{Q}_{\boldsymbol{k}}^{(T)}(\boldsymbol{r}) \otimes \boldsymbol{Q}_{\boldsymbol{k}}^{(T)\dagger}(\boldsymbol{r}') + \boldsymbol{Q}_{\boldsymbol{k}}^{(L)}(\boldsymbol{r}) \otimes \boldsymbol{Q}_{\boldsymbol{k}}^{(L)\dagger}(\boldsymbol{r}')\Big]\frac{1}{\sqrt{\varepsilon(\boldsymbol{r}')}}\boldsymbol{P}_{ext}(\boldsymbol{r}',t)$$

$$+\frac{1}{\varepsilon_0 V}\sum_{\boldsymbol{k}}\int_V d\boldsymbol{r}' \int_{-\infty}^{t} dt' \Big[\omega_{\boldsymbol{k}}^{(T)}\sin\omega_{\boldsymbol{k}}^{(T)}(t-t') \times$$

$$\boldsymbol{Q}_{\boldsymbol{k}}^{(T)}(\boldsymbol{r}) \otimes \boldsymbol{Q}_{\boldsymbol{k}}^{(T)\dagger}(\boldsymbol{r}')\Big]\frac{1}{\sqrt{\varepsilon(\boldsymbol{r}')}}\boldsymbol{P}_{ext}(\boldsymbol{r}',t). \tag{6.44}$$

The direct products can be eliminated by using

$$\sum_{\boldsymbol{k}}\boldsymbol{Q}_{\boldsymbol{k}}^{(T)}(\boldsymbol{r}) \otimes \boldsymbol{Q}_{\boldsymbol{k}}^{(T)\dagger}(\boldsymbol{r}') + \sum_{k}\boldsymbol{Q}_{\boldsymbol{k}}^{(L)}(\boldsymbol{r}) \otimes \boldsymbol{Q}_{\boldsymbol{k}}^{(L)\dagger} = V\vec{I}\delta(\boldsymbol{r}-\boldsymbol{r}'). \tag{6.45}$$

Equation (6.44) then becomes

$$\boldsymbol{Q}(\boldsymbol{r},t) = \frac{1}{\varepsilon_0 V}\sum_{\boldsymbol{k}}\boldsymbol{Q}_{\boldsymbol{k}}^{(T)}(\boldsymbol{r})\int_V d\boldsymbol{r}' \int_{-\infty}^{t} dt'$$

$$\times \frac{\boldsymbol{Q}_{\boldsymbol{k}}^{(T)\dagger}(\boldsymbol{r}')\cdot\boldsymbol{P}_{ext}(\boldsymbol{r}',t')}{\sqrt{\varepsilon(\boldsymbol{r}')}}\omega_{\boldsymbol{k}}^{(T)}\sin\omega_{\boldsymbol{k}}^{(T)}(t-t') - \frac{\boldsymbol{P}_{ext}(\boldsymbol{r},t)}{\varepsilon_0\sqrt{\varepsilon(\boldsymbol{r})}}. \tag{6.46}$$

Substituting into the equation (6.39) to change back to the electric field and placing all the integtals on one side of the equation

$$\boldsymbol{E}(\boldsymbol{r},t) + \frac{\boldsymbol{P}_{ext}(\boldsymbol{r},t)}{\varepsilon_0\varepsilon(\boldsymbol{r})} = \frac{1}{\varepsilon_0 V}\sum_{k}\boldsymbol{E}_{\boldsymbol{k}}^{(T)}(\boldsymbol{r})\int_V d\boldsymbol{r}' \int_{-\infty}^{t} dt'\boldsymbol{E}_{\boldsymbol{k}}^{(T)\dagger}(\boldsymbol{r}')\cdot\boldsymbol{P}_{ext}(\boldsymbol{r}',t')$$

$$\times \omega_{\boldsymbol{k}}^{(T)}\sin\omega_{\boldsymbol{k}}^{(T)}(t-t'). \tag{6.47}$$

Substituting equation (6.24) into equation (6.47) yields

$$E_p(r,t) + \frac{P_p(r,t)}{\varepsilon_0 \varepsilon(r)} = \frac{1}{\varepsilon_0 V}\frac{e^{-i\omega t}}{2}\sum_k \omega_k^{(T)} E_k^{(T)}(r)\left(E_k^{(T)\dagger}(r_i)\cdot p\right)$$

$$\times\left(\frac{1}{\omega+\omega_k^{(T)}+i\eta} - \frac{1}{\omega-\omega_k^{(T)}+i\eta}\right) \tag{6.48}$$

Poynting's vector describes the energy per unit time per unit area transported by the electric and magnetic fields and is given by

$$\boldsymbol{S}(\boldsymbol{r},t) \equiv \boldsymbol{E}(\boldsymbol{r},t)\times\boldsymbol{H}(\boldsymbol{r},t)$$

and in terms of real and imaginary parts by

$$\boldsymbol{S}(\boldsymbol{r},t) = \left[\boldsymbol{E}_p(\boldsymbol{r},t) + \boldsymbol{E}_p{}^*(\boldsymbol{r},t)\right]\times\left[\boldsymbol{H}_p(\boldsymbol{r},t) + \boldsymbol{H}_p{}^*(\boldsymbol{r},t)\right]. \tag{6.49}$$

Taking the time average of Poynting's vector

$$\overline{\boldsymbol{S}(\boldsymbol{r},t)} = \overline{\left[\boldsymbol{E}_p(\boldsymbol{r},t) + \boldsymbol{E}_p^*(\boldsymbol{r},t)\right]\times\left[\boldsymbol{H}_p(\boldsymbol{r},t) + \boldsymbol{H}_p^*(\boldsymbol{r},t)\right]}. \tag{6.50}$$

Using a vector identity to group the vectors

$$\overline{\boldsymbol{S}(\boldsymbol{r},t)} = \left[\boldsymbol{E}_p(\boldsymbol{r},t)\times\boldsymbol{H}_p^*(\boldsymbol{r},t)\right] + \left[\boldsymbol{E}_p^*(\boldsymbol{r},t)\times\boldsymbol{H}_p(\boldsymbol{r},t)\right]. \tag{6.51}$$

Now using equation (6.35) $\boldsymbol{H}_p(\boldsymbol{r},t)$ can be written in terms of $\boldsymbol{E}_p(\boldsymbol{r},t)$. Both $\boldsymbol{H}_p(\boldsymbol{r},t)$ and $\boldsymbol{E}_p(\boldsymbol{r},t)$ are proportional to $e^{-i\omega t}$, thus

$$\boldsymbol{H}_p(\boldsymbol{r},t) = \frac{1}{i\omega\mu_o}\boldsymbol{\nabla}\times\boldsymbol{E}_p(\boldsymbol{r},t). \tag{6.52}$$

Substituting (6.52) and (6.40) and taking the divergence of equation (6.51)

$$\boldsymbol{\nabla}\cdot\overline{\boldsymbol{S}(\boldsymbol{r},t)} = \left[\boldsymbol{H}_p^*(\boldsymbol{r},t)\cdot\left(\boldsymbol{\nabla}\times\boldsymbol{E}_p(\boldsymbol{r},t)\right) - \boldsymbol{E}_p(\boldsymbol{r},t)\cdot\left(\boldsymbol{\nabla}\times\boldsymbol{H}_p^*(\boldsymbol{r},t)\right) + \right.$$

$$\left.\boldsymbol{H}_p(\boldsymbol{r},t)\cdot\left(\boldsymbol{\nabla}\times\boldsymbol{E}_p^*(\boldsymbol{r},t)\right) - \boldsymbol{E}_p^*(\boldsymbol{r},t)\cdot\left(\boldsymbol{\nabla}\times\boldsymbol{H}_p(\boldsymbol{r},t)\right)\right] \tag{6.53}$$

Simplifying

$$\boldsymbol{\nabla}\cdot\overline{\boldsymbol{S}(\boldsymbol{r},t)} = i\omega\left[\left(\boldsymbol{E}_p^*(\boldsymbol{r},t)\cdot\boldsymbol{P}_p(\boldsymbol{r},t)\right) - \left(\boldsymbol{E}_p(\boldsymbol{r},t)\cdot\boldsymbol{P}_p^*(\boldsymbol{r},t)\right)\right] \tag{6.54}$$

Using Cauchy's principle value, $\wp$

$$\frac{1}{\omega - \omega_o \pm i\delta} = \frac{\wp}{\omega - \omega_o} \mp \pi i \delta(\omega - \omega_o) \tag{6.55}$$

and substituting (6.48) into (6.53)

$$\boldsymbol{\nabla} \cdot \overline{\boldsymbol{S}(\boldsymbol{r}, t)} = \frac{\pi \omega^2}{\varepsilon_o V} \delta(\boldsymbol{r} - \boldsymbol{r}_i) \sum_{\boldsymbol{k}} \left| \boldsymbol{p} \cdot \boldsymbol{E}_{\boldsymbol{k}}^{(T)*}(\boldsymbol{r}_i) \right|^2 \delta\left(\omega - \omega_{\boldsymbol{k}}^{(T)}\right) \tag{6.56}$$

The energy density of the fields in the EM wave per unit time is given by

$$U = \oint_{\sigma} d\boldsymbol{\sigma}\, \overline{\boldsymbol{S}(\boldsymbol{r}, t)} = \int_V d\tau\, \boldsymbol{\nabla} \cdot \overline{\boldsymbol{S}(\boldsymbol{r}, t)} \tag{6.57}$$

Substituting (6.56) into equation (6.57)

$$U = \frac{\pi \omega^2}{\varepsilon_o V} \sum_{kn} \left| \boldsymbol{d} \cdot \boldsymbol{E}_{kn}^{(T)*}(\boldsymbol{r}_i) \right|^2 \delta\left(\omega - \omega_{kn}^{(T)}\right). \tag{6.58}$$

The energy emitted per unit time by the oscillating dipole in the photonic crystal can be approximated using the density of states $D(\omega)$. The number of eigenmodes whose eigenfrequencies fall between ω and $\omega + \Delta\omega$ is indicated by $D(\omega)d\omega$. The approximation we make is time averaging to give

$$U \cong \frac{\pi \omega^2}{\varepsilon_o V} \overline{\left| \boldsymbol{d} \cdot \boldsymbol{E}_{kn}^{(T)*}(\boldsymbol{r}_o) \right|^2} \int_0^{\infty} d\omega' D(\omega') \delta(\omega - \omega'). \tag{6.59}$$

Performing the integral

$$U = \frac{\pi \omega^2}{\varepsilon_o V} \overline{\left| \boldsymbol{d} \cdot \boldsymbol{E}_{kn}^{(T)*}(\boldsymbol{r}_o) \right|^2} D(\omega) \tag{6.60}$$

Therefore, the energy radiated form the oscillating dipole is proportional to $D(\omega)$. If $D(\omega) = 0$ in a particular frequency interval then no spontaneous emission takes place.

6.5.2 Proof of Bloch's Theorem for EM Waves

Bloch's theorem in traditional solid state physics describes the interaction of an electron with the potentials from a periodic atomic crystal. In this section instead of

regular atomic nuclei creating the crystal, dielectrics will create the periodic structure, forming the photonic crystal. Bloch's theorem for the electric and magnetic fields are

$$\boldsymbol{E}(\boldsymbol{r}) = \boldsymbol{E}_{\boldsymbol{k}}(\boldsymbol{r}) = \boldsymbol{u}_{\boldsymbol{k}}(\boldsymbol{r})e^{i\boldsymbol{k}\cdot\boldsymbol{r}} \tag{6.61}$$

$$\boldsymbol{H}(\boldsymbol{r}) = \boldsymbol{H}_{\boldsymbol{k}}(\boldsymbol{r}) = \boldsymbol{v}_{\boldsymbol{k}}(\boldsymbol{r})e^{i\boldsymbol{k}\cdot\boldsymbol{r}}. \tag{6.62}$$

and ω represents the angular eigenfrequency. Since the proof for the electric field and magnetic field[131] are similar only the proof for the electric field is shown. The eigenfunction for the electric filed is given by the Maxwell's equations

$$\frac{1}{\varepsilon(\boldsymbol{r})}\boldsymbol{\nabla}\times\boldsymbol{\nabla}\times\boldsymbol{E}(\boldsymbol{r}) = \frac{\omega^2}{c^2}\boldsymbol{E}(\boldsymbol{r}), \tag{6.63}$$

or

$$\boldsymbol{\nabla}\times\boldsymbol{\nabla}\times\boldsymbol{E}(\boldsymbol{r}) - \frac{\omega^2}{c^2}\varepsilon(\boldsymbol{r})\boldsymbol{E}(\boldsymbol{r}) = 0. \tag{6.64}$$

The periodic dielectric function can be expanded in terms of a Fourier series

$$\varepsilon(\boldsymbol{r}) = \sum_{\boldsymbol{G}} \lambda(\boldsymbol{G})e^{i\boldsymbol{G}\cdot\boldsymbol{r}}. \tag{6.65}$$

where $\boldsymbol{G}$ represents the reciprocal lattice vectors. Finally, a Fourier integral can be used to express the eigenfunction of the electric field

$$\boldsymbol{E}(\boldsymbol{r}) = \int d\boldsymbol{k}\, \boldsymbol{E}(\boldsymbol{k})e^{i\boldsymbol{k}\cdot\boldsymbol{r}}. \tag{6.66}$$

Substituting equations (6.65) and (6.66) into equation (6.64) gives

$$\int d\boldsymbol{k}\left[\boldsymbol{k}\times\left(\boldsymbol{k}\times\boldsymbol{E}(\boldsymbol{k})\right)\right]e^{i\boldsymbol{k}\cdot\boldsymbol{r}} + \frac{\omega^2}{c^2}\sum_{G}\int d\boldsymbol{k}\,\lambda(\boldsymbol{G})\boldsymbol{E}(\boldsymbol{k}-\boldsymbol{G})e^{i\boldsymbol{k}\cdot\boldsymbol{r}} = 0 \tag{6.67}$$

Equation (6.67) is a function of $\boldsymbol{r}$ only, thus the integrand disappears

$$\boldsymbol{k}\times\left(\boldsymbol{k}\times\boldsymbol{E}(\boldsymbol{k})\right) + \frac{\omega^2}{c^2}\sum_{\boldsymbol{G}}\lambda(\boldsymbol{G})\boldsymbol{E}(\boldsymbol{k}-\boldsymbol{G}) = 0 \tag{6.68}$$

Thus, only the Fourier components $\boldsymbol{E}(\boldsymbol{k})$ related to the reciprocal lattice vectors $\boldsymbol{G}$ form a set of eigenvalues equations.

$$\boldsymbol{E}_{\boldsymbol{k}}(\boldsymbol{r}) = \sum_{\boldsymbol{G}} \boldsymbol{E}(\boldsymbol{k}-\boldsymbol{G}) e^{i(\boldsymbol{k}-\boldsymbol{G})\cdot\boldsymbol{r}}. \tag{6.69}$$

Defining

$$\boldsymbol{u}_{\boldsymbol{k}}(\boldsymbol{r}) = \sum_{\boldsymbol{G}} \boldsymbol{E}(\boldsymbol{k}-\boldsymbol{G}) e^{-i\boldsymbol{G}\cdot\boldsymbol{r}} \tag{6.70}$$

allows equation (6.69) to be written as

$$\boldsymbol{E}_{\boldsymbol{k}}(\boldsymbol{r}) = \boldsymbol{u}_{\boldsymbol{k}}(\boldsymbol{r}) e^{i\boldsymbol{k}\cdot\boldsymbol{r}}. \tag{6.71}$$

Equation (6.71) is Bloch's theorem derived for the electric field portion of an electromagnetic wave. Individual eigenvalues and eigenfunctions are typically denoted by a subscript.

---

[1] K. Sakoda, *Optical Properties of Photonic Crystals*, 2nd ed. (Springer, New York 2005), p. 2.

[2] E. M. Purcell, "Spontaneous Emission Probabilities at Radio Frequencies" Phys. Rev. **69**, 681 (1946).

[3] K. Yoshino, S. Tatsuhara, Y. Kawagishi, M. Ozaki, A. A. Zakhidov, Z. V. Vardeny, "Spectral Narrowing of Photoluminescence in Conducting Polymer and Fluorescent Dyes Infiltrated in Photonic Crystal, Synthetic Opal," Jpn. J. Appl. Phys. **37**, L1187-L1189 (1998).

[4] K. Yoshino, S. Tatsuhara, Y. Kawagishi, M. Ozaki, A. A. Zakhidov, Z. V. Vardeny, "Amplified spontaneous emission and lasing in conducting polymers and fluorescent dyes in opals as photonic crystals," Appl. Phys. Lett. **74**, 2590-2592 (1999).

[5] J. G. Fleming, Shawn-Yu Lin, "Three-dimensional photonic crystal with a stop band from 1.35 to 1.95 μm," Opt. Lett. **24**, 49-51 (1999).

[6] M. Haraguchi, T. Nakai, A. Shinya, T. Okamoto, M. Fukui, T. Koda, R. Shimada, K. Ohtaka, K. Takeda, "Optical Modes in Two-dimensionally Ordered Dielectric Spheres," Jpn. J. Appl. Phys. **39**, 1747 (2000).

[7] T. Fujimura, T. Itoh, A. Imada, R. Shimada, T. Koda, N. Chiba, H. Muramatsu, H. Miyazaki, K. Ohtaka, "Near-field optical images of ordered polystyrene particle layers and their photonic band effect," J. Lumin. **87-89**, 954-956 (2000).

[8] T. Fujimura, T. Itoh, K. Hayashibe, K. Edamatsu, K. Shimoyama, R. Shimada, A. Imada, T. Koda, Y. Segawa, N. Chiba, H. Muramatsu, T. Ataka, Observation of local light propagation in ordered latex layers by scanning near-field optical microscope," Mater. Sci. Eng. B **48**, 94-102 (1997).

[9] H. T. Miyazaki, H. Miyazaki, K. Ohtaka, T. Sato, "Photonic band in two-dimensional lattices of micrometer-sied spheres mechanically arranged under a scanning electron microscope," J. Appl. Phys. **87**, 7152-7158 (2000).

[10] S. Fan, P. R. Villeneuve, J. D. Joannopoulos, E. F. Schubert, "High Extraction Efficiency of Spontaneous Emission from Slabs of Photonic Crystals," Phys. Rev. Lett. **78**, 3294-3297 (1997).

[11] D. Labilloy, H. Benisty, C. Weisbuch, C. J. M. Smith, T. F. Krauss, R. Houdré, U. Oestrele, "Finely resolved transmission spectra and band structure of two-dimensional photonic crystals using emission from InAs quantum dots," Phys. Rev. B **59**, 1649-1652 (1999).

[12] O. Painter, R. K. Lee, A. Scherer, A. Yariv, J. D. O'Brien, P. D. Dapkus, I. Kim, "Two-Dimensional Photonic Band-Gap Defect Mode Laser," Science **284**, 1819-1821 (1999).

[13] J. C. Maxwell, "A dynamical theory of the electromagnetic field," Phil. Trans. Roy. Soc. (London) **155**, 459-512 (1865).

[14] S. G. Johnson, S. D. Joannopoulos, *Photonic Crystals: The Road from Theory to Practice*, ed. (Springer, New York 2002), p. 17.

[15] Lord Rayleigh, "On the maintenance of vibrations by force of double frequency, and on the propagation of waves through a medium endowed with a periodic structure," Phil. Mag. **26**, 145-159 (1887).

[16] Lord Rayleigh, "On the reflection of light from a regularly stratified medium," Proc. Roy. Soc. London **93**, 565-577 (1917).

[17] G. Floquet, "Sur les équations différentielles linéaries à coefficients périodiques," Ann. École Norm. Sup. **12**, 47-48 (1883); F. Bloch, "Über die quantenmechanik der electronen in kristallgittern," Z. Physik **52**, 555-600 (1928).

[18] K. Ohtaka, "Energy band of photons and low-energy photon diffraction," Phys. Rev B **19**, 5057-5067 (1979).

[19] K. Ohtaka, "Scattering theory of low-energy photon diffraction," J. Phys. C: Solid St. Phys. **13**, 667-680 (1980).

[20] P. A. Hiltner and I. M. Krieger, "Diffraction of Light by Ordered Suspensions," J. Phys. Chem. **73**, 2386-2389 (1969).

[21] R. Williams, R. S. Crandall, P. J. Wojtwicz, "Melting of Crystalline Suspensions of Polystyrene Spheres," Phys. Rev. Lett. **37**, 348-351 (1976).

[22] H. Fujita and K. Ametani, "Optical Properties of Colloidal Crystal Latex near the Melting Point," Jpn. J. Appl. Phys. **16**, 1907-1917 (1977).

[23] G. B. Street and R. L. Greene, "Preparation and Properties of $(SN)_x$," IBM J. Res. Develop. **21**, 99-110 (1977).

[24] J. H. Evans, "Observations of a Regular Void Array in High Purity Molybdenum irradiated with 2 MeV Nitrogen Ions," Nature **229**, 403-404 (1971).

[25] B. L. Eyre, J. M. Evans, *Void Formed by Irradiation of Reactor Materials*, ed. S. H. Pugh et. al. (London, BNES 1971).

[26] B. K. Vainstein, *Diffraction of X-rays by Chain Molecules*, (Amsterdam, Elsevier 1966).

[27] K. Kambe, Z. Naturf **22a** 322-330 (1967).

[28] K. Kambe, Z. Naturf. **22a** 422-431 (1967).

[29] K. Kambe, Z Naturf **23a**, 1280 (1968).

[30] J. Korringa, "On the calculation of the energy of a Bloch wave in a metal," Physica **13**, 392-400 (1947).

[31] W. Kohn and N. Rostoker, "Solution of the Schrödinger Equation in Periodic Lattices with an Application to Metallic Lithium," Phys. Rev. **94**, 1111-1120 (1954).

[32] D. S. Boudreaux and V. Heine, "Band structure treatment of low energy electron diffraction intensities," Surf. Sci. **8**, 426-444 (1967).

[33] J. B. Pendry, "The application of pseudopotentials to low-energy diffraction II: Calculation of the reflected intensities," J. Phys. C: Solid St. Phys. **2**, 2273-2282 (1969).

[34] D. R. Hartree, "Results of Calculations of Atomic Wave Functions. I. Survey, and Self-consistent Fields for Cl^- and Cu^+," Proc. Roy. Soc. London A **141**, 282-301 (1933). J. C. Slater, "Not on Hartree's Method," Phys. Rev. **35**, 210-211 (1930); V. Fock, Z. Physic **61**, 126

(1930); L. Brillouin, *Les Champs Self-Consistents de Hartree et de Fock*, Actualiés Scientifiques et Industrielles No. 159 (Herman et Cie. 1934).

[35] J. B. Pendry, "Ion core scattering and low energy electron diffraction I J. Phys. C. Solid St. Phys. **4**, 2501-2513 (1971).

[36] J. B. Pendry, "Ion core scattering and low energy electron diffraction II J. Phys. C. Solid St. Phys. **4**, 2514-2523 (1971).

[37] E. Yablanovitch, "Inhibited Spontaneous Emission in Solid-State Physics and Electronics," Phys. Rev. Lett. **58**, 2059 (1987).

[38] H. A. Haus, C. V. Shank, "Antisymmetric Taper of Distributed Feedback Lasers," IEEE J. Quantum Electron. **12**, 532-539 (1976).

[39] E. Yablonovitch, R. Bhat, J. P. Harbison, R. A. Logan, "Survey of defect-mediated recombination lifetimes in GaAs epilayers grown by different methods," Appl. Phys. Lett. **50**, 1197-1199 (1987).

[40] E. Yablonovitch, E. O. Kane, "Reduction of lasing threshold current density by the lowering of valence band effective mass," J. Lightwave Technol. **4**, 504-506 (1986).

[41] E. Yablonovitch, "Statistical ray optics," J. Opt. Soc. Am. **72**, 899 (1982).

[42] A. Z. Genack, "Optical Transmission in Disordered Media," Phys. Rev. Lett. **58**, 2043-2046 (1987).

[43] G. Watson, P. Fleury, S. McCall, "Searching for photon localization in the time domain," Phys. Rev. Lett. **58**, 945-948 (1987).

[44] W. Chen, D. L. Mills, "Gap solitons and the nonlinear optical response of superlattices," Phys. Rev. Lett. **58**, 160-163 (1987).

[45] S. John, "Strong Localization of Photons in Certain Disordered Dielectric Superlattices," Phys. Rev. Lett. **58**, 2486 (1987).

[46] P. W. Anderson, "Absence of Diffusion in Certain Random Lattices," Phys. Rev. **109**, 1492-1505 (1958).

[47] E. Abrahams, P. W. Anderson, D. C. Licciardello, T. V. Ramakrishnan, "Scaling Theory of Localization: Absence of Quantum Diffusion in Two Dimensions," Phys. Rev. Lett. **42**, 673-676 (1979).

[48] S. John, "Electromagnetic Absorption in a Disordered Medium near a Photon Mobility Edge," Phys. Rev. Lett. **53**, 2169-2172 (1984).

[49] S. John, M. J. Stephen, "Wave propagation and localization in a long-range correlated random potential," Phys. Rev. B **28**, 6358-6368 (1983).

[50] R. D. Meade, A. Devenyi, J. D. Joannopoulos, O. L. Alerhand, D. A. Smith, K. Kash, "Novel applications of photonic band gap materials: Low-loss bends and high Q cavities," J. Appl. Phys. **75** 4753-4755 (1994).

[51] A. Mekis, J.C. Chen, I. Kurland, S. Fan, P.R. Villeneuve and J.D. Joannopoulos, "High Transmission through Sharp Bends in Photonic Crystal Waveguides," Phys. Rev. Lett. **77**, 3787 (1996).

[52] S.Y. Lin, E. Chow, V. Hietala, P.R. Villeneuve, and J.D. Joannopoulos, "Experimental Demonstration of Guiding and Bending of Electromagnetic Waves in a Photonic Crystal," Science **282**, 274 (1998).

[53] A. Scherer, O. Painter, J. Vuckovic, M. Loncar, T. Yoshie, "Photonic Crystals for Confining and Guiding and Emitting Light," Trans. Nanotech. **1** 4-11 (2002).

[54] M. Notomi, K. Yamada, A. Shinya, J. Takahashi, C. Takahashi, I, Yokohama, "Extremely Large Group-Velocity Dispersion of Line-Defect Waveguides in Photonic Crystal Slabs," Phys. Rev. Lett. **87**, 253902-1 (2001).

[55] M. Lončar, D. Nedeljković, T. Doll, J. Vučković, A. Sherer, T. P. Pearsall, "Waveguiding in planar photonic crystals," App. Phys. Lett. **77** 1937-1939 (2000).

[56] S. G. Johnson, S. Fan, P. R. Villeneuve, J. D. Joannopoulos, and L. A. Kolodziejski, "Guided modes in photonic crystal slabs," Phys. Rev. B **60**, 5751-5758 (1999).

[57] S. G. Johnson, P. R. Villeneuve, S. Fan, J. D. Joannopoulos, "Linear waveguides in photonic-crystal slabs," Phys. Rev. B **62**, 8212-8222 (2000).

[58] K. Ohtaka, Y. Tanabe, "Photonic Bands Using Vector Spherical Waves. III. Group-Theoretical Treatment," J. Phys. Soc. Jpn. **65**, 2670-2684 (1996).

[59] K. Sakoda, "Symmetry, degeneracy, and uncoupled modes in two-dimensional photonic lattices," Phys. Rev. B **52**, 7982-7986 (1995).

[60] K. Sakoda, "Group-theoretical classification of eigenmodes in three dimensional photonic lattices," Phys. Rev. B **55**, 15345-15348 (1997).

[61] P. L. Gourley, J. R. Wendt, G. A. Vawter, T. M. Brennan, B. E. Hammons, "Optical properties of two-dimensional photonic lattices fabricated as honeycomb nanostructures in compound semiconductors," Appl. Phys. Lett. **64**, 687-689 (1994).

[62] A. Mekis, S. Fan, J. D. Joannopoulos, "Bound states in photonic crystal waveguides and waveguide bends," Phys. Rev. B **58**, 4809-4817 (1998).

[63] S. G. Johnson, P. R. Villeneuve, S. Fan, J. D. Joannopoulos, "Linear waveguides in photonic-crystal slabs," Phys. Rev. B **62**, 8212-8221 (2000).

[64] S. G. Johnson, S. Fan, P. R. Villeneuve, J. D. Joannopoulos, and L. A. Kolodziejski, "Guided modes in photonic crystal slabs," Phys. Rev. B **60**, 5751-5758 (1999).

[65] H. Benisty, "Modal analysis of optical guides with two-dimensional photonic band-gap boundaries," J. Appl. Phys. **79**, 7483-7492 (1996).

[66] P. L. Gourley, J. R. Wendt, G. A. Vawter, T. M. Brennan, B. E. Hammons, "Optical properties of two-dimensional photonic lattices fabricated as honeycomb nanostructures in compound semiconductors," Appl. Phys. Lett. **64**, 687-689 (1994).

[67] Y. Chen, G. Faini, H. Launois, J. Etrillard, "Fabrication of two-dimensional photonic lattices in GaAs: the regular graphite structures," Supperlattices and Microsctructres **22**, 109-113 (1997).

[68] R. D. Meade, A. Devenyi, J. D. Joannopoulos, O. L. Alerhand, D. A. Smith, K. Kash, "Novel applications of photonic band gap materials: Low loss bends and high Q cavities," J. Appl. Phys. **75**, 4753-4755 (1994).

[69] T. Kraus, R. De La Rue, S. Band, "Two-dimensional photonic bandgap structures operating at near-infrared wavelengths," Nature **383**, 699-702 (1996).

[70] M. D. B. Charlton, S. W. Roberts, G. J. Parker, "Guided mode analysis, and fabrication of a 2-dimensional visible photonic band structure confined within a planar semiconductor waveguide," Material Sci. and Eng. B **49**, 155-165 (1997).

[71] J. S. Foresi, P. R. Villeneuve, J. Ferrera, E. R. Thoen, G. Steinmeyer, S. Fan, J. D. Joannopoulos, L. C. Kimerling, H. I. Smith, E. P. Ippen, "Photonic-bandgap microcavities in optical waveguides," Nature **390**, 143-145 (1997).

[72] W. Bogaerts, D. Taillaert, B. Luyssaert, P. Dumon, J. Van Campenhour, P. Bienstman, D. Van Thourhout, R. Baets, V. Wiaux, S. Beckx, "Basic structures for photonic integrated circuits in Silicon-on-insulator," Optics Express **12**, 1583-1591 (2004).

[73] M. Kanskar, P. Paddon, V. Pacradouni, R. Morin, A. Busch, J. F. Young, S. R. Johnson, J. Mackenzie, T. Tiedje,"Observation of leaky slab modes in an airbridged semiconductor waveguide with a two-dimensional photonic lattice," Appl. Phys. Lett. **70**, 1438-1440 (1997).

[74] J. D. Joannopoulos, P. R. Villeneuve, S. Fan, "Photonic crystals: putting a new twist on light," Nature **386**, 143-149 (1997).

[75] N. Kawai, K. Inoue, N. Carlsson, N. Ikeda, Y. Sugimoto, K. Asakawa, and T. Takemori, "Confined Band Gap in an Air-Bridge Type of Two-Dimensional AlGaAs Photonic Crystal," Phys. Rev. Lett. **86**, 2289-2292 (2001).

[76] Y. Sugimoto, Y. Tanaka, N. Ikeda, Y. Nakamura, K. Asakawa, K. Inoue, "Low propagation loss of 0.76 db/mm in GaAs-based single-line-defect two-dimensional photonic crystal slab waveguides up to 1cm in length," Opt. Express **12**, 1090-1096 (2004).

[77] Y. Sugimoto, N. Ikeda, N. Carlsson, K. Asakawa, N. Kawai, and K. Inoue, "Fabrication and Characterization of different types of two-dimensional AlGaAs photonic crystal slabs," J. Appl. Phys. **91**, 922-929, (2002).

[78] Y. Sugimoto, N. Ikeda, N. Carlsson, K. Asakawa, N. Kawai, K. Inoue, "Theoretical and experimental investigation of straight defect waveguides in AlGaAs-based air-bridge-type two-dimensional slabs," Appl. Phys. Lett. **79**, 4286-4288 (2001).

[79] P. R. Villeneuve, S. Fan, J. D. Joannopoulos, K. –Y. Lim, G. S. Petrich, L. A. Kolodziejski, R. Reif, "Air-Bridge microcavities," Appl. Phys. Lett. **67**, 167-169 (1995).

[80] A. Scherer, O. Painter, B. D'Urso, R. Lee, A. Yariv, "InGaAsP photonic bandgap crystal membrane microresonators," J. Vac. Sci. & Technol. B: Microelectronics and Nanometer Structures **16**, 3906-3910 (1998).

[81] M. Kanskar, P. Paddon, V. Pacraouni, R. Morin, A. Busch, J. F. Young, S. R. Johnson, J. MacKenzie, T. Tiedje, "Observation of leaky slab modes in an air-bridge semiconductor waveguide with a two-dimensional photonic lattice," Appl. Phys. Lett. **70**, 1438-1440 (1997).

[82] Y. Sugimoto, N. Ikeda, N. Carlsson, K. Asakawa, N. Kawai, K. Inoue, "AlGaAs-Based Two-Dimensional Photonic Crystal Slab With Defect Waveguides for Planar Lightwave Circuit Applications," IEEE J. Quantum Electron. **38**, 760-769 (2002).

[83] P. I. Borel, B. Bilenberg, L. H. Frandsen, T. Nielsen, J. Fage-Pedersen, A. V. Lavrinenko, J. S. Jensen, O. Sigmund, A. Kristensen, "Imprinted silicon-based nanophotonics," Optics Express **15**, 1261-1266 (2007).

[84] M. Lončar, D. Nedeljković, T. Doll, J. Vučković A. Scherer, T. P. Pearsall, "Waveguiding in planar photonic crystals," Appl. Phys. Lett. **77**, 19371939 (2000).

[85] S. McNab, N. Moll, Y. Vlasov, "Ultra-low loss photonic integrated circuit with membrane-type photonic crystal waveguides," Optics Express **11**, 2927-2939 (2003).

[86] S. Kuchinsky, D. C. Allan, N. F. Borrelli, J. C. Cotteverte, "3D localization in a channel waveguide in a photonic crystal with 2D periodicity," Opt. Commun. **175**, 147-152 (2000).

[87] D. Labilloy, H. Benisty, C. Weisbuch, T. F. Krauss, R. M. De La Rue, V. Bardinal, R. Houdré, U. Oesterle, D. Cassagne, C. Jouanin, "Quantitative Measurement of Transmission, Reflection, and Diffraction of Two-Dimensional Photonic Band Gap Structures at Near-Infrared Wavelengths," Phys. Rev. Lett. **79**, 4147-4150 (1997).

[88] Masatoshi Tokushima and Hirohito Yamada, "Light Propagation in a Photonic-Crystal-Slab Line-Defect Waveguide," J. Quantum Elect. **38**, 753-759 (2002).

[89] M. Notomi, A. Shinya, K. Yamada, J. Takahashi, C. Takahashi, and I. Yokoyama, "Singlemode transmission within photonic bandgap of width-varied single-line-defect photonic crystal waveguides on SOI substrates," Electron. Lett. **37**, 293-295, (2001).

[90] A. Mekis, J. C. Chen, I. Kurland, S. Fan, P. R. Villeneuve, J. D. Joannopoulos, "High Transmission through Sharp Bends in Photonic Crystal Waveguides," Phys. Rev. Lett. **77**, 3787-3790 (1996).

[91] S. Y. Lin, E. Chow, V. Hietch, P. R. Villeneuve, J. D. Joannopoulos, "Experimental Demonstration of Guiding and Bending of Electromagnetic Waves in a Photonic Crystal," Science **282**, 274-275 (1998)

[92] J. Yonekura, M. Ikeda, and T. Baba," Analysis of finite 2D photonic crystals of columns and lightwave devices using the scattering matrix method," J. Lightwave Technol. **17**, 1500-1508 (1999).

[93] M. Lončar, D. Nedelijkoović, T. Doll, J. Vučković, A. Scherer, and T.P. Pearsall, "Waveguiding in planar photonic crystals," Appl. Phys. Lett. **77**, 1937-1939 (2000).

[94] M. Tokushima, H. Kosaka, A. Tomita, H. Yamada, "Lightwave propagation through a 120° sharply bent single-line-defect photonic crystal waveguide," Appl. Phys. Lett. **76**, 952-954 (2000).

[95] "Waveguides and waveguide bends in two dimensional photonic crystal slabs," Phys. Rev. B **62**, 4488-4492 (2000).

[96] S. Fan, G. Johnson, J.D. Joannopoulos, C. Manolatou, and H.A. Haus, "Waveguide branches in photonic crystals," J. Opt. Soc. Am. B **18**, 162-165 (2001).

[97] E. Chow, A. Grot, L. W. Mirkarimi, M. Sigalas, and G. Girolami, "Ultracompact biochemical sensor built with two-dimensional photonic crystal microcavity," Opt. Lett. **29**, 1093-1095 (2004).

[98] M. Notomi, A. Shinya, K. Yamada, J. –I. Takahashi, C. Takahashi, I. Yokohama, "Structural tuning of guided modes of line-defect waveguides of silicon-on-insulator photonic crystal slabs," IEEE J. Quantum Electron. **38**, 736-742 (2002).

[99] P. Halevi and F. Ramos-Mendieta, "Tunable Photonic Crystals with Semiconducting Constituents," Phys. Rev. Lett. **85**, 1875 - 1878 (2000).

[100] H. Němec, P. Kužel, L. Duvillaret, A. Pashkin, M. Dressel, M. T. Sebastian, "Highly tunable photonic crystal filter for the terahertz range," Opt. Lett. **30**, 549-551 (2005).

[101] C. Xu, X. Hu, Y. Li, X. Liu, R. Fu, and J. Zi, "Semiconductor-based tunable photonic crystals by means of an external magnetic field," Phys. Rev. B **68**, 193201 (2003).

[102] M. Harold, H. Chong and R.M. De La Rue, "Tuning of Photonic Crystal Waveguide Microcavity by Thermooptic Effect," Photonic Tech. Lett. **16**, 1528-1530 (2004).

[103] T. Chu. H. Yamada, S. Ishida, Y. Arakawa, "Thermooptic switch based on photonic-crystal line-defect waveguides," IEEE Photon. Technol. Lett. **17**, 2083-2085 (2005).

[104] L. Gu, W. Jiang, X. Chen, R. T. Chen, "Thermooptically Tuned Photonic Crystal Waveguide Silicon-on-Insulator Mach-Zehnder Interferometers," IEEE Photon. Technol. Lett. **19**, 342-344 (2007)

[105] W. Park, E. Schonbrun, M. Tinker, J. –B. Lee, "Tunable nanophotonic device based on flexible photonic crystal," Proc. SPIE **5111**, 165-172 (2004).

[106] M. T. Tinker and J-B. Lee, "Thermal and optical simulation of a photonic crystal light modulator based on the thermo-optic shift of the cut-off frequency," Optics Express **13**, 7174-7188 (2005).

[107] V. Berger, "From photonic band gaps to refractive index engineering," Opt. Mater. **11**, 131-142 (1999).

[108] M. Schmidt, M. Eich, U. Huebner and R. Boucher, "Electro-optically tunable photonic crystals," Appl. Phys. Lett. **87**, 121110 (2005).

[109] Nina Skivesen, Amélie Têtu, Martin Kristensen, Jørgen Kjems, Lars H. Frandsen, and Peter I. Borel, "Photonic-crystal waveguide biosensor," Optics Express **15**, 3169-3176 (2007).

[110] K. Busch, S. John, "Liquid-Crystal Photonic-Band-Gap Materials: The Tunable Electromagnetic Vacuum," Phys. Rev. Lett. **83**, 967-970 (1999).

[111] K. Yoshino, Y. Shimoda, Y. Kawagishi, K. Nakayama, M. Ozaki, "Temperature tuning of the stop band in transmission spectra of liquid-crystal infiltrated synthetic opal as tunable photonic crystal," Appl. Phys. Lett. **75**, 932-934 (1999).

[112] K. Yoshino, S. Satoh, Y. Shimoda, T. Kawagishi, K. Nakayama, M. Ozaki, "Tunable Optical Stop Band and Reflection Peak in Synthetic Opal Infiltrated with Liquid Crystal and Conducting Polymer as Photonic Crystal," Jpn. J. Appl. Phys. **38**, L961-L963 (1999).

[113] A. Blanco, E. Chomski, S. Grabtchak, M. Ibisate, S. John, S. W. Leonard, C. Lopez, F. Meseguer, H. Miguez, J. P. Mondia, G. A. Ozin, O. Toader and H. M. van Driel, "Large-scale synthesis of a silicon photonic crystal with a complete three-dimensional bandgap near 1.5 micrometres," Nature **405**, 437-440 (2000).

[114] S. W. Leonard, J. P. Mondia, H. M. van Driel, O. Toader, S. John, "Tunable two-dimensional photonic crystals using liquid crystal infiltration," Phys. Rev. B **61**, R2389-R2392 (2000).

[115] E. P. Kosmidou, E. E. Kriezis, T. D. Tsiboukis, "Analysis of Tunable Photonic Crystal Devices Comprising Liquid Crystal Materials as Defects," J. Quantum Electon. **41**, 657-665 (2005).

[116] D. Kang, J. E. Maclennan, N. A. Clark, A. A. Zakhidov, R. H. Baughman, "Electro-optic Behavior of Liquid-Crystal-Filled Silica Opal Photonic Crystals: Effect of Liquid-Crystal alignment," Phys. Rev. Lett. **86**, 4052-4055 (2001).

[117] F. Du, Y. –Q. Lu, S. –T. Wu, "Electrically tunable liquid crystal photonic crystal fiber," Appl. Phys. Lett. **85**, 2181-2183 (2004).

[118] M. W. Haakestad, T. T. Alkeskold, M. D. Nielsen, L. Scolari, J. Riishede, H. E. Engan, A. Bjarklev, "Electrically Tunable Photonic Crystal Bandgap Guidance in a Liquid-Crystal-Filled Photonic Fiber," Photonics Technol. Lett. **17**, 819-821 (2005).

[119] T. T. Larsen, A. Bjarkley, D. S. Hermann, and J. Broeng, "Optical devices based on liquid crystal photonic bandgap fibres," Optics Express **11**, 2589-2586 (2003).

[120] M. J. Escuti, J. Qi, and G. P. Crawford, "Two-dimensional tunable photonic crystal formed in a liquid-crystal/polymer composite: Threshold behavior and morphology," App. Phys. Lett. **83**, 1331-1333 (2003).

[121] C. Schuller, F. Klopf, J. P. Reithmaier, M. Kamp, and A. Forchel, "Tunable photonic crystals fabricated in III-V semiconductor slab waveguides using infiltrated liquid crystals," App. Phys. Lett. **82**, 2767-2769 (2003).

[122] G. Mertens, T. Röder, R. Schweins, K. Huber, H. S. Kitzerow, "Shift of the photonic band gap in two photonic crystal/liquid crystal composites," Appl. Phys. Lett. **80**, 1885-1887 (2002).

[123] D. McPhail, M. Straub, and M. Gu, “Electrical tuning of three-dimensional photonic crystals using polymer dispersed liquid crystals,” Appl. Phys. Lett. **86**, 051103 (2005).

[124] J. H. Holtz and S. A. Asher, “Polymerized colloidal crystal hydrogel films as intelligent chemical sensing materials,” Nature **389**, 829-832 (1997).

[125] D. Erickson, T. Rockwood, T. Emery, A. Scherer, D. Psaltis, “Nanofluidic tuning of photonic crystal circuits,” Optics Lett. **31**, 59-61 (2006).

[126] A. Sidorenko, T. Krupenkin, A. Taylor, P. Fratzl, J. Aizenberg, “Reversible Switching of Hydrogel-Actuated Nanostructures into Complex Micropatterns,” Science **315**, 487-490 (2007).

[127] Y. J. Kang, J. J. Walish, T. Goishnyy, E. L. Thomas, "Broad-wavelength-range chemically tunable block-copolymer photonic gels," Nature Mater. **6**, 957-960 (2007).

[128] K. Sakoda, K. Ohtaka, "Optical response of three-dimensional photonic lattices: Solutions of inhomogeneous Maxwell's equations and their applications," Phys. Rev. B **54**, 5732-5741 (1996).

[129] J. P. Dowling, C. M. Bowden, "Atomic emission rates in inhomogeneous media with applications to photonic band structures," Phys. Rev. A **46**, 612-622 (1992).

[130] R. J. Glauber, M. Lewenstein, "Quantum optics of dielectric media," Phys. Rev. A **43**, 467-491 (1991).

[131] S. G. Johnson, J. D. Joannopoulos, "Introduction to Photonic Crystals: Bloch's Theorem, Band Diagrams, and Gaps (But no defect)," http://ab-initio.mit.edu/photons/tutorial/photonic-intro.pdf, (Accessed Feb 2008).

CHAPTER 7

PHOTONIC CRYSTAL SIMULATIONS

7.1 Bandgap Calculation—Plane Wave Method

The software used in performing photonic bandgap simulations is made by the RSoft Design Corporation of Ossining, New York. The packaged used in the bandgap simulations is the BandSolve portion of the RSoft suite. In this section the plane wave method calculating the bandgap of a photonic crystal will be described in general. Although there are other methods for calculating the bandgap the plane wave method has been widely used and generally accepted since 2D and 3D photonic bandgaps were found.[1, 2, 3] As in the previous chapter, free charges and free currents are absent in the photonic crystal. Maxwell's equations in matter are given by

$$\boldsymbol{\nabla} \cdot \boldsymbol{D}(\boldsymbol{r}, t) = 0 \tag{7.1}$$

$$\boldsymbol{\nabla} \cdot \boldsymbol{B}(\boldsymbol{r}, t) = 0 \tag{7.2}$$

$$\boldsymbol{\nabla} \times \boldsymbol{E}(\boldsymbol{r}, t) = -\frac{\partial}{\partial t}\boldsymbol{B}(\boldsymbol{r}, t) \tag{7.3}$$

$$\boldsymbol{\nabla} \times \boldsymbol{H}(\boldsymbol{r}, t) = \frac{d}{dt}\boldsymbol{D}(\boldsymbol{r}, t) \tag{7.4}$$

To solve find the wave equation Maxwell's equations must be put in terms of $\boldsymbol{E}(\boldsymbol{r}, t)$ and $\boldsymbol{H}(r, t)$. The displacement vector $\boldsymbol{D}(\boldsymbol{r}, t)$ in terms of the dielectric constant $\varepsilon(\boldsymbol{r})$ and the permittivity of free space ε_0 is given by

$$\boldsymbol{D}(r, t) = \varepsilon_0 \varepsilon(\boldsymbol{r})\boldsymbol{E}(\boldsymbol{r}, t), \tag{7.5}$$

where $\varepsilon(\boldsymbol{r})$ is assumed to be periodic, such that

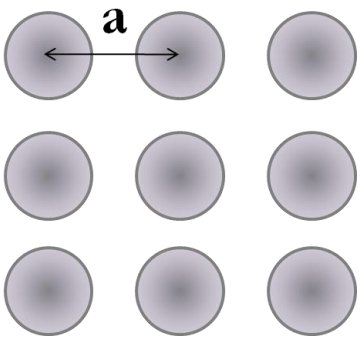

Figure 7.1 A depiction of the lattice spacing a.

$$\varepsilon(\boldsymbol{r} + \boldsymbol{a}_i) = \varepsilon(\boldsymbol{r}). \tag{7.6}$$

The periodic spacing of the scatterers in the photonic crystal are given by the primitive lattice vector $\boldsymbol{a}_i$, where i denotes the i^{th} scatterer. The lattice vector is shown in figure 7.1 for a cubic lattice and figure 7.2 for a hexagonal lattice. And the relationship between B and H is

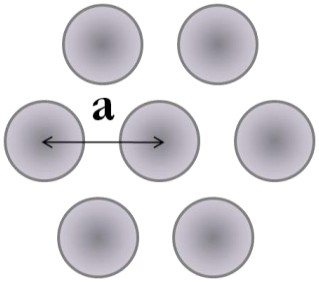

Figure 7.2 The lattice vectors for a hexagonal geometry photonic crystal.

$$\boldsymbol{B}(\boldsymbol{r}, t) = \mu_0 \boldsymbol{H}(\boldsymbol{r}, t) \tag{7.7}$$

where the magnetic permeability of free space is equivalent to that of the photonic crystal. Thus, substituting (7.5) and (7.7) into (7.1), (7.2), (7.3) and (7.4) allows Maxwell's equation to be written as

$$\boldsymbol{\nabla} \cdot \{\varepsilon(\boldsymbol{r})\boldsymbol{E}(\boldsymbol{r}, t)\} = 0 \tag{7.8}$$

$$\boldsymbol{\nabla} \cdot \boldsymbol{H}(\boldsymbol{r}, t) = 0 \tag{7.9}$$

$$\boldsymbol{\nabla} \times \boldsymbol{E}(\boldsymbol{r}, t) = -\mu_0 \frac{\partial}{\partial t} \boldsymbol{H}(\boldsymbol{r}, t) \tag{7.10}$$

$$\boldsymbol{\nabla} \times \boldsymbol{H}(\boldsymbol{r}, t) = \varepsilon_0 \varepsilon(\boldsymbol{r}) \frac{\partial}{\partial t} \boldsymbol{E}(\boldsymbol{r}, t) \tag{7.11}$$

Eliminating either $\boldsymbol{E}(\boldsymbol{r}, t)$ or $\boldsymbol{H}(\boldsymbol{r}, t)$ yields the wave equations for the magnetic and electric fields of an EM wave

$$\frac{1}{\varepsilon(\boldsymbol{r})} \boldsymbol{\nabla} \times [\boldsymbol{\nabla} \times \boldsymbol{E}(\boldsymbol{r}, t)] = -\frac{1}{c^2} \frac{\partial^2}{\partial t^2} \boldsymbol{E}(\boldsymbol{r}, t) \tag{7.12}$$

$$\boldsymbol{\nabla} \times \left[\frac{1}{\varepsilon(\boldsymbol{r})} \boldsymbol{\nabla} \times \boldsymbol{H}(\boldsymbol{r}, t)\right] = -\frac{1}{c^2} \frac{\partial^2}{\partial t^2} \boldsymbol{H}(\boldsymbol{r}, t) \tag{7.13}$$

where

$$c = \frac{1}{\sqrt{\varepsilon_0 \mu_0}},$$

is the speed of light. Solutions to equations (7.12) and (7.13) will have the general forms

$$\boldsymbol{E}(\boldsymbol{r},t)=\boldsymbol{E}(\boldsymbol{r})e^{-i\omega t}, \tag{7.14}$$

and

$$\boldsymbol{H}(\boldsymbol{r},t)=\boldsymbol{H}(\boldsymbol{r})e^{-i\omega t}. \tag{7.15}$$

where $E(\boldsymbol{r})$ and $H(\boldsymbol{r})$ are the eigenfunctions of the wave equation. Writing equations (7.12) and (7.13) in terms of the eigenfunction (7.14) and (7.15 yield the eigenvalues equations

$$\mathcal{L}_E\boldsymbol{E}(\boldsymbol{r})\equiv\frac{1}{\varepsilon(\boldsymbol{r})}\boldsymbol{\nabla}\times[\boldsymbol{\nabla}\times\boldsymbol{E}(\boldsymbol{r})]=\frac{\omega^2}{c^2}\boldsymbol{E}(\boldsymbol{r}) \tag{7.16}$$

and

$$\mathcal{L}_H\boldsymbol{H}(\boldsymbol{r})\equiv\nabla\times\left[\frac{1}{\varepsilon(\boldsymbol{r})}\nabla\times\boldsymbol{H}(\boldsymbol{r})\right]=\frac{\omega^2}{c^2}\boldsymbol{H}(\boldsymbol{r}) \tag{7.17}$$

where the differential operator $\mathcal{L}$ represents the second time derivative of the respective fields. Bloch's theorem must now be applied but to do so two periodic functions $\boldsymbol{u}_{\boldsymbol{k}n}(\boldsymbol{r})$ and $\boldsymbol{v}_{\boldsymbol{k}n}(\boldsymbol{r})$ are defined by

$$\boldsymbol{u}_{\boldsymbol{k}}(\boldsymbol{r})\equiv\boldsymbol{u}_{\boldsymbol{k}}(\boldsymbol{r}+\boldsymbol{a}_i), \tag{7.18}$$

and

$$\boldsymbol{v}_{\boldsymbol{k}}(\boldsymbol{r})\equiv\boldsymbol{v}_{\boldsymbol{k}}(\boldsymbol{r}+\boldsymbol{a}_i). \tag{7.19}$$

Using equations (7.18) and (7.19) $E(\boldsymbol{r})$ and $H(\boldsymbol{r})$ can be written as

$$\boldsymbol{E}(\boldsymbol{r})=\boldsymbol{E}_{\boldsymbol{k}}(\boldsymbol{r})=\boldsymbol{u}_{\boldsymbol{k}}(\boldsymbol{r})e^{i\boldsymbol{k}\cdot\boldsymbol{r}} \tag{7.20}$$

and

$$\boldsymbol{H}(\boldsymbol{r})=\boldsymbol{H}_{\boldsymbol{k}}(\boldsymbol{r})=\boldsymbol{v}_{\boldsymbol{k}}(\boldsymbol{r})e^{i\boldsymbol{k}\cdot\boldsymbol{r}}, \tag{7.21}$$

where $\boldsymbol{k}$ is the wave vector in the first Brillouin zone. The term $\varepsilon^{-1}(\boldsymbol{r})$ in equations (7.12) and (7.13) must be expanded as a Fourier series in terms of the primitive reciprocal lattice vectors $\boldsymbol{b}$ where

$$\boldsymbol{a}_i \cdot \boldsymbol{b}_i = 2\pi\delta_{ij}, \tag{7.22}$$

and the reciprocal lattice vectors $\boldsymbol{G}$ such that

$$\boldsymbol{G} = l_1\boldsymbol{b}_1 + l_2\boldsymbol{b}_2 + l_3\boldsymbol{b}_3. \tag{7.23}$$

The terms l_i terms in (7.15) are arbitrary integers and δ_{ij} is the Kronecker delta.[i] Thus, the reciprocal of the dielectric constant expressed as a Fourier series can be written as

$$\frac{1}{\varepsilon(\boldsymbol{r})} = \sum_{\boldsymbol{G}} \lambda(\boldsymbol{G}) e^{i\boldsymbol{G}\cdot\boldsymbol{r}} \tag{7.24}$$

Likewise, because of the spatial periodicity equations (7.20) and (7.21) can also be expanded in terms of the reciprocal lattice vectors

$$\boldsymbol{E}_{\boldsymbol{k}}(\boldsymbol{r}) = \sum_{\boldsymbol{G}} \boldsymbol{E}_{\boldsymbol{k}}(\boldsymbol{G}) e^{i(\boldsymbol{k}+\boldsymbol{G})\cdot\boldsymbol{r}} \tag{7.25}$$

$$\boldsymbol{H}_{\boldsymbol{k}}(\boldsymbol{r}) = \sum_{\boldsymbol{G}} \boldsymbol{H}_{\boldsymbol{k}}(\boldsymbol{G}) e^{i(\boldsymbol{k}+\boldsymbol{G})\cdot\boldsymbol{r}} \tag{7.26}$$

Substituting (7.24), (7.25) and (7.26) into equations (7.16) and (1.17) yield

[i] As a historical side note, the first concept of the Kronecker delta appears in the work of Poisson [S. D. Poisson, *Traité de Mécanique*, (Bachelier, Paris, 1833); Memoir read before the Paris Academy 1815], Fourier [J. Fourier, *Théorie Analytique de la Chaleur*, translated by Alexander Freeman 1822 (Dover Publication, New York 2003)] and Cauchy [A. L. Cauchy, "Résumé des leçons données à l'école royale polytechnique sur le calcul infinitésimal, " *Paris*, **1** (1823)]. These first uses were more arguments than rigorous use. Poisson and Cauchy implied a Lorentzian representation of the delta function, while Fourier derived a series expansion of an impulse function. The first mathematical use appears in the work of Kirchhoff [G. Kirchhoff, *Gesammelte Abhandlungen*, (Barth, Leipzig, 1882, supplement 1891)] who dealt with the three-dimensional wave equation and Heaviside [O. Heaviside, *Electromagnetic Theory*, ed. vol. 1 and 2 (MacMillan and Co. London 1892)] in his operational calculus. Finally, it was Dirac [P. A. M. Dirac, "The Fundamental Equations of Quantum Mechanics," *Proc. Roy. Soc. London Series A* **109**, 642-653 (1925)] who introduced a continuous version of the function in his quantum theory and thereafter the use of the Kronecker delta became commonplace.

$$-\sum_{G'}\lambda(G-G')(k+G')\times\{(k+G')\times E_k(G')\}=\frac{\omega_k^2}{c^2}E_k(G) \qquad (7.27)$$

$$-\sum_{G'}\lambda(G-G')(k+G')\times\{(k+G')\times H_k(G')\}=\frac{\omega_{kn}^2}{c^2}H_k(G) \qquad (7.28)$$

Solving either (7.27) or (7.28) by numerical computations the dispersion relations for the eigenmodes are found and thus, the photonic band structure.[4, 5, 6]

7.2 Band-Gap Simulations

Calculation in RSoft BandSolve package are performed on objects that are created in a Cad program that is capable of creating 1D, 2D and 3D objects. In performing a bandgap calculation, the scatterers are defined in the Cad area as individual objects or if the same object is being repeated, as an array. The scatterers are defined either as holes (low refractive scatterers) or as columns (high refractive scatterers. The simulation is run by defining the relative refractive index of the scatterer and the background material.

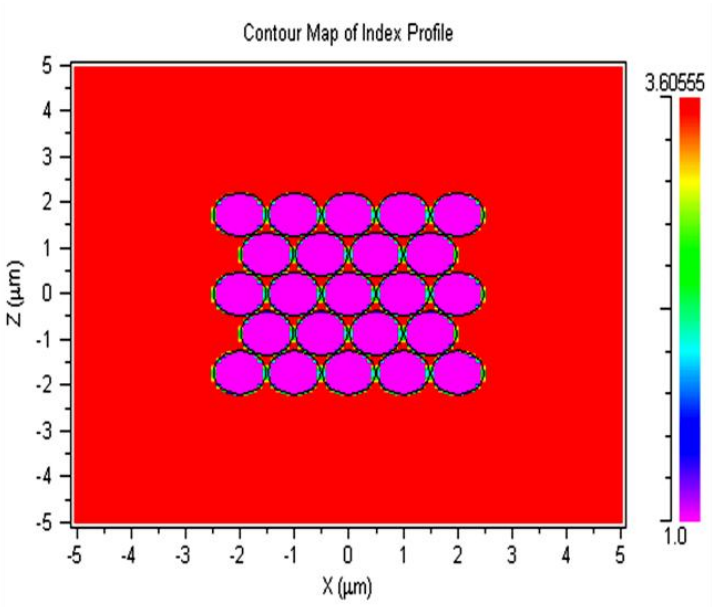

Figure 7.3 The index profile for an array of low refractive scatterers in a high refractive index background material.

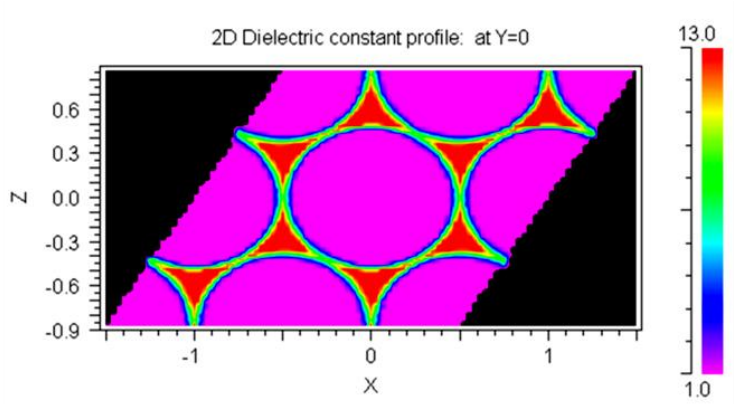

Figure 7.4 A profile of the dielectric constants the comprise the array. The dielectric constant is merely the square of the refractive index.

For example, consider the 2D array in figure 7.3 where the background in red represents a refractive index of 3.6, while the scatterers, in pink, have a refractive index of 1. Further, it is possible to view the profile in terms of the dielectric constants, as shown in figure 7.4.

The calculation of the bandgap is performed over the first Brillouin zone, which is uniquely defined in the frequency domain, by the reciprocal lattice. The first Brillouin zone is a space which comprises the points closer to the origin that other reciprocal lattice vectors. For the example illustrated above of the hexagonal array of scatterers, the Brillouin zone will be hexagonal in figure 7.5. The points M, K, and Γ correspond to points of high symmetry.

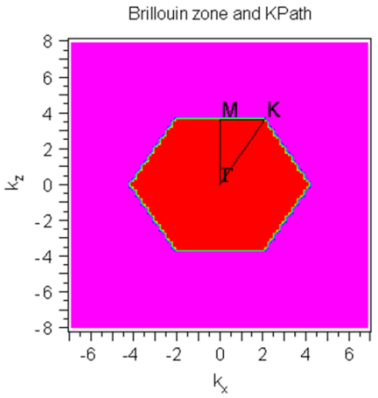

Figure 7.5 The first Brillouin zone for a hexagonal array of scatterers.

The radius and diameter of the scatterers also must be defined for the calculation to be made. If the radius is defined as $radius = 0.48 \times Period$ and the

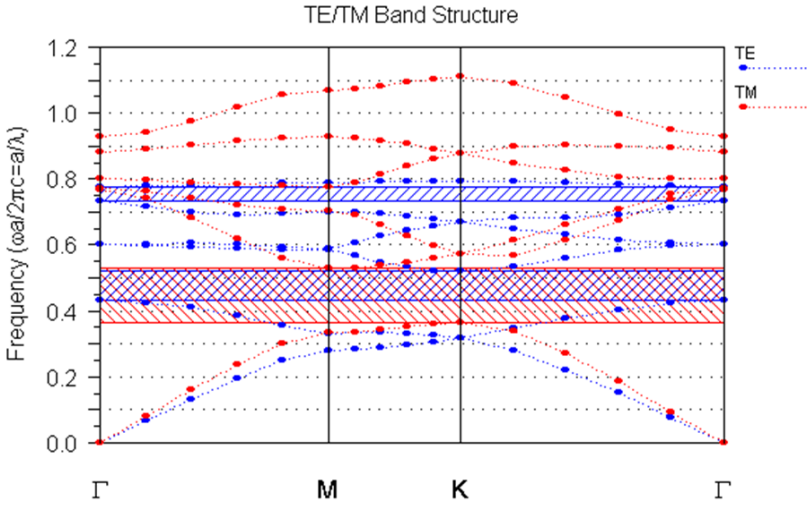

Figure 7.6 depicts the both the TE and TM polarizations in the illustrated photonic crystal of figure 7.2.1.

period is set to $Period = 1$, the historically significant, band structure can be calculated. The bandgap structure of figure 7.6 shows the overlap of the TE and TM bandgaps, which provides a photonic crystal that is independent of polarization.

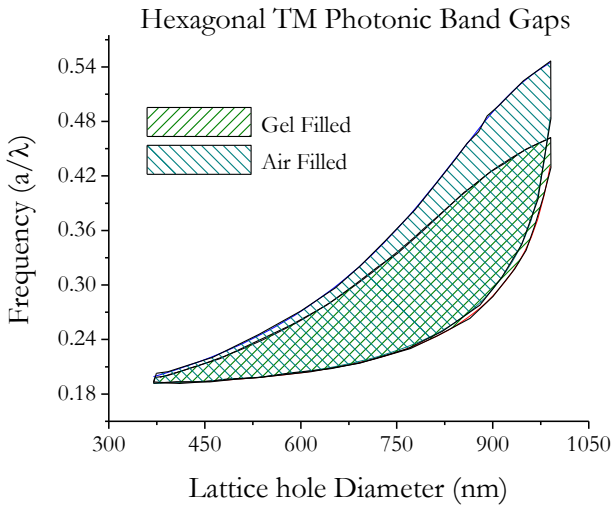

Figure 7.7 The TM bandgaps of a photonic crystal with hexagonal symmetry. Scatterers filled with air and with hydrogel below LCST are depicted.

7.2.1 Hydrogel Parameters

The interest in this study is the behavior a photonic crystal array filled with the hydrogel discussed in the previous chapter. As the photonic crystal is globally heated the hydrogel infiltrated in the lattice structure will undergo a phase change, changing the refractive index. The refractive indies of the hydrogel are 1.3288 at a temperature below LCST and 1.3816 above LCST.

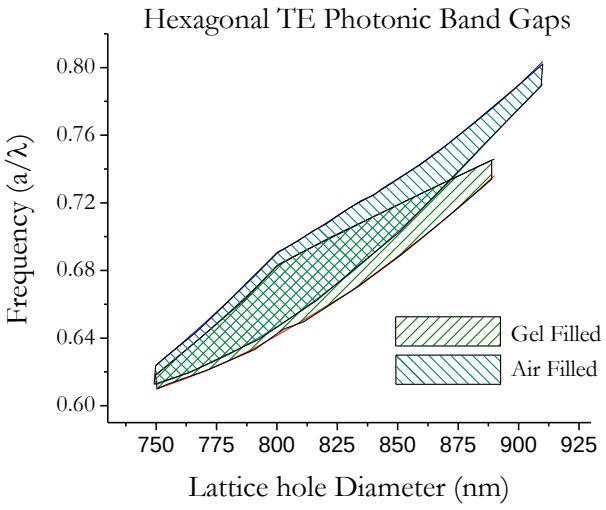

Figure 7.8 The TE bandgaps of a photonic crystal with hexagonal symmetry. Scatterers are shown filled with air and with hydrogel below LCST

7.2.2 Introducing an Index Material

In plotting the bandgaps, it is simply infeasible to place the thousands of bandgap calculations such as figure 7.6 into the dissertation. The main concern is the bandgaps and whether they exist in the Brillouin

zone or not. Therefore, in an effort to convey this information, the individual bandgaps for particular hole diameters are plotted in a compressed format.

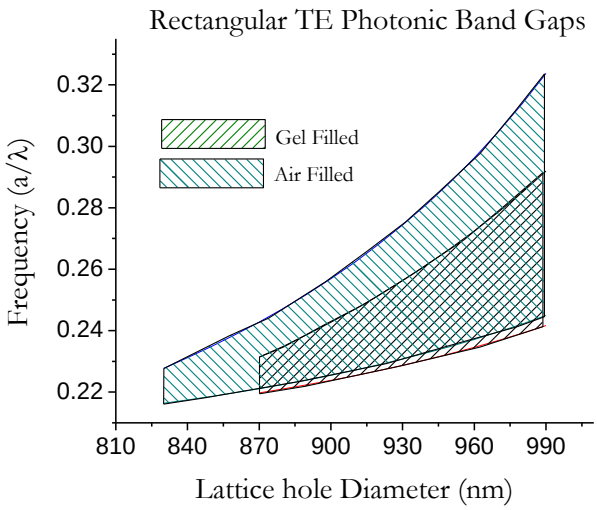

Figure 7.9 The bandgaps of a photonic crystal with square or rectangular symmetry. Scatterers filled with air and with hydrogel below LCST are depicted.

In figures 7.7 and 7.8, the band gaps for the TM and TE modes are shown over a range of hole diameters for a photonic crystal with and without hydrogel. Likewise, figure 7.9 depicts a photonic crystal with square symmetry, with air scatterers and with hydrogel scatterers. The calculation of the hydrogel is made for a hydrogel below LCST. The importance of these plots is to see that when a material such as the hydrogel is introduces the bandgap of the crystal changes from the bandgap of an air-filled photonic crystal.

7.2.3 Tuning with Hydrogel

In designing a tunable photonic crystal, the exhibited shift of the bandgap is one of the paramount considerations. The other major consideration is the wavelength of interest. In figures 7.10

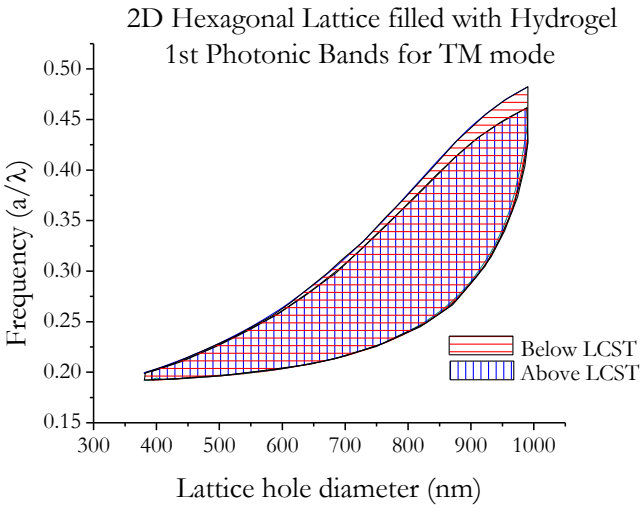

Figure 7.10 A hexagonal lattice filled with gel above and below LCST.

and 7.11, the bandgap shifts of an infiltrated hexagonal lattice structure, are depicted. Figure 7.11 clearly indicates that this photonic crystal structure is not well suited for the TE modes, since the bandgaps for the hydrogel above and below LCST lie nearly on top of one another.

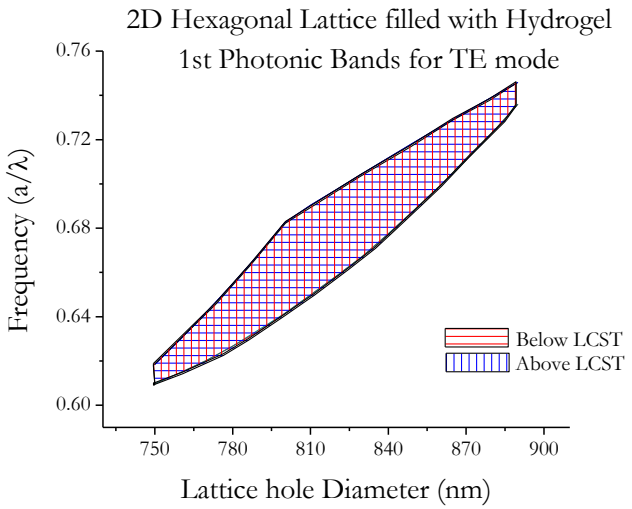

Figure 7.11 A hexagonal lattice filled with gel above and below LCST. These band gaps exhibit poor tunability.

Figure 7.10 indicate a small degree of tunability which increases at higher frequencies, most of which lie outside the communications range. In conjunction with figure 7.10, figure 7.12 depicts a second bandgap, which exhibits a high degree of tunability. In figure 7.13, the only bandgap for the rectangular lattice is depicted for TE polarized light. Although the square lattice symmetry shows a good degree of tunability the wavelengths of interest are outside the communications range. Although, these simulations do not show an ideal candidate for infiltrating the lattice with hydrogel for tunability, recall that these are 2D simulations. To gain a more correct

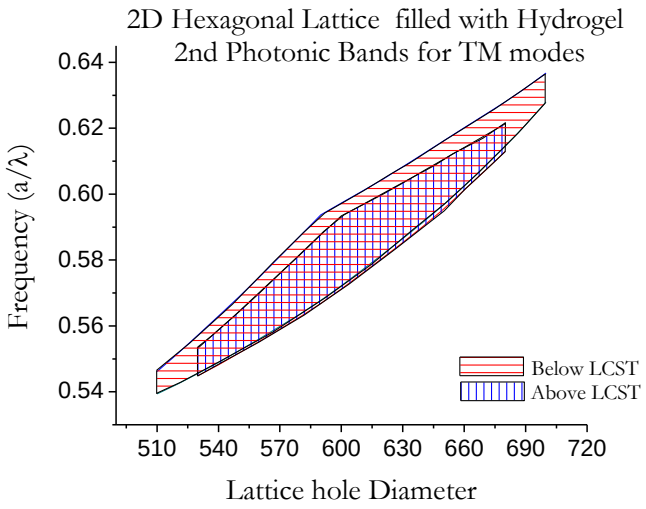

Figure 7.12 The second TM bandgap for a 2D hexagonal array.

view of the tunability the next section will show similar simulations for a photonic crystal on a SOI wafer.

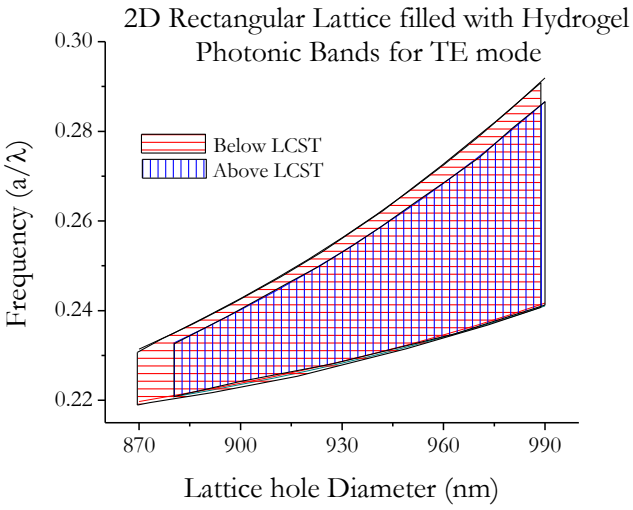

Figure 7.13 The bandgaps for a rectangular array filled with hydrogel above and below LCST.

7.2.4 SOI Approximation

Silicon-on-Insulator possesses an increased difficulty in modeling because it is now a three dimensional structure. In figure 7.14, a cross section view of the SOI wafer is shown, where the pink represents hydrogel below LCST, the red is silicon containing a periodic lattice structure and the purple is the SiO_2 layer acting as an insulator. Similarly, in figure 7.15 a top view a SOI wafer is shown with the lattice structure infiltrated with hydrogel below LCST.

The refractive index of SiO_2 is approximately 1.45 in the communication

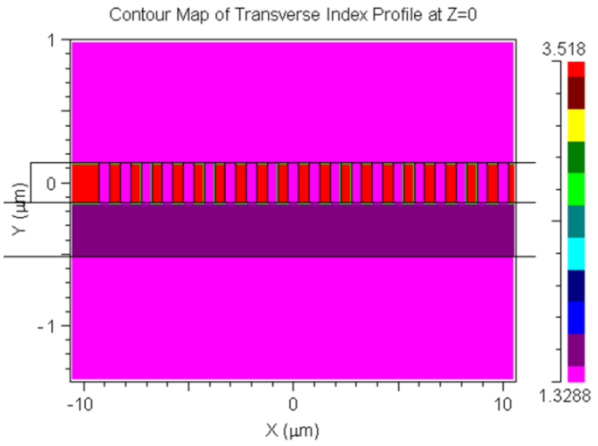

Figure 7.14 A cross sectional view along the z=0 axis, depicting the layers of SOI and the photonic crystal scatterers.

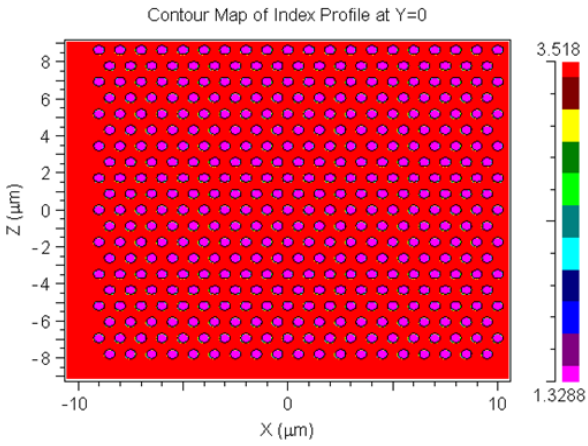

Figure 7.15 A top view along the y=0 axis, depicting the silicon layer and the hydrogel infiltrating the scattering holes.

wavelengths and is clearly shown in figure 7.14. However, once the hydrogel undergoes the phase change, the surrounding refractive index increases to 1.3816. The refractive index between the SiO_2 and the hydrogel is insufficient to be seen any longer on the contour maps. Therefore, more colors where added color scale creating more of a continuous spectrum as shown in figures 7.16 and 7.17. Figure 7.16 shows a cross sectional view along the z-axis, while, figure 7.17 shows a cross sectional view along the x-axis. Using

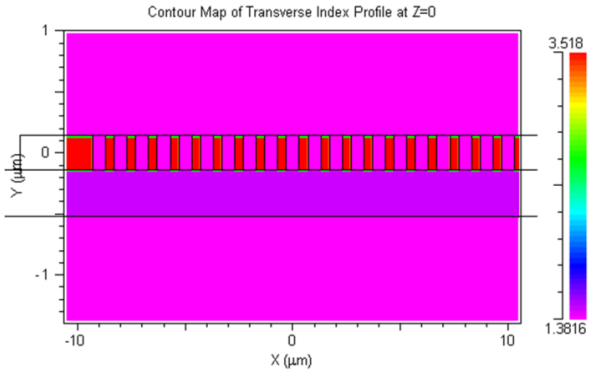

Figure 7.16 The SOI structure with hydrogel above LCST. The SiO_2 layer is now in a light purple, representing a refractive index near that of the hydrogel.

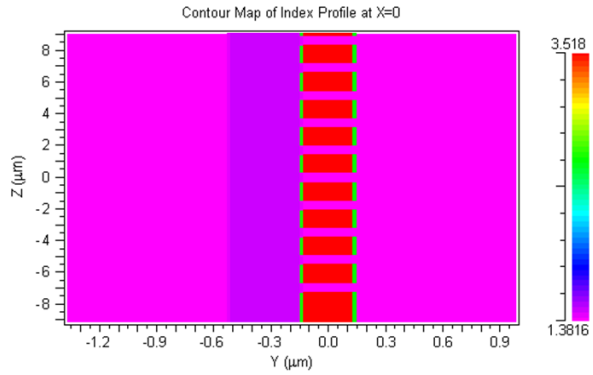

Figure 7.17 A side view along the x-axis of the SOI structure with a photonic crystal lattice in the Si layer.

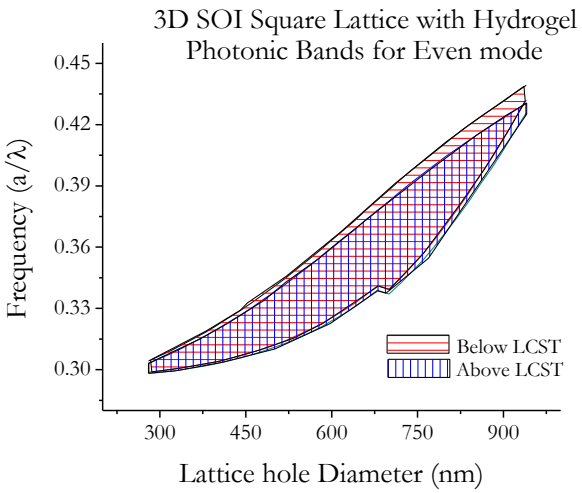

Figure 7.18 Improper gridding leads to discontinuities in the composite band structure.

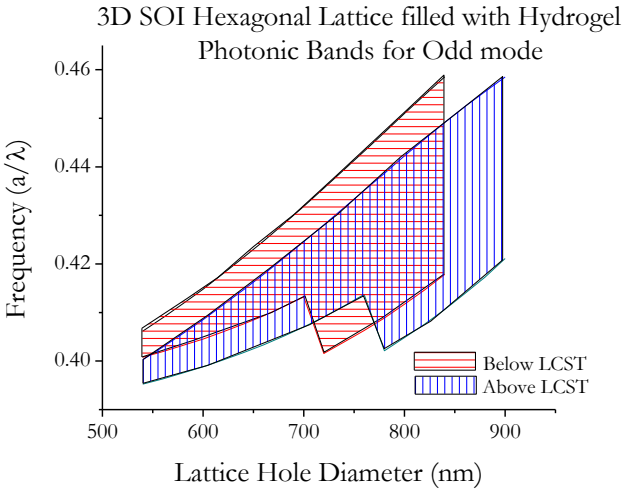

Figure 7.19 Improper gridding leads for odd modes.

this method of checking the refractive indices of the structure, the correct structure can be modeled.

Careful attention must be made when modeling 3D layered structure when gridding is performed. Artifacts such as those in figures 7.18 and 7.19 can arise from too coarse a grid.

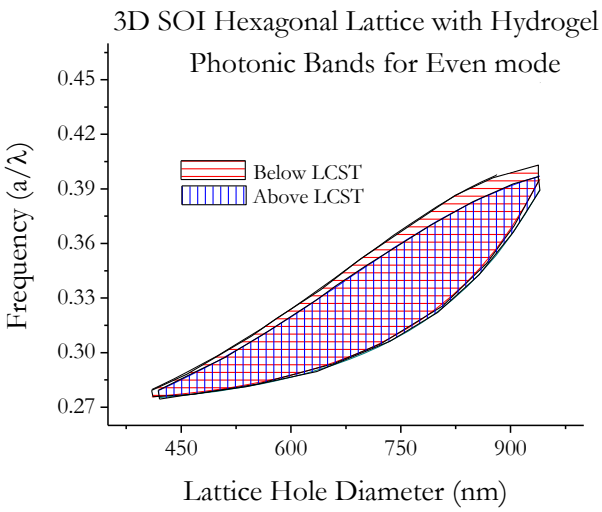

Figure 7.20 A composite of the even mode bandgaps in SOI

The modes in a photonic crystal slab are no longer purely TM or TE. However these modes can be approximated as even and odd modes. In figure 7.20 a composite of the bandgaps is depicted the even modes and shows some tunability. Further, figure 7.21 also shows the greater promise of tunability for odd modes.

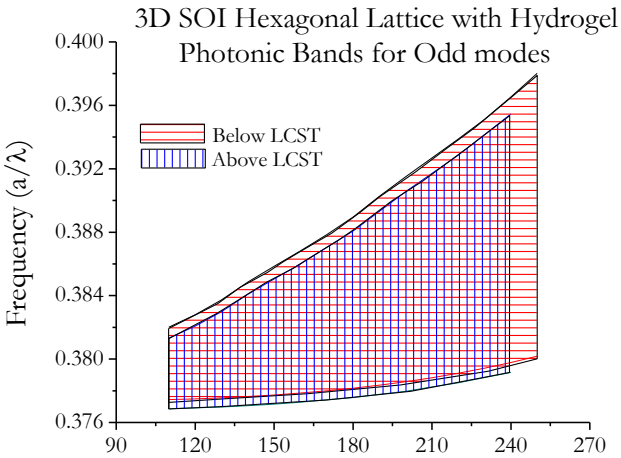

Figure 7.21 A composite of the odd mode bandgaps in SOI

7.3 Transmission Simulation—FDTD Method

The Finite-Difference Time-Domain numerical method has become one of the most popular an extensively used techniques for solving electromagnetic problems. The main methods for modeling the propagation of an EM wave in a photonic crystal are: (1) FDTD[7, 8, 9]; (2) transfer matrix theory[10]; (3) spherical wave expansion[11, 12, 13], (4) plane wave

method[14, 15],finite element method[16]. FDTD has become the standard in calculating the transmission of an EM wave, around bends, junctions, and crossings in photonic crystals.[17, 18]

The FDTD method was first proposed, in 1966 by Yee, as a way to make the differential forms of Maxwell's equations discrete.[19] In his paper, Yee replaced Maxwell's equations were by a set of finite difference equations. In particular, Yee offset an electric field spatially and temporally from a magnetic field, in order to construct update equations, which represented present fields in the computational area in terms of the past fields. Once the update equations were constructed they were used to step the electric and magnetic fields forward in time.

Yee's original algorithm suffered from numerical-dispersion and grid-anisotropy errors. Taflove began studying the errors and was able to introduce stability criteria to improve the Yee algorithm.[20] As time has passed there have been many variations and improvements of the original Yee algorithm each having its own strengths and weaknesses.[21, 22] For example, Merewether[23] in 1971 and Holland[24] in 1983 introduced alternative coordinate systems. Other improvements have included update equations for modeling sub-cellular structures like wires and narrow slots.[25, 26] FDTD has become a powerful tool for analysis of scattered EM waves in a medium.[27]

7.3.1 FDTD 2D Formalism[28]

The FDTD method was used by the Rsoft package FullWave in the simulations discussed at the end of this chapter. Although many of the simulations discussed are 3D models the formalism is presented here in 2D for simplicity and illustration.

Consider an electromagnetic wave propagating in the z-direction in a waveguide with the general fields

$$\boldsymbol{E} = \boldsymbol{E}_0 e^{-i(\omega t - \beta t)} \tag{7.29}$$

and

$$\boldsymbol{H} = \boldsymbol{H}_0 e^{-i(\omega t - \beta t)} \tag{7.30}$$

where β is the propagation constant and ω is the angular frequency. Maxwell's curl equations can be written as six equations in terms of the x and y electric and magnetic field components

$$\varepsilon_r E_x = \frac{i}{\omega \mu_0}\left(\frac{\partial H_z}{\partial y} - i\beta H_y\right) \tag{7.31}$$

$$\varepsilon_r E_y = \frac{i}{\omega \varepsilon_0}\left(i\beta H_x - \frac{\partial H_z}{\partial x}\right) \tag{7.32}$$

$$\varepsilon_r E_z = \frac{i}{\omega \varepsilon_0}\left(\frac{\partial H_y}{\partial x} - \frac{\partial H_x}{\partial y}\right) \tag{7.33}$$

$$H_x = -\frac{i}{\omega \mu_0}\left(\frac{\partial E_z}{\partial y} - i\beta E_y\right) \tag{7.34}$$

$$H_y = -\frac{i}{\omega \mu_0}\left(i\beta E_x - \frac{\partial E_z}{\partial x}\right) \tag{7.35}$$

$$H_z = -\frac{i}{\omega \mu_0}\left(\frac{\partial E_y}{\partial x} - \frac{\partial E_x}{\partial y}\right) \tag{7.36}$$

where ε_0 is the permittivity of free space μ_0 is the permeability of free space and ε the permittivity of the material is a function of position $\varepsilon = \varepsilon(x, y)$. To apply Yee's meshing scheme, as shown in figure 7.22 the electric and magnetic fields of equations (7.31)—(7.36)

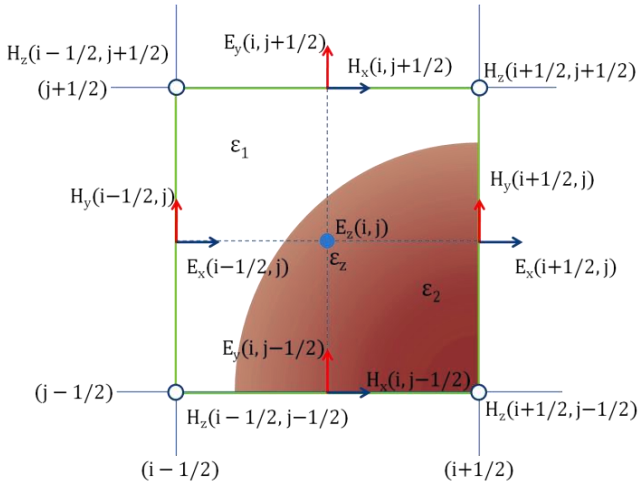

Figure 7.22 A schematic of a changing dielectric and the constituent electric and magnetic field components.

must be written in terms of indices. The x-direction index is represented by i, while the y-direction is represented by the j index.

$$(\varepsilon E_x)_{i+\frac{1}{2},j} = \frac{i}{\omega\varepsilon_0}\left(\left.\frac{\partial H_z}{\partial y}\right|_{i+\frac{1}{2},j} - i\beta\left(H_y\right)_{i+\frac{1}{2},j}\right) \tag{7.37}$$

$$\left(\varepsilon E_y\right)_{i,j+\frac{1}{2}} = \frac{i}{\omega\varepsilon_0}\left(i\beta(H_x)_{i,j+\frac{1}{2}} - \left.\frac{\partial H_z}{\partial x}\right|_{i,j+\frac{1}{2}}\right) \tag{7.38}$$

$$(\varepsilon E_z)_{i,j} = \frac{i}{\omega\varepsilon_0}\left(\left.\frac{\partial H_y}{\partial x}\right|_{i,j} - \left.\frac{\partial H_x}{\partial y}\right|_{i,j}\right) \tag{7.39}$$

$$(H_x)_{i,j+\frac{1}{2}} = -\frac{i}{\omega\mu_0}\left(\left.\frac{\partial E_z}{\partial y}\right|_{i,j+\frac{1}{2}} - i\beta\left(E_y\right)_{i,j+\frac{1}{2}}\right) \tag{7.40}$$

$$\left(H_y\right)_{i+\frac{1}{2},j} = -\frac{i}{\omega\mu_0}\left(-i\beta(E_x)_{i+\frac{1}{2},j} - \left.\frac{\partial E_z}{\partial x}\right|_{i+\frac{1}{2},j}\right) \tag{7.41}$$

$$(H_z)_{i+\frac{1}{2},j+\frac{1}{2}} = -\frac{i}{\omega\mu_0}\left(\left.\frac{\partial E_y}{\partial x}\right|_{i+\frac{1}{2},j+\frac{1}{2}} - \left.\frac{\partial E_x}{\partial y}\right|_{i+\frac{1}{2},j+\frac{1}{2}}\right) \tag{7.42}$$

Using the second fundamental theorem of calculus, the differentials in equations (7.37)—(7.42) can be expanded to

$$(\varepsilon_x)_{i+\frac{1}{2},j}E_{x\,i+\frac{1}{2},j} = \frac{i}{\omega\varepsilon_0}\left[\frac{(H_z)_{i+\frac{1}{2},j+\frac{1}{2}} - (H_z)_{i+\frac{1}{2},j-\frac{1}{2}}}{\Delta y} - i\beta\left(H_y\right)_{i+\frac{1}{2},j}\right] \tag{7.43}$$

$$\left(\varepsilon_y\right)_{i,j+\frac{1}{2}}\left(E_y\right)_{i,j+\frac{1}{2}} = \frac{i}{\omega\varepsilon_0}\left[i\beta(H_x)_{i,j+\frac{1}{2}} - \frac{(H_z)_{i+\frac{1}{2},j+\frac{1}{2}} - (H_z)_{i-\frac{1}{2},j+\frac{1}{2}}}{\Delta x}\right] \tag{7.44}$$

$$(\varepsilon_z)_{i,j}(E_z)_{i,j} = \frac{i}{\omega\varepsilon_0}\left[\frac{\left(H_y\right)_{i+\frac{1}{2},j} - \left(H_y\right)_{i-\frac{1}{2},j}}{\Delta x} - \frac{(H_x)_{i,j+\frac{1}{2}} - (H_x)_{i,j-\frac{1}{2}}}{\Delta y}\right] \tag{7.45}$$

$$(H_x)_{i,j+\frac{1}{2}} = -\frac{i}{\omega\varepsilon_0}\left[\frac{(E_z)_{i,j+\frac{1}{2}} - (E_x)_{i,j}}{\Delta y} - i\beta\left(E_y\right)_{i,j+\frac{1}{2}}\right] \tag{7.46}$$

$$\left(H_y\right)_{i+\frac{1}{2},j} = -\frac{i}{\omega\mu_0}\left[-i\beta(E_x)_{i+\frac{1}{2},j} - \frac{(E_z)_{i+1,j} - (E_z)_{i,j}}{\Delta x}\right] \tag{7.47}$$

$$(H_z)_{i+\frac{1}{2},j+\frac{1}{2}} = -\frac{i}{\omega\mu_0}\left[\frac{\left(E_y\right)_{i+1,j+\frac{1}{2}} - \left(E_y\right)_{i,j+\frac{1}{2}}}{\Delta x} - \frac{(E_x)_{i+\frac{1}{2},j+1} - (E_x)_{i+\frac{1}{2},j}}{\Delta y}\right]. \tag{7.48}$$

Equations (7.43)—(7.48) can be written in matrix form in conjunction with the square matrices $\boldsymbol{U_x}, \boldsymbol{U_y}, \boldsymbol{V_x}, \boldsymbol{V_y}$, which are dependent on the boundary conditions of the computation window. For example, the matrix $\boldsymbol{U_x}$ for the zero-value boundary condition will be

$$\boldsymbol{U_x} = \frac{1}{\Delta x}\begin{bmatrix} -1 & 1 & 0 & 0 & 0 \\ 0 & -1 & 1 & 0 & 0 \\ 0 & 0 & \ddots & \ddots & 0 \\ 0 & 0 & 0 & -1 & 1 \\ 0 & 0 & 0 & 0 & -1 \end{bmatrix}. \tag{7.49}$$

Therefore, equations (7.43)—(7.48) become

$$\begin{bmatrix} \boldsymbol{\varepsilon_x} & 0 & 0 \\ 0 & \boldsymbol{\varepsilon_y} & 0 \\ 0 & 0 & \varepsilon_z \end{bmatrix}\begin{bmatrix} \boldsymbol{E_x} \\ \boldsymbol{E_y} \\ \boldsymbol{E_z} \end{bmatrix} = \frac{i}{\omega\varepsilon_0}\begin{bmatrix} 0 & -i\beta\mathbf{I} & \boldsymbol{V_x} \\ i\beta\mathbf{I} & 0 & -\boldsymbol{V_x} \\ -\boldsymbol{V_y} & \boldsymbol{V_x} & 0 \end{bmatrix}\begin{bmatrix} \boldsymbol{H_x} \\ \boldsymbol{H_y} \\ \boldsymbol{H_z} \end{bmatrix} \tag{7.50}$$

$$\begin{bmatrix} \boldsymbol{H_x} \\ \boldsymbol{H_y} \\ \boldsymbol{H_z} \end{bmatrix} = -\frac{i}{\omega\mu_0}\begin{bmatrix} 0 & -i\beta\mathbf{I} & \boldsymbol{U_y} \\ i\beta\mathbf{I} & 0 & -\boldsymbol{U_x} \\ -\boldsymbol{U_y} & \boldsymbol{U_x} & 0 \end{bmatrix}\begin{bmatrix} \boldsymbol{H_x} \\ \boldsymbol{H_y} \\ \boldsymbol{H_z} \end{bmatrix} \tag{7.51}$$

where I is the identity matrix. Finally two equivalent eigenvalue equations can be derived from equations (7.50) and (7.51)

$$\boldsymbol{A}\begin{bmatrix} \boldsymbol{E_x} \\ \boldsymbol{E_y} \end{bmatrix} = \begin{bmatrix} \boldsymbol{A_{xx}} & \boldsymbol{A_{xy}} \\ \boldsymbol{A_{yx}} & \boldsymbol{A_{yy}} \end{bmatrix}\begin{bmatrix} \boldsymbol{E_x} \\ \boldsymbol{E_y} \end{bmatrix} = \beta^2\begin{bmatrix} \boldsymbol{E_x} \\ \boldsymbol{E_y} \end{bmatrix} \tag{7.52}$$

and

$$\boldsymbol{B}\begin{bmatrix}\boldsymbol{H_x}\\ \boldsymbol{H_y}\end{bmatrix}=\begin{bmatrix}\boldsymbol{B_{xx}} & \boldsymbol{B_{xy}}\\ \boldsymbol{B_{yx}} & \boldsymbol{B_{yy}}\end{bmatrix}\begin{bmatrix}\boldsymbol{H_x}\\ \boldsymbol{H_y}\end{bmatrix}=\beta^2\begin{bmatrix}\boldsymbol{H_x}\\ \boldsymbol{H_y}\end{bmatrix}. \tag{7.53}$$

The matrix elements of the eigenvalues problem of (7.52) are

$$\boldsymbol{A_{xx}}=-k_0^2\boldsymbol{U_x\varepsilon_z^{-1}V_yV_xU_y}+[k_0^2\mathbf{I}+\boldsymbol{U_x\varepsilon_z^{-1}V_x}]\left[\boldsymbol{\varepsilon_x}+\frac{1}{k_0^2}\boldsymbol{V_yU_y}\right] \tag{7.54}$$

$$\boldsymbol{A_{yy}}=-\frac{1}{k_0^2}\boldsymbol{U_y\varepsilon_z^{-1}V_xV_yU_x}+\left[k_0^2\mathbf{I}+\boldsymbol{U_y\varepsilon_z^{-1}V_y}\right]\left[\left(\boldsymbol{\varepsilon_y}+\frac{1}{k_0^2}\boldsymbol{V_xU_x}\right)\right] \tag{7.55}$$

$$\boldsymbol{A_{xy}}=-\left[\mathbf{I}+\frac{1}{k_0^2}\boldsymbol{U_x\varepsilon_z^{-1}V_x}\right]\boldsymbol{V_yU_x}+\boldsymbol{U_x}\varepsilon_z^{-1}\boldsymbol{V_y}\left[\boldsymbol{\varepsilon_y}+\frac{1}{k_0^2}\boldsymbol{V_xU_x}\right] \tag{7.56}$$

$$\boldsymbol{A_{yx}}=-\left[\mathbf{I}+\frac{1}{k_0^2}\boldsymbol{U_y\varepsilon_z^{-1}V_y}\right]\boldsymbol{V_xU_y}+\boldsymbol{U_y\varepsilon_z^{-1}V_x}\left[\boldsymbol{\varepsilon_x}+\frac{1}{k_0^2}\boldsymbol{V_yU_y}\right] \tag{7.57}$$

where k_0 is the wavenumber in free space. And the matrix elements for (7.53) are

$$\boldsymbol{B_{xx}}=-\frac{1}{k_0^2}\boldsymbol{V_xU_yU_x\varepsilon_z^{-1}V_y}+\left[\varepsilon_y+\frac{1}{k_0^2}\boldsymbol{V_xU_x}\right]\left[k_0^2\mathbf{I}+\boldsymbol{U_y\varepsilon_z^{-1}V_y}\right] \tag{7.58}$$

$$\boldsymbol{B_{yy}}=-\frac{1}{k_0^2}\boldsymbol{V_yU_xU_y\varepsilon_z^{-1}V_x}+\left[\varepsilon_x+\frac{1}{k_0^2}\boldsymbol{V_yU_y}\right]\left[k_0^2\mathbf{I}+\boldsymbol{U_x}\varepsilon_z^{-1}\boldsymbol{V_x}\right] \tag{7.59}$$

$$\boldsymbol{B_{xy}}=\boldsymbol{V_xU_y}\left[\mathbf{I}+\frac{1}{k_0^2}\boldsymbol{U_x\varepsilon_z^{-1}V_x}\right]-\left[\boldsymbol{\varepsilon_y}+\frac{1}{k_0^2}\boldsymbol{V_xU_x}\right]\boldsymbol{U_y\varepsilon_z^{-1}V_x} \tag{7.60}$$

$$\boldsymbol{B_{yx}}=\boldsymbol{V_yU_x}\left[\mathbf{I}+\frac{1}{k_0^2}\boldsymbol{U_y\varepsilon_z^{-1}V_y}\right]-\left[\boldsymbol{\varepsilon_x}+\frac{1}{k_0^2}\boldsymbol{V_yU_y}\right]U_x\boldsymbol{\varepsilon_z^{-1}V_y} \tag{7.61}$$

Therefore, once the transverse electric fields $\boldsymbol{E}^{(T)}$are derived the other transverse field components can be found by equation (7.52). Likewise, once the transverse magnetic field $\boldsymbol{H}^{(T)}$is found the other components are found by equation (7.53).

Although the ideas present in this section have been for a 2D model, the method can be extended to 3D. The simulations in the following section were performed using the FDTD method.

7.4 Waveguiding Simulations

The RSoft package FullWave makes use of the FDTD algorithm in modeling the propagation of an EM wave through a medium. The Cad program is again used to create an appropriate structure for simulation. Once a structure has been created in the Cad the band structure can be found with BandSolve and then transmission modeling can be performed on the same structure. In this manner a photonic crystal with a desired bandgap and characteristics can be engineered. However, FullWave requires additional information beyond that of BandSolve. Since FullWave models the transmission of an EM wave the transmitted wave must also be modeled.

7.4.1 Transmission Simulation

Since FullWave is modeling the predicted response of the photonic crystal, it is possible to find the transmission bandgap. This is accomplished by designing a defect waveguide in a lattice array. Assuming a scatterer diameter of 200nm and a lattice constant of 320 nm the TM transmission gap can be simulated as shown in figure 7.4.1. It should be noted that there is a red-shift in the spectrum as the hydrogel undergoes its phase change. Further, there is an increase in intensity above LCST.

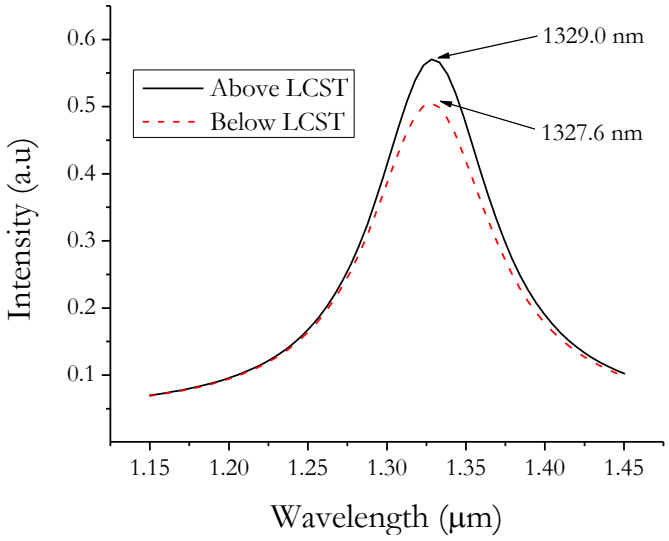

Figure 7.23 Transmission bandwidth through a linear defect in a 2D hexagonal photonic crystal.

7.4.2 Photonic Crystal Bends

The second use of FullWave is for modeling the transmission of EM waves around bend. In figure 4.2.3 a 2D simulation of a linear defect with a 120° bend is shown. A continuous EM wave is emitted from the source on the left side of the crystal and a monitor on the right side records the transmitted wave. There is some loss of radiation through leakage around each of the bends. Further, some radiation is lost by reflection at the first bend and can be seen leaving the waveguide by the source.

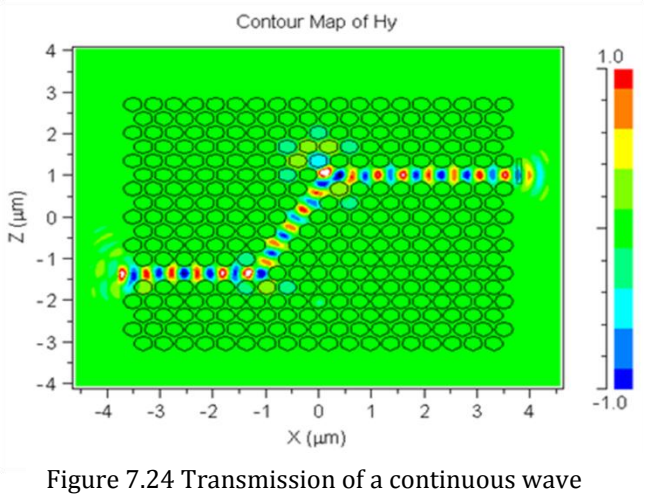

Figure 7.24 Transmission of a continuous wave through a 120° bend defect.

---

[1] S. John, R. Rangarajan, "Optimal structures for classical wave localization: an alternative to the ioffe-regel criterion," Phys. Rev. B **38**, 10101-10104 (1988).

[2] E. N. Economou, A. Zdetsis, "Classical wave propagation in periodic structures," Phys. Rev. B **40**, 1334-1337 (1989).

[3] P. R. Villenieve, M. Piché, "Photonic bandgaps: what is the best numerical representation of periodic structures?" J. Mod. Opt. **41**, 241 (1994).

[4] K. M. Leung, Y. F. Liu, "Full vector wave calculation of photonic structures in face-centered cubic dielectric media," Phys. Rev. Lett. **65**, 2646 (1990).

[5] Z. Zhang, S. Satpathy, "Electromagnetic wave propagation in periodic structures: Bloch wave solution of Maxwell's equations," Phys. Rev. Lett. **65**, 2650 (1990).

[6] K. M. Ho, C. T. Chan, C. M. Soukoulis, "Existence of a photonic gap in periodic dielectric structures," Phys. Rev. Lett. **65**, 3152 (1990).

[7] A. Taflov, S. C. Hagness, *Computational Electrodynamics: The Finite-Difference Time-Domain Method*, 2nd ed. (Artech House, Boston 2000).

[8] H. Benisty, "Modal analysis of optical guides with two-dimensional photonic band-gap boundaries," J. Appl. Phys. **79**, 7483-7492 (1996).

[9] M. Qui, "Analysis of guided modes in photonic crystal fibers using the finite-difference time-domain method," Microwave Opt. Technol. Lett. **30**, 327-330 (2001).

[10] J. B. Pendry, A. MacKinnon, "Calculation of Photon Dispersion Relations," Phys. Rev. Lett. **69**, 2772-2775 (1992).

[11] K. Ohtaka, "Energy band of photons and low-energy photon diffraction," Phys. Rev. B **19**, 5057-5067 (1979).

[12] N. Stefanou, V. Karathanos, A. Modinos, "Scattering of electromagnetic waves by periodic structures," J. Phys..: Condes. Matter **4**, 7389-7400 (1992).

[13] A. Modinos, "Scattering of electromagnetic waves by a plane of spheres-formalism," Physica A: Statistical and Theoretical Phys. **141**, 575-588 (1987).

[14] S. E. Barkou, J. Broenh, A. Bjarklev, "Silica-sir photonic crystal fiber design that permits waveguiding by a true photonic band gap effect," Opt. Lett. **24**, 46-48 (1999).

[15] A. Ferrando, E. Silvestre, J. J. Miret, P. Andrés, M. V. Andrés, "Full-vector analysis of a realistic photonic crystal fiber," Opt. Lett. **24**, 276-278 (1999).

[16] F. Brechet, J. Marcou, D. Pagnoux, P. Roy, "Complete analysis of the characteristics of propagation into photonic crystal fibers, by the finite element method," Opt. Fiber. Technol. **6**, 181-191 (2000).

[17] C. Manolatau, S. G. Johnson, S. Fan, P. R. Villeneuce, H. A. Haus, J. D. Joannopoulos, "High-Density Integrated Optics," J. Lightwave Tech. **17**, 1682 (1999).

[18] B. D'Urso, O. Painter, J. O'Brien, T. Tombrello, A. Yariv, A. Scherer, "Modal reflectivity in finite-depth two-dimensional photonic crystal microcavities," J. Opt. Soc. Am. B **15**, 1155-1159 (1997).

[19] K. S. Yee, "Numerical solution of initial boundary value problems involving Maxwell's equations in isotropic media," IEEE Trans. Antennas and Propagation **AP-14**, 302-307 (1966).

[20] A. Taflove, M. E. Brodwin, "Numerical Solution of Steady-State Electromagnetic Scattering Problems Using the Time-Dependent Maxwell's Equations," Microwave Theory and Techniques **MTT-23**, 623-630 (1975).

[21] A. Taflove, "Application of the Finite-Difference Time-Domain Method to Sinusoidal Steady-State Electromagnetic-Penetration Problems," IEEE Trans. Electromagnetic Compatibility **EMC-22**, 191-202 (1980).

[22] A. C. Cangellaris and D. B Wright, "Analysis of the numerical error caused by the stair-stepped approximation of a conducting boundary in FDTD simulations of electromagnetic phenomena," IEEE Trans. Antennas and Propagation, **AP-39**, 1518-1525 (1991).

[23] D. E. Merewether, "Transient currents on a body of revolution by an electromagnetic pulse," IEEE Trans. Electromagnetic Compatibility, **EMC-13**, 41-44 (1971).

[24] R. Holland, "THREDS: A finite-difference time-domain EMP code in 3D spherical coordinates," IEEE Trans. Nuclear Science **NS-30**, 4592-4595 (1983)

[25] K. R. Umashankar, A. Taflove, B. Becker, "Calculation and experimental validation of induced currents on coupled wires in an arbitrary shaped cavity," IEEE Trans. Antennas and Propagation **AP-35**, 1258-1257 (1987).

[26] A. Taflove, K. R. Umashankar, B. Becker, F. Harfoush, K. S. Yee, "Detailed FD-TD analysis of electromagnetic fields penetrating narrow slots and lapped joints in thick conducting screens," IEEE Trans. Antennas and Propagation, **AP-36**, 247-257 (1988).

[27] K. Umashankar, A. Taflove, "A Novel Method to Analyze Electromagnetic Scattering of Complex Objects," IEEE Trans. Electromagnetic Compatibility **EMC-24**, 397-405 (1982).

[28] C. –P. Yu, H. –C. Chang, "Yee-mesh-based finite difference eigenmode solver with PML absorbing boundary conditions for optical waveguides and photonic crystal fibers," Opt. Express **12**, 6165-6177 (2004).

CHAPTER 8

TUNABLE HYDROGEL BASED PHOTONIC CRYSTAL

8.1 Introduction

The basic goal of this section is to describe the device simulated in the previous chapter. Specifically, a tunable photonic crystal comprised of a linear waveguide and air-holes infiltrated with NIPA hydrogel. In this chapter the construction of such a tunable photonic crystal will be presented as well as the necessary tools to accomplish the task. These tasks include a description of the photonic crystal, gel insertion instrumentation and transmission measurement instrumentation.

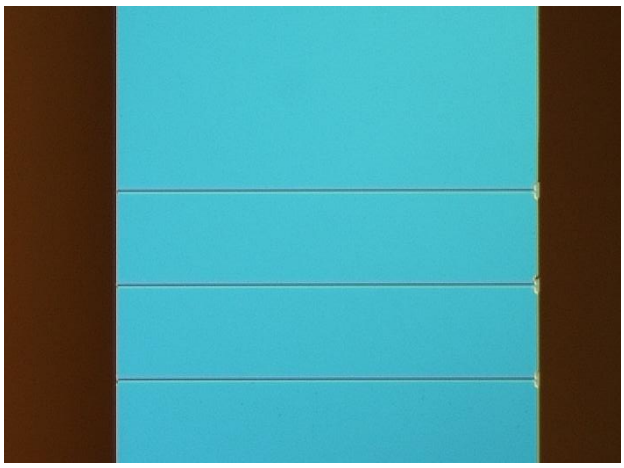

Figure 8.1 A photo of the photonic crystal used in the experiment. The center line is the waveguide used throughout this chapter.

8.2 The Photonic Crystal

The photonic crystal consists of a single line defect in a hexagonal array of air-hole scatterers. The crystal was formed in a GaAs wafer with hole diameters of 200 nm and lattice spacing of 330 nm. The lattice matrix is a bridge or membrane structure suspended in air. In figure 8.1, a photo at 20x magnification is shown. There are in fact three

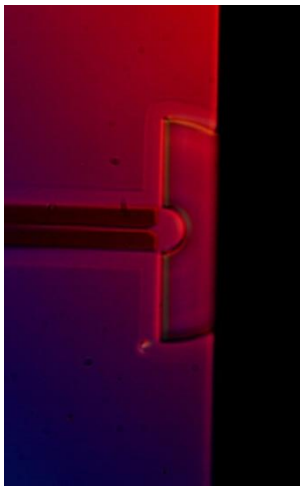

Figure 8.2 A close up of the lens structure used to focus the light onto the linear defect waveguide in the photonic crystal.

photonic crystals shown with linear defects, however, only the center waveguide was used because of defects in the matrix in the first and third lines.

One of the major issues in photonic crystal research is the coupling of light into and out of the linear defect. The coupling process is the largest source of intensity loss, when measuring the transmission bandgap. In figure 8.1, notice the structures on the right hand side of the line. These structures are lens fabricated to collect and focus the light onto the linear defect. In figure 8.2, a close up of the structure is shown at 100x magnification. The use of this structure will be discussed in the section on the transmission experiment.

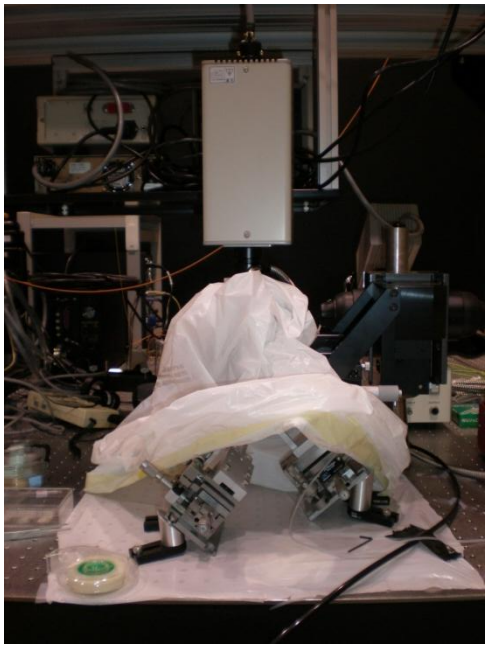

Figure 8.3 The microscope used for inserting the gel. A CCD camera was mounted for viewing the procedure with two 3-axis stages for manipulating the sample and monomer.

8.3 Infiltrating the Photonic Crystal

The first step in constructing the photonic crystal is infiltrating the NIPA hydrogel into the lattice matrix of the photonic crystal. Since the NIPA gel is semi-rigid it is not possible to simply place the NIPA gel into the 200 nm diameter holes of the matrix. However, the precursor to the NIPA polymer is a liquid monomer solution. Therefore, the monomer can infiltrate the lattice matrix and then polymerize in the matrix. In this fashion, the semi-rigid polymer is

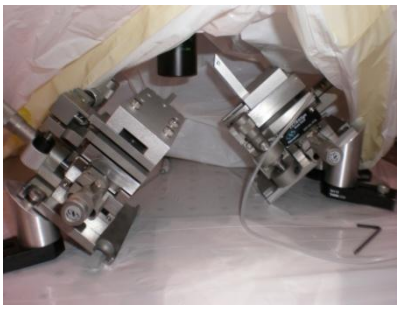

Figure 8.4 The 3-axis stages used for manipulating the photonic crystal and monomer.

grown in the matrix. Although the monomer is a liquid there were still issues to overcome in infiltrating the matrix.

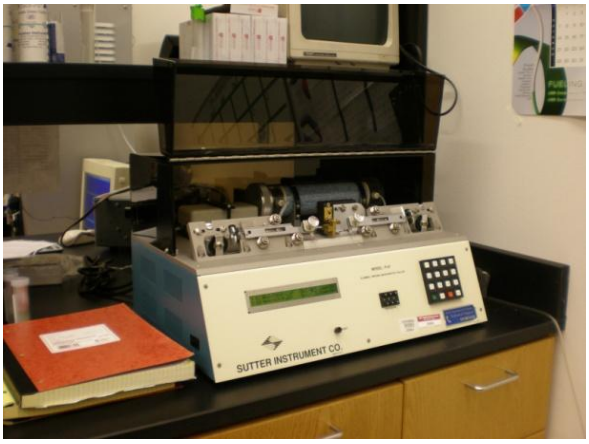

Figure 8.5 Sutter P-87 used to make 20 μm diameter tips.

First, the amount of monomer placed on the photonic crystal is crucial. The drop placed on the matrix must be small enough to leave the edges of the wafer clear from obstruction. If the monomer is allowed to cover the wafer surface and contact the edge of the wafer, the coupling of the light into the waveguide will be impossible. Second the placement of the droplet on the surface must be gentle. The bridge photonic crystal structure on the GaAs is extremely fragile and the slightest touch will cause fracturing and total collapse. The precision necessary, required the infiltration to be performed under a microscope, as seen in figure 8.3. The manipulation of the monomer and photonic crystal required two 3-axis stages, shown in figure 8.4. The plastic bag seen in figure 8.3 and 8.4 is used to

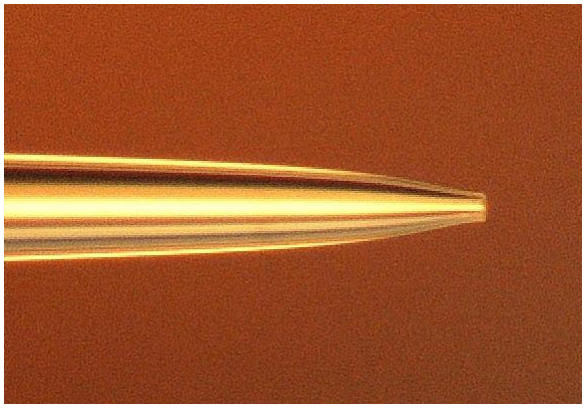

Figure 8.6 A pristine tip shown under 20x magnification.

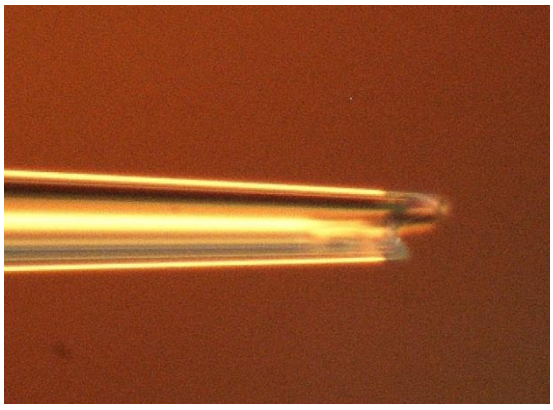

Figure 8.7 A damaged tip that broke as the pipette was pulled. The opening is approximately 50 μm.

maintain a nitrogen atmosphere around the monomer environment. If there is not a nitrogen rich atmosphere in the proximity of the monomer, the contamination will cause the monomer will fail to polymerize.

The solution to placing a small droplet on the surface was to use a micro-pipette. Pipettes were pulled using a P-87 pipette puller manufactured by Sutter, shown in figure 8.5. The target diameter of the pipette tips was 20 μm, however for every one tip at 20 μm four at 1 μm—5μm were made. The difficulty in making the large tip accounts for the high cost in commercially available tips ($10 per 20 μm tip). In figure 8.6 a pristine 20 μm tip is shown. Conversely, a tip that broke during the pulling process is shown in figure 8.7.

The micro-pipette is next aligned over the photonic crystal of interest. The 3-axis stages are tilted at 45° angles to allow for a visually controlled alignment of the micropipette with the photonic crystal. As the pipette approaches the surface of the wafer a reflection of the pipette can be seen. When the reflection and the real image of the pipette nearly meet, the pipette is close enough to dispense the monomer. The 45° tilt allows the alignment to be made with a single microscope objective rather that two, which saves money.

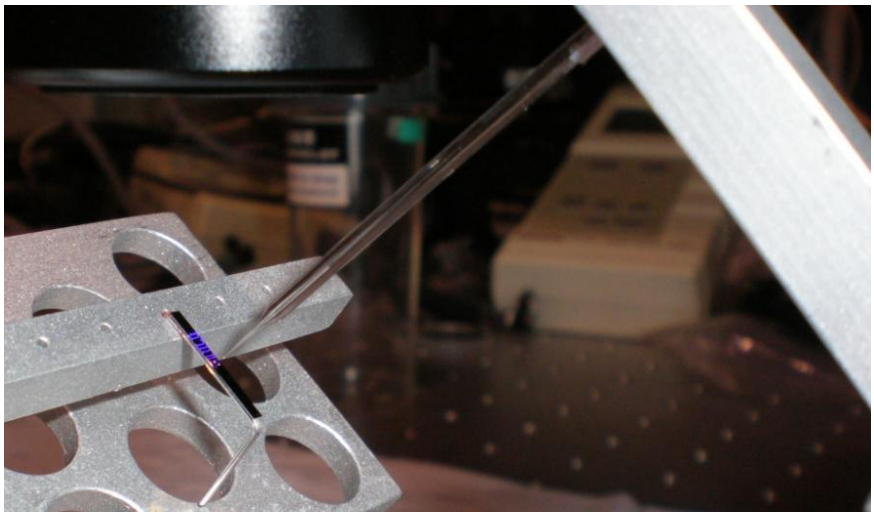

Figure 8.8 A micro-pipette aligned over a GaAs wafer containing a photonic crystal.

Once the tip has been placed over the region of interest the monomer is back filled into the pipette and allowed to settle into the tip. The tip is then lowered the remaining distance to the wafer surface. When the tip reaches a critical distance a syringe pump is used to apply a slight positive pressure to the liquid. The meniscus in the tip then slightly protrudes from the tip and attaches to the surface.

Pristine tips such as those in figure 8.6 have more surface tension that damaged tips in figure 8.7. With the greater surface tension in a pristine tip control of the droplet size is lost. The tip used in the experiment was the damaged tip. As the damaged tip is lowered to the surface the meniscus naturally protrudes from the tip negating the need to for pushing the monomer out (the syringe pump is necessary to remove the air trapped in the tip). When the protruding meniscus touches the surface of the GaAs it attaches and the tip is withdrawn leaving a single droplet on the surface. Figure 8.9 shows a droplet that was placed on the side of the waveguide.

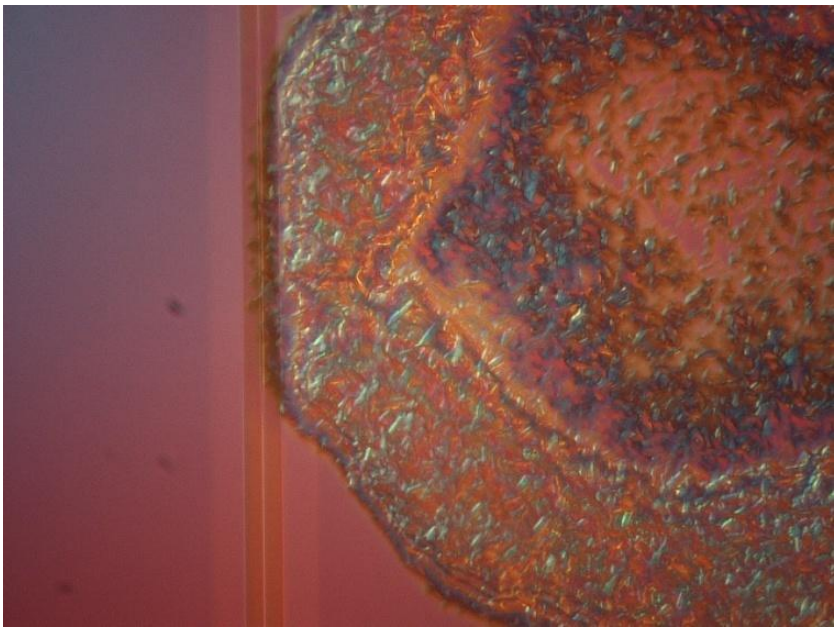

Figure 8.9 A desiccated droplet of polymerized NIPA infiltrating a photonic crystal.

The droplet was polymerized using a UV lamp at a wavelength of 295 nm, manufacture by Phillips, for 15 minutes. The sample was placed in an ice bath during polymerization to maintain a temperature below LCST. If the monomer reaches LCST

during polymerization, as polymerization occurs it will undergo the phase change and will remain in its collapsed state even when the temperature is reduced below LCST.

8.4 Transmission Characterization

The transmission measurement is performed by sending a broad band light source through one side of the line defect waveguide and recording the light emitted from the waveguide. Light falling within the bandgap will be confined to the waveguide by the surrounding photonic crystal lattice, while light outside the bandgap will continue to expand. When the light is gathered and recorded the light confined to the waveguide will have a much, much higher intensity than the unconfined light. In figure 8.10 the incoming light comes from the right and is coupled into the waveguide by the lens structure in figure 8.2, and finally the light is gathered to the left of the photonic crystal by an optical fiber.

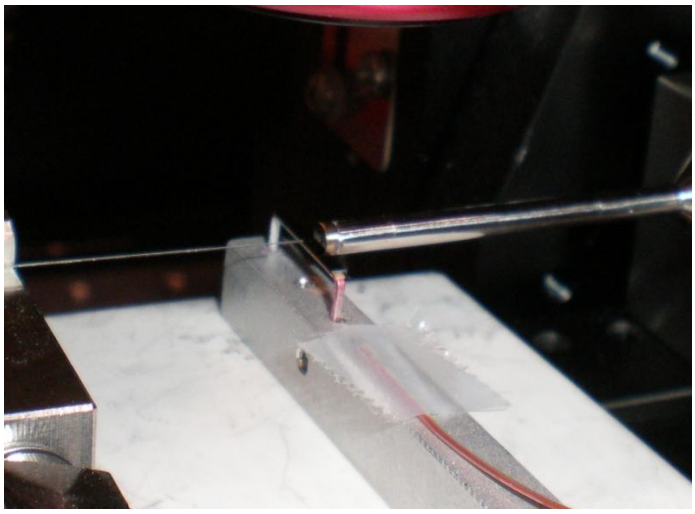

Figure 8.10 A photo of the polarizer, photonic crystal and optical fiber.

The first step in the transmission experiment is align the incoming light, the waveguide and the optical fiber. This is accomplished using a tunable laser source operating at a wavelength lying within the bandgap. The light from the laser is fed via a polarization maintaining optical fiber to a focusing/polarizer assembly. The polarization maintaining fiber is used to reduce polarization changes caused by movement of the fiber, which in turn will cause drops in recorded intensity. The

polarizer/focuser assembly is pictured in figure 8.10. The polarizer is rotated to excite either the TE modes or the TM modes photonic crystal. In this experiment the TM modes were analyzed. Alignment of the polarizer and the photonic crystal can be visually seen be a circular focus point on entrance to the waveguide and a bright circular point emitting form the waveguide. The distance of the polarizer assembly to the photonic crystal is approximately 300 μm. Next, the output fiber is aligned to gather the coupled light and stands at a distance of approximately 20 μm from the waveguide output. The output waveguide is attached to a light-wave multimeter, which measures the intensity of the laser light. Fine tuning of the alignment is performed by adjusting each axis in turn, maximizing the recorded intensity,

Once the system is aligned, a white light source replaces the laser source. In this experiment Santec's Ultra-Wideband Source (UWS-1000) was used to generate a spectrum from 1200nm to 2000nm. The light-wave multimeter was removed and a monochromater was used to record the transmission spectra.

The white base in figure 8.9 is a TE heater that provided a range of temperature from 21°C to 40°C. The temperature was controlled by a Lakeshore 322 temperature control using a thermocouple, also pictured in figure 8.9 at the base of the staple.

8.5 Transmission Measurement Results

Measurements were taken over temperatures form 21°C to 36°C and are shown in figure 8.11. The peak transmission is consistently 1317.1 nm until the critical temperature is attained where the peak redshifts to 1318.2 nm. Further, there is an increase in intensity as the NIPA hydrogel undergoes its phase change. Recall from the previous chapter figure 8.12, which predicts a 1.4 nm redshift and an increase in intensity. However, the spectral

range of the simulation remains much larger than the recorded bandgap and is most likely due to the bridge structure being a 3D object and the simulation being performed as 2D structure.

The photonic crystal was then heated to a temperature of 40°C to ensure the polymer phase change. When the phase change was complete the water which was previously locked in the gel network was expelled and quickly evaporated. Once the evaporation had occurred the spectral peak of the transmission bandwidth shifted back to a position equivalent to the photonic crystal without hydrogel. However, the intensity remained low as shown in figure 8.13. This is expected. Since the hydrogel is composed of 97% water, once the water has evaporated the peak should shift back to its original

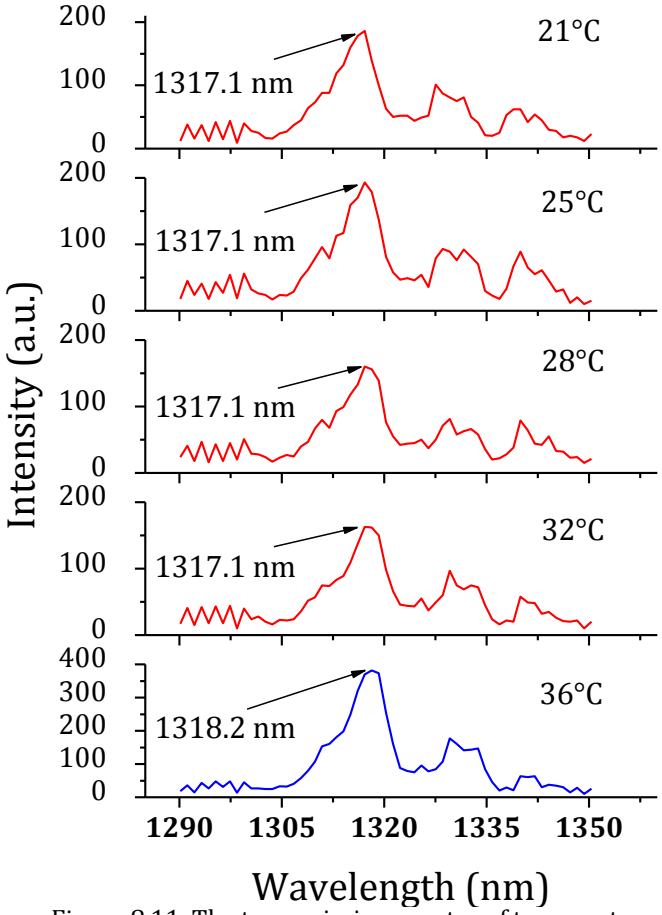

Figure 8.11 The transmission spectra of temperatures from 21°C to 36°C.

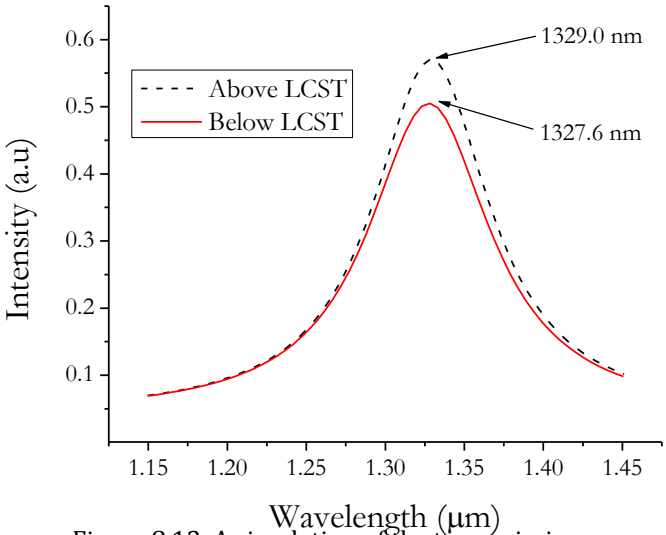

Figure 8.12 A simulation of the transmission bandwidth above and below LCST.

position. The fact that the peak intensity is not recovered shows that gel has infiltrated the photonic crystal matrix. Further, notice in figure 8.8, the desiccated gel network can be seen as clumps of fibrous material over the photonic crystal and along the edges. This indicates that polymerization occurred and the remaining polymer remains after the water has evaporated.

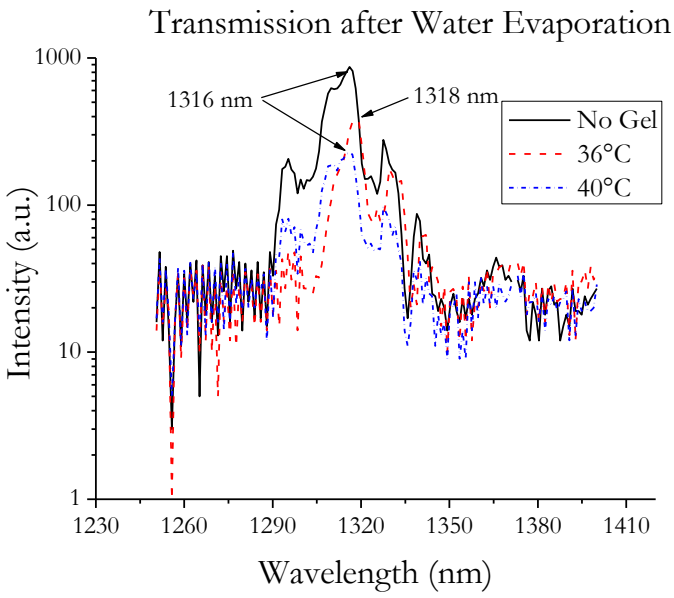

Figure 8.13 The transmission in the photonic crystal without gel above LCST and at 40°C when the hydrogel became desiccated.

Of course one of the unique abilities of NIPA hydrogel is its ability to be rehydrated. The photonic crystal was placed in a cold bath, reducing the surface temperature of the wafer. Humidity was allowed to collect on the surface and partially rehydrate the hydrogel. In figure 8.14 a shift is observed, although not to the extent of the first experiment. The peak intensity also is not fully

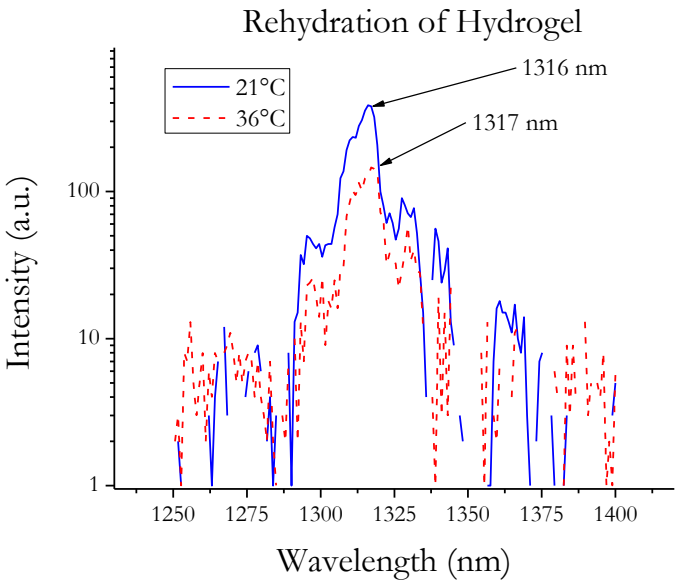

Figure 8.14 The transmission spectra showing the relative peaks for no gel, and a rehydrated photonic crystal above and below LCST.

realized and is most likely due to water vapor around the bridge structure causing scattering.

Thus, the red-shift of the recorded data taken into account with the simulation and the rehydration of the gel show a tunable photonic crystal.

CHAPTER 9

SUMMARY AND CONCLUSIONS

The objective of this dissertation was to show uses of N-isopropylacramide hydrogel as a means for controlling photonic devices. This was accomplished by first characterizing the hydrogel.

Employing the use of ellipsometer for the measurement of the index of refraction of a fluid, particularly NIPA have been presented. The great significance of the measurement is the jump in index of refraction as the temperature is increased over the critical temperature. The shrinking of the NIPA gel particles cause an increase in scattering and hence an increase in the refractive index. This work may lead to further technological applications of the NIPA material, particularly in the optical field, making use of the change in refractive index.

The first device made was a PNIPAM—Quantum Dot hybrid material which is capable of controlling resonant energy transfer through externally applied stimuli. Enhancement of the photoluminescent was shown as functions of temperature and electric field. Such a device can be used as a sensor, which increase the photoluminescence as the environmental conditions change.

The second device is a tunable photonic crystal with the NIPA hydrogel infiltrating the crystal matrix. By globally changing the temperature a shift in the transmission bandwidth was shown as well as a change in transmission intensity. This again is useful as a sensor, where the transmission is observed as environmental conditions change.

BIBLIOGRAPHY

E. Abrahams, P. W. Anderson, D. C. Licciardello, T. V. Ramakrishnan, "Scaling Theory of Localization: Absence of Quantum Diffusion in Two Dimensions," Phys. Rev. Lett. **42**, 673-676 (1979).

M. Abramowitz, I. A. Stegun, "Riccati-Bessel Functions." §10.3 in *Handbook of Mathematical Functions with Formulas, Graphs, and Mathematical Tables*, (Dover, New York 1972) p. 445.

E. I. Adirowitsch, *Einige Fragen Zur Theorie der Lumineszens der Kristalle*, (Akademie-Verlag, Berlin 1953).

ALV Laser Vertiebsgesellschaft, *ALV/DLS/SLS 5000 Digital Correlator Reference Manual*, June 1993.

T. Amiya, T. Tanaka, "Phase Transitions in Cross-Linked Gels of Natural Polymers," Macromolecules **20**, 1162-1164 (1987).

—, Y. Hirokawa, Y. Hirose, Y. Li, T. Tanaka, "Reentrant phase transition of N-isopropylacrylamide gels in mixed solvents," J. Chem Phys. **86**, 2375-2379 (1987).

P. W. Anderson, "Absence of Diffusion in Certain Random Lattices," Phys. Rev. **109**, 1492-1505 (1958).

R. Apkarian, E. R. Wright, V. A. Seredyuk, S. Eustis, L. A. Lyon, V. P. Conticelo, F. M. Menger, "In-Lens Cry-High Resolution Scanning Electron Microscopy: Methodologies for Molecular Imaging of Self-Assembled Organic Hydrogels," Microsc. Microanal. **9**, 286-295 (2003).

Aristotle, *On the Soul II* (335 BC) ; translated by R. D. Hicks (Cambridge 1907); in M. R. Cohen, I. E. Drabkin, *A source book in Greek science*, (Cabbridge, Harvard University Press, 1958) p. 285-286.

—, *De Anima*, Book II, Ch. 7, Sec. 4; translated by R. D. Hicks, *Aristotle De Anima*, (Cambridge Press, 1907) p. 80-81.

L. Arleth, X. Xia, R. P. Hjelm, J. Wu, Z. Hu, "Volume transition and internal structures of small poly(N-isopropylacrylamide) microgels," J. Polym. Sci. Part B **43**, 849-860 (2004).

D. E. Aspnes, "Characterization of Materials and Interfaces by Visible-Near UV Spectrophotometry and Ellipsometry," J. Mat. Educ. **7**, 849-901 (1985).

R. M. A. Azzam, N. M. Bashara, *Ellipsometry and Polarized Light*, (North-Holland, New York 1977).

F. Bacon, *Topics of inquiry concerning light and the nature of light*, (1612); in Basil Montagu, Esq, *The works of Francis Bacon*, **15**, 82-87 (London, 1834).

Y. H. Bae, T. Okano, S. W. Kim, "'On—Off' Thermocontrol of Solute Transport. I. Temperature Dependence of Swelling of N-Isopropylacrylamide Networks Modified with Hydrophobic Components in Water," Pharm. Res. **8**, 531-537 (1991).

S. E. Barkou, J. Broenh, A. Bjarklev, "Silica-sir photonic crystal fiber design that permits waveguiding by a true photonic band gap effect," Opt. Lett. **24**, 46-48 (1999).

M. G. Bawendi, W. L. Wilson, L. Rothberg, P.J. Carroll, T.M. Jedju, M. L. Steigerwald, L. E. Brus, "Electronic structure and photo excited-carrier dynamics in nanometer-size CdSe clusters," Phys. Rev. Lett. **65**, 1623-1626 (1990).

E. Becquerel, *La Lumière, ses causes et ses effets*, (Grautheir-Villars, Paris 1867).

A. Beer, "Versuch die Absorptions-Verhältnisse des Cordierites für rothes Licht zu bestimmen," Ann. der Physik (Leipzig) **84**, 37-44 (1951).

—, "Bestimmung der Absorption des rothen Lichts in farbigen Flüssigkeiten," Ann. der Physik (Leizig) **86**, 78-88 (1852).

T. M. Bender, R. J. Lewis, R. Pecora, "Absolute Rayleigh ratios of four solvents at 488 nm," Macromolecules **19**, 244-245 (1986).

H. Benisty, "Modal analysis of optical guides with two-dimensional photonic band-gap boundaries," J. Appl. Phys. **79**, 7483-7492 (1996).

V. Berger, "From photonic band gaps to refractive index engineering," Opt. Mater. **11**, 131-142 (1999).

R. G. Berra, A. García-Valenzuela, "Coherent reflectance in a system of random Mie scatterers and its relation to the effective-medium approach," J. Opt. Soc. Am. A **20**, 296-311 (2003).

C. L. A. Berli, D. L. Quemada, "Prediction of the Interaction Potential of Microgel Particles from Rheometric Data. Comparison with Different Models," Langmuir **16**, 10509-10514 (2000).

B. J. Berne, R. Pecora, *Dynamic Light Scattering*, ed. (John Wiley & Sons, New York 1976).

R. N. Bhargave, D. Gallagher, X. Hong, A. Nurmikko, "Optical properties of manganese-doped nanocrystals of ZnS," Phys. Rev. Lett, **72**, 416-419 (1994).

A. Blanco, E. Chomski, S. Grabtchak, M. Ibisate, S. John, S. W. Leonard, C. Lopez, F. Meseguer, H. Miguez, J. P. Mondia, G. A. Ozin, O. Toader and H. M. van Driel, "Large-scale synthesis of a silicon photonic crystal with a complete three-dimensional bandgap near 1.5 micrometers," Nature **405**, 437-440 (2000).

W. Bogaerts, D. Taillaert, B. Luyssaert, P. Dumon, J. Van Campenhour, P. Bienstman, D. Van Thourhout, R. Baets, V. Wiaux, S. Beckx, "Basic structures for photonic integrated circuits in Silicon-on-insulator," Optics Express **12**, 1583-1591 (2004).

C. F. Bohren, D. R. Huffman, *Absorption and Scattering of Light by Small Particles*, (Wiley, New York 1983).

P. I. Borel, B. Bilenberg, L. H. Frandsen, T. Nielsen, J. Fage-Pedersen, A. V. Lavrinenko, J. S. Jensen, O. Sigmund, A. Kristensen, "Imprinted silicon-based nanophotonics," Opt. Express **15**, 1261-1266 (2007).

D. S. Boudreaux and V. Heine, "Band structure treatment of low energy electron diffraction intensities," Surf. Sci. **8**, 426-444 (1967).

W.L. Bragg, "The Diffraction of Short Electromagnetic Waves by a Crystal", Proc. of the Cambridge Phil. Soc. **17**, 43–57 (1914).

F. Brechet, J. Marcou, D. Pagnoux, P. Roy, "Complete analysis of the characteristics of propagation into photonic crystal fibers, by the finite element method," Opt. Fiber. Technol. **6**, 181-191 (2000).

D. Brewster, "On the Laws Which Regulate the Polarisation of Light by Reflexion from Transparent Bodies," Phil. Trans. Roy. Soc. **105**, 125-159 (1815).

—, "Experiments on the Depolarisation of Light as Exhibited by Various Mineral, Animal and Vegetable Bodies, with a Reference of the Phenomena to the General Principles of Polarisation, Phil. Trans. Roy. Soc. **105**, 29-53 (1815).

L. Brillouin," Über die Fortpflanzung des Lichtes in dispergierenden Medien," Annalen der Physik (Leipzig) **349**, 203-240 (1914).

—, "Diffusion de la lumiere et des rayonnes X par un corps transparent homogene; influence del'agitation thermique," Annales de Physique (Paris) **17**, 88-122 (1922).

—, *Les Champs Self-Consistents de Hartree et de Fock*, Actualiés Scientifiques et Industrielles No. 159 (Herman et Cie. 1934).

W. Brown, *Dynamic Light Scattering*, edited by W. Brown, (Clarendon Press, Oxford 1993), Preface.

R. G. W. Brown, "Homodyne Optical Fiber Dynamic Light Scattering," App. Opt. **40**, 4004-4010 (2001).

W. Bruchard, M. Schmidt, W. H. Stockmayer, "Information on Polydispersity and Branching from Combined Quasi-Elastic and Integrated Scattering," Macromolecules **13**, 1265-1272 (1980).

L. E. Brus, "A simple model for the ionization potential, electron affinity and aqueous redox potential of small semiconductor crystallites," J. Chem. Phys. **79**, 5566-5571 (1983).

—, "Electron-electron and electron-hole interactions in small semiconductor crystallites: The size dependence of the lowest excited electronic state," J. Chem. Phys., **80**, 4403-4409 (1984).

J. Z. Buchwald, *The Rise of the Wave Theory of Light: Optical Theory and Experiment in the Early Nineteenth Century*, ed. (University of Chicago Press, Chicago 1989).

H. Buecher, K. H. Drexhage, M. Fleck, H. Kuhn, D. Mobius, F. Schafer, J. Sondermann, W. Sperling, P. Tillman, J. Weigand, Controlled transfer of excitation energy through thin layers, Mod. Cryst. **2**, 199-230 (1967).

K. Busch, S. John, "Liquid-Crystal Photonic-Band-Gap Materials: The Tunable Electromagnetic Vacuum," Phys. Rev. Lett. **83**, 967-970 (1999).

J. Butty, N. Peyghambarian, "Room temperature optical gain in sol-gel derived CdS quantum dots," Appl. Phys. Lett. **69**, 3224-3226 (1996).

A. C. Cangellaris, D. B Wright, "Analysis of the numerical error caused by the stair-stepped approximation of a conducting boundary in FDTD simulations of electromagnetic phenomena," IEEE Trans. Antennas and Propagation, **AP-39**, 1518-1525 (1991).

S.R. Carter, S. Rimmer "Aqueous compatible polymers in bionanotechnology," IEE Proc.-Nanobiotechnol. **152**, 169 (2005).

Caykara T., C. Ozyurek, O. Kantoglu, O.J. Guven, "Equilibrium swelling behavior of pH- and temperature-sensitive poly(N-vinyl 2-pyrrolidone-g-citric acid) polyelectrolyte hydrogels," Polym. Sci. B **38**, 2063-2071 (2000).

M. Cellio, *Il Fosforo o vero la Pietra Bolognese*, (1680) original volume at University Library of Bologna, Italy.

M. Chamarro, C. Gourdon, P. Lavallard, O. Lublinskaya, A. I. Ekimov, "Enhancement of electron-hole exchange interaction in CdSe nanocrystals: A quantum confinement effect," Phys. Rev. B **53**, 1336-1342 (1996).

M. D. B. Charlton, S. W. Roberts, G. J. Parker, "Guided mode analysis, and fabrication of a 2-dimensional visible photonic band structure confined within a planar semiconductor waveguide," Material Sci. and Eng. B **49**, 155-165 (1997).

W. Chen, D. L. Mills, "Gap solitons and the nonlinear optical response of superlattices," Phys. Rev. Lett. **58**, 160-163 (1987).

Y. Chen, G. Faini, H. Launois, J. Etrillard, "Fabrication of two-dimensional photonic lattices in GaAs: the regular graphite structures," Supperlattices and Microsctructres **22**, 109-113 (1997).

H. C. Cheung, "Resonance Energy Transfer," in *Topics in Fluorescence Spectroscopy, Volume 2: Principles*, ed. by J. R. Lakowicz, (Plenum Press, New York 1991).

E. Chow, A. Grot, L. W. Mirkarimi, M. Sigalas, and G. Girolami, "Ultracompact biochemical sensor built with two-dimensional photonic crystal microcavity," Opt. Lett. **29**, 1093-1095 (2004).

B. Chu, Q. Ying, C. Wu, J. R. Ford, H. S. Dhadal "Characterization of poly(1,4-phenyleneterephthalamide) in concentrated sulfuric acid. 2: Determination of molecular weight distributions," Polymer **26**, 1408 (1985).

—, *Laser Light Scattering,* 2nd ed. (Academic Press, San Diego, CA, 1991).

T. Chu. H. Yamada, S. Ishida, Y. Arakawa, "Thermooptic switch based on photonic-crystal line-defect waveguides," IEEE Photon. Technol. Lett. **17**, 2083-2085 (2005).

A. Chutinan, S. Noda, "Waveguides and waveguide bends in two dimensional photonic crystal slabs," Phys. Rev. B **62**, 4488-4492 (2000).

R. Clapp, I. L. Medintz, H. T. Uyeda, E. R. Goldman, H. Mattoussi, "Quantum dot-based multiplexed fluorescence resonance energy transfer," in Genetically Engineered and Optical Probes for Biomedical Applications III, edited by D. J. Bornhop, S. I Achilefu, R. Raghavachari, A. P. Savitsky (2005).

R. W. Collins and Y. –T. Kim, "Ellipsometry for Thin-Film and Surface Analysis," Anal. Chem. **62**, 887A-900a (1990).

H. Z. Cummins, N. Knable, L. Yeh, "Observation of Diffusion Broadening of Rayleigh Scattered Light," Phys. Rev. Lett. **12**, 150 (1964).

D. Curie, *Luminescence in Crystals,* (Wiley, New York 1963).

P. Debye, "Das Verhalten von Lichtwellen in der Nähe eines Brennpunktes oder einer Brennlinie, Annalen der Physik (Leipzig) **335**, 755-776 (1909).

—, "Zerstreuung von Röntgenstrahlen," Annalen der Physik (Leipzig) **351**, 809-823 (1915).

—, "Light Scattering in Solutions," J. Appl. Phys. **15**, 338-342 (1944).

—, " Molecular-weight determination by light scattering," J. Phys. Coll. Chem. **51**, 18-32 (1947).

V. Degiorgoi, J. B. Lastovka, "Intensity—correlation spectroscopy," Phys. Rev. A **4**, 2033-2050 (1971).

R. Descartes, *La Dioptrique*, (Leiden, 1639); Discourse on Method, Optics, Geometry and Meterology (Indianapolis: Bobbs-Merrill 1965).

J. P. Dowling, C. M. Bowden, "Atomic emission rates in inhomogeneous media with applications to photonic band structures," Phys. Rev. A **46**, 612-622 (1992).

R. Drevillon, "Spectroscopic Ellipsometry of Ultrathin Films: From UV to IR," Thin Solid Films **163** 157-166 (1988).

F. Du, Y. –Q. Lu, S. –T. Wu, "Electrically tunable liquid crystal photonic crystal fiber," Appl. Phys. Lett. **85**, 2181-2183 (2004).

B. D'Urso, O. Painter, J. O'Brien, T. Tombrello, A. Yariv, A. Scherer, "Modal reflectivity in finite-depth two-dimensional photonic crystal microcavities," J. Opt. Soc. Am. B **15**, 1155-1159 (1997).

K. Dušek, D. Patterson, "Transition in Swollen Polymer Networks Induced by Intramolecular Condensation," J. Polym. Sci. **6**, 1209-1216 (1968).

E. N. Economou, A. Zdetsis, "Classical wave propagation in periodic structures," Phys. Rev. B **40**, 1334-1337 (1989).

O. J. Ehl, C. Loucheux, C. Reiss, H. Benoit, "Mesure de l' incrément d' indice de refraction de différentes solutions de hauts polymers, et du rapport de Rayleigh de quelques liquids, en function de la temperature," Makromol. Chem. **75**, 35-51 (1964).

A. Einstein, "Theorie der Opaleszenz von homogenen Flüssigkeitsgemischen in der Nähe des kritischen Zustandes," Annalen der Physik (Leipzig) **14,** 368-391 (1910).

A. I. Ekimov, A. A. Onuschenko, "Quantum size effect in the spectra of semiconductor microcrysals," Sov. Phys. Semicond. **16**, 775-778 (1982).

—, A. L. Efros, A. A. Onushcenko, "Quantum Size Effect in Semiconductor Microcrystals," Solid St. Comm., **56**, 921-924 (1985).

—, "Optical Properties of Semiconductor Quantum Dots in Glass Matrix'" Phys. Scr. **T39**, 217-222 (1991).

—, F. Hache, M. C. Schanne-Klein, D. Ricard, C. Flytzanis, I. A. Judryavtsec, T. V. Yazeva, A. V. Rodina, A. L. Efros, "Absorption and intensity-dependent photoluminescence measurements on CdSe quantum dots: assignment of the first electronic transitions," J. Opt. Soc. Am. B **10**, 100 (1993).

D. Erickson, T. Rockwood, T. Emery, A. Scherer, D. Psaltis, "Nanofluidic tuning of photonic crystal circuits," Optics Lett. **31**, 59-61 (2006).

M. J. Escuti, J. Qi, and G. P. Crawford, "Two-dimensional tunable photonic crystal formed in a liquid-crystal/polymer composite: Threshold behavior and morphology," App. Phys. Lett. **83**, 1331-1333 (2003).

Euclid, *Optica*, (300 BC); translated by Heiberg; in M. R. Cohen, I. E. Drabkin, *A source book in Greek science*, (Cambridge, Harvard University Press, 1958) p. 257-168.

L. Euler, "Nova theoria lucis et colorum," Opuscala varii argumenti **1**, 169 (Berlin 1746).

J. H. Evans, "Observations of a Regular Void Array in High Purity Molybdenum irradiated with 2 MeV Nitrogen Ions," Nature **229**, 403-404 (1971).

B. L. Eyre, J. M. Evans, *Void Formed by Irradiation of Reactor Materials*, ed. S. H. Pugh et. al. (London, BNES 1971).

S. Fan, P. R. Villeneuve, J. D. Joannopoulos, E. F. Schubert, "High Extraction Efficiency of Spontaneous Emission from Slabs of Photonic Crystals," Phys. Rev. Lett. **78**, 3294-3297 (1997).

—, G. Johnson, J.D. Joannopoulos, C. Manolatou, and H.A. Haus, "Waveguide branches in photonic crystals," J. Opt. Soc. Am. B **18**, 162-165 (2001).

M. Faraday, *Extraits des recherché expérimentales en électricité,* edited by Germaine Hirtz (Paris, Gauthier-Villars, 1967).

J. Feldmann, G. Peter, E. O. Göbel, P. Dawson, K. Moore, C. Foxon, R. J. Elliott, "Linewidth dependence of radiative excitons lifetimes in quantum wells," Phys Rev. Lett. **59**, 2337-2340 (1987).

P. de Fermat, "Principle of Least Time," Oeuvres de Fermat vol 2, (Paris, 1891) p. 354.

V. V. Fernandez, N. Tepale, J. F. A. Soltero, "Thermoresponsive nanostructured poly(N-isopropylacrylamide) hydrogels made via inverse microemulsion polymerization," Colloid. Polym. Sci. **284**, 387-395 (2006).

A. Ferrando, E. Silvestre, J. J. Miret, P. Andrés, M. V. Andrés, "Full-vector analysis of a realistic photonic crystal fiber," Opt. Lett. **24**, 276-278 (1999).

J. G. Fleming, Shawn-Yu Lin, "Three-dimensional photonic crystal with a stop band from 1.35 to 1.95 μm," Opt. Lett. **24**, 49-51 (1999).

G. Floquet, “Sur les équations différentielles linéaries à coefficients périodiques,” Ann. École Norm. Sup. **12**, 47-48 (1883); F. Bloch, “Über die quantenmechanik der electronen in kristallgittern,” Z. Physik **52**, 555-600 (1928).

P. J. Flory, "Thermodynamics of High Polymer Solutions," J. Chem. Phys. **10**, 51-61 (1942).

—, J. Rehner Jr., "Statistical Mechanics of Cross-Linked Polymer Networks II. Swelling," J. Chem. Phys. **11**, 521-526 (1943).

—, "Statistical Mechanics of Swelling of Network Structures," J. Chem. Phys. **18**, 108-111 (1950).

J. A. Finnigan, D. J. Jacobs, "Light scattering from benzene, toluene, carbon disulphide and carbon tetrachloride," Chem. Phys. Lett. **6**, 141-143 (1970).

M. Fixman, "Molecular Theory of Light Scattering," J. Chem. Phys. **23**, 2074-2079 (1955).

A. H. L. Fizeau, Compt. Rend. Acad. Sci. Paris **30**, 562, 771 (1850).

V. Fock, Z. Physic **61**, 126 (1930).

J. S. Foresi, P. R. Villeneuve, J. Ferrera, E. R. Thoen, G. Steinmeyer, S. Fan, J. D. Joannopoulos, L. C. Kimerling, H. I. Smith, E. P. Ippen, "Photonic-bandgap microcavities in optical waveguides," Nature **390**, 143-145 (1997).

A. T. Forrester, R. A. Gudmandesen, P. O. Johnson, "Photoelectric Mixing of Incoherent Light," Phys. Rev. **99**, 1691 (1955).

T. Förster, "Zwischenmolekulare Energiewanderung und Fluoreszenz," Annalen der Physik (Leipzig) **437**, 55-75 (1948); Translation by R.S. Knox, "Intermolecular energy migration and fluorescence."

—, "Transfer Mechanisms of Electronic Excitation," Discuss. Faraday Soc. **27**, 7-17 (1959).

—, "Part III Action of Light and Organic Crystals," In *Modern Quantum Chemistry*, ed. O Sinanoglu, (Academic Press, New York 1965).

—, Mechanism of energy transfer, in: Comprehensive Biochemistry (M. Florkin and E. H. Statz, eds), Vol. 22, pp. 61-77, (Elsevier, New York 1967).

L. Foucault, Compt. Ren. Acad. Sci. Paris **30**, 551 (1850).

A. Fresnel, " Mémoire sur la diffraction de la lumière," Ann. Chim, et Phys. **1**, 239-281 (1816).

—, *Oeuvres Complètes d'Augustin Fresnel*, Edited by H. de Senarmont, É. Verdet, L. Fresnel, (IImprimiere Imperiale, Paris 1866-1870).

T. Fujimura, T. Itoh, K. Hayashibe, K. Edamatsu, K. Shimoyama, R. Shimada, A. Imada, T. Koda, Y. Segawa, N. Chiba, H. Muramatsu, T. Ataka, "Observation of local light propagation in ordered latex layers by scanning near-field optical microscope," Mat. Sci. Eng. B **48**, 94-102 (1997).

—, T. Itoh, A. Imada, R. Shimada, T. Koda, N. Chiba, H. Muramatsu, H. Miyazaki, K. Ohtaka, "Near-field optical images of ordered polystyrene particle layers and their photonic band effect," J. Lumin. **87-89**, 954-956 (2000).

H. Fujita and K. Ametani, "Optical Properties of Colloidal Crystal Latex near the Melting Point," Jpn. J. Appl. Phys. **16**, 1907-1917 (1977).

R. Gans, "Uber die from ultramikroskopischer Goldteilchen," Annalen der Physik (Leipzig) **342**, 881 (1912).

—, "Über die Form ultramikroskopischer Silberteilchen," Annalen der Physik (Leipzig) **352**, 270-284 (1915).

—, "Strahlunsdiagramme ultramikroskopischer Teilchen," Annalen der Physik (Leipzig) **381**, 29-38 (1925).

J. Gao, B. J. Frisken, "Cross-Linker-Free N-Isopropylacrylamide Gel Nanospheres," Langmuir **19**, 5212-5216 (2003).

A. García-Valenzuela, R. G. Barrera, "Electromagnetic response of a random half-space of Mie scatterers within the effective medium approximation and the determination of the effective optical coefficients," J. Quant. Spectrosc. Radiat. Transfer **79-80**, 627-647(2003).

A. Z. Genack, "Optical Transmission in Disordered Media," Phys. Rev. Lett. **58**, 2043-2046 (1987).

R. J. Glauber, M. Lewenstein, "Quantum optics of dielectric media," Phys. Rev. A **43**, 467-491 (1991).

Y. Gong, M. Gao, D. Wang, H. Möhwald, "Incorporating Fluorescent CdTe Nanocrystals into a Hydrogel via Hydrogen Bonding: Toward Fluorescent Microspheres with Temerature-Responsive Properties," Chem. Mater., **17**, 2648-2653 (2005).

P. L. Gourley, J. R. Wendt, G. A. Vawter, T. M. Brennan, B. E. Hammons, "Optical properties of two-dimensional photonic lattices fabricated as honeycomb nanostructures in compound semiconductors," Appl. Phys. Lett. **64**, 687-689 (1994).

H. E. Grecco, K. A. Lidke, R. Heintzmann, D. S. Lidke, C. Spagnuolo, O. E. Martinez, E. A. Jares-Erijman, T. M. Jovin, "Ensamble and Single Particle Photophysical Properties (Two-Photon Excitation, Anisotropy, FRET, Lifetime Spectral Conversion) of Commercial Quantum Dots in Solution and in Live Cells," Micro. Res. Tech., **65**, 169-179 (2004).

S. E. Green, C. M. Herzinger, B. D. Johs, J. A. Woollam, U.S patent 5,757,494 (26 May 1998).

C. Gesner, *De raris et admirandis herbis quae sive nactu luceant, sive alias ob causas, Lunariae nominantur et obiter de alia etiam rebus, quae in tenebris lucent, Commentariolus*, (Tiguri 1555) p. 82; in E. N. Harvey, *A History of Luminescence: From the Earliest Times Until 1900*, (J. H. Furst, Baltimore, MD 1957).

E. Gross, "Change of wave-length of light due to elastic heat waves at scattering in liquids," Nature **126**, 201 (1930).

—, "Modification of light quanta by elastic heat oscillations in scattering media," Nature **129**, 722 (1932).

L. Gu, W. Jiang, X. Chen, R. T. Chen, "Thermooptically Tuned Photonic Crystal Waveguide Silicon-on-Insulator Mach-Zehnder Interferometers," IEEE Photon. Technol. Lett. **19**, 342-344 (2007).

T. Ha, T. Enderle, D. F. Ogletree, D. S. Chemla, P. R. Selvins, S. Weiss, "Probing the interaction between two single molecules: Fluorescence resonance energy transfer between a single donor and a single acceptor," Proc. Natl. Acad. Sci. U.S.A. **93**, 6264-6268 (1996).

M. W. Haakestad, T. T. Alkeskold, M. D. Nielsen, L. Scolari, J. Riishede, H. E. Engan, A. Bjarklev, "Electrically Tunable Photonic Crystal Bandgap Guidance in a Liquid-Crystal-Filled Photonic Fiber," Photonics Technol. Lett. **17** 819-821 (2005).

P. Halevi and F. Ramos-Mendieta, "Tunable Photonic Crystals with Semiconducting Constituents," Phys. Rev. Lett. **85**, 1875 - 1878 (2000).

A. C. Hall, "A century of ellipsometry," Surf. Sci. **16**, 1-13 (1969).

R. Hamlen, C. Kent, S. Shafer, "Electrochemically activated contractile polymer," Nature **206**, 1149-1150 (1965).

M. Haraguchi, T. Nakai, A. Shinya, T. Okamoto, M. Fukui, T. Koda, R. Shimada, K. Ohtaka, K. Takeda, "Optical Modes in Two-dimensionally Ordered Dielectric Spheres," Jpn. J. Appl. Phys. **39**, 1747 (2000).

M. Harold, H. Chong and R.M. De La Rue, “Tuning of Photonic Crystal Waveguide Microcavity by Thermooptic Effect,” Photonic Tech. Lett. **16** 1528-1530 (2004).

D. R. Hartree, "Results of Calculations of Atomic Wave Functions. I. Survey, and Self-consistent Fields for Cl^- and Cu^+," Proc. Roy. Soc. London A **141**, 282-301 (1933).

R. P. Haugland, G. J. Yguerabide, L. Stryer, Dependence of the kinetics of singlet-singlet energy transfer on the spectral overap integral, Proc. Natl. Acad. Sci. U.S.A. **63**, 23-30 (1969).

H. A. Haus, C. V. Shank, "Antisymmetric Taper of Distributed Feedback Lasers," IEEE J. Quantum Electron. **12**, 532-539 (1976).

H. Hertz, "The Forces of Electrical Oscillations Treated According to Maxwell's Theory," Weidemann's Ann. **36**, 1 (1889); reprinted in Chap. 9 of H. Hertz, *Electric Waves*, Dover, New York 1962).

J. Hilfiker, J. Woollam, G. Mowry, P. Chow, J. Elman, "Automated Spectroscopic Ellipsometry," Industrial Physicist **2**, 30-34 (1996).

—, B. Singh, R.A. Synowicki, C. L. Bungay, “Optical characterization in the vacuum ultraviolet with Variable Angle Spectroscopic Ellipsometry: 157nm and below,” SPIE Microlithography Conf. (2000).

P. A. Hiltner and I. M. Krieger, "Diffraction of Light by Ordered Suspensions," J. Phys. Chem. **73**, 2386-2389 (1969).

T. Hino, J. M. Prausnitz, "Swelling equlibria for heterogeneous polyacrylamide gels," J. App. Polym. Sci. **62**, 1635-1640 (1996).

Y. Hirokawa and T. Tanaka, "Volume phase transition in a nonionic gel," J. Chem. Phys. **81** 6379-6380 (1984).

S. Hirotsu, "Electric-Field Induced Phase Transition in Polymer Gels," Jpn. J. Appl. Phys. Suppl. **24**, 396-388 (1985).

—Y. Hirokawa, T. Tanaka, "Volume-phase transitions of ionized N-isopropylacrylamide gels," J. Chem Phys. **87**, 1392-1395 (1987).

—, "Phase Transition of a Polymer Gel in Pure and Mixed Solvent Media," J. Phys. Soc. Jpn. **56**, 233-242 (1987).

—, T. Hirokawa, T. Tanaka, "Volume-phase transitions of ionized N-isopropylacrylamide gels," J. Chem. Phys. **87**, 1392-1395 (1987).

K. M. Ho, C. T. Chan, C. M. Soukoulis, "Existence of a photonic gap in periodic dielectric structures," Phys. Rev. Lett. **65**, 3152 (1990).

S. Hohng, T. Ha, "Single-Molecule Quantum Dot Fluorescence Resonance Energy Transfer," Chem. Phys. Chem. **6**, 956-960 (2005).

R. Holland, "THREDS: A finite-difference time-domain EMP code in 3D spherical coordinates," IEEE Trans. Nuclear Science **NS-30**, 4592-4595 (1983)

J. H. Holtz and S. A. Asher, "Polymerized colloidal crystal hydrogel films as intelligent chemical sensing materials," Nature **389**, 829-832 (1997).

Z. Hu, X. Lu, J. Gao, "Hydrogel Opals," Adv. Maters. **13**, 1708-1712 (2001).

G. Huang, J. Gao, Z. Hu, J. V. St. John, B. C. Ponder, D. Moro, "Controlled drug release from hydrogel nanoparticle networks," J. Cont. Rel. **94**, 303-311 (2004).

M. L. Huggins, "Solutions of Long Chain Compounds," J. Chem. Phys. **9**, 440 (1941).

H. C. van de Hulst, *Light Scattering by Small Particles*, (Wiley, New York 1957).

J. Humlicek, "Sensitivity extrema in multiple-angle ellipsometry," J. Opt. Soc. Am. A **2**, 713-722 (1985).

O. Hunderi, "On the problems of multiple overlayers in ellipsometry and a new look at multiple angle of incidence ellipsometry," Surf. Sci. **61**, 515-520 (1976).

C. Huygens, *Traité de la lumière*, (Leyden 1960).

M. Ilavsky, "Phase transition is Swollen Gels. 2. Effect of Charge Concentration on the Collapse and Mechanical Behavior of Polyacrylamide Networks," Macromolecules **15**, 782-788 (1982).

M. M. Ibrahim, N. M. Bashara, "Parameter-Correlation and Computational Considerations in Multiple-Angle Ellipsometry," J. Opt. Soc. Am. **61**, 1622-1629 (1971).

F. Ilmain, T. Tanaka, E. Kokufuta, "Volume transition in a gel driven by hydrogen bonding," Nature **349**, 400 (1991).

M. Irie, "Photoresponsive Polymers. Reversible Bending of Rod-Shaped Acrylamide Gels in an Electric Field," Macromolecules **19**, 2890-2892 (1986).

T. Itoh, T. Kirihara, "Excitons in CuCl Microcrystals Embedded in NaCl," J. Lumin, **31**, 120-22 (1984).

—, T. Iwabuchi, M. Kataoka, "Study on the Size and Shape of CuCl Microcrystals Embeddedin Alkali-Chloride Matrices and Their Correlation with Exciton Confinement," Phys. Stat. Solidi (b) **145**, 567-577 (1988).

A. Jabloński, “Efficiency of anti-Stokes fluorescence in dyes,” Nature **131**, 839 (1933).

D. Jackson, *Classical Electrodynamics*, 3rd ed., (John Wiley & Sons, New York 1998), p. 456.

E. Jakeman, E. R. Pike, S. Sqain, "Statistical accuracy in the digital autocorrelation of photon counting fluctuations," J. Phys. A : Gen. Phys. **4**, 517-534 (1971).

S. John, M. J. Stephen, "Wave propagation and localization in a long-range correlated random potential," Phys. Rev. B **28**, 6358-6368 (1983).

—, "Electromagnetic Absorption in a Disordered Medium near a Photon Mobility Edge," Phys. Rev. Lett. **53**, 2169-2172 (1984).

—, “Strong Localization of Photons in Certain Disordered Dielectric Superlattices,” Phys. Rev. Lett. **58**, 2486 (1987).

—, R. Rangarajan, "Optimal structures for classical wave localization: an alternative to the ioffe-regel criterion," Phys. Rev. B **38**, 10101-10104 (1988).

R. P. Johnson, “Luminescence of sulfide and silicate phosphors,” J. Opt. Soc. Am. **29**, 387-391 (1939).

J. G. Joannopoulos, P. R. Villeneuve, S. Fan, "Photonic crystals: putting a new twist on light," Nature **386**, 143-149 (1997).

S. G. Johnson, S. Fan, P. R. Villeneuve, J. D. Joannopoulos, and L. A. Kolodziejski, “Guided modes in photonic crystal slabs,” Phys. Rev. B **60**, 5751-5758 (1999).

—, S. Fan, P. R. Villeneuve, J. D. Joannopoulos, and L. A. Kolodziejski, “Guided modes in photonic crystal slabs,” Phys. Rev. B **60**, 5751-5758 (1999).

—, P. R. Villeneuve, S. Fan, J. D. Joannopoulos, “Linear waveguides in photonic-crystal slabs,” Phys. Rev. B **62** 8212-8222 (2000).

—, P. R. Villeneuve, S. Fan, J. D. Joannopoulos, "Linear waveguides in photoni-crystal slabs," Phys. Rev. B **62**, 8212-8221 (2000).

—, S. D. Joannopoulos, *Photonic Crystals: The Road from Theory to Practice*, ed. (Springer, New York 2002), p. 17.

—, J. D. Joannopoulos, "Introduction to Photonic Crystals: Bloch's Theorem, Band Diagrams, and Gaps (But no defect)," http://ab-initio.mit.edu/photons/tutorial/photonic-intro.pdf, (Accessed February 2008).

T. M. Jovin, "Quantum dots finally come of age," Nature Biotechnol., **21**, 32-33 (2003).

K. Jubota, S. Fujishige, I. Ando, "Single-Chain Transition of Poly(N-isopropylacrylamide) in Water," J. Phys. Chem. **94**, 5154-5158 (1990).

B. G. Kabra, S. H. Gehrke, R. J. Spontak, "Microporous, Responsive Hydroxypropyl Cellulose Gels. 1. Synthesis and Microstructure," Macromolecules **31**, 2166-2173 (1998).

K. Kambe, Z. Naturf **22a** 322-330 (1967).

—, Z. Naturf. **22a** 422-431 (1967).

—, Z Naturf **23a**, 1280 (1968).

D. Kang, J. E. Maclennan, N. A. Clark, A. A. Zakhidov, R. H. Baughman, "Electro-optic Behavior of Liquid-Crystal-Filled Silica Opal Photonic Crystals: Effect of Liquid-Crystal alignment," Phys. Rev. Lett. **86**, 4052-4055 (2001).

Y. J. Kang, J. J. Walish, T. Goishnyy, E. L. Thomas, "Broad-wavelength-range chemically tunable block-copolymer photonic gels," Nature Mater. **6**, 957-960 (2007).

M. Kanskar, P. Paddon, V. Pacraouni, R. Morin, A. Busch, J. F. Young, S. R. Johnson, J. MacKenzie, T. Tiedje, "Observation of leaky slab modes in an air-bridge semiconductor waveguide with a two-dimensional photonic lattice," Appl. Phys. Lett. **70**, 1438-1440 (1997).

G. Karreman, R. H. Steele, A. Szent-Györgyi, "On Resonance Transfer of Excitation Energy Between Aromatic Amino acids in Proteins," Proc. Nat. Acd. Sci. U.S.A. **44**, 140-143 (1958).

S. Katayama, Y. Hirokawa, T. Tanaka "Reentrant Phase Transition in Acrylamide-Derivative Copolymer Gels," Macromolecules **17**, 2641-2643 (1984).

N. Kawai, K. Inoue, N. Carlsson, N. Ikeda, Y. Sugimoto, K. Asakawa, and T. Takemori, "Confined Band Gap in an Air-Bridge Type of Two-Dimensional AlGaAs Photonic Crystal," Phys. Rev. Lett. **86**, 2289-2292 (2001).

A. Kikuchi, T. Okano, "Pulsatile drug release control using hydrogels," Adv. Drug Deliv. Rev. **54**, 53 (2002).

J. Kim, M.J. Serpe, A.L. Lyon, "Hydrogel Microparticles as Dynamically Tunable Microlenses," J. Am. Chem. Soc. **126**, 9512-9513 (2004).

W. Kohn and N. Rostoker, "Solution of the Schrödinger Equation in Periodic Lattices with an Application to Metallic Lithium," Phys. Rev. **94**, 1111-1120 (1954).

Z. Kojro, "Influence of statistical errors on size distributions obtained from dynamic light scattering data. Experimental limitations in size distribution determination," J. Phys. A: Math. Gen. **23**, 1363-1383 (1990).

E. P. Kosmidou, E. E. Kriezis, T. D. Tsiboukis, "Analysis of Tunable Photonic Crystal Devices Comprising Liquid Crystal Materials as Defects," J. Quantum Electon. **41**, 657-665 (2005).

J. Korringa, "On the calculation of the energy of a Bloch wave in a metal," Physica **13**, 392-400 (1947).

J. P. Kratohvil, Gj. Deželić, M. Kerker, E. Matijević, "Calibratin of Light Scattering Instruments: A Critical Survey," J. Poly. Sci. **57**, 59-78 (1962).

T. Kraus, R. De La Rue, S. Band, "Two-dimensional photonic bandgap structures operating at near-infrared wavelengths," Nature **383**, 699-702 (1996).

F. A. Kröger, W. Hoogenstraaten, "Decay and quenching of fluorescence in willemite," Physica, **14**, 425-441 (1948).

M. Kuang, D. Wang, H. Möhwald, "Fabrication of Thermoresponsive Plasmonic Microspheres with Long-Term Stability from Hydrogel Spheres," Adv. Mater., **15**, 1611-1616 (2005).

K. Kubota, S. Fujishige, I. Ando, "Solution properties of poly(N-isopropyl-acrylamide) in water," Polym. J. **22**, 15-20 (1990).

S. Kuchinsky, D. C. Allan, N. F. Borrelli, J. C. Cotteverte, "3D localization in a channel waveguide in a photonic crystal with 2D periodicity," Opt. Commun. **175**, 147-152 (2000).

W. Kuhn, B. Hargitay, A. Katchalsky, H. Eisenberg, "Reversible Dilation and Contraction by Changing the State of Ionization of High-Polymer Acid Networks," Nature **165**, 514-516 (1950).

D. Labilloy, H. Benisty, C. Weisbuch, C. J. M. Smith, T. F. Krauss, R. Houdré, U. Oestrele, "Finely resolved transmission spectra and band structure of two-dimensional photonic crystals using emission from InAs quantum dots," Phys. Rev. B **59**, 1649-1652 (1999).

D. Labilloy, H. Benisty, C. Weisbuch, T. F. Krauss, R. M. De La Rue, V. Bardinal, R. Houdré, U. Oesterle, D. Cassagne, C. Jouanin, "Quantitative Measurement of Transmission, Reflection, and Diffraction of Two-Dimensional Photonic Band Gap Structures at Near-Infrared Wavelengths," Phys. Rev. Lett. **79**, 4147-4150 (1997).

L. Landau, G. Placzek, "Struktur der unverschobenen Streulinie," Phys. Zeitt. Sow. **5**, 172-173 (1934).

—, E. M. Lifshitz, Electrodynamics of Continuous Media, 2nd ed. Translated by J. B. Sykes, J. S. Bell, M. J. Kearsley (Pergamon Press, New York 1984) p. 422-462.

T. T. Larsen, A. Bjarkley, D. S. Hermann, and J. Broeng, "Optical devices based on liquid crystal photonic bandgap fibres," Optics Express **11**, 2589-2586 (2003).

S. Latt, H. T. Cheung, E. R. Blout, "Energy Transfer: A system with relatively fixed donor-acceptor separation," J. Am. Chem. Soc. **87**, 995-1003 (1965).

M. Lax, "Multiple scattering of waves II. The effective field in dense systems," Phys. Rev. **85**, 621-629 (1952).

H. B. Lee, M. S. John, J. D. Andrade, "Nature of water in synthetic hydrogels. I Dilatometry, specific conductivity, and differential scanning calorimetry of polyhydroxyethyl methacrylate," J. Colloid Interface Sci. **51**, 225-231 (1975).

J. Legge, *The Chinese classics*, vol. 4, (1893) pp. 237.

P. Leonard, *Handbuch der Experimental Physik* **23**, Pt. 1 and 2 "Phosphoreszenz und Fluoreszenz," (Akad. Verlagsges. Leipzig, 1928).

S. W. Leonard, J. P. Mondia, H. M. van Driel, O. Toader, S. John, "Tunable two-dimensional photonic crystals using liquid crystal infiltration," Phys. Rev. B **61**, R2389-R2392 (2000).

K. M. Leung, Y. F. Liu, "Full vector wave calculation of photonic structures in face-centered cubic dielectric media," Phys. Rev. Lett. **65**, 2646 (1990).

Y. Li, T. Tanaka, "Kinetics of swelling and shrinking of gels," J. Chem. Phys. **92**, 1365-1371 (1990).

—, T. Tanaka, "Phase Transitions of Gels," Annu. Rev. Mater. Sci. **22**, 243-277 (1992).

J. Li, X. Hong, Y. Liu, D. Li, Y. Wang, J. Li, Y. Bai, T. Li, "Highly Photoluminescent CdTe/Poly(N-isopropylacrylamide Temperature-Sensitive Gels," Adv. Mater., **17**, 163-166 (2005).

J. Li, B. Lin, J. Li, "Controllable Self-Assembly of CdTe/Poly(N-isopropylacrylamide-acrylic acid) Microgels in Response to pH Stimuli," Langmuir, **22**, 528-531 (2006).

S. Y. Lin, E. Chow, V. Hietch, P. R. Villeneuve, J. D. Joannopoulos, "Experimental Demonstration of Guiding and Bending of Electromagnetic Waves in a Photonic Crystal," Science **282**, 274-275 (1998)

M. Lončar, D. Nedeljković, T. Doll, J. Vučković, A. Sherer, T. P. Pearsall, “Waveguiding in planar photonic crystals,” App. Phys. Lett. **77** 1937-1939 (2000).

X. Lu, Z. Hu, J. Gao, "Synthesis and Light Scattering Study of Hydroxypropyl Celloulose Microgels," Macromolecules **33**, 8698-8702 (2000).

C. Manolatau, S. G. Johnson, S. Fan, P. R. Villeneuce, H. A. Haus, J. D. Joannopoulos, "High-Density Integrated Optics," J. Lightwave Tech. **17**, 1682 (1999).

A. Mamada. T. Tanaka, D. Kungwatchakun, M. Irie, "Photoinduced Phase Transistion of Gels," Macromolecules **23**, 1517-1519 (1990).

É. L Malus, "Mémoire sur la mesure du pouvoir réfringent des corps opaques," Nouveau Bull. D. Sci. par. la Soc. Philimatique **1**, 77-81 (1807); Also in"Ueber die Messung des Brechungsvermögens der undurchsichtigen Körper," Annalen der Physik (Leipzig) **31**, 225-234 (1809).

—, "Sur une propriété de la lumière réfléchie," Nouveau Bull. D. Sci. par. la Soc. Philimatique **1**, 266-269 (1808), translation in Ann. Phys. **31**, 286-297, 1809.

L. Mandel, Prog. Opt. **2**, 181 (1963).

Masatoshi Tokushima and Hirohito Yamada, “Light Propagation in a Photonic-Crystal-Slab Line-Defect Waveguide,” J. Quantum Elect. **38**, 753-759 (2002).

Y. Masumoto, T. Kawamura, K. Era, "Biexciton lasing in CuCl quantum dots," Appl. Phys. Lett. **62**, 225-227 (1993).

Y. Matsumoto, T. Kawamura, T. Ohzeki, S. Urabe, "Lifetime of indirect excitons in AgBr quantum dots," Phys. Rev. B, **46**, 1827-1830 (1992).

M. Matsuura, T. Kamizoto, "Oscillator strength of excitons in quantum wells," Surf. Sci. **174**, 183-187 (1986).

J. C. Maxwell, On the physical lines of force IV. The teory of molecular vortices applied to the action of magnetism on polarized light," Proc. Roy. Soc. **13**, 531-536 (1862).

J. C. Maxwell, "A dynamical theory of the electromagnetic field," Phil. Trans. Roy. Soc. **155**, 459-512 (1865).

—, "On double diffraction of a viscous fluid in motion," Proc. Roy. Soc. **22**, 46-47 (1873).

P. J. McMarr, K. Vedam, J. Narayan, "Spectroscopic Ellipsometry: A New Tool for Nondesctructive Depth Profiling and Characterization of Interfaces," J. Appl. Phys. **59**, 664-701 (1986).

S. McNab, N. Moll, Y. Vlasov, "Ultra-low loss photonic integrated circuit with membrane-type photonic crystal waveguides," Optics Express **11**, 2927-2939 (2003).

D. McPhail, M. Straub, and M. Gu, "Electrical tuning of three-dimensional photonic crystals using polymer dispersed liquid crystals," Appl. Phys. Lett. **86**, 051103 (2005).

R. D. Meade, A. Devenyi, J. D. Joannopoulos, O. L. Alerhand, D. A. Smith, K. Kash, "Novel applications of photonic band gap materials: Low-loss bends and high Q cavities," J. Appl. Phys. **75** 4753-4755 (1994).

M. Meewes, J. Rička, M. De Silva. R. Nyffenegger, Th. Binkert, "Coil-Globule Transition of Poly(N-isopropylacrylamide). A study of Surfactant Effects by Light Scattering," Macromolecules **24**, 5811-5816 (1991).

A. Mekis, J. C. Chen, I. Kurland, S. Fan, P. R. Villeneuve, J. D. Joannopoulos, "High Transmission through Sharp Bends in Photonic Crystal Waveguides," Phys. Rev. Lett. **77**, 3787-3790 (1996).

—, S. Fan, J. D. Joannopoulos, "Bound states in photonic crystal waveguides and waveguide bends," Phys. Rev. B **58**, 4809-4817 (1998).

D. E. Merewether, "Transient currents on a body of revolution by an electromagnetic pulse," IEEE Trans. Electromagnetic Compatibility, **EMC-13**, 41-44 (1971).

G. Mertens, T. Röder, R. Schweins, K. Huber, H. S. Kitzerow, "Shift of the photonic band gap in two photonic crystal/liquid crystal composites," Appl. Phys. Lett. **80**, 1885-1887 (2002).

G. Mie, "Beiträge zur Optik tuber Medien, speziell kolloidaler Metallösungen," Annalen der Physik (Leipzig) **330**, 377-445(1908).

T. Miyata, T. Uragami, K. Nakamae, "Biomolecule-sensitive hydrogels," Adv. Drug Delivery Rev. **54**, 79-98 (2002).

H. T. Miyazaki, H. Miyazaki, K. Ohtaka, T. Sato, "Photonic band in two-dimensional lattices of micrometer-sied spheres mechanically arranged under a scanning electron microscope," J. Appl. Phys. **87**, 7152-7158 (2000).

A. Modinos, "Scattering of electromagnetic waves by a plane of spheres-formalism," Physica A: Statistical and Theoretical Phys. **141**, 575-588 (1987).

N. F. Mott, "The theory of Crystal Rectifiers," Proc. Roy. Soc. A (London), **171**, 27-38 (1939).

C. Nanavati, J. M. Fernandez, "The secretory granule matrix: a fast-acting smart polymer," Science **259**, 963-965 (1993).

A. Neogi, S. Ghosh, J. Li, T. Cai, Z. Hu, "Enhanced Luminesence Efficiency from Hydrogel Microbead Encapsulated Quantum Dots," Mater. Res. Soc. Symp. Proc. **959**, 0959-M02-09 (2007).

H. Němec, P. Kužel, L. Duvillaret, A. Pashkin, M. Dressel, M. T. Sebastian, "Highly tunable photonic crystal filter for the terahertz range," Opt. Lett. **30**, 549-551 (2005).

I. Newton, *Opticks: or, A Treatise on the Reflexions, Refractions, Inflexions and Colours of Light*, (Printers of the Royal Society, London, 1705).

I. Nisho, G. Swislow, S. –T. Sun, T. Tanaka, "Critical density fluctuations within a single polymer chain," Nature **300**, 243-244 (1982).

M. Notomi, A. Shinya, K. Yamada, J. Takahashi, C. Takahashi, and I. Yokoyama, "Singlemode transmission within photonic bandgap of width-varied single-line-defect photonic crystal waveguides on SOI substrates," Electron. Lett. **37**, 293-295, (2001).

—, K. Yamada, A. Shinya, J. Takahashi, C. Takahashi, I, Yokohama, "Extremely Large Group-Velocity Dispersion of Line-Defect Waveguides in Photonic Crystal Slabs," Phys. Rev. Lett. **87** 253902-1 (2001).

—, A. Shinya, K. Yamada, J. –I. Takahashi, C. Takahashi, I. Yokohama, "Structural tuning of guided modes of line-defect waveguides of silicon-on-insulator photonic crystal slabs," IEEE J. Quantum Electron. **38**, 736-742 (2002).

T. Okano, Y. H. Bae, H. Jacobs, S. W. Kim, "Thermally on-off switching polymers for drug permeation and release," J. Conrl. Rel. **11**, 255-265 (1990).

A. Onuki, "Paradox in phase transitions with volume change," Phys. Rev. A **38**, 2192-2195 (1988).

L. S. Ornstein, F. Zernike, "Accidental deviation of density and opalescence at the critical point of a substance," Proc. Acad. Sci. Amst. **17**, 793 (1914).

—, F. Zernike, Proc. Acad. Sci. Amst. **19**, 1312 (1916).

—, F. Zernike, Z. Phys. **27**, 761 (1926).

Lucretius, *On the Nature of Things II*, (55 BC); translated by Cyril Bailey (Oxford, 1921); in M. R. Cohen, I. E. Drabkin, *A source book in Greek science*, (Cabbridge, Harvard University Press, 1958) p. 212-217.

K. Ohtaka, "Energy band of photons and low-energy photon diffraction," Phys. Rev B **19**, 5057-5067 (1979).

—, "Scattering theory of low-energy photon diffraction," J. Phys. C: Solid St. Phys. **13**, 667-680 (1980).

—, Y. Tanabe, "Photonic Bands Using Vector Spherical Waves. III. Group-Theoretical Treatment," J. Phys. Soc. Jpn. **65**, 2670-2684 (1996).

K. Otake, H. Inomata, M. Konno, S. Saito, "Thermal Analysis of the Volume Phase Transition with N-Isopropylacrylamide Gels," Macromolecules **23**, 283-289 (1990).

O. Painter, R. K. Lee, A. Scherer, A. Yariv, J. D. O'Brien, P. D. Dapkus, I. Kim, "Two-Dimensional Photonic Band-Gap Defect Mode Laser," Science, **284**, 1819-1821 (1999).

W. Park, E. Schonbrun, M. Tinker, J. –B. Lee, "Tunable nanophotonic device based on flexible photonic crystal," Proc. SPIE **5111**, 165-172 (2004).

C. A. Parker, *Photoluminescence of Solutions: With Applications to Photochemistry and Analytical Chemistry*, (Elsevier Pub. Co., New York 1968).

F. L. Pedrotti, L. S. Pedrotti, *Introduction to Optics*, 2nd ed. (Prentics Hall, New Jersey, 1993), p. 305.

R. Pecora, "Doppler Shifts in Light Scattering from Pure Liquids and Polymer Solutions," J. Chem. Phys. **40**, 1604-1614 (1964).

R. H. Pelton, P. Chibante, "Preparation of aqueous lattices with N-isopropylacrylamide," Colloids and Surf. **20**, 247-256 (1986).

J. B. Pendry, "The application of pseudopotentials to low-energy diffraction II: Calculation of the reflected intensities," J. Phys. C: Solid St. Phys. **2**, 2273-2282 (1969).

—, A. MacKinnon, "Calculation of Photon Dispersion Relations," Phys. Rev. Lett. **69**, 2772-2775 (1992).

—, "Ion core scattering and low energy electron diffraction I J. Phys. C. Solid St. Phys. **4**, 2501-2513 (1971).

—, "Ion core scattering and low energy electron diffraction II J. Phys. C. Solid St. Phys. **4**, 2514-2523 (1971).

A. Peters, S. J. Candau, "Kinetics of Swelling Polyacrylamide Gels," Macromolecules **19**, 1952-1955 (1986).

—, S. J. Candau, "Kinetics of Swelling of Spherical and Cylindrical Gels," Macromolecules **21**, 2278-2282 (1988).

P. N. Prasad, *Nanophotonics*, ed. (Wiley-Interscience, New York 2004) p. 3-8.

P. Pringsheim, *Fluorescence and Phosphorescence*, (Interscience Publishers, New York 1949).

Ptolemy, *Almagest*, (140 AD); in M. R. Cohen, I. E. Drabkin, *A source book in Greek science*, (Cabbridge, Harvard University Press, 1958) p. 212-217.

E. M. Purcell, "Spontaneous Emission Probabilities at Radio Frequencies" Phys. Rev. **69**, 681 (1946).

M. Qui, "Analysis of guided modes in photonic crystal fibers using the finite-difference time-domain method," Microwave Opt. Technol. Lett. **30**, 327-330 (2001).

X. Qui, C. M. S. Kwan, C. Wu, "Laser Light Scattering Study of the Formation and Structure of Poly(N-isopropylacrylamide-co-acrylic acid) Nanoparticles," Macromolecules **30**, 6090-6094 (1997).

Y. Qui, K. Park, "Environment-sensitive hydrogels for drug delivery," Adv. Drug Del. Rev. **53**, 321-339 (2001).

K. R. Ramanathan, Indian J. Phys. **1**, 413 (1927).

V. V. Raman, K. S. Krishnan, "A new type of secondary radiation," Nature **121**, 501-502 (1928).

Lord Rayleigh, "On the light from the sky, its polarization and coulour," Phil. Mag. **41**, 107-120 (1871).

—, "On the scattering of light by small particles," Phil. Mag. **41**, 274-279, 447, (1871).

—, "On the electromagnetic theory of light," Phil. Mag. **12**, 81-102 (1881).

—, “On the maintenance of vibrations by force of double frequency, and on the propagation of waves through a medium endowed with a periodic structure,” Phil. Mag. **26**, 145-159 (1887).

—, "On the transmission of light through an atmosphere containing small particles in suspension, and on the origin of the blue sky," Phil. Mag. **47**, 375-394 (1899).

—, "The Incidence of Light upon a Transparent Sphere of Dimensions Comparable with the Wave-Length," Proc. Roy. Soc. A, **84**, 25-46 (1910).

—, "On the Diffraction of Light by Spheres of Small Relative Index," Proc. Roy. Soc. A **90**, 219-225 (1914).

—, “On the reflection of light from a regularly stratified medium,” Proceedings of the Royal Society of London **93**, 565-577 (1917).

—, "On the Scattering of Light by Spherical Shells, and by Complete Spheres of Periodic Structure, when the Refractivity is Small," Proc. Roy. Soc. A **94**, 296-300 (1918).

A. Reyes-Coronado, A. García, C. Sánchez-Pérez, R. G. Barrera, "Measurement of the effective refractive index of a turbid colloidal suspension using light refraction," New J. Phys. **7**, 89 (2005).

N. Riehl, M. Schön, “Der Leuchtmechanismus von Kristallphosphoren,” Z. Physik **114**, 682 (1939).

A. Righi, "Sui campi elettromagnetici e particolarmente su quelli create da cariche elettriche o da poli magnetic in movimento," Nuovo Cimento **2**, 104-121 (1901).

—, "Sulla questione del campo magneico generato dalla convenzione elettrica, e su alter questioni, Nuovo Cimento **2**, 233-256 (1901).

Y. Rocard, Annales de Physique (Paris) **10**, 116 (1928).

A. Roda, *The Discovery of Luminescence: "The Bolognian Stone"* International Society of Bioluminescence and Chemiluminescence (http://www.isbc.unibo.it/Files/10_SE_BoStone.htm) accessed on February 13, 2008)

A. Roda, M. Pazzagli, L. J. Kricka, P.E. Stanley, *Bioluminescence & Chemiluminescence: Perspectives for the 21st Century*, (Wiley, New York, 1999).

R. Roseler, *Infared Spectroscopic Ellipsometry*, (Akademie-Verlag, Berlin 1990).

A. Rothen, "The Ellipsometer, an Apparatus to Measure Thickness of Thin Surface Films," Rev. Sci. Instrum. **16**, 26-30 (1945).

J.W. Ryde, B. S. Cooper, “Scattering of Light by Turbid Media—Part I,” Proc. Roy. Soc. Series A **131**, 451 (1931).

—, B. S. Cooper, “Scattering of Light by Turbid Media—Part II,” Proc. Roy. Soc. Series A **131**, 464 (1931).

B. E. A. Saleh, M. F. Cordoso, "The effect of channel correlation on the accuracy of photon counting digital autocorrelators," J. Phys. A.: Math. Nuc. Gen. **6**, 1897-1909 (1973).

K. Sakoda, "Symmetry, degeneracy, and uncoupled modes in two-dimensional photonic lattices," Phys. Rev. B **52**, 7982-7986 (1995).

—, K. Ohtaka, "Optical response of three-dimensional photonic lattices: Solutions of inhomogeneous Maxwell's equations and their applications," Phys. Rev. B **54**, 5732-5741 (1996).

—, "Group-theoretical classification of eigenmodes in three dimensional photonic lattices," Phys. Rev. B **55**, 15345-15348 (1997).

—, *Optical Properties of Photonic Crystals*, 2nd ed. (Springer, New York 2005).

K. Schätzel, M. Drewel, "Laser light scattering and correlation techniques for characterization of colloidal suspensions," Z. Physik B **68**, 229-232 (1987).

—, "Noise on photon correlation data: I. Autocorrelation functions," Quantum Opt. **2**, 287-305 (1990).

—, "Correlation techniques in dynamic light scattering," App. Phys. B **42**, 193-213 (2004).

A. Scherer, O. Painter, B. D'Urso, R. Lee, A. Yariv, "InGaAsP photonic bandgap crystal membrane microresonators," J. Vac. Sci. & Technol. B: Microelectronics and Nanometer Structures **16**, 3906-3910 (1998).

—, O. Painter, J. Vuckovic, M. Loncar, T. Yoshie, "Photonic Crystals for Confining and Guiding and Emitting Light," Trans. Nanotech. **1** 4-11 (2002).

M. Schmidt, M. Eich, U. Huebner and R. Boucher, "Electro-optically tunable photonic crystals," Appl. Phys. Lett. **87**, 121110 (2005).

R. L. Schmidt, H. L. Clever, "Thermodynamics of Binary Liquid Mixtures by Rayleigh Light Scattering," J. Chem. Phys. **72**, 1529-1536 (1968).

C. Schuller, F. Klopf, J. P. Reithmaier, M. Kamp, and A. Forchel, "Tunable photonic crystals fabricated in III-V semiconductor slab waveguides using infiltrated liquid crystals," App. Phys. Lett. **82**, 2767-2769 (2003).

E. O. Schulz-Du Bois, In *Photon Correlation Techniques in Fluid Mechanics* ed., edited by E. O. Schulz-Du Bois, (Springer-Verlag, Berlin 1983) p. 15.

T. Schica, Y. Hirose, A. Okada, T. Kurauchi, "Bending of Poly (Vinal Alcohol) –Poly (Sodium Acrylate) Composite Hdrogels in Electric Fields," J. App. Polymer. Sci. **44**, 249-253 (1992).

P. Schiebener, J. Straub, J. M. H. Levelt Sengers, and J. S. Gallagher, "Refractive index of water and steam as function of wavelength, temperature and density," *J. Phys. Chem. Ref. Data* **19**, 677-717 (1990).

A. J. F. Seigert, "MIT Radiation Lab. Report" *No. 465*, (1943).

F. Seitz, “Interpretation of the properties of Alkali Halide-Thallium phosphors,” J. Chem. Phys. **6**, 150-162 (1938).

P. R. Selvin, "The renaissance of fluorescence resonance energy transfer," Nat. Struct. Bio., **7**, 730-734 (2000).

M. Shibayama, T. Fujikawa, S. Nomura, "Dynamic Light Scattering Study of Poly(N-isopropylacrylamide-co-acrylic acid) Gels," Macromolecules **29**, 6535-6540 (1996).

T. Shiga, T. Kurauchi, “Deformation of Polyelectrolyte Gels under the Influence of Electric Field,” J. App. Poly. Sci. **39**, 2305-2320 (1990).

S. Shionoya, "Introduction to the Handbook," in *Phosphor Handbook*, edited by S. Shionoya, W. M. Yen, (CRC Press, New York 1999).

Y. Shen, C. S. Friend, Y. Jiang, D. Jakubczyk, J. Swiatkiewics, P. N. Prasad, "Nanophotonics: Interactions, Materials, and Applications," J. Phys. Chem. **104**, 7577-7587 (2000).

N. Skivesen, A. Têtu, M. Kristensen, J. Kjems, L. H. Frandsen, P. I. Borel, “Photonic-crystal waveguide biosensor,” Optics Express, **15**, 3169-3176 (2007).

J. C. Slater, "Not on Hartree's Method," Phys. Rev. **35**, 210-211 (1930).

A. Sidorenko, T. Krupenkin, A. Taylor, P. Fratzl, J. Aizenberg, “Reversible Switching of Hydrogel-Actuated Nanostructures into Complex Micropatterns,” Science **315** 487-490 (2007).

M. Smoluchowski, "Molekular-kinetische Theorie der Opaleszenz von Gasen im kritischen Zustande, sowie einiger verwandter Erscheinungen," Annalen der Physik (Leipzig) **25**, 205-226 (1908).

P. G. Snyder, M. C. Rost, G. H. Bu-Abbud, J. A. Woollam, J. Appl. Phys. **60**, 3293-3302 (1986).

G. B. Street and R. L. Greene, "Preparation and Properties of $(SN)_x$," IBM J. Res. Develop. **21**, 99-110 (1977).

N. Stefanou, V. Karathanos, A. Modinos, "Scattering of electromagnetic waves by periodic structures," J. Phys..: Condes. Matter **4**, 7389-7400 (1992).

L. Stryer R. P. Haugland, "Energy transfer: A spectroscopic ruler," Proc. Natl. Acad. Sci. U.S.A. **58**, 718-726 (1967).

—, "Fluorescence Energy Transfer as a Spectroscopic Ruler," Ann. Rev. Biochem., **47**, 819-846 (1978).

G. Q. Stokes, "On the change of refrangibility of light," Phil. Trans. Roy. Soc. London **142**, 463-562 (1852).

Y. Sugimoto, N. Ikeda, N. Carlsson, K. Asakawa, N. Kawai, K. Inoue, "Theoretical and experimental investigation of straight defect waveguides in AlGaAs-based air-bridge-type two-dimensional slabs," Appl. Phys. Lett. **79**, 4286-4288 (2001).

—, N. Ikeda, N. Carlsson, K. Asakawa, N. Kawai, K. Inoue, "AlGaAs-Based Two-Dimensional Photonic Crystal Slab With Defect Waveguides for Planar Lightwave Circuit Applications," IEEE J. Quantum Electron. **38**, 760-769 (2002).

—, N. Ikeda, N. Carlsson, K. Asakawa, N. Kawai, and K. Inoue, "Fabrication and Characterization of different types of two-dimensional AlGaAs photonic crystal slabs," J. Appl. Phys. **91**, 922-929, (2002).

—, Y. Tanaka, N. Ikeda, Y. Nakamura, K. Asakawa, K. Inoue, "Low propagation loss of 0.76 db/mm in GaAs-based single-line-defect two-dimensional photonic crystal slab waveguides up to 1cm in length," Opt. Express **12**, 1090-1096 (2004).

A. Suzuki, T. Tanaka, "Phase transition in polymer gels induced by visible light," Nature **346**, 345-347 (1990).

G. Swislow, S. –T. Sun, I. Nisho, T. Tanaka, "Coil-Globule Phase Transition in a Single Polystyrene Chain in Cyclohexane," Phys. Rev. Lett. **44**, 796-798 (1980).

R. A. Synowicki, G. K. Pribil, G. Cooney, C. M. Heringer, S. E. Green, R. H. French, M. K. Yang, J. H. Burnett, S. Kaplan, "Fluid refractive index measurements using rough surface and prism minimum deviation techniques," J. Vac. Sci Technol. B **22**, 3450-3453 (2004).

—, T. E. Tiwald, U.S. Patent No. 6,738,139 (18 May 2004).

A. Takizawa, T. Kinoshita, O. Nomura, Y. Tsujita, "Characteristics of Water in Copoly(methyl methacrylate—N—vinylpyrrolidone) Membranes," Polym. J. **17**, 747-752 (1985).

T. Tanaka, L. O. Hocker, G. B. Benedek, "Spectrum of light scattered from a viscoelastic gel," J. Chem. Phys. **59**, 5151-5159 (1973).

—, S. Ishiwata, C. Ishimoto, "Critical Behavior of Density Fluctuations in Gels," Phys. Rev. Lett. **38**, 771-774 (1977).

—, "Collapse of Gels and the Critical Endpoint," Phys. Rev. Lett. **40**, 820-823 (1978).

—, "Dynamics of critical concentration fluctuations in gels," Phys. Rev. A **17**, 763-766 (1978).

—, D. J. Fillmore, "Kinetics of swelling of gels," J. Chem. Phys. **70**, 1214-1218 (1979).

—, D. Fillmore, S. –T. Sun, I. Nishio, G. Swislow, A. Shah, "Phase Transitions in Ionic Gels," Phys. Rev. Lett. **45**, 1636-1639 (1980).

—, I. Nishio, S. Sun, S. Nisho, "Collapse of Gels in an Electric Field," Science **218**, 467-469 (1982).

—, E. Sato, Y. Hirokawa, S. Hirotsu, J. Peetermans, "Critical Kinetics of Volume Phase Transition of Gels," Phys. Rev. Lett. **55**, 2455 (1985).

A. Taflove, M. E. Brodwin, "Numerical Solution of Steady-State Electromagnetic Scattering Problems Using the Time-Dependent Maxwell's Equations," Microwave Theory and Techniques **MTT-23**, 623-630 (1975).

—, "Application of the Finite-Difference Time-Domain Method to Sinusoidal Steady-State Electromagnetic-Penetration Problems," IEEE Trans. Electromagnetic Compatibility **EMC-22**, 191-202 (1980).

—, K. R. Umashankar, B. Becker, F. Harfoush, K. S. Yee, "Detailed FD-TD analysis of electromagnetic fields penetrating narrow slots and lapped joints in thick conducting screens," IEEE Trans. Antennas and Propagation, **AP-36**, 247-257 (1988).

—, S. C. Hagness, *Computational Electrodynamics: The Finite-Difference Time-Domain Method*, 2nd ed. (Artech House, Boston 2000).

M. Tokushima, H. Kosaka, A. Tomita, H. Yamada, "Lightwave propagation through a 120° sharply bent single-line-defect photonic crystal waveguide," Appl. Phys. Lett. **76**, 952-954 (2000).

M. T. Tinker and J-B. Lee, “Thermal and optical simulation of a photonic crystal light modulator based on the thermo-optic shift of the cut-off frequency,” Optics Express **13**, 7174-7188 (2005).

L. Tsang, J. A. Kong, "Effective propagation constants for coherent electromagnetic waves propagating in media embedded with dielectric scatterers," J. Appl. Phys. **53**, 7162-7173 (1982).

—, J. A. Kong, *Scattering of Electromagnetic Waves: Advanced Topics*, (Wiley, New York 2001).

J. Tyndall, "On the blue colour of the sky, the polarisation of skylight, and the polarisation of light by cloudy matter generally," Phil. Mag. **37**, 384-394 (1869).

—, "On the chemical rays, and the light from the sky," Proc. Roy. Inst. **5**, 429-450 (1869).

—, "On the action of rays of high refrangibility upon gaseous matter, Phil Trans. Roy. Soc. **160**, 333-365 (1870).

—, *Faraday as a discoverer*, electronic ed. (Champaign, Ill, Project Gutenberg; Boulder, Co, Netlibrary 1999).

K. Umashankar, A. Taflove, "A Novel Method to Analyze Electromagnetic Scattering of Complex Objects," IEEE Trans. Electromagnetic Compatibility **EMC-24**, 397-405 (1982).

—, A. Taflove, B. Becker, "Calculation and experimental validation of induced currents on coupled wires in an arbitrary shaped cavity," IEEE Trans. Antennas and Propagation **AP-35**, 1258-1257 (1987).

B. K. Vainstein, *Diffraction of X-rays by Chain Molecules*, (Amsterdam, Elsevier 1966).

P. R. Villenieve, M. Piché, "Photonic bandgaps: what is the best numerical representation of periodic structures?" J. Mod. Opt. **41**, 241 (1994).

—, S. Fan, J. D. Joannopoulos, K. –Y. Lim, G. S. Petrich, L. A. Kolodziejski, R. Reif, "Air-Bridge microcavities," Appl. Phys. Lett. **67**, 167-169 (1995).

J. A. Vollgraff, "Snellius' Notes on the Reflection and Refraction of Rays," Osiris, **1**, 718-725 (1936).

A. T. Walter, "Elastic Properties of Polvinyl Chloride gels," J. Poly. Sci. **8**, 207-228 (1954).

C. Wang, Y. Li, Z. Hu, "Swelling Kinetics of Polymer Gels," Macromolecules **30**, 4727-4732 (1997).

X. Wang, C. Wu, "Light-Scattering Study of Coil-to-Globule Transition of a Poly(N-isopropyacrylamide) Chain in Deuterated Water," Macromolecules **32**, 4299-4301 (1999).

G. Watson, P. Fleury, S. McCall, "Searching for photon localization in the time domain," Phys. Rev. Lett. **58**, 945-948 (1987).

N. Wax, *Selected Papers on Noise and Stochastic Processes*, edited by N. Wax (Dover, New York 1954).

W. H. Weedon, S. W. McKnight, A. J. Devaney, "Selection of optimal angles for inversion of multiple-angle ellipsometry and reflectometry equations," J. Opt. Soc. Am. A **8**, 1881-1891 (1991).

C. Weisbuch, B. Vinter, *Quantum Semiconductor Structures*, (Academic Press, Boston 1991).

S. Weiss, Fluorescence Spectroscopy of Single Biomolecules," Science **283**, 1676-1683 (1999).

—, "Measuring conformational dynamics of biomolecules by single molecule fluorescence spectroscopy," Nat. Struct. Bio. **7**, 724-729 (2000).

N. C. Wickramasinghe, Light Scattering Functions for Small Particles with Applications in Astronomy, (Wiley, New York 1973).

F. Williams, *Luminescence of Inorganic Solids*, edited by P. Goldberg, (Academic Press, New York 1966) p. 5.

R. Williams, R. S. Crandall, P. J. Wojtwicz, "Melting of Crystalline Suspensions of Polystyrene Spheres," Phys. Rev. Lett. **37**, 348-351 (1976).

C. Wu, K. K. Chan, K. Q. Xia, "Experimental Study of the Spectral Distribution of the Light Scattered from Flexible Macromolecules in Very Dilute Solution," Macromolecules **28**, 1032-1037 (1995).

—, S. Zhou, "Laser Light Scattering Study of the Phase Transition of Poly(N-isopropylacrylamide in Water. 1. Single Chain," Macromolecules **28**, 8381-8387 (1995).

—, B. Chu, in *Experimental Methods in Polymer Science: Modern Methods in Polymer Research and Technology*, edited by T. Tanaka, (Academic Press, San Diego, CA 2000).

J. Wu, B. Zhou, Z. Hu, "Phase Behavior of Thermally Responsive Microgel Colloids," Phys. Rev. Lett. **90**, 48304 (2003).

C. Xu, X. Hu, Y. Li, X. Liu, R. Fu, and J. Zi, "Semiconductor-based tunable photonic crystals by means of an external magnetic field," Phys. Rev. B **68**, 193201 (2003).

E. Yablonovitch, "Statistical ray optics," J. Opt. Soc. Am. **72**, 899 (1982).

—, E. O. Kane, "Reduction of lasing threshold current density by the lowering of valence band effective mass," J. Lightwave Technol. **4**, 504-506 (1986).

—, "Inhibited Spontaneous Emission in Solid-State Physics and Electronics," Phys. Rev. Lett. **58**, 2059 (1987).

—, R. Bhat, J. P. Harbison, R. A. Logan, "Survey of defect-mediated recombination lifetimes in GaAs epilayers grown by different methods," Appl. Phys. Lett. **50**, 1197-1199 (1987).

Yamashita, K., O. Hashimoto, T. Nishimura, M. Nango, "Preparation of stimuli-responsive water absorbent," React. Funct. Poly. **51**, 61 (2002).

M. Yamato, C. Konno, M. Utsumi, A. Kikuchi, T. Oano, "Thermally responsive polymer-grafted surfaces facilitate patterned cell seeding and co-culture," Biomaterials. **23**, 561 (2002).

Y. Yang, Z. Wen, Y. Dong, M. Gao, "Incorporating CdTe Nanocrystals into Polystyrene Microspheres: Towards Robust Fluorescent Beads," Small, **2**, 898-901 (2006).

K. S. Yee, "Numerical solution of initial boundary value problems involving Maxwell's equations in isotropic media," IEEE Trans. Antennas and Propagation **AP-14**, 302-307 (1966).

A. D. Yoffe, "Low-dimensional systems; quantum size effects and electronic properties of semiconductor microcrytallites (zero-dimensional systems) and some quasi-two-dimensional systems," Adv. Phys. **42**, 173-262 (1993).

J. Yonekura, M. Ikeda, and T. Baba," Analysis of finite 2D photonic crystals of columns and lightwave devices using the scattering matrix method," J. Lightwave Technol. **17**, 1500-1508 (1999).

K. Yoshino, S. Tatsuhara, Y. Kawagishi, M. Ozaki, A. A. Zakhidov, Z. V. Vardeny, "Spectral Narrowing of Photoluminescence in Conducting Polymer and Fluorescent Dyes Infiltrated in Photonic Crystal, Synthetic Opal," Jpn. J. Appl. Phys. **37**, L1187-L1189 (1998).

—, S. Tatsuhara, Y. Kawagishi, M. Ozaki, A. A. Zakhidov, Z. V. Vardeny, "Amplified spontaneous emission and lasing in conducting polymers and fluorescent dyes in opals as photonic crystals," Appl. Phys. Lett. **74**, 2590-2592 (1999).

—, Y. Shimoda, Y. Kawagishi, K. Nakayama, M. Ozaki, "Temperature tuning of the stop band in transmission spectra of liquid-crystal infiltrated synthetic opal as tunable photonic crystal," Appl. Phys. Lett. **75**, 932-934 (1999).

—, S. Satoh, Y. Shimoda, T. Kawagishi, K. Nakayama, M. Ozaki, "Tunable Optical Stop Band and Reflection Peak in Synthetic Opal Infiltrated with Liquid Crystal and Conducting Polymer as Photonic Crystal," Jpn. J. Appl. Phys. **38**, L961-L963 (1999).

T. Young, "The Bakerian Lecture: On the Theory of Light and Colours," Phil. Trans. Roy. Soc. London **92**, 12-48 (1802)

—, "An Account of Some Cases of the Production of Colours, not Hitherto Describes," Phil. Trans. Roy. Soc. **92**, 387-397 (1802).

—, "The Bakerian Lecture: Experiments and Calculations Relative to Physical Optics," Phil. Trans. Roy Soc. **94**, 1-16 (1804).

C. –P. Yu, H. –C. Chang, "Yee-mesh-based finite difference eigenmode solver with PML absorbing boundary conditions for optical waveguides and photonic crystal fibers," Opt. Express **12**, 6165-6177 (2004).

F. Zernike, T. H. Prins, Z. Physik. **41**, 184 (1927).

G. Zhang, C. Wu, "The Water/Methanol Complexation Induced Reentrant Coil-to-Globule Transition of Individual Homopolymer Chains in Extremely Dilute Solution," J. Am Chem. Soc. **123**, 1376-1380 (2001).

Z. Zhang, S. Satpathy, "Electromagnetic wave propagation in periodic structures: Bloch wave solution of Maxwell's equations," Phys. Rev. Lett. **65**, 2650 (1990).

B. H. Zimm, "Molecular Theory of Scattering of Light in Fluids," J. Chem Phys. **13**, 141-145 (1945).

—"The Scattering of Light and the Radial Distribution Function of High Polymer Solutions," J. Chem. Phys. **16**, 1093-1099 (1948).

M. Zrìnyi, "Intelligent polymer gels controlled by magnetic fields," Colloid Poly. Sci. **278**, 98-103 (2000).

R. Zwanzig, "Time-Correlation Functions and Transport Coefficients in Statistical Mechanics," Ann. Rev. Phys. Chem. **16**, 67-102 (1965).